



O'Connor, Cairíona (2016) TRIB2 in normal and malignant hematopoiesis - a transcription factor network. PhD thesis.

<http://theses.gla.ac.uk/7354/>

Copyright and moral rights for this thesis are retained by the author

A copy can be downloaded for personal non-commercial research or study, without prior permission or charge

This thesis cannot be reproduced or quoted extensively from without first obtaining permission in writing from the Author

The content must not be changed in any way or sold commercially in any format or medium without the formal permission of the Author

When referring to this work, full bibliographic details including the author, title, awarding institution and date of the thesis must be given

# **TRIB2 in normal and malignant hematopoiesis - a transcription factor network**

**Caitriona O'Connor, BSc**

*A thesis submitted in fulfilment of the requirements for a Doctor of  
Philosophy at the University of Glasgow*

*Faculty of Medical, Veterinary and Life Sciences  
Institute of Cancer Science*

*Submitted: February 2016*

© Caitriona O'Connor

## Abstract

Hematopoiesis is the tightly controlled and complex process in which the entire blood system is formed and maintained by a rare pool of hematopoietic stem cells (HSCs), and its dysregulation results in the formation of leukaemia. TRIB2, a member of the *Tribbles* family of serine/threonine pseudokinases, has been implicated in a variety of cancers and is a potent murine oncogene that induces acute myeloid leukaemia (AML) *in vivo* via modulation of the essential myeloid transcription factor CCAAT-enhancer binding protein  $\alpha$  (C/EBP $\alpha$ ). C/EBP $\alpha$ , which is crucial for myeloid cell differentiation, is commonly dysregulated in a variety of cancers, including AML.

Two isoforms of C/EBP $\alpha$  exist - the full-length p42 isoform, and the truncated oncogenic p30 isoform. TRIB2 has been shown to selectively degrade the p42 isoform of C/EBP $\alpha$  and induce p30 expression in AML. In this study, overexpression of the p30 isoform in a bone marrow transplant (BMT) leads to perturbation of myelopoiesis, and in the presence of physiological levels of p42, this oncogene exhibited weak transformative ability. It was also shown by BMT that despite their degradative relationship, expression of C/EBP $\alpha$  was essential for TRIB2 mediated leukaemia. A conditional mouse model was used to demonstrate that oncogenic p30 cooperates with TRIB2 to reduce disease latency, only in the presence of p42. At the molecular level, a ubiquitination assay was used to show that TRIB2 degrades p42 by K48-mediated proteasomal ubiquitination and was unable to ubiquitinate p30. Mutation of a critical lysine residue in the C-terminus of C/EBP $\alpha$  abrogated TRIB2 mediated C/EBP $\alpha$  ubiquitination suggesting that this site, which is frequently mutated in AML, is the site at which TRIB2 mediates its degradative effects. The TRIB2-C/EBP $\alpha$  axis was effectively targeted by proteasome inhibition.

AML is a very difficult disease to target therapeutically due to the extensive array of chromosomal translocations and genetic aberrations that contribute to the disease. The cell from which a specific leukaemia arises, or leukaemia initiating cell (LIC), can affect the phenotype and chemotherapeutic response of the resultant disease. The LIC has been elucidated for some common oncogenes but it is unknown for TRIB2. The data presented in this thesis investigate the ability of the oncogene TRIB2 to transform hematopoietic stem and progenitor

cells *in vitro* and *in vivo*. TRIB2 overexpression conferred *in vitro* serially replating ability to all stem and progenitor cells studied. Upon transplantation, only TRIB2 overexpressing HSCs and granulocyte/macrophage progenitors (GMPs) resulted in the generation of leukaemia *in vivo*. TRIB2 induced a mature myeloid leukaemia from the GMP, and a mixed lineage leukaemia from the HSC. As such the role of TRIB2 in steady state hematopoiesis was also explored using a *Trib2*<sup>-/-</sup> mouse and it was determined that loss of Trib2 had no effect on lineage distribution in the hematopoietic compartment under steady-state conditions.

The process of hematopoiesis is controlled by a host of lineage restricted transcription factors. Recently members of the Nuclear Factor 1 family of transcription factors (NFIA, NFIB, NFIC and NFIX) have been implicated in hematopoiesis. Little is known about the role of NFIX in lineage determination. Here we describe a novel role for NFIX in lineage fate determination. In human and murine datasets the expression of *Nfix* was shown to decrease as cells differentiated along the lymphoid pathway. NFIX overexpression resulted in enhanced myelopoiesis *in vivo* and *in vitro* and a block in B cell development at the pre-pro-B cell stage. Loss of NFIX resulted in disruption of myeloid and lymphoid differentiation *in vivo*. These effects on stem and progenitor cell fate correlated with changes in the expression levels of key transcription factors involved in hematopoietic differentiation including a 15-fold increase in *Cebpa* expression in *Nfix* overexpressing cells. The data presented support a role for NFIX as an important transcription factor influencing hematopoietic lineage specification.

The identification of NFIX as a novel transcription factor influencing lineage determination will lead to further study of its role in hematopoiesis, and contribute to a better understanding of the process of differentiation. Elucidating the relationship between TRIB2 and C/EBP $\alpha$  not only impacts on our understanding of the pathophysiology of AML but is also relevant in other cancer types including lung and liver cancer. Thus in summary, the data presented in this thesis provide important insights into key areas which will facilitate the development of future therapeutic approaches in cancer treatment.

# Table of Contents

Abstract .....	2
List of tables.....	10
List of figures.....	11
Acknowledgements.....	15
Author's declaration .....	16
Abbreviations.....	17
<b>1 Introduction.....</b>	<b>23</b>
1.1 Hematopoiesis.....	23
1.1.1 Hematopoietic hierarchy .....	24
1.1.2 Identification of stem and progenitor populations .....	26
1.1.3 Myelopoiesis .....	27
1.1.3.1 Cytokines in myeloid differentiation .....	28
1.1.3.2 Transcription factors in myeloid differentiation .....	29
1.1.3.3 C/EBP $\alpha$ .....	30
1.1.3.3.1 C/EBP $\alpha$ in myelopoiesis .....	31
1.1.3.3.2 Fetal to adult switch .....	33
1.1.4 B cell lymphopoiesis.....	34
1.1.5 T cell lymphopoiesis.....	36
1.2 AML .....	38
1.2.1 AML classifications.....	38
1.2.1.1 FAB classification .....	39
1.2.1.2 The WHO classification .....	39
1.2.2 Common mutations and abnormalities .....	40
1.2.2.1 Class I mutations.....	40
1.2.2.2 Class II mutations.....	41
1.2.2.2.1 <i>CEBPA</i> mutations .....	41
1.2.2.2.2 <i>NPM1</i> .....	42
1.2.2.2.3 Mixed-lineage leukaemia fusion genes .....	43
1.2.2.2.4 Dysregulation of <i>HOX</i> genes .....	43
1.2.2.2.5 <i>PML RAR<math>\alpha</math></i> .....	44
1.2.2.2.6 <i>RUNX1</i> .....	45
1.2.2.3 Mutations of epigenetic modifiers .....	45
1.2.3 Chemotherapeutic treatment of AML.....	45

1.3	Trib2.....	47
1.3.1	Discovery.....	47
1.3.2	Structure of TRIB proteins.....	48
1.3.3	Functions of TRIB2.....	49
1.3.3.1	Protein degradation .....	49
1.3.3.2	MAPK/ERK Signalling .....	50
1.3.3.3	AKT Signalling .....	51
1.3.3.4	Toll-like receptor signalling.....	51
1.3.3.5	Hematopoiesis.....	52
1.3.4	The role of TRIB2 in cancer .....	53
1.3.4.1	TRIB2 in acute leukaemia .....	53
1.3.4.1.1	AML.....	53
1.3.4.1.2	T-ALL.....	56
1.3.4.2	TRIB2 in solid tumour cancer .....	57
1.3.4.2.1	Melanoma .....	57
1.3.4.2.2	Lung Cancer.....	58
1.3.4.2.3	Liver Cancer .....	59
<b>2</b>	<b>Materials &amp; Methods .....</b>	<b>61</b>
2.1	Plasmids and cell lines .....	61
2.1.1	Plasmids.....	61
2.1.2	Cell Lines .....	62
2.1.2.1	HEK293T Cells.....	63
2.1.2.2	NIH/3T3 Cells.....	63
2.1.2.3	OP9 cells .....	63
2.1.2.4	WEHI-3B cells.....	64
2.1.2.4.1	WEHI conditioned media production .....	64
2.1.2.5	BHK/MKL cells.....	64
2.1.2.6	Ba/F3 cells.....	64
2.1.2.7	32D cells .....	64
2.1.2.8	C/EBP $\alpha^{-/-}$ cells.....	65
2.1.2.9	Human leukaemia cell lines.....	65
2.2	Tissue culture .....	65
2.2.1	Transfection .....	66
2.2.1.1	Production of retrovirus by calcium phosphate transfection....	66
2.2.1.1.1	Titration of viruses using 3T3 cells .....	67

2.2.1.2	TurboFect transfection for ubiquitination assays .....	68
2.2.2	Retroviral transduction .....	68
2.2.2.1	Suspension cell transduction .....	68
2.2.2.2	Primary cell transduction.....	68
2.2.3	Differentiation Assays.....	69
2.2.3.1	32D Differentiation Assay.....	69
2.2.3.2	Colony forming unit assay .....	69
2.2.3.3	OP9 B cell differentiation assay .....	71
2.2.4	Dual-luciferase reporter assay.....	72
2.2.5	Magnetic-activated cell sorting.....	73
2.2.5.1	cKit Purification.....	74
2.2.5.2	Lineage Depletion .....	74
2.2.5.3	Magnetic separation.....	75
2.3	Animal Work.....	75
2.3.1	BMT .....	75
2.3.2	Harvesting tissues .....	77
2.3.3	Transgenic mouse models .....	77
2.3.3.1	<i>Trib2</i> <sup>-/-</sup> mice.....	77
2.3.3.1.1	Genotyping and evaluation of Trib2 excision .....	77
2.3.3.2	<i>Cebpa</i> conditional model .....	78
2.3.3.2.1	Genotyping and evaluation of C/EBPα excision .....	79
2.4	Flow Cytometry .....	79
2.4.1	Determining surface antigen expression .....	80
2.4.2	Apoptosis staining .....	80
2.4.3	Proliferation assay.....	81
2.4.4	Fluorescence activated cell sorting.....	82
2.5	Protein Assays.....	82
2.5.1	Western Blotting.....	82
2.5.1.1	Preparation of cell lysates .....	82
2.5.1.1.1	Tris or RIPA lysis.....	82
2.5.1.1.2	Direct lysis .....	83
2.5.1.2	SDS-PAGE and membrane transfer .....	83
2.5.1.3	Antibody labelling and detection.....	84
2.5.1.4	Stripping for re-probing.....	84
2.5.2	Ubiquitination assay.....	85

2.5.2.1	Setting up the Ubiquitination IP .....	86
2.5.2.2	Elution.....	86
2.6	Gene Expression Analysis .....	87
2.6.1	RNA extraction .....	87
2.6.2	cDNA synthesis .....	87
2.6.3	qRT-PCR.....	87
2.6.4	Fluidigm™ high-throughput qPCR .....	88
2.6.4.1	Preamplification and exonuclease treatment .....	88
2.6.4.2	Loading the chip .....	88
2.7	Statistical analysis.....	89
<b>3</b>	<b>Results: C/EBP<math>\alpha</math> in TRIB2 mediated AML induction .....</b>	<b>98</b>
3.1	Introduction .....	99
3.1.1	C/EBP $\alpha$ p30 targets .....	99
3.1.1.1	C/EBP $\alpha$ p42.....	101
3.1.1.2	Ubiquitin conjugating enzyme 9.....	101
3.1.1.3	Peptidyl-prolyl cis/trans isomerase .....	102
3.1.1.4	WD repeat-containing protein 5 .....	103
3.1.2	Experimental mouse models of p30 in AML .....	103
3.1.2.1	The BRM2 knock-in murine model.....	104
3.1.2.2	The L/+ and L/L knock-in murine model.....	105
3.1.2.3	The K/L and K/K knock-in murine model .....	105
3.1.2.4	The C/EBP $\alpha$ -N <sup>m</sup> and C/EBP $\alpha$ -C <sup>m</sup> overexpression murine model	106
3.2	Aims and objectives .....	108
3.3	Results.....	109
3.3.1	C/EBP $\alpha$ -p30 disrupts myelopoiesis <i>in vivo</i> .....	109
3.3.2	Overexpression of C/EBP $\alpha$ -p30 induces AML <i>in vivo</i> .....	116
3.3.3	Trib2 degrades p42, but not p30, via K48 mediated ubiquitination	125
3.3.4	Degradation of p42 is the key driver of TRIB2-induced AML .....	133
3.4	Discussion .....	147
<b>4</b>	<b>Results: Identifying the TRIB2 leukaemia initiating cell.....</b>	<b>152</b>
4.1	Introduction .....	153
4.1.1	Modelling tumour development .....	153
4.1.1.1	The stochastic model .....	153
4.1.1.2	The cancer stem cell model.....	154
4.1.2	Leukaemia stem cell heterogeneity and plasticity .....	156

4.1.3	The leukaemia initiating cell .....	158
4.1.3.1	MLL rearranged AML.....	159
4.1.3.1.1	MLL-ENL .....	159
4.1.3.1.2	MLL-GAS7.....	160
4.1.3.1.3	MLL-AF9.....	160
4.1.3.2	AML fusion proteins from other common chromosomal rearrangements.....	161
4.1.3.2.1	MOZ-TIF2 and BCR-ABL.....	161
4.1.3.2.2	CALM/AF10 .....	161
4.1.3.2.3	DEK/CAN.....	162
4.1.3.2.4	PML-RAR $\alpha$ .....	162
4.1.3.2.5	NUP98/HOXA9 .....	163
4.1.3.2.6	MN1.....	163
4.1.3.3	C/EBP $\alpha$ .....	164
4.2	Aims and Objectives.....	167
4.3	Results.....	168
4.3.1	<i>Trib2</i> can transform all cell populations <i>in vitro</i> .....	168
4.3.2	<i>Trib2</i> generates leukaemia <i>in vivo</i> with different latencies from the HSC and GMP, but not the MPP or CMP .....	178
4.3.3	TRIB2 propagates phenotypically different diseases from the HSC and GMP	186
4.3.4	Loss of <i>Trib2</i> does not perturb bone marrow hematopoiesis <i>in vivo</i>	195
4.4	Discussion .....	205
<b>5</b>	<b>Results: NFIX expression critically modulates early B lymphopoiesis and myelopoiesis.....</b>	<b>212</b>
5.1	Introduction .....	213
5.1.1	Nuclear factor one (NFI).....	213
5.1.2	Structure of NFI.....	213
5.1.3	NFI proteins in hematopoiesis .....	214
5.1.3.1	NFIA.....	214
5.1.3.2	NFIB.....	215
5.1.3.3	NFIC.....	216
5.1.3.4	NFIX.....	216
5.2	Aims and Objectives.....	217
5.3	Results.....	218

5.3.1	NFIX overexpression favours myelopoiesis over B cell lymphopoiesis <i>in vivo</i>	218
5.3.2	NFIX expression decreases during B cell development.....	224
5.3.3	NFIX expression favours myelopoiesis over B cell lymphopoiesis...	229
5.3.4	Loss of <i>Nfix</i> expression promotes B lymphopoiesis while impairing myelopoiesis .....	242
5.4	Discussion .....	251
<b>6</b>	<b>General discussion .....</b>	<b>257</b>
<b>7</b>	<b>References .....</b>	<b>260</b>
<b>8</b>	<b>Publications .....</b>	<b>275</b>

## List of tables

Table 2. 1 -Suppliers .....	90
Table 2. 2 -Recipes.....	92
Table 2. 3 -DNA primer sequences.....	94
Table 2. 4 -Flow cytometry antibodies.....	96
Table 2. 5 -Western blot antibodies .....	97

## List of figures

Figure 1. 1 - Diagram of the hierarchical arrangement of the hematopoietic system.....	25
Figure 1. 2 - Flow cytometric gating strategy used to identify murine HSPCs. ..	27
Figure 1. 3 - Schematic representation of myeloid differentiation from the HSC	29
Figure 1. 4 - Schematic diagram of the structure of C/EBP $\alpha$ .....	31
Figure 1. 5 - Schematic representation of the stages of B cell development ....	35
Figure 1. 6 - Diagram of T cell development in the BM and thymus .....	37
Figure 1. 7 - Schematic diagram of the Trib family .....	49
Figure 1. 8 - Diagram depicting Trib2 mediated degradation of p42, and p30 driven positive feedback loop of E2F1 regulation of Trib2 expression .....	54
Figure 2. 1 - Plasmid map of retroviral expression vector MigR1.....	61
Figure 2. 2- Overview of retroviral production and titration process .....	67
Figure 2. 3 - Schematic depiction of CFU assay.....	70
Figure 2. 4 - Diagram depicting OP9 co-culture system used to differentiate B cells .....	72
Figure 2. 5 - Schematic diagram depicting MACS cell sorting.....	74
Figure 2. 6 - Experimental outline of a primary and secondary BMT. ....	76
Figure 2. 7 - Schematic depiction of the generation of <i>Cebpa<sup>fl/f</sup></i> , <i>Cebpa<sup><math>\Delta/\Delta</math></sup></i> , <i>Cebpa<sup>fl/+</sup></i> , <i>Cebpa<sup>fl/p30</sup></i> and <i>Cebpa<sup><math>\Delta/p30</math></sup></i> mice .....	79
Figure 2. 8 - Gating strategy for detecting stages of apoptosis using flow cytometry.....	81
Figure 2. 9 - Diagram of the gel/membrane transfer sandwich .....	84
Figure 2. 10 - Diagram of the process of ubiquitination .....	85
Figure 2. 11 - Fluidigm <sup>TM</sup> 48.48 Dynamic Array .....	89
Figure 3. 1 - BMT model to determine the effect of p30 overexpression on hematopoiesis.....	111
Figure 3. 2 - Analysis of GFP expression in MigR1 and p30 transplanted mice ..	112
Figure 3. 3 - Overexpression of p30 enhances myelopoiesis <i>in vivo</i> . ....	113
Figure 3. 4 - Overexpression of p30 results in a decrease in mature B cells <i>in vivo</i> . ....	114
Figure 3. 5 - The effect of p30 overexpression on CD4 and CD8 expression <i>in vivo</i> . ....	115
Figure 3. 6 - Overexpression of p30 induces leukaemia <i>in vivo</i> .....	118
Figure 3. 7 - Analysis of p30 leukemic mice .....	119
Figure 3. 8 - Flow cytometric analysis of GFP clones of M1 leukemic BM cells .	120
Figure 3. 9 - Flow cytometric analysis of GFP clones of M2 leukemic BM cells .	121
Figure 3. 10 - Schematic overview of secondary and tertiary p30 overexpression transplants .....	122
Figure 3. 11 - M2 but not M1 transplanted cells induce AML in secondary recipients.....	123

Figure 3. 12 - Flow cytometric analysis of BM of p30 (M2) secondary leukaemia. .....	124
Figure 3. 13 - Analysis of TRIB2 mediated ubiquitination of C/EBP $\alpha$ .....	128
Figure 3. 14 - Degradation of p42 by TRIB2 can be targeted by Bortezomib induced proteasome inhibition in leukaemia cell lines. ....	129
Figure 3. 15 - Analysis of TRIB2 mediated ubiquitination of C/EBP $\alpha$ isoforms p42 and p30 .....	130
Figure 3. 16 - Analysis of TRIB2 mediated ubiquitination of K313R mutant .....	131
Figure 3. 17 - C/EBP $\alpha$ mutant K313R retains transcriptional and differentiation activity.....	132
Figure 3. 18 - C/EBP $\alpha$ is required for TRIB2 mediated AML induction .....	136
Figure 3. 19 - Schematic overview of BM transplantation experiment .....	137
Figure 3. 20 - Schematic overview of predicted outcomes of bone marrow transplant experiment.....	138
Figure 3. 21 - Engraftment of donor cells in recipient mice. ....	139
Figure 3. 22 - Analysis of GFP expression in CD45.2 <sup>+</sup> cells in the PB over time .	140
Figure 3. 23 - Analysis of PB cells and spleen weights in control groups.....	141
Figure 3. 24 - Flow cytometric analysis of tissues from control mice .....	142
Figure 3. 25 - Survival curve of <i>Cebpa</i> <sup>fl/+</sup> and <i>Cebpa</i> <sup>fl/p30</sup> transplanted mice ....	143
Figure 3. 26 - Survival curve of <i>Cebpa</i> <sup><math>\Delta</math>/p30</sup> transplanted mice .....	144
Figure 3. 27 - Expression of cKit in BM cells of transplanted mice.....	145
Figure 3. 28 - Western blot analysis of C/EBP $\alpha$ expression in BM cells from transplant cohorts.....	146
Figure 4. 1- Schematic diagram of the stochastic and cancer stem cell models of tumour development.....	154
Figure 4. 2 - Schematic representation of CD34 and CD38 expression on human stem and progenitor cells .....	156
Figure 4. 3 - Schematic overview of CFU experiment used to identify the leukaemia initiating cell.....	170
Figure 4. 4 - TRIB2 transforms stem and progenitor populations <i>in vitro</i> with different efficiencies .....	171
Figure 4. 5 - Colony size and type differs between TRIB2 transformed stem and progenitor groups.....	172
Figure 4. 6 - Cellular morphology of TRIB2 transformed stem and progenitor cells .....	173
Figure 4. 7 - Comparison of CD11b and Gr1 expression in transformed stem and progenitor cells from P3, 4 and P5.....	174
Figure 4. 8 - Comparison of cKit expression in transformed stem and progenitor cells from P3, 4 and P5 .....	175
Figure 4. 9 - Differential expression of mature myeloid markers in cKit <sup>+</sup> and cKit <sup>-</sup> populations of transformed stem and progenitor cells at P3 .....	176
Figure 4. 10- Differential expression of mature myeloid markers in cKit <sup>+</sup> and cKit <sup>-</sup> populations of transformed stem and progenitor cells at P5.....	177
Figure 4. 11 - Schematic overview of transplantation model used to identify the TRIB2 leukaemia initiating cell.....	180

Figure 4. 12 - Varying engraftment levels in TRIB2 LIC transplanted mice .....	181
Figure 4. 13 - Normal hematopoiesis in mice that failed to engraft transplanted cells .....	182
Figure 4. 14 - No BM or splenic engraftment of donor cells at 16 weeks in mice failing to display peripheral engraftment at 7 weeks post BMT .....	183
Figure 4. 15 - TRIB2 generates leukaemia from the HSC and GMP with different latencies, but not the MPP or CMP.....	184
Figure 4. 16 - HSC and CMP transplanted mice that engrafted the donor cells, but did not succumb to disease displayed normal hematopoiesis after 1 year .....	185
Figure 4. 17 - Physically distinct diseases arose from the TRIB2 transformed HSC and GMP.....	188
Figure 4. 18 - TRIB2 generates phenotypically different diseases from the HSC and GMP.....	189
Figure 4. 19 - HSC and GMP derived leukemic cells infiltrate the spleen and peripheral blood .....	190
Figure 4. 20 - Absolute frequency of BM and PB CD11b <sup>+</sup> Gr1 <sup>+</sup> in leukemic mice .	191
Figure 4. 21 - Distinct B cell surface marker expression patterns on HSC derived leukemic cells compared with GMP derived leukemic cells.....	192
Figure 4. 22 - Aberrant T cell surface marker expression patterns on HSC derived leukemic cells compared with GMP derived leukemic cells.....	193
Figure 4. 23 - Differential myeloid cell surface marker expression patterns on HSC and GMP derived leukemic cells .....	194
Figure 4. 24 - Normal levels of circulating leukocytes in <i>Trib2</i> <sup>-/-</sup> mice.....	197
Figure 4. 25 - Normal distribution of splenic leukocytes in <i>Trib2</i> <sup>-/-</sup> mice .....	198
Figure 4. 26 - Normal BM hematopoiesis in <i>Trib2</i> <sup>-/-</sup> mice.....	199
Figure 4. 27 - Normal BM erythropoiesis in <i>Trib2</i> <sup>-/-</sup> mice .....	200
Figure 4. 28 - Normal distribution of stem and progenitor cells in <i>Trib2</i> <sup>-/-</sup> mouse .....	201
Figure 4. 29 - Normal distribution of myeloid progenitor cells in <i>Trib2</i> <sup>-/-</sup> BM ...	202
Figure 4. 30 - Absence of <i>Trib2</i> does not impair BM colony forming ability .....	203
Figure 4. 31 - No differences in the expression of mature myeloid markers on cells from P1 WT and <i>Trib2</i> <sup>-/-</sup> colonies .....	204
<b>Figure 5. 1 - Generalised structure of <i>NFI</i> genes.....</b>	<b>214</b>
Figure 5. 2 - NFIX overexpression results in decreased B220 and CD19 expression in the PB. ....	219
Figure 5. 3 - NFIX overexpression does not affect T cell maturation <i>in vivo</i> . ...	220
Figure 5. 4 - NFIX overexpression results in a higher percentage of peripheral myeloid cells <i>in vivo</i> . ....	221
Figure 5. 5 - Disrupted hematopoiesis in the BM of NFIX mice. ....	222
Figure 5. 6 - Disrupted hematopoiesis in the spleen of NFIX mice. ....	223
Figure 5. 7 - Gene expression in murine B cell progenitor populations. ....	226
Figure 5. 8 - <i>NFIX</i> expression in stem and progenitor populations. ....	227
Figure 5. 9 - NFIX overexpression results in a block at the pro-B cell stage of B cell differentiation. ....	228

Figure 5. 10 - NFIX blocks B cell differentiation <i>in vitro</i> in favour of myelopoiesis. .....	232
Figure 5. 11 - NFIX blocks B cell differentiation from the HSPC.....	233
Figure 5. 12 - Gene expression analysis of NFIX expressing BM relative to MigR1 control. ....	234
Figure 5. 13 - Ectopic NFIX expression does not affect BA/F3 cell growth. ....	235
Figure 5. 14 - Ectopic NFIX expression does not affect BA/F3 cell viability. ....	236
Figure 5. 15 - NFIX enhances myeloid differentiation <i>in vitro</i> .....	237
Figure 5. 16 - Differentiation of myeloid progenitor populations by NFIX <i>in vitro</i> . .....	238
Figure 5. 17 - NFIX promotes differentiation of 32D cells in the presence of IL-3. .....	239
Figure 5. 18 - NFIX enhances 32D cell differentiation in the presence of G-CSF. .....	240
Figure 5. 19 - Gene expression changes in NFIX expressing cells.....	241
Figure 5. 20 - <i>Nfix</i> expression in fetal and adult HSC and HSPC.....	244
Figure 5. 21 - <i>Nfix</i> <sup>-/-</sup> FLCs do not display abnormal hematopoiesis. ....	245
Figure 5. 22 - Loss of <i>Nfix</i> in the FLC does not affect myeloid differentiation <i>in vitro</i> . .....	246
Figure 5. 23 - <i>Nfix</i> <sup>-/-</sup> neonatal (P10) BM does not display abnormal hematopoiesis. ....	247
Figure 5. 24 Loss of <i>Nfix</i> disrupts myeloid differentiation <i>in vitro</i> .....	248
Figure 5. 25- Loss of <i>Nfix</i> enhances B cell differentiation in neonatal BM <i>in vitro</i> .....	249
Figure 5. 26 - Gene expression analysis of WT and <i>Nfix</i> <sup>-/-</sup> BM. ....	250

## Acknowledgements

First and foremost, I would like to thank my supervisor, Dr. Karen Keeshan, for all of her help and support since I joined her lab in 2008. You've been a role model for me personally and professionally, thank you for everything! I would also like to thank my co-supervisor Dr. Alison Michie for her help and advice throughout my time in POG-LRC. I'm very lucky and thankful to have had great colleagues, now friends, during my PhD with special mention to (almost Dr.) Joana Campos and (almost Dr.) Kai Ling Liang, as well as all of the Keeshan lab members past and present in particular Shahzya, Mara and Jenny, and everyone past and present at POG-LRC in particular Chris, Susan and Leena. I do and will miss the camaraderie, support and fun we had - POG-LRC was such a collegiate work environment, and ye all made those unsociable hours very sociable! I am also indebted to several people in POG-LRC for their technical support in particular Karen Dunn and Jen Cassels, two very helpful, patient and talented ladies. A special mention to Michelle Bradley, Michelle you made me feel so welcome from day one, and made me laugh every day after that! Thanks to Trish Collins for the late night science chats, my go-to UB guru and the best roomie a girl could ask for!

I would like to thank the University of Glasgow, the Children's Leukaemia Research Project and Leukaemia & Lymphoma Research (Bloodwise) for supporting this work.

Finally, and most importantly, I would like to thank my friends and family. Thanks in particular to Ellen, Elaine, Denise, Aoife, Helen, and Karen, ye're friendship and support means the world to me, and a special thanks to Niall - Drew I'll miss my wee office!

To Mam and Dad, ye are fantastic parents who have always made me feel loved, safe and supported. Thank you both for everything. To my sister (almost Dr.) Siobhan, Shiv girl thank you! Without your support over the last few years I wouldn't have gotten here at all. I can't wait to celebrate your graduation soon!

This thesis is dedicated to the wonderful life of my brother Liam who was, is and will continue to be an inspiration to me.

## Author's declaration

I declare that, except where explicit reference is made to the contribution of others, this dissertation is the result of my own work and has not been submitted for any other degree at the University of Glasgow or any other institution.

Signed name: 

Printed name: CAITRIONA O'CONNOR

## Abbreviations

5-FU	5-Fluorouracil
$\alpha^{-/-}$	C/EBP $\alpha^{-/-}$
ABL	Acute biphenotypic leukaemia
ACC	Acetyl-coenzyme A carboxylase
AcLDL	Acetylated low-density lipoprotein
ADCC	Antibody-dependent cellular cytotoxicity
AGM	Aorta-gonad-mesonephros
ALL	Acute lymphoblastic leukaemia
AML	Acute myeloid leukaemia
AML1	Acute myeloid leukaemia 1 protein
APL	Acute promyelocytic leukaemia
APS	Ammonium persulfate
ASPA	Animals Scientific Procedures Act
ATF4	Activating transcription factor 4
ATP	Adenosine triphosphate
BA	Basophils
B-ALL	B cell acute lymphoblastic leukaemia
BCR	B cell receptor
BHK-MKL	Baby hamster kidney - murine kit ligand
BM	Bone marrow
BME	2-mercaptoethanol
BMT	Bone marrow transplant
bp	Base pair
bZIP	Basic-leucine zipper
C/EBP	CCAAT-enhancer binding protein
CBF-AML	Core binding factor AML
CBFB/MYH11	Core binding factor beta/myosin heavy chain 11
CFU	Colony forming unit
ChIP	Chromatin immunoprecipitation
CLP	Common lymphoid progenitor
CML	Chronic myeloid leukaemia
CMP	Common myeloid progenitor
CN	Cytogenetically normal
CO-IP	Co-immunoprecipitation
COP1	Constitutive photomorphogenic 1
CRC	Colorectal cancer
CSC	Cancer stem cell
CSF	Colony-stimulating factor

CSF3R	Colony stimulating factor 3 receptor
CSFR1	Macrophage colony-stimulating factor
CSL	CBF1/Suppressor of Hairless/LAG-1
CTF	CCAAT-binding transcription factor
CTV	CellTrace™ Violet
CXCL12	Stromal cell-derived factor-1
CXCR4	C-X-C chemokine receptor type 4
D	Aspartic acid
ddH2O	Double distilled water
DMEM	Dulbecco's modified Eagles medium
DN	Double negative
DNMT3A	DNA (cytosine-5)-methyltransferase 3A
DP	Double positive
E	Embryonic day
E2A	E box binding protein 2A
EBF1	Early B cell factor-1
ECD	Extracellular domain
EMSA	Electrophoretic mobility shift assay
EO	Eosinophil
EPO	Erythropoietin
ER	Estradiol
ERK	Extracellular signal-regulated protein kinase
EtOH	Ethanol
ETP	Early thymocyte progenitor
Exol	Exonuclease I
FAB	French-American British
FACS	Fluorescence-activated cell sorting
FBS	Fetal Bovine Serum
FL	Fetal liver
FLC	Fetal liver cell
FLT3	FMS-like tyrosine kinase 3
FOG1	Friends of GATA 1
FOX	Forkhead box proteins
G-CSF	Granulocyte colony-stimulating factor
GCSFR	Granulocyte colony-stimulating factor receptor
GEMM	Granulocyte/erythroid/macrophage/megakaryocyte
GFP	Green fluorescent protein
GM	Granulocyte/macrophage
GM-CSF	Granulocyte/macrophage colony-stimulating factor
GMCSFR	Granulocyte/macrophage colony-stimulating factor receptor

GMP	Granulocyte/macrophage progenitor
Gy	Grays
H	Histidine
H3K4	Histone H3 Lysine 4
Hb	Hemoglobin
HBSS	Hank's balanced salt solution
HCT	Hematocrit
HD	Heterodimerization domain
HOX	Homeodomain-containing transcription factor
HPC	Hematopoietic progenitor cells
HRP	Horseradish-peroxidase
Hrs	Hours
HSC	Hematopoietic stem cell
HSPC	Hematopoietic stem and progenitor cell
ICD	Intracellular domain
ICN	Intracellular Notch
IDH	Isocitrate dehydrogenase
IFC	Integrated fluidic circuit
Ig	Immunoglobulin
IGF1	Insulin-like growth factor
IL-3	Multi-CSF or Interleukin-3
IL-7	Interleukin 7
IL7R	Interleukin-7 receptor
IL-8	Interleukin-8
IMDM	Iscove's modified Dulbecco's medium
inv	Inversion
IP	Intraperitoneal
IPTG	Isopropyl $\beta$ -D-1-thiogalactopyranoside
IRES	Internal ribosome entry site
ITD	Internal tandem duplication
IV	Intravenous
JNK	c-Jun N-terminal Kinase
K	Lysine
kD	Kilodalton
KLF4	Kruppel-like Factor 4
KO	Knock out
L	Leucine
L-Glut	L-Glutamine
LIC	Leukaemia initiating cell
Lin	Lineage

LK	Lineage <sup>-</sup> cKit <sup>+</sup>
LMPP	Lymphoid-primed multipotent progenitor
LPS	Lipopolysaccharide
LSC	Leukaemia stem cell
LSK	Lineage <sup>-</sup> cKit <sup>+</sup> Sca1 <sup>+</sup>
LT-HSC	Long-term hematopoietic stem cell
LY	Lymphocyte
MACS	Magnetic-activated cell sorting
MAPK	Mitogen-activated protein kinases
MAPKK	MAPK kinase
MAPKKK	MAPK kinase kinase
M-CSF	Macrophage colony-stimulating factor
MCSFR	Macrophage colony-stimulating factor receptor
MDS	Myelodysplastic syndrome
MEIS	Myeloid ecotropic insertion site
MEK1	MAPK/extracellular-signal regulated kinase-1
MEP	Megakaryocyte/erythrocyte progenitor
Mins	Minutes
MkE	Megakaryocyte-erythroid
MKK	MAPK kinase
MLL	Mixed-lineage leukaemia
MMP9	Metalloprotease 9
MO	Monocyte
MPP	Multipotent progenitor
MPV	Mean platelet volume
N	Asparagine
Na3V04	Sodium Orthovanadate
NaF	Sodium fluoride
ND13	NUP98-HOXD13
NE	Neutrophil
NEM	N-Ethylmaleimide
NES	Nuclear export signal
NFI	Nuclear factor one
NK	Natural killer
NOD/SCID	Non-obese diabetic/severe combined immune-deficient
NPM1	Nucleophosmin
NSCLC	Non-small cell lung cancers
NSG	NOD/SCID/IL2R $\gamma$ <sup>null</sup>
ORF	Open reading frame
P	Plating

p30	C/EBP $\alpha$ - p30
p42	C/EBP $\alpha$ - p42
PB	Peripheral blood
PBS	Phosphate-buffered saline
PBS-t	PBS-tween
PBX	Pre-B-cell leukaemia
PEST	Region rich in proline, glutamic acid, serine and threonine
PHMA	pcDNA3.1-myc-HIS
PI3K	Phosphatidylinositol 3-kinase
PIN1	Peptidyl-prolyl cis/trans isomerase
PLT	Platelet
PML	Promyelocytic gene
PMSF	Phenylmethylsulfonyl fluoride
Poly I:C	Polyinosinic-polycytidylic acid
PS	Penicillin/Streptomycin
PU.1	Purine box factor 1
PV	Polycythaemia vera
R	Arginine
RA	All-trans retinoic acid
RAR $\alpha$	Retinoic acid receptor alpha
RBC	Red blood cell
rh	Recombinant human
rm	Recombinant murine
RT	Room temperature
RUNX1	Runt-related transcription factor 1
S	Serine
Sca-1	Stem cell antigen-1
SCF	Stem cell factor
SD	Standard deviation
SDS-PAGE	Sodium dodecyl sulphate-polyacrilamide gel electrophoresis
sec	Second
SFM	Serum free media
shRNA	Short hairpin RNA
SIRP1 $\alpha$	Signal regulatory protein 1 $\alpha$
SP	Single positive
STAT	Signal transducer and activator of transcription
ST-HSC	Short-term hematopoietic stem cell
SUMO	Small ubiquitin-like modifier
SWI/SNK	Switch/Sucrose Non-Fermentable
t	Translocation
TAD	Transactivation domain

T-ALL	T cell acute lymphoblastic leukaemia
TCF	T cell factor
TCR	T cell receptor
TEMED	Tetramethylethylenediamine
TET2	Tet methylcytosine dioxygenase 2
TIM3	T-cell Ig mucin-3
TKD	Tyrosine kinase domain
TLR	Toll-like receptor
TPO	Thrombopoietin
Ub	Ubiquitin
UBC9	Ubiquitin conjugating enzyme
UCA1	Urothelial carcinoma associated 1
VSVG	pCMV-VSV-G
WBC	White blood cell
WDR5	WD repeat-containing protein 5
WHO	World Health Organisation
WNT	Wingless-type MMTV integration site
WT	Wild-type

# 1 Introduction

## 1.1 Hematopoiesis

The term hematopoiesis describes the formation of all of the components of our blood system from a small pool of hematopoietic stem cells (HSCs). Prior to the 1960's it was known that our blood cells had a short lifespan, but the source of their constant turnover was not discovered until a seminal paper by Till & McCulloch (Till and McCulloch, 1961). Murine bone marrow (BM) cells were injected into irradiated mice and the formation of large hematopoietic colonies was observed in the recipient spleens. These colonies were formed from a single initiating cell, and the daughter cells could produce different hematopoietic lineages. This discovery provided the first evidence for HSCs with the defining characteristics of self-renewal and multi-potency. Since then, HSCs and hematopoiesis have been extensively studied.

Fetal hematopoiesis occurs in sequential steps arising from several sites, beginning with primitive erythropoiesis in the yolk sac at embryonic day (E) 7.5, followed by the aorta-gonad-mesonephros (AGM) where the first HSCs can be detected at E11 (Dzierzak and Speck, 2008). These areas are succeeded by the fetal liver (FL) and spleen, with hematopoiesis moving to the thymus and finally the BM where definitive post-natal hematopoiesis is established. Fetal HSCs rapidly divide and expand while adult HSCs rarely divide with most remaining in a quiescent phase. In the adult, HSCs reside in the hypoxic niche of BM cavities and are capable of long-term self-renewal, as well as terminal differentiation into cells of the myeloid, lymphoid and erythroid lineages. Because differentiated cells are relatively short lived, HSCs are responsible for the generation of millions of new blood cells every day in order to satisfy the life-long demands of the blood system. Various secreted growth factors and cytokines maintain a healthy growing environment for these self-renewing stem cells. They also turn on signal transduction pathways which alter a host of lineage specific transcription factors that are ultimately responsible for the cell fate decisions that drive differentiation.

### 1.1.1 Hematopoietic hierarchy

The hematopoietic system is hierarchically arranged with a small population of multipotent hematopoietic stem and progenitor cells (HSPCs) lying at the apex of this hierarchy. During cell division the daughter cells of a HSC may either, remain a HSC (self-renewal), commit along a path of differentiation, or go through apoptosis. The HSC compartment contains cells termed long-term HSCs (LT-HSCs) which provide life-long renewal and short-term HSCs (ST-HSC) with limited repopulating activity (~8 weeks). With each step towards maturation, the cells lose self-renewal capacity and become more restricted within a given lineage branch. Multipotent HSPCs give rise to more restricted oligopotent progenitor cells which subsequently produce lineage restricted progenitor cells that will terminally differentiate into mature effector cells. HSCs which enter differentiation, first give rise to multipotent progenitor cells (MPPs) that lack self-renewal capacity but retain multi-lineage potential. Multi-colour flow cytometry has been used in combination with murine transplant studies to identify and characterise functional stem and progenitor cell populations in the mouse and human. HSC and MPP activities have been shown to reside in a small population of BM cells which lack lineage markers found on mature blood cells, and also express a receptor for the cytokine stem cell factor (SCF) called cKit, as well as stem cell antigen-1 (Sca-1). This population of cells are termed Lin<sup>-</sup>Sca-1<sup>+</sup>cKit<sup>+</sup> or LSKs (Weissman et al., 2001). A description of the identification of stem and progenitor populations based on cell surface markers is provided in 1.1.2.

Our understanding of the hierarchical arrangement of the hematopoietic system is constantly being challenged by new approaches, technologies and hypotheses. It had been thought that following the emergence of the MPP from the HSC, a myeloid/lymphoid branching occurs with the emergence of either the oligopotent common lymphoid progenitor (CLP) or common myeloid progenitor (CMP). The CLP will generate cells of lymphoid origin - B, T and NK cells. The CMP produces further and more restricted oligopotent precursors in the granulocyte macrophage progenitor (GMP) which gives rise to granulocytes and macrophages, or the megakaryocyte/erythrocyte progenitor (MEP) which gives rise to erythrocytes and platelets. The origin of dendritic cells, which is not fully understood, was suggested to be both from the CMP and the CLP. However, in

recent years this pyramidal model has been challenged and persuasive evidence has emerged suggesting that the MPP first differentiates into a lymphoid primed multipotent progenitor (LMPP) which has lymphoid and granulocyte-macrophage (GM) potential but lacks megakaryocyte-erythroid (MkE) potential, and another progenitor with MkE potential (Adolfsson et al., 2005, Arinobu et al., 2007). Indeed the putative LMPP compartment has also been suggested to have strong dendritic cell potential (Naik et al., 2013). Contrasting studies indicate that MkE progenitors may diverge from the MPP before the CMP/CLP branch-point (Pronk et al., 2007) and it was subsequently demonstrated that MkE progenitors may be derived directly from the HSC (Yamamoto et al., 2013). More recently a “two-tier” hierarchy was proposed by John Dick and colleagues whereby in the adult hematopoietic system the top tier is composed of multipotent HSCs and MPPs and these cells give rise to a bottom tier of unipotent progenitors, with the megakaryocyte lineage progenitor (MkP) residing closer to the top tier (Notta et al., 2015). The pyramidal, LMPP and two-tier model are depicted in Figure 1. 1.

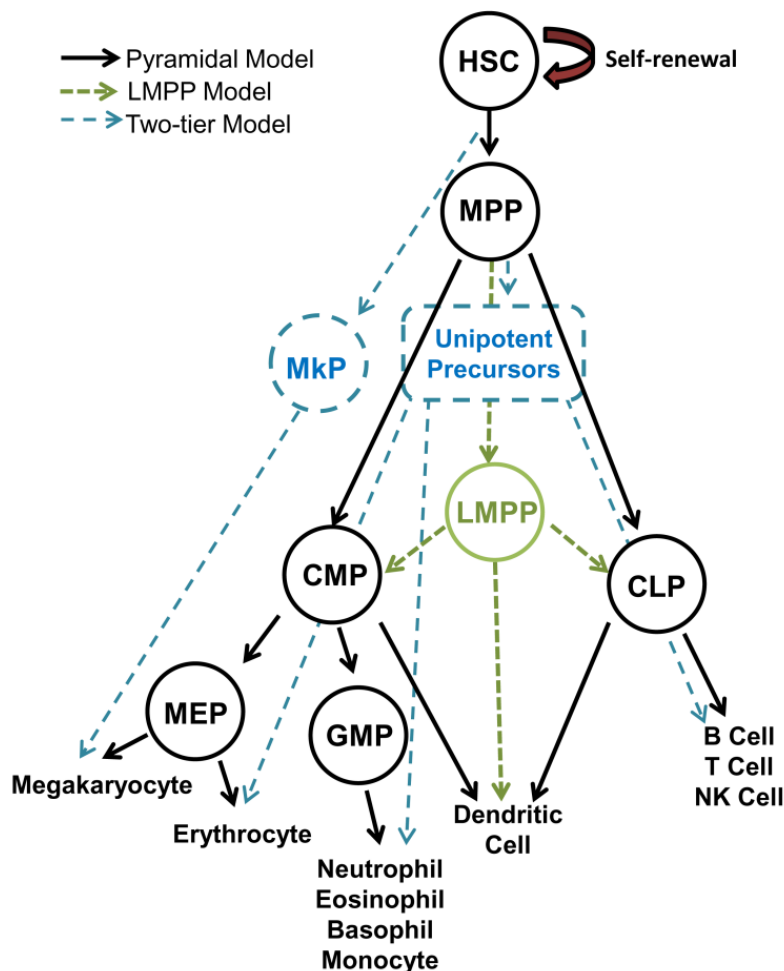


Figure 1. 1 – Diagram of the hierarchical arrangement of the hematopoietic system.

### 1.1.2 Identification of stem and progenitor populations

Using multicolour flow cytometry and murine BMT, functional stem and progenitor cells have been identified and characterised. In order for a cell to be classified as a bona fide HSC, it must be able to provide long-term reconstitution of the entire hematopoietic system when transplanted into lethally irradiated recipient mice. As outlined in 1.1.1, HSC and MPP populations reside in the LSK fraction of adult BM which comprises approximately 0.1% of total BM cells. The cKit receptor, also known as CD117, whose ligand is stem cell factor (SCF), is highly expressed on early hematopoietic stem and progenitor cells and its expression decreases as cells differentiate. Sca-1 is almost exclusively expressed on HSCs and MPPs and so can be used in conjunction with lineage markers and cKit to distinguish them (LSK compartment) from myeloid progenitor populations (CMP, GMP and MEP) which reside in the Lin<sup>-</sup>Sca-1<sup>-</sup>cKit<sup>+</sup> (LK) fraction. There are 2 main systems for sub-classifying the LSK population into functional groups - use of Thy-1.1 (also known as CD90) and Flk-2 (also known as FMS-like tyrosine kinase 3 or Flt3), and use of the SLAM family of molecules. Thy-1.1 (also known as CD90) is a cell surface glycoprotein expressed on HSCs but absent from more committed cells (Christensen and Weissman, 2001). Flt3, a cytokine receptor for the Flt3 ligand, is expressed on progenitor populations (MPP, CLP) but not HSCs. Using this system the loss of Thy-1.1 and gain of Flt3 expression signifies HSC maturation and loss of self-renewal. Therefore functional LT-HSCs reside in the Lin<sup>-</sup>Sca-1<sup>+</sup>cKit<sup>+</sup>Thy<sup>lo</sup>Flt3<sup>-</sup> population while ST-HSCs are contained within the Lin<sup>-</sup>Sca-1<sup>+</sup>cKit<sup>+</sup>Thy<sup>lo</sup>Flt3<sup>+</sup> population, with MPP cells shown to be Lin<sup>-</sup>Sca-1<sup>+</sup>cKit<sup>+</sup>Thy<sup>lo</sup>Flt3<sup>+</sup>.

The SLAM family of molecules, including CD150 (Slamf1) and CD48 (Slamf2), are used to segregate the LSK compartment into HSCs, MPPs and more restricted hematopoietic progenitors (HPC-1 and HPC-2) (Oguro et al., 2013). As CD150 expression decreases cells lose self-renewal ability i.e. functional HSCs express CD150 while MPPs are CD150<sup>-</sup>. CD48 expression increases as cells lose self-renewal activity thus HSCs and MPPs are CD48<sup>-</sup> while HPC-1 and HPC-2 cells express CD48. The HPC-1 population (CD150<sup>-</sup>), which comprise approximately 67% of LSKs, were shown to contain Flt3<sup>+</sup> LSKs with myeloid and lymphoid potential, akin to an LMPP. HPC-2 cells, the smallest fraction at just 2% of LSKs, possessed a more myeloerythroid/megakaryocyte potential. It is worth noting



damaged cells and invading pathogens. Myeloid cells can be detected by flow cytometry in the murine system where neutrophils express high levels of the GPI-anchored protein Gr1 as well as the integrin CD11b (also known as Mac-1), while eosinophils express intermediate levels of Gr1. Cells of the monocyte and macrophage lineage express CD11b and the adhesion G protein-coupled receptor F4/80, while erythroid cells are routinely detected with antibodies against TER119. Myeloid differentiation occurs initially in the BM with terminal differentiation occurring in the blood or peripheral tissues.

### 1.1.3.1 Cytokines in myeloid differentiation

An extensive family of cytokines regulate myelopoiesis and influence lineage choices of stem and progenitor cells including colony-stimulating factors (CSFs), IL-6, erythropoietin (EPO) and thrombopoietin (TPO) (Figure 1. 3). The CSF family consists of macrophage-CSF (M-CSF), granulocyte-CSF (G-CSF), granulocyte/macrophage-CSF (GM-CSF) and multi-CSF (Interleukin-3 or IL-3). The effects of M-CSF, which is synthesised by many cell types including endothelial and BM stromal cells, are mediated via the M-CSF receptor (MCSFR) which is primarily expressed on macrophages (Barreda et al., 2004). It promotes the proliferation, differentiation and survival of progenitor cells as they differentiate into macrophages. G-CSF is essential for the differentiation and survival of neutrophils. It is primarily produced by monocytes and macrophages and the G-CSF receptor (GCSFR) is expressed in immature and mature neutrophils. GCSFR expression is regulated by the key myeloid transcription factors CCAAT-enhancer binding protein  $\alpha$  (C/EBP $\alpha$ ) and Purine box factor 1 (PU.1) (Smith et al., 1996). *Gcsf*<sup>-/-</sup> mice exhibit neutropenia with defects in myeloid progenitor cells (Liongue et al., 2009) and administration of G-CSF is widely used to treat neutropenia in humans as it stimulates production and survival of neutrophils. GM-CSF mediates proliferation and differentiation of the macrophage and neutrophil lineages and functionally overlaps with M-CSF, G-CSF and IL-3. As with G-CSF, GM-CSF is regulated by C/EBP $\alpha$  and PU.1 (Hohaus et al., 1995), and is also used to therapeutically treat neutropenia caused by chemotherapy. Similar to GM-CSF, IL-3 is an early acting cytokine. It works with GM-CSF, IL-6 and EPO to stimulate multipotent stem and progenitor cells to differentiate into all of the myeloid lineages. IL-6 has been shown to synergise with IL-3 to promote proliferation of murine HSPCs *in vitro* (Heike and Nakahata,

2002) and IL-3 is commonly used in conjunction with IL-6 and SCF in *in vitro* assays to stimulate proliferation and survival of HSPCs. EPO is essential for definitive erythropoiesis while TPO is the main stimulatory cytokine involved in megakaryocytic commitment (Metcalf, 2008).

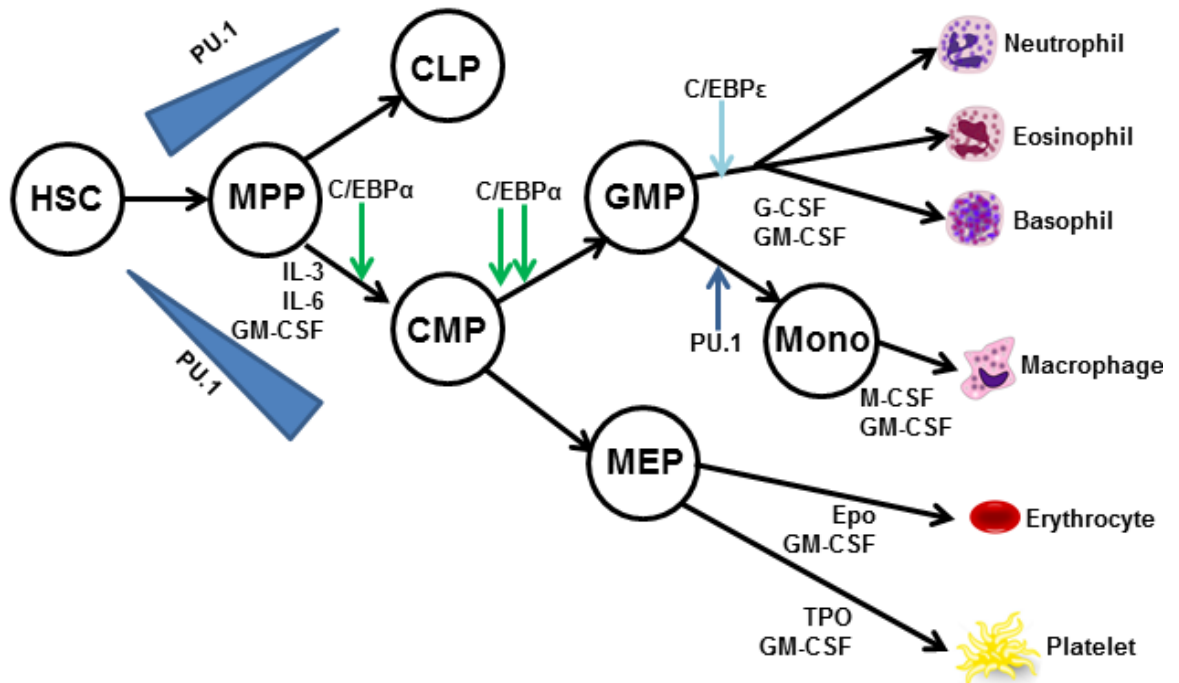


Figure 1. 3 – Schematic representation of myeloid differentiation from the HSC

### 1.1.3.2 Transcription factors in myeloid differentiation

The lineage decisions of stem and progenitor cells to differentiate in the myeloid lineage are directed by the action of a variety of lineage specific transcription factors including PU.1, and members of the GATA family and C/EBP family (Figure 1. 3). PU.1, the protein encoded by the *SPI1* gene, is an ETS-domain transcription factor essential for hematopoiesis. *Spi1*<sup>-/-</sup> mice are embryonic lethal with a complete absence of macrophages and B cells (Scott et al., 1994), and loss of PU.1 in the HSC impairs its repopulating ability (Dakic et al., 2005). PU.1 mediates the formation of CMPs and CLPs from the HSC. HSCs lacking *Pu1* fail to generate early myeloid and lymphoid precursors (Iwasaki et al., 2005). *Pu1* is highly expressed in mature myeloid cells and is also detectable in the HSC, MPP, CMP, CLP and B cells. While *Pu1* expression is downregulated during T cell and erythroid differentiation, the amount of PU.1 present in the MPP determines whether the cell will differentiate into a macrophage or a B cell. B cell development is favoured where *Pu1* is expressed at lower levels, while high

*Pu1* expression promotes macrophage differentiation (DeKoter and Singh, 2000). PU.1 has also been shown to be required for terminal granulopoiesis as granulocytes from *Spi<sup>-/-</sup>* fetal liver fail to fully differentiate *in vitro* (Dahl et al., 2003).

The GATA family comprise 6 transcription factors that bind to the DNA consensus sequence (A/T)GATA(A/G), with GATA1, GATA2 and GATA3 expressed in the hematopoietic system. GATA1 is essential for normal erythropoiesis. *Gata1<sup>-/-</sup>* mice die from severe anaemia at E10.5-11.5 (Fujiwara et al., 1996). Embryonic stem cells lacking GATA1 are unable to form mature red blood cells, while all other lineages are unperturbed (Pevny et al., 1995). *Pu1* and *Gata1* expression are mutually exclusive and there is evidence to suggest that PU.1 and GATA1 directly interact and antagonise one another (Zhang et al., 1999). GATA1 has also been linked with megakaryocyte development where absence of GATA1 leads to uncontrolled proliferation and disrupted maturation of megakaryocyte progenitors (Vyas et al., 1999). *Gata2* is primarily expressed in HSCs where it regulates quiescence and apoptosis, and myeloid progenitors (Rodrigues et al., 2012). Recently, low-level overexpression of GATA2 in mice was shown to promote myeloid progenitor cell turnover and block lymphoid differentiation (Nandakumar et al., 2015). GATA3 is involved in T cell differentiation and is described in brief in section 1.1.5.

### 1.1.3.3 C/EBP $\alpha$

C/EBPs are a family of 6 transcription factors ( $\alpha$ ,  $\beta$ ,  $\gamma$ ,  $\delta$ ,  $\epsilon$ ,  $\zeta$ ) that modulate gene expression through interaction with promoters that possess the CCAAT box motif. They contain a highly conserved 86 residue C-terminal basic-leucine zipper (bZIP) domain which is responsible for DNA binding and dimerization, where the C/EBP family can form homodimers or heterodimers with other C/EBPs or other transcription factors (Figure 1. 4). Dimerization is required for DNA binding. C/EBPs are differentially expressed throughout the body and regulate a host of different activities including proliferation, growth and differentiation. *CEBPA*, the first of the C/EBP family to be discovered, is an intronless gene located on chromosome 19q13.1. C/EBP $\alpha$  is expressed in a variety of tissues including lung, liver and the hematopoietic compartment. There are 2 translated isoforms of the *CEBPA* gene - a full-length 358 amino acid

42 kilodalton (kD) product (p42) and an N-terminal truncated 30kD product (p30) which is translated from an alternative ATG start site at amino acid 120. Full-length C/EBP $\alpha$  (henceforth referred to as p42), contains two transactivation domains (TAD1 and TAD2) while the p30 isoform, lacks the first 117 amino acids of p42 where TAD1 is located. The p30 isoform of C/EBP $\alpha$  is a main focus in chapter 3 of this thesis and it is described in more detail in section 3.1. Amongst other functions, TAD1 has been shown to be essential for C/EBP $\alpha$  mediated E2F1 repression (Porse et al., 2001). TAD2, present in both p42 and p30, interacts with p21. Overexpression of C/EBP $\alpha$  induces growth arrest in numerous human cell lines including Hep3B2, HeLa and human fibrosarcoma cells HT1080 (Timchenko et al., 1997). Protein expression was analysed in an HT1080 cell line engineered with an isopropyl B-D-1-thiogalactopyranoside (IPTG) inducible C/EBP $\alpha$  construct and cells were analysed 2, 4, 8 and 24 hours (hrs) post IPTG addition. Induced expression of C/EBP $\alpha$  led to a significant increase in the expression of *P21*, but no change in the expression of other key cell cycle regulators including *CDK2* and *CDK4*. Subsequently it was demonstrated that C/EBP $\alpha$  directly inhibits CDK activity through TAD2 mediated P21 interaction (Harris et al., 2001). Switch/Sucrose Non-Fermentable (SWI/SNF) is a chromatin remodelling complex which is involved in the regulation of lineage specific genes. TAD2 of C/EBP $\alpha$  has been shown to regulate adipocyte differentiation (Pedersen et al., 2001) and proliferation (Muller et al., 2004) through SWI/SNF interaction, discussed further in section 3.1.1.

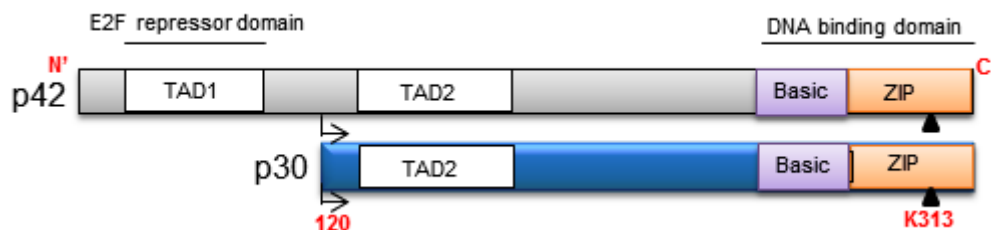


**Figure 1. 4 – Schematic diagram of the structure of C/EBP $\alpha$**

#### 1.1.3.3.1 C/EBP $\alpha$ in myelopoiesis

C/EBP $\alpha$  is an essential transcription factor in hematopoiesis and lineage determination. It is differentially expressed in stem and progenitor cells. With low expression in the HSC, its expression increases as cells progress towards terminal myeloid differentiation. Its expression is highest in GMPs where it is

switched off and another family member, C/EBP $\epsilon$  is switched on to drive terminal differentiation (Lekstrom-Himes, 2001). Mice lacking *Cebpe* display disrupted granulopoiesis and fail to generate neutrophils and eosinophils (Yamanaka et al., 1997). C/EBP $\alpha$  has been shown to be essential for granulopoiesis (Zhang et al., 1997). *Cebpa*<sup>-/-</sup> mice died within 8 hours of birth. At birth they were indistinguishable from wild-type and heterozygous littermates, however analysis of the blood revealed a complete absence of mature neutrophils in *Cebpa*<sup>-/-</sup> mice compared with wild-type (WT) and heterozygous controls where 87% of white blood cells (WBCs) comprise neutrophils. While *Cebpa*<sup>-/-</sup> mice had the same numbers of monocytes and lymphocytes, their WBCs had the appearance of immature myeloid cells and stained positive for a marker of myeloid progenitor cells (Sudan black). Northern blot analysis was used to show that there were no differences in *Mcsfr* and *Gmcsfr* mRNA levels in fetal liver cells (FLCs) of WT, heterozygous and *Cebpa*<sup>-/-</sup> mice. However *Gcsfr* mRNA expression was virtually absent in *Cebpa*<sup>-/-</sup> mice and they also exhibited a 4-fold increase in *Epor* mRNA. Indeed G-CSF, which can cross the placental barrier, administered to pregnant heterozygous mice caused a marked increase in mature granulocytes in the livers of WT mice, whereas the *Cebpa*<sup>-/-</sup> mice did not respond to G-CSF administration. Considering the presence of immature myeloid cells in the blood of *Cebpa*<sup>-/-</sup> mice, these data show that C/EBP $\alpha$  is essential for granulopoiesis and mediates differentiation in part via stimulation of the G-CSF receptor.

Progression through the cell cycle is strictly controlled by a variety of regulators which coordinate entry into and transition between the sequential stages. The E2F family play a major role in the G1 to S phase transition where they act as either activators with cyclical expression (E2F1, E2F2, E2F3a) or repressors with constant expression (E2F4 and E2F5). Several studies have described E2F repression by C/EBP $\alpha$  and this function, which is unique to TAD1, present only in the p42 isoform of C/EBP $\alpha$ , is central to terminal granulocytic differentiation. Electrophoretic mobility shift assay (EMSA) analysis of nuclear extracts from mouse hepatocytes and 3T3 cells revealed, that C/EBP $\alpha$  associates in a complex with E2F although does not bind directly to it (Slomiany et al., 2000). The authors use an *E2f* responsive promoter in a reporter assay to show that C/EBP $\alpha$  directly represses transcriptional activation of the promoter by E2F.

Furthermore in cell lines C/EBP $\alpha$  could repress cell cycle activation of the *E2f1* promoter. Down-regulation of *c-Myc* is required for myeloid differentiation and it has been identified as a target gene of C/EBP $\alpha$  by oligonucleotide array screening and representational difference analysis (Johansen et al., 2001). The authors mapped an E2F binding site on the *c-Myc* promoter which is critical for C/EBP $\alpha$  mediated negative regulation of *c-Myc*. Enforced expression of WT C/EBP $\alpha$  in 3T3 cells induced their differentiation, while an N-terminal mutant (D1-70) which lacks TAD1 was unable to induce differentiation (Porse et al., 2001). D1-70 showed a 10-fold decrease in the ability to repress E2F1 mediated transcription compared to WT C/EBP $\alpha$ . The authors also created basic region (between TAD2 and ZIP) mutants - BRM1, 2, 3 and 5. In BRM1 (V287A, E290A), BRM2 (I294A, R297A) and BRM3 (D301A, K304A) point mutations were introduced in the non-DNA binding face of the basic region while the BRM5 (Y285A) mutation was introduced in the bZIP domain. They showed that BRM2 and BRM5 had impaired ability to repress E2F1 dependent transcription. BRM2 and BRM5 transgenic mice, also lacked mature granulocytes in the BM and peripheral blood (PB) with no effect on other lineages apart from an increase in Ter119<sup>+</sup> erythroid cells, paralleling observations made in the *Cebpa*<sup>-/-</sup> mice. It was subsequently shown that unlike WT C/EBP $\alpha$ , the mutant BRM2 could not induce granulocytic differentiation in 32D myeloblast cell line (Keeshan et al., 2003). While BRM2 was able to bind E2F1, it was unable to induce expression of a C/EBP $\alpha$  target gene promoter. These data demonstrate that C/EBP $\alpha$  mediated inhibition of E2F1 is necessary for granulopoiesis and this activity is restricted to the p42 isoform as p30 lacks the transactivation domain necessary for E2F1 repression.

#### 1.1.3.3.2 Fetal to adult switch

C/EBP $\alpha$  has been shown to mediate the murine fetal to adult switch which occurs in HSCs 3-4 weeks after birth (Ye et al., 2013). Using a conditional deletion model the authors showed that loss of *Cebpa*, despite causing a significant reduction in BM cellularity, resulted in a 70 fold increase in LSK frequency. Analysis of the LSKs using SLAM markers showed an enriched LT-HSC population in the *Cebpa* knock out (KO) BM. It was shown that loss of *Cebpa* resulted in increased expression of cell-cycle related genes such as *Ccna2*, *Ccnb2* and *Cdk4*, and cell cycle analysis confirmed that loss of *Cebpa* induced proliferation of LT-HSCs. Gene expression analysis revealed that adult KO HSCs clustered with E15.5 FL HSCs from WT mice with over 1000 overlapping gene

changes, and differed significantly from control adult HSCs. Analysis of *Cebpa* expression showed a dramatic increase in HSCs from 4 week old mice compared to 2 week old mice. Indeed overexpression of C/EBP $\alpha$  in fetal HSCs was able to switch them from a proliferative to a quiescent state. The authors identify N-Myc as a direct target of C/EBP $\alpha$  and suggest that inhibition of N-Myc by C/EBP $\alpha$  blocks proliferation in new-born HSCs and promotes HSC quiescence in the adult system.

In addition to playing critical roles in steady state hematopoiesis, C/EBP $\alpha$  is also one of the most commonly mutated genes in acute myeloid leukaemia (AML) and these mutations are described in detail in 1.2.2.2.1.

### 1.1.4 B cell lymphopoiesis

Lymphopoiesis is the differentiation of lymphoid cells, which encompass B, T and NK cells. B cells are a key component of the adaptive immune system where they secrete antibodies to fight invading pathogens. B cells express B cell receptors (BCR) composed of immunoglobulin (Ig) M or D on their cell surface, which permit binding to specific antigens to initiate an immune response. B cells are formed and mature in the BM before migration to peripheral lymphoid tissues such as the spleen and lymph nodes. In the BM, B cell differentiation occurs in a number of well-defined phases governed by the sequential action of increasingly lineage-restricted transcription factors (Figure 1. 5). Early B cell development is characterised by the rearrangement of the Ig H and L chain loci in a process known as V(D)J rearrangement. Pre-pro-B cells are the earliest B cell precursor generated by the CLP and there is evidence to suggest that these cells may still maintain multi-lineage potential. They give rise to the fully committed pro-B cell which in turn gives rise to the pre-B cell. The pre-B cell does not express surface IgM but, unlike the pro-B cell, initiation of V(D)J rearrangement takes place, and it also expresses a surface IgM precursor called the pre-BCR. Pre-B cells give rise to immature B cells which express surface IgM (BCR) and V(D)J rearrangement is complete. These cells in turn produce mature B cells which express both IgM and IgD on the cells surface as well as other surface proteins including B220 and CD19. B220, a 220kD CD45 tyrosine phosphatase (also known as CD45RA), is a pan B-cell marker expressed on all committed B cells and is essential in regulating antigen receptor mediated

signalling. Expression of B220 is not restricted to B cells however, and can also be found on subsets of T and dendritic cells. CD19 expression emerges at the pro-B stage and it is expressed on all B cells downstream of this point. CD19 is a phosphoglycoprotein that facilitates signal transduction via surface Ig and is expressed on all B cells from the pro-B cell stage of differentiation onwards. Anti-B220 and anti-CD19 fluorochrome conjugated antibodies are used throughout this thesis to identify mature B cells in the BM, spleen and PB by flow cytometry.

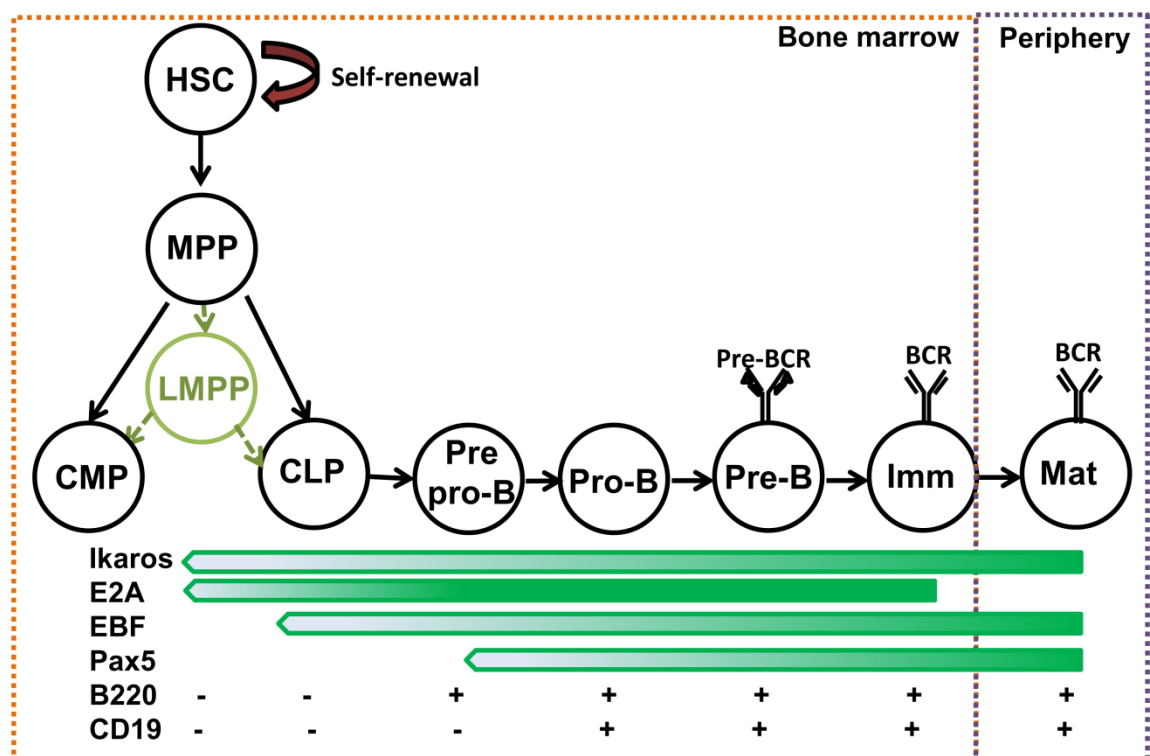


Figure 1. 5 – Schematic representation of the stages of B cell development

Each step of B cell development is regulated by the action of key transcription factors. Lineage priming of the HSC by Ikaros is an essential step in B cell lineage commitment and the generation of the pre-pro-B cell. *Ikaros* deficient mice display a developmental arrest at the LMPP stage of differentiation resulting in a complete lack of B cell production while myeloid differentiation is undisrupted (Georgopoulos et al., 1994). Ikaros was subsequently shown to repress genetic programs associated with self-renewal in the HSC and promote those associated with B lineage commitment (Ng et al., 2009). Indeed Ikaros is also necessary for the normal expression of key lymphoid signalling receptors Flt3, IL7R $\alpha$  and Notch1 (Sitnicka et al., 2003). As described in 1.1.3, PU.1 is a master regulator

of the myeloid/lymphoid bifurcation step whereby low concentrations of PU.1 promote B lineage commitment from the MPP/LMPP while higher levels drive myelopoiesis. E box binding protein 2A (E2A) is an essential transcription factor in early B cell lineage commitment. *E2a*<sup>-/-</sup> mice exhibit a B cell arrest at the pre-pro-B cell stage with mice completely devoid of mature B cells (Bain et al., 1994). E2A is required for initiating and maintaining expression of downstream effectors of B cell commitment from the pre-pro-B cell, including early B cell factor (EBF1) and Pax5 (Kwon et al., 2008). EBF1 expression is initiated via either E2A or IL-7 mediated promoter activation in the CLP. It has been shown to regulate the transcription factor network in CLPs responsible for downstream B lineage commitment. *Ebf1*<sup>-/-</sup> CLPs lack B-lineage associated genes including *Pax5* (Zandi et al., 2008), while enforced expression of EBF1 in MPPs drives B cell differentiation *in vitro* and suppresses myeloid differentiation through down-regulation of PU.1 and C/EBP $\alpha$  (Pongubala et al., 2008). In the hematopoietic system, *Pax5* is exclusively expressed in cells of the B lineage but absent from the earliest precursor the pre-pro-B cell. *Pax5*<sup>-/-</sup> mice display arrested B cell differentiation at the early pro-B cell stage (Nutt et al., 1999). *Pax5*<sup>-/-</sup> progenitor cells express *E2a* and *Ebf1* but lack expression of target gene *Cd19* indicating that *Pax5* operates downstream of *E2a* and *Ebf1*. PAX5 controls B lineage commitment through down-regulation of key genes including *Notch1* and *Csfr1* and maintains their repression during the later stages of lymphopoiesis (Delogu et al., 2006).

### 1.1.5 T cell lymphopoiesis

T cells originate in the BM before committed lymphoid progenitor cells migrate into the thymus via the cortico-medullary junction to form early thymocyte progenitors (ETPs) which subsequently differentiate into mature T and NK cells (Figure 1. 6). Within the thymic cortex the earliest developing thymocytes lack expression of the T cell glycoproteins CD4 and CD8 and thus are termed double negative (DN) cells. During the DN stage, T cells lose all other lineage potential and the T cell receptor (TCR)  $\alpha$ ,  $\gamma$  and  $\beta$  gene loci undergo rearrangement. DN cells with successful rearrangement of TCR- $\beta$  migrate through the cortex of the thymus towards the medulla where they proliferate extensively and differentiate into double positive (DP) T cells which express both CD4 and CD8. DP T cells migrate into the medulla proper where they mature into either CD4 single

positive (SP) or CD8 SP cells that will eventually leave the thymus via blood vessels and travel to peripheral lymphoid organs. One of the key transcriptional regulators of T cell development is Notch1.

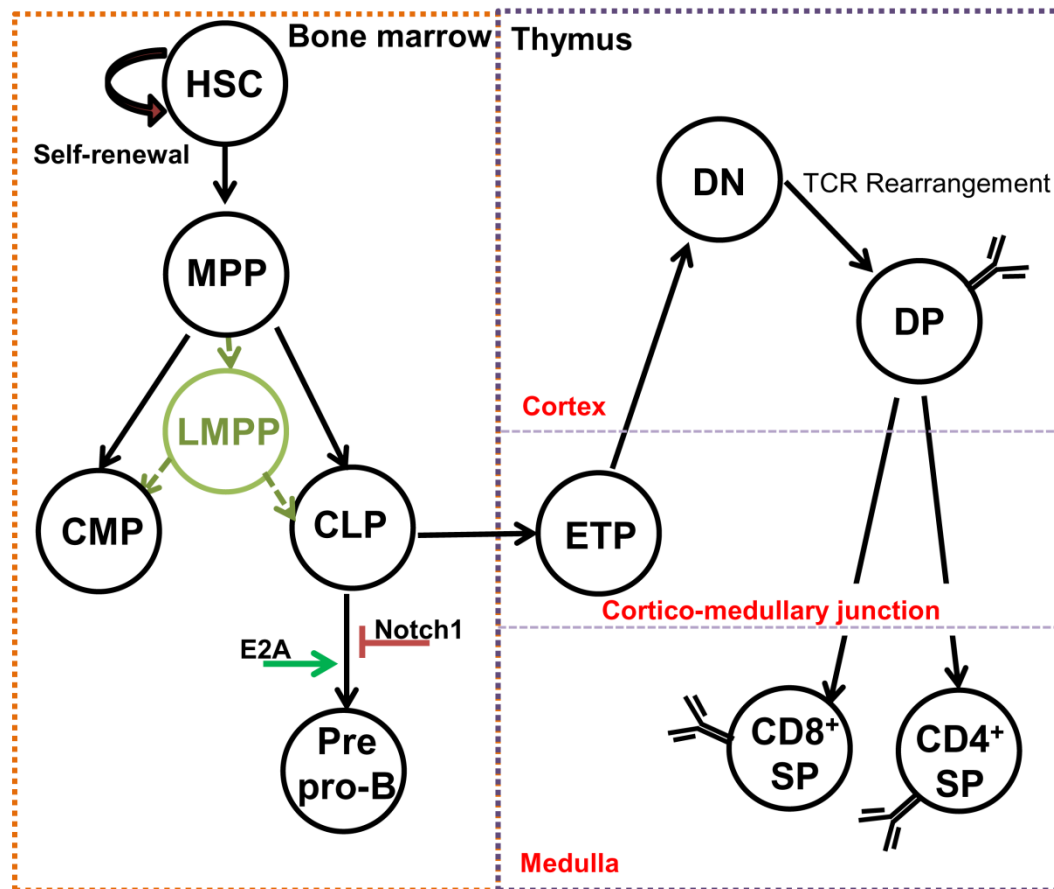


Figure 1. 6 – Diagram of T cell development in the BM and thymus

Notch1 belongs to a family of 4 class 1 transmembrane glycoproteins (NOTCH 1-4) that have a highly conserved canonical signalling pathway which is involved in a variety of developmental cell processes. Notch signalling plays an imperative role in hematopoiesis. In KO mouse studies the lymphoid progenitors of *Notch1*<sup>-/-</sup> mice migrate to the thymus where they become B cells, demonstrating the necessity for NOTCH1 in T cell commitment (Wilson et al., 2001). Conversely mice transplanted with BM transduced with NOTCH1 showed a block in B cell differentiation and increased T cells in the bone marrow (Pui et al., 1999). NOTCH1 signalling is essential for commitment to the T cell lineage and for early stages of differentiation but during  $\beta$ -selection (TCR rearrangement) NOTCH1 signalling is switched off and very low levels of NOTCH1 are detected in later stages of T cell development. NOTCH1 mutations are present in approximately

50% of all T-ALLs and in some cases of AML. NOTCH1 has two domains that are frequently mutated in T-cell acute lymphoblastic leukaemia (T-ALL) - the heterodimerization domain (HD) and the C-terminal PEST (region rich in proline, glutamic acid, serine and threonine) degradation domain. Gain-of-function mutations in these regions result in upregulated NOTCH1 expression by either ligand activation or a decrease in protein degradation respectively.

Thus the expression of cell-restricted transcription factors is essential to initiate or inhibit expression of lineage-instructive genes, as stem and progenitor cells progress through different stages of maturation.

## **1.2 AML**

Leukaemia is broadly divided into two subtypes; acute and chronic leukaemia. Acute leukaemia is characterised by a block in differentiation in a blood cell, and uncontrolled proliferation of these immature blast cells. The most common forms of acute leukaemia are found in the myeloid and lymphoid blood lineages. Acute lymphoblastic leukaemia (ALL) accounts for 78% of all paediatric leukaemia cases (Grigoropoulos et al., 2013). AML, the most common adult form, accounts for less than 1% of new leukaemia diagnoses in the UK (4.5 new diagnoses per 100,000 people per year) but represents 33% of all leukaemia cases (Cancer Research UK, 2012). This is because AML is a particularly heterogeneous disease with a plethora of genetic lesions contributing to its pathology, making it very difficult to effectively target therapeutically. Studying normal hematopoiesis allows us to gain insight into the complex network of pathways involved in differentiation, and understanding how these pathways become dysregulated is central to better comprehension of the disease.

### **1.2.1 AML classifications**

AML is a clinically and biologically heterogeneous disease and for many years the development of AML was thought to occur through a “two-hit” process i.e. two types of mutations are required to induce AML. Class I mutations (which include Flt3 and cKit) result in uncontrolled proliferation of cells, and class II mutations including C/EBP $\alpha$ , nucleophosmin1 (NPM1), homeodomain-containing transcription factor (HOX) and promyelocytic leukaemia-retinoic acid receptor  $\alpha$

(PML-RAR $\alpha$ ), that affect myeloid transcription factors causing a block in differentiation so that the cells fail to mature. However approximately 50% of AML patients do not carry a class I mutation and recent research has revealed several common mutations which cannot be identified as class I or II (Shih et al., 2012). These mutations, broadly termed class III, incorporate mutations in epigenetic modifiers such as DNA (cytosine-5)-methyltransferase 3A (DNMT3A), and mutations in the hydroxymethylation pathway such as tet methylcytosine dioxygenase 2 (TET2) and isocitrate dehydrogenase 1/2 (IDH1/2) mutations. Demonstrating the limitations of the “two-hit” model, the identification of these groups of mutations extends our understanding of the complex pathogenesis of AML.

There are two established systems used to classify AML into subtypes, the French-American-British (FAB) and World Health Organization (WHO) systems.

#### **1.2.1.1 FAB classification**

The FAB classification system was first published in 1976 and is based primarily on morphologic observations from blood and BM films (Bennett et al., 1976). 8 categories of AML were described with M0, M1 and M2 representing a myeloblastic phenotype with increasing maturation and M3 encompassing promyelocytic leukaemia. Myelomonocytic leukaemia is denoted M4 (without eosinophils) or M4eos (with eosinophils). Acute monocytic leukaemia is represented by M5, M6 describes leukaemia of early erythroid precursors (acute erythroid leukaemia) and M7 leukaemia of early platelet cells (acute megakaryoblastic leukaemia). Because the FAB system relies primarily on morphologic characteristics of patient samples, and does not take into account the diverse cytogenetic background of AML patients within a given group, it provides limited prognostic information.

#### **1.2.1.2 The WHO classification**

The WHO system is based on biological, clinical, genetic and immunophenotypic features, allowing a more integrated approach to the identification of a given AML (Swerdlow et al., 2008). It categorises samples broadly into 7 groups - AML with certain genetic abnormalities, AML with myelodysplasia-related changes,

AML related to previous chemotherapy or radiation, AML not otherwise specified, myeloid sarcoma, myeloid proliferation related to Down's syndrome and undifferentiated and biphenotypic acute leukaemias. AMLs with certain genetic abnormalities are further characterised as those with favourable or unfavourable outcome. Favourable karyotypes include translocation (t)(8;21) which results in the formation of the runt-related transcription factor 1 (RUNX1)/ETO fusion gene (also known as AML1/ETO), inversion (inv)(16) which produces the core binding factor  $\beta$ /myosin heavy chain 11 (CBFB/MYH11) fusion gene, and t(15;17) which causes the fusion of the PML and RAR $\alpha$  genes resulting in acute promyelocytic leukaemia (APL) (Chaudhury et al., 2015). AML with RUNX1-ETO or CBFB/MYH11 present are collectively known as core binding factor AML (CBF-AML). Those within the 'AML not otherwise specified' category fall into similar categories as the FAB subtypes M0-M7 with the addition of 2 further groups - acute basophilic leukaemia and acute panmyelosis fibrosis. In the most recent update the WHO classification system added 2 additional categories - AML with mutated *CEBPA*, and AML with mutated *NPM1*, due to the prevalence of these mutations in AML (Vardiman et al., 2009).

## 1.2.2 Common mutations and abnormalities

In addition to the aforementioned chromosomal rearrangements, approximately half of AML patients have cytogenetically normal AML (CN-AML). Within the diverse pool of genetic aberrations found in AML, there are some which are found more frequently than others.

### 1.2.2.1 Class I mutations

Flt3 (also known as CD135) is a cytokine receptor expressed on hematopoietic progenitor cells in particular MPPs and CLPs. *FLT3* is found mutated in up to 30% of AML patients and is broadly associated with a poor clinical outcome. There are 2 classes of *FLT3* mutations which result in constitutive activation of FLT3 signalling - internal tandem duplications (ITD) found in up to 25% of AML patients (Nakao et al., 1996), and point mutations in the tyrosine kinase domain (TKD) found in 5-10% of AML patients. Activating *FLT3* mutations result in aberrant activation of downstream pathways including phosphatidylinositol 3-kinase (PI3K)/AKT and signal transducer and activator of transcription (*STAT5*), which

promote cellular proliferation. The cKit receptor is a tyrosine kinase structurally related to Flt3 that, as alluded to earlier, plays an important role in hematopoiesis and stem cell proliferation through its ligand SCF. Up to 80% of myeloblasts in AML express cKIT (Ikeda et al., 1991). Activating mutations in the *cKIT* gene are found in up to 25% of CBF-AMLs, and are also common in other cancers including testicular, melanoma and gastrointestinal. Similar to Flt3, they may be point mutations affecting the TKD or ITD mutations resulting in activation of the cKIT receptor (Wakita et al., 2011).

### 1.2.2.2 Class II mutations

#### 1.2.2.2.1 *CEBPA* mutations

One of the most commonly mutated genes in AML is *CEBPA*, with mutations reported in between 5% and 14% of AML cases (Pabst and Mueller, 2009). *CEBPA* mutations are primarily of two types either an N-terminal frame-shift, or C-terminal in-frame mutation (Pabst et al., 2001). N-terminal *CEBPA* mutations cause a truncation of the full length 42kD isoform (p42) resulting in the expression of the 30kD isoform (p30) which, as outlined in 1.1.3.3.1, lacks a transactivation domain necessary for C/EBP $\alpha$  mediated E2F repression. C-terminal mutations exhibit insertions or deletions in the bZIP domain which affect the DNA binding activity of C/EBP $\alpha$ . *CEBPA* mutations are associated with M1 or M2 (myeloblastic) CN-AML with a favourable outcome, and, unusually, with expression of the T-cell surface marker CD7 and increased expression of erythroid genes including *GATA1* and *EPOR*. In over 70% of *CEBPA* mutated AMLs, both alleles exhibit a mutation but despite their prevalence, biallelic *CEBPA* mutations almost never result in a complete loss of C/EBP $\alpha$ . Over 90% of patients with biallelic mutations carry both the N- and C-terminal mutation (Pabst and Mueller, 2007). Indeed there is a growing body of evidence to suggest that C/EBP $\alpha$  expression is necessary for the induction of AML in some instances. MLL translocations (discussed in 1.2.2.2.3) are a very common lesion found in AML, present in around 10% of patients and resulting in the increased expression of genes including *MEIS1* and *HOXA9*. A study has shown that expression of C/EBP $\alpha$  is required for the initiation but not maintenance of MLL-rearranged AML (Ohlsson et al., 2014). A conditional deletion mutant *Cebpa<sup>fl/fl</sup>;Mx1Cre* was treated with polyinosinic-polycytidylic acid (poly I:C) and control (*Cebpa<sup>fl/fl</sup>*) and *Cebpa*-deleted (*Cebpa<sup>Δ/Δ</sup>*) HSPCs were isolated and transduced with control or

MLL-ENL overexpressing retrovirus. When transplanted into irradiated recipients control *Cebpa<sup>fl/fl</sup>* mice developed lethal AML with a latency of just 10 weeks where as *Cebpa<sup>Δ/Δ</sup>* transplanted mice remained healthy. The authors generated primary MLL-ENL AMLs from *Cebpa<sup>fl/fl</sup>;Mx1Cre* and *Cebpa<sup>fl/fl</sup>* before transplanting into secondary recipients. The recipients were then treated with poly I:C to delete *Cebpa* from the established leukaemia. Loss of *Cebpa* at this stage had no effect on the latency or phenotype of this disease. In another study loss of *Cebpa* from established *Hoxa9/Meis1*-induced leukaemia resulted in improved survival (Collins et al., 2014). As with the aforementioned study, overexpression of HOXA9/MEIS1 in a *Cebpa* null background was unable to drive leukaemogenesis, but in this case deletion of *Cebpa* from an established HOXA9/MEIS1 leukaemia resulted in a delay in disease latency from 40 to 60 days.

In addition to these commonly occurring mutations, C/EBPα is dysregulated in a variety of other ways e.g. hypermethylation of the *CEBPA* promoter leading to gene silencing (Chim et al., 2002). Common AML mutations resulting in fusion oncoproteins can inhibit *CEBPA* mRNA transcription including AML1-ETO (1.2.2.2.6), PML-RARα (1.2.2.2.5) and CBFβ/MYH11 (Paz-Priel and Friedman, 2011). Several posttranslational modifications of the C/EBPα protein have also been documented. C/EBPα is phosphorylated at serine 21, resulting in a conformational change which inhibits its ability to induce granulocytic differentiation (Ross et al., 2004). The p42 isoform of C/EBPα has also been shown to be sumoylated (Hankey et al., 2011). It has been suggested that p42 sumoylation may occur as a result of increased p30 expression (Geletu et al., 2007) which itself cannot be sumoylated, highlighting a dominant negative role for p30 over p42, discussed in more detail in section 3.1.1.1. Proteasomal degradation of C/EBPα mediated by TRIB2 induces AML *in vivo* (Keeshan et al., 2006) and is discussed in detail in 1.3.4.1.1, and elucidating the nature of this relationship is a major focus in chapter 3.

#### 1.2.2.2.2 NPM1

NPM1 is a ubiquitously expressed phosphorylated protein which shuttles between the cytoplasm and nucleus where it mediates a range of activities including regulation of p53 and ribosome assembly and transport (Lindstrom, 2011). *NPM1* mutations, which occur in one third of all AMLs and up to 60% of CN-AML cases,

result primarily from a frameshift caused by an insertion into exon 12 of the gene. The resultant protein, termed NPM1c<sup>+</sup>, lacks at least one key tryptophan residue in the C terminal nuclear export signal (NES) region, resulting in NPM1 transiting out of the nucleus and into the cytoplasm (Falini et al., 2006). It is not fully understood how cytoplasmic NPM1c<sup>+</sup> contributes to leukaemogenesis nor the prognostic significance of NPM1 mutations, however a recent review of 13 previously published studies suggested that NPM1 mutations correlate with a favourable outcome for AML patients (Liu et al., 2014).

#### 1.2.2.2.3 Mixed-lineage leukaemia fusion genes

Mixed-lineage leukaemia (MLL) is a histone methyltransferase protein essential for regulating gene expression in hematopoiesis. MLL forms a large multi-subunit protein complex which negotiates chromatin modification through methylation, acetylation and nucleosome remodelling (Slany, 2009). It also associates with the WD repeat-containing protein 5 (WDR5), discussed further in section 3.1.1.4, which recognises a methylation mark introduced by MLL at histone 3 lysine 4 (H3K4). While MLL mediated chromatin modification is a requirement for the transcription of many genes, HOX genes are among those most dependent on it and as discussed next are frequently dysregulated as a result of the formation of MLL fusion genes. Translocations affecting *MLL* (11q23) are found in both myeloid and lymphoid leukaemia. To date *MLL* has been associated with 79 translocation partner genes (Meyer et al., 2013) but the most common are *ENL*, *AF9*, *AF4*, *ELL* and *AF10*. MLL-ENL overexpression in BM cells in a B cell permissive serial replating assay resulted in immortalisation of a B220<sup>+</sup>CD19<sup>-</sup> cell capable of continuous replating and generating B220<sup>+</sup>CD19<sup>-</sup> leukaemia growth *in vivo* when transplanted into recipient mice (Zeisig et al., 2003). The MLL-ENL leukemic cells also expressed CD11b and cKit to a lesser extent. MLL leukaemia is typically aggressive and common in paediatric patients.

#### 1.2.2.2.4 Dysregulation of HOX genes

In vertebrates the genes that encode the highly conserved HOX proteins are found in 4 clusters - A, B, C, and D - on separate chromosomes. In the hematopoietic system HOX genes are differentially expressed on stem and progenitor cells. They are highly expressed in primitive cells and their expression is downregulated with differentiation. *HOXA* genes are expressed in the myeloid lineage, *HOXB* in erythroid and *HOXC* in the lymphoid lineage (Alharbi et al.,

2013). *HOXA9* is the most highly expressed HOX family member in human HSCs and progenitor populations. Its overexpression *in vivo* results in a long latency murine AML (Kroon et al., 1998). HOX proteins usually require the binding of a cofactor to mediate their effects the most common belonging to the pre-B-cell leukaemia (PBX), and myeloid ecotropic insertion site (MEIS) families which also have essential roles in hematopoiesis. *HOX* mutations are one of the most common Class II mutations found in AML and *NUP98* is one of the most frequent *HOX* fusion partners. Fusion with *NUP98* has been documented for *HOXA9*, *A11*, *A13*, *D11*, *D13* and *C13*. Murine AML induced by *HOXA9/NUP98* fusion protein overexpression is associated with long latency (~1 year) but with co-overexpression of cofactors *MEIS1* the latency is greatly decreased. In addition to dysregulation by mutation, *HOX* gene expression is frequently upregulated by other common chromosomal rearrangements in AML. Usually *MLL* regulates *HOX* gene transcription through direct binding, however *MLL* fusion proteins hyper-activate *HOX* transcription resulting in a block in myeloid differentiation (Slany, 2009). *HOX* gene expression is used as a prognostic factor as it correlates with intermediate or unfavourable outcome.

#### 1.2.2.2.5 PML RAR $\alpha$

Over 98% of APL (M3) patients, and 13% of all AML patients, are positive for the t(15;17) translocation which results in the fusion of *RARA* with *PML* producing the oncoprotein PML-RAR $\alpha$  (Goddard et al., 1991). RAR $\alpha$  is a transcription factor that is activated by all-trans retinoic acid (RA) and 9-cis retinoic acid. Its activity controls the transcription of genes involved in apoptosis, differentiation and granulopoiesis. RAR $\alpha$  binds to regions of DNA and recruits corepressors to repress gene transcription but stimulation with its ligand results in recruitment of a coactivator protein which induces transcription. *PML* is a tumour suppressor protein involved in a wide range of processes including repression of cell growth and proliferation and induction of apoptosis. The PML-RAR $\alpha$  oncoprotein results in a block in differentiation of granulocytes and uncontrolled growth resulting in an accumulation of leukemic promyelocytes. APL is one of the most treatable forms of leukaemia as it responds to RA therapy which reverses RAR $\alpha$  repression of transcription and induces differentiation of leukemic blasts leading to apoptosis. As a single agent ATRA treatment has been reported to induce complete remission in 85% of patients, and in combination with standard chemotherapeutics up to 95% (Coombs et al., 2015).

#### 1.2.2.2.6 RUNX1

RUNX1, also called acute myeloid leukaemia 1 (AML1) protein, is a transcription factor involved in the regulation of HSC differentiation through interaction with an array of genes including *PU1* and *CEBPA*. Several chromosomal translocations in AML pathophysiology involve the RUNX1 gene. t(8;21) is one of the most common AML rearrangements and results in the fusion of the RUNX1 gene with ETO. The RUNX1-ETO or AML1-ETO fusion protein is present in approximately 12% of AML patients (Lam and Zhang, 2012).

#### 1.2.2.3 Mutations of epigenetic modifiers

DNMT3A is a highly conserved 130kD protein which catalyses DNA methylation, an epigenetic modification in which a methyl group is added to DNA that can stably alter gene expression by switching on or off gene transcription. Aberrant DNA methylation is a hallmark of cancer. Mutations in *DNMT3A* are present in approximately 20% of AML cases. Despite much research, the mechanism through which *DNMT3A* mutations contribute to leukaemogenesis remains elusive. There are some patterns emerging for co-occurring mutations. *DNMT3A* mutations do not exist in patients with t(15;17), inv(16) or t(8;21), nor in MLL-rearranged leukaemia (Yang et al., 2015). However 60% of patients carrying a *DNMT3A* mutation also carry an *NPM1* mutation and they are also positively correlated with *FLT3*-ITD and *IDH1* mutations albeit to a lesser extent, but how these mutations interact in the pathology of AML is unknown.

The commonly recurring chromosomal translocations and molecular abnormalities in AML are briefly discussed here but many other less frequently occurring genetic lesions have been described in AML. Most gene mutations identified in CN-AML, also occur in AML with abnormal and complex karyotypes, and frequently in the presence of additional mutations further increasing the complexity of this disease. It is this complexity and heterogeneity that makes AML such a difficult disease to target therapeutically.

### 1.2.3 Chemotherapeutic treatment of AML

The treatment of AML with chemotherapeutic drugs occurs in 2 phases - intensive induction therapy to destroy the bulk of leukaemia cells, and consolidation therapy to destroy long-lasting leukaemia cells. Induction

treatment usually involves two drugs - namely cytarabine (also known as ara-C) and an anthracycline such as liposomal daunorubicin. Cytarabine is an anti-metabolite which damages DNA in the S-phase of the cell cycle halting cancer cell division. Daunorubicin interacts with DNA by intercalation and inhibits the progression of topoisomerase II. The standard approach termed “7+3” involves 7 days of cytarabine administration followed by 3 days of an anthracycline. Etoposide, which forms a complex with DNA and topoisomerase II to prevent the re-ligation of DNA strands, is also frequently administered with cytarabine and daunorubicin in patients below 60 years of age. Consolidation therapy usually involves several cycles of cytarabine (Kadia et al., 2014). As mentioned briefly, APL is induced by t(15;17) and is treatable with RA but the overall prognosis for AML in general is poor with only 40% of patients under 60 years of age surviving more than 5 years (Stein and Tallman, 2016).

Many commonly recurring cytogenetic lesions confer poor prognosis and as such extensive work is being carried out to develop additional chemotherapeutic agents based on the molecular phenotype of a given AML. Patients with *FLT3*-ITD mutations have a high relapse rate and poor prognosis. Small molecule tyrosine kinase inhibitors (namely gilteritinib, quizartinib and midostaurin) are currently being investigated for their efficacy in AML treatment with limited success thus far. Patients with *IDH1/2* mutations fall into the intermediate to poor outcome groups and inhibitors of mutant *IDH1/2* are currently in clinical trials. In addition to molecularly targeted agents, several antibody-drug conjugates against unique cell surface receptors expressed on leukemic cells are also being developed. Despite the clear complexity of AML as eluded to above, the standard “7+3” treatment prevails even for patients with molecularly and cytogenetically complex AML. The development of new therapies such as those mentioned for *FLT3* and *IDH1/2* mutations are the result of extensive characterisation of a given lesion. Thus it is imperative to gain a better understanding of molecular perturbations that contribute to AML pathogenesis in order to expose new targets for more tailored treatment. There is a strong correlation between dysregulated *TRIB2* expression and human acute leukaemia and this thesis aims to further examine the role of *TRIB2* in hematopoiesis and AML pathogenesis.

## 1.3 Trib2

Trib2 is a member of the *Tribbles* family of pseudokinases that comprise 3 members; Trib1, Trib2 and Trib3.

### 1.3.1 Discovery

*Tribbles (trbl)* was first identified as a novel regulator of *string* - a CDC25 homolog - in *Drosophila*. Genetic screening for mutations resulting in improperly formed ventral furrows in *Drosophila* embryos revealed *trbl* as a candidate gene (Seher and Leptin, 2000). Sequencing of *trbl* revealed that it encodes a protein similar to the SNF1 class of serine/threonine kinases but with an asparagine (N) to arginine (R) substitution in the catalytic loop domain. In the *Drosophila* embryo, *string* controls entry into mitosis but during gastrulation a delay in mitosis of cells on the ventral side of the embryo is required for the formation of the ventral furrow. A parallel study subsequently showed that *trbl* inhibited *string*, permitting formation of the ventral furrow (Grosshans and Wieschaus, 2000). Embryos lacking *trbl* did not exhibit the mitotic delay during gastrulation, and by injecting synthetic *trbl* mRNA into *Drosophila* embryos, the authors demonstrated that *trbl* overexpression inhibited mitosis. The authors also further characterised the kinase domain of *trbl* and found changes in 3 additional residues; a lysine (K) to R swap in the adenosine triphosphate (ATP) binding site, an aspartic acid (D) to serine (S) exchange, and a highly conserved histidine (H) residue in the catalytic loop was substituted with a leucine (L). The authors hypothesised that such deviations would mean *trbl* may lack kinase function.

In a gain-of-function screen for genes whose overexpression would affect cell division during oogenesis in the developing *Drosophila*, authors identified 15 (out of 8500) lines with aberrant cell division (Mata et al., 2000). In one of the 15 lines, overexpressed *trbl* was shown to result in extra cell divisions with very high frequency. Co-transfection of *trbl* and *string* resulted in a reduction of *string* protein levels and in the presence of a proteasome inhibitor, the degradation was reversed indicating that *trbl* controls *string* protein turnover in a proteasome-dependent manner. In *Drosophila* oogenesis the C/EBP transcription factor *slbo* is required for the migration of border cells. *Trbl* was

shown to negatively regulate *slbo* *in vivo* by targeting it for ubiquitin mediated degradation (Rorth et al., 2000). These 4 studies identified *trbl* as a regulator of key developmental stages by mediating protein degradation.

### 1.3.2 Structure of TRIB proteins

The three mammalian homologs of *trbl*, TRIB1, TRIB2 and TRIB3, are highly conserved among vertebrates and share substantial sequence similarity, in particular TRIB1 and TRIB2 exhibit 71.3% overlap with one another (Yokoyama and Nakamura, 2011). Structurally the TRIB family are composed of an N-terminal region, a C-terminal region and a central pseudokinase domain (Figure 1. 7). The N-terminal domain is rich in proline and serine residues, a common feature of proteins with a short half-life. The C-terminal domain contains a highly conserved constitutive photomorphogenic 1 (COP1) E3 ubiquitin ligase binding motif, and a mitogen-activated kinase/extracellular-signal-regulated kinase-1 (MEK1) binding motif (Qi et al., 2006, Yokoyama et al., 2010). As mentioned above the TRIB pseudokinase domain has characteristic features of a canonical kinase but lacks critical motifs and residues including a motif required for anchoring ATP (GXGX<sub>2</sub>GXV), and a sequence (DFG) required for catalysis (Hanks and Hunter, 1995). The conserved amino acids of canonical kinases, absent in the TRIB family, bind to divalent metal ions and align ATP before phosphoryl-transfer. Until recently no kinase activity had been reported for the TRIB family of proteins thus the persistent classification of the family as pseudokinases. However recently recombinant human TRIB2 protein was used in a fluorescence-based ligand interaction assay and demonstrated weak ATP binding activity in the absence of divalent metal cations, which can be targeted by small molecule inhibitors (Bailey et al., 2015).

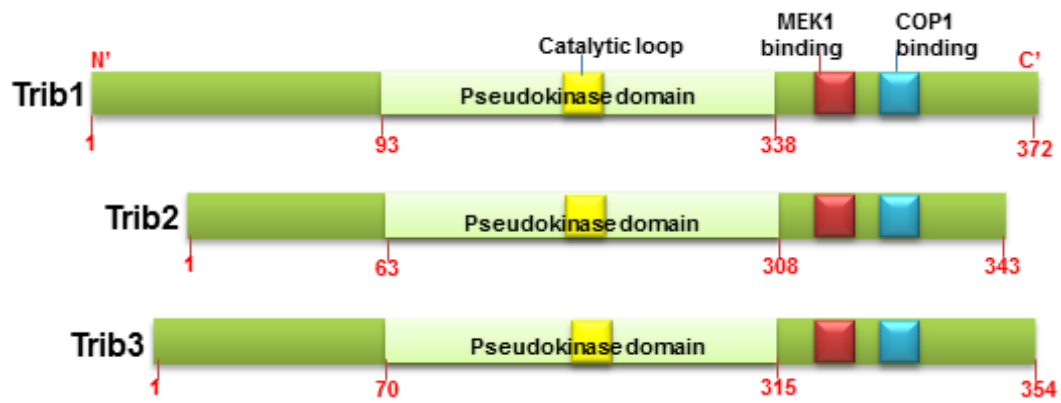


Figure 1. 7 – Schematic diagram of the Trib family

### 1.3.3 Functions of TRIB2

The TRIB family have been shown to be dispensable for development in the vertebrate system (Yamamoto et al., 2007, Takasato et al., 2008, Okamoto et al., 2007) suggesting overlapping functions between the 3 mammalian isoforms. *TRIBs* are expressed in most human tissues with *TRIB2* expression highest in PB leukocytes (Kiss-Toth et al., 2004). TRIB proteins localize in both the cytoplasm where they mediate proteasomal degradation of signalling proteins including mitogen-activated protein kinase kinase (MKK) and C/EBP $\alpha$ , and also in the nucleus where they associate with target promoters such as C/EBP $\zeta$  (CHOP) and activating transcription factor 4 (ATF4) (Lohan and Keeshan, 2013).

#### 1.3.3.1 Protein degradation

The proteolytic function of Trbl has been conserved in vertebrates where the TRIB family regulate cell cycle and differentiation in a cell-specific context. TRIB2 mediates protein degradation by binding directly to target proteins and recruiting the E3 ubiquitin ligase COP1 into a protein complex, marking the target protein for degradation. Members of the C/EBP family ( $\alpha$ ,  $\beta$ ,  $\gamma$ ) have been shown to regulate adipocyte differentiation, a process which is also modulated by sets of signal cascades including mitogen-activated protein kinases (MAPK), extracellular signal-regulated protein kinase (ERK) and jun kinase (JNK). Overexpression of TRIB2, and also TRIB3, inhibits the differentiation of 3T3-L1 adipocytes *in vitro* (Naiki et al., 2007). Gene expression analysis in TRIB2 overexpressing 3T3-L1 cells showed that *Cebpb* mRNA levels were unchanged in

the presence of TRIB2 or TRIB3 but *Cebpa* levels were significantly reduced. At the protein level TRIB2 (but not TRIB3) overexpression resulted in reduction of the LAP isoform of CEBPB which contains the DNA binding and trans-activation domains with no effect on the LIP isoform - an inhibitory isoform which lacks the trans-activating domain and is translated from an alternative start site.

Treatment with MG132, a cell permeable proteasome inhibitor, rescued LAP protein levels and in a co-immunoprecipitation (CO-IP) experiment TRIB2 was shown to bind to LAP but not LIP suggesting that TRIB2 selectively degrades this CEBPB isoform in a proteasome dependent manner to inhibit adipogenesis.

It is worth noting that while TRIB3 overexpression in adipocytes did not lead to C/EBPB degradation it did inhibit adipocyte differentiation through suppression of AKT phosphorylation. TRIB2 mediated proteasomal dependent degradation of C/EBP $\alpha$  has also been demonstrated in the lung (Grandinetti et al., 2011) and hematopoietic system (Keeshan et al., 2006) and is discussed in detail in 1.3.4.2.2 and 1.3.4.1.1 respectively. Indeed TRIB1 has also been shown to degrade C/EBP $\alpha$  in the hematopoietic system (Yokoyama et al., 2010). Acetyl-coenzyme A carboxylase (ACC) is a multi-subunit enzyme that catalyses carboxylation of acetyl-CoA providing a substrate for the biosynthesis of fatty acids. TRIB3 was the first to be shown to degrade ACC in adipose tissue in a COP-1 dependent manner (Qi et al., 2006), and this was subsequently demonstrated for TRIB1 and TRIB2 (Dedhia et al., 2010).

### 1.3.3.2 MAPK/ERK Signalling

MAPKs are a highly conserved serine/threonine kinase family integral to fundamental cellular processes like proliferation, differentiation and survival. MAPK activation involves a three step process whereby MAPK is activated upon phosphorylation by MAPK kinase (MAPKK) which is first phosphorylated by MAPKK kinase (MAPKKK) in response to stimuli such as mitogens, cytokines and growth factors. Six groups of MAPKs have been characterized including ERK which responds to growth factors and mitogens, and JNK and p38 which primarily respond to stress stimuli. Activation of MAPK is involved in the inflammatory activation of monocytes. In a study of regulators of monocyte activation, *TRIB2* was shown to be downregulated following treatment of a human monocytic leukaemia cell line, THP-1, with either acetylated low-density lipoprotein

(AcLDL) or lipopolysaccharide (LPS) (Eder et al., 2008). Alone AcLDL treatment of THP-1 cells does not induce production of the proinflammatory cytokine interleukin-8 (IL-8), but in combination with LPS treatment it further increases LPS-induced IL-8 production. When *TRIB2* expression was targeted using an siRNA, IL-8 production in response to LPS treatment was significantly higher in cells with silenced *TRIB2* than in cells expressing *TRIB2*. *IL8* expression is regulated by MAPK pathways and pharmacologically blocking JNK or MEK1 (but not p38) inhibits LPS-induced IL-8 production. In *TRIB2* silenced THP-1 cells MAPK activation was potentiated in response to LPS-dependent MAPK activation suggesting a negative regulatory role for *TRIB2* in MAPK specific inflammatory activation. CO-IP studies showed that *TRIB2* specifically interacts with MEK1 and MKK7 but not with MKK4 in monocytes and this binding is dependent on the *TRIB2* kinase-like domain. Thus the authors hypothesise that monocytes downregulate *TRIB2* in response to stimulation, shown here by AcLDL or LPS, resulting in loss of *TRIB2* binding to MEK1 or MKK7 thus, increasing activation of ERK and JNK respectively, resulting in increased IL-8 production.

### 1.3.3.3 AKT Signalling

Activated AKT, a serine/threonine kinase, mediates a host of downstream responses including glucose homeostasis. The AKT signal transduction pathway is usually activated by PI3K which in turn is activated by a range of stimuli such as hormones and growth factors. A yeast two-hybrid assay, used to identify proteins upstream of *AKT* which could attenuate its activity, revealed *TRIB3* as a putative regulator of *AKT* activity (Du et al., 2003). To validate this link the authors overexpressed *AKT* in the HepG2 cell line and performed a CO-IP experiment and found that both *TRIB2* and *TRIB3* interact with *AKT*. To address whether these interactions affect *AKT* activity, HEK293 cells were treated with Insulin-like growth factor (IGF1) to induce *AKT* phosphorylation at Thr<sup>308</sup> and Ser<sup>473</sup>. Overexpression of *TRIB2* and *TRIB3* blocked IGF1 induced *AKT* phosphorylation in 293T cells.

### 1.3.3.4 Toll-like receptor signalling

Toll-like receptors (TLRs) comprise a family of ten type 1 transmembrane proteins expressed on cells involved in the innate immune response such as

macrophages and dendritic cells where they detect a wide range of pathogens and molecules to initiate the innate and adaptive immune response. TLR5 recognises flagellin, the principle component of bacterial flagella, and TRIB2 has been identified as a binding partner of TLR5. A study of colonic tissue biopsies in patients with inflammatory bowel disease showed *TRIB2* expression was decreased when compared with normal control tissue samples, and those cells displaying decreased *TRIB2* were mainly epithelial cells (Wei et al., 2012). 293T cells transfected with TLR2, TLR4, TLR5 and TLR9 were each stimulated with the appropriate ligand and it was shown that *TRIB2* mRNA and protein expression was upregulated upon TLR5 stimulation by flagellin. In an NF- $\kappa$ B luciferase reporter assay, TRIB2 inhibited NF- $\kappa$ B activation by TLR-5 in a dose dependent manner. Conversely knockdown of *TRIB2* resulted in an increase NF- $\kappa$ B activity when TLR5 expressing cells were stimulated with flagellin. The authors showed that knockdown of *TRIB2* significantly reduced TLR5 mediated phosphorylation of the JNK and p38 pathway but no effect on the ERK pathway was observed. By CO-IP the authors showed that NF- $\kappa$ B2 (p100) interacts with Trib2. Thus the authors demonstrated a novel role for TRIB2 in regulation of TLR5 signalling through modulation of specific MAPK pathways to inhibit NF- $\kappa$ B activity.

### 1.3.3.5 Hematopoiesis

In the human hematopoietic system gene expression analysis has revealed that *TRIB1* expression is highest in mature BM granulocytes, monocytes and B cells, while *TRIB2* expression is significantly higher in the T cell compartment (Liang et al., 2013). *TRIB3* expression is generally low in the hematopoietic compartment. Recently TRIB2 was implicated in the development of the megakaryocyte and erythroid lineages (Mancini et al., 2012). The authors used *Cebpa*, *Gata1* and friends of GATA-1 (*Fog1*) conditional knockout mice to study the role of these transcription factors in megakaryocyte and erythroid differentiation and showed that GATA-1 is required for erythroid development, FOG-1 is required for the formation of megakaryocyte and erythroid precursor cells, and also that FOG-1 could suppress myeloid progenitor specification. They suggest that TRIB2 mediated degradation of C/EBP $\alpha$  may be the mechanism through which FOG-1 can suppress myeloid potential. Microarray analysis showed *Trib2* to be expressed in MkE precursor cells but down-regulated in pre-GMs and CLPs. They also found a binding site on the *Trib2* promoter that binds both GATA-2 and FOG-

1 and this was confirmed by chromatin immunoprecipitation (ChIP) assay. Furthermore they show that in the conditional *Fog1* KO mice, there is a strong reduction in *Trib2* expression. These findings point towards a role for Trib2 in erythroid development. However, *Trib2* has also been shown to be downregulated by EPO (Flygare et al., 2011) a cytokine essential for erythroblast development and survival. Thus far it has not been determined whether or not loss of Trib2 from the hematopoietic compartment affects lineage distribution and stem and progenitor cell differentiation and this is a major focus of chapter 4, section 4.3.4.

### 1.3.4 The role of TRIB2 in cancer

The *Tribbles* family have been implicated in many different types of cancer including acute leukaemia, melanoma, lung and liver cancer.

#### 1.3.4.1 TRIB2 in acute leukaemia

##### 1.3.4.1.1 AML

Trib2 was first identified as a murine oncogene, when its overexpression in a BMT led to the development of a potent AML with a 6 month latency (Keeshan et al., 2006). In this model, TRIB2 preferentially degrades the p42 isoform of the myeloid transcription factor C/EBP $\alpha$  and causes an increase in the truncated p30 isoform which has oncogenic functions. As discussed in detail in 1.1.3.3.1, in the hematopoietic system C/EBP $\alpha$  is essential for granulopoiesis (Zhang et al., 1997) and TRIB2 mediated degradation of p42 blocks granulopoiesis. This block in granulopoiesis is coupled with uncontrolled proliferation of the myeloblast cells and leads to a transplantable AML with 100% penetrance and a median latency of 25.5 weeks. Degradation of C/EBP $\alpha$  by TRIB2 was shown to be via a proteasome dependent pathway as in a CO-IP experiment TRIB2 only associated with p42 in the presence of the proteasome inhibitor MG132. Structure-function analysis of TRIB2 revealed that deletion or mutation of the C-terminal COP1-binding site prevented TRIB2 mediated degradation of C/EBP $\alpha$  and thus failure to induce AML *in vivo* (Keeshan et al., 2010). Mutation of the TRIB2 pseudokinase domain prevented TRIB2 mediated C/EBP $\alpha$  degradation.

The TRIB2 induced increase in the p30 isoform has not yet been explained. TRIB2 might be proteolytically cleaving the p42 isoform or it could be switching on the

translation of the p30 isoform which has its own alternative translation initiation site (Lin et al., 1993). While it lacks the N-terminal, p30 still contains the transactivation domain TAD2 and, as will be discussed in detail in section 3.1.1.1, p30 has been shown to be a dominant negative regulator of the p42 isoform and also binds different target genes (Pabst et al., 2001). A recent publication described a regulatory loop involving E2F1 and TRIB2, whereby E2F1 binds to the *TRIB2* promoter to increase translation of the TRIB2 protein (Rishi et al., 2014). TRIB2 then degrades p42 so that E2F1 repression is decreased. TRIB2 also causes an increase in p30, which lacks the ability to repress E2F1, and in this study p30 was shown to synergise with E2F1 to increase the level of TRIB2 promoter activation thus creating a positive feedback loop that contributes to the oncogenicity of TRIB2 (Figure 1. 8).

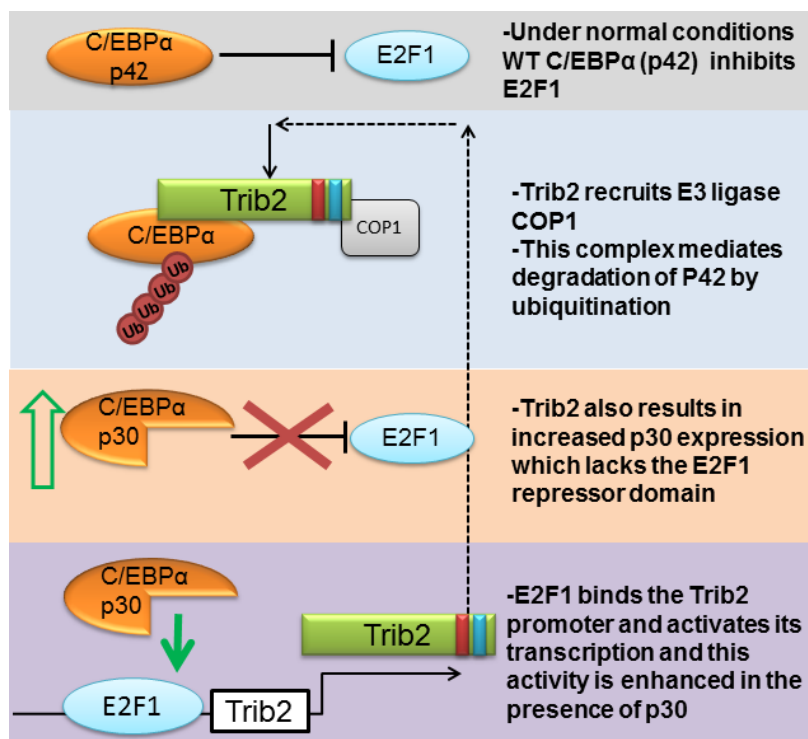


Figure 1. 8 – Diagram depicting Trib2 mediated degradation of p42, and p30 driven positive feedback loop of E2F1 regulation of Trib2 expression

As discussed in 1.2.2.2.4, overexpression of the HOX or HOX-NUP98 induces AML *in vivo* and *Meis1* overexpression is a co-operating event in their leukaemogenesis, although *Meis1* alone has no transforming ability. MEIS1 was retrovirally overexpressed in preleukemic *NUP98-HOXD13* (ND13) cells and CHIP analysis revealed occupation of *TRIB2* by MEIS1 (Argiropoulos et al., 2008). The authors showed that overexpression of TRIB2 on ND13 BM cells resulted in

increased cell growth. The site of integration of recombinant viral vectors can lead to activation of proto-oncogenes or inactivation of tumour suppressor genes, thereby contributing to leukaemogenesis. Viral insertion mutagenesis screens have been used to identify many oncogenes in murine tumours. Analysis of insertion sites in TRIB2 tumours uncovered *HoxA9* as a site of proviral insertion in 1 out of 4 tumours, which resulted in significantly increased HOXA9 expression (Keeshan et al., 2008). Mice transplanted with BM cells overexpressing both TRIB2 and HOXA9 rapidly develop AML with a much shorter latency (79 days) than those transplanted with TRIB2 (169 days) or HOXA9 (152 days) alone. In a study of HOXA9/MEIS1 tumours, *Trib1* was identified as a viral insertion site with TRIB1 expression upregulated as a result of the insertion (Jin et al., 2007). Like TRIB2, transplantation of BM cells co-expressing TRIB1 and HOXA9 generated a much more aggressive AML *in vivo* than induced by TRIB1 or HOXA9 alone.

Gene expression analysis of 13,000 genes in 285 human AML samples clustered patients into 16 groups based on their molecular signatures (Valk et al., 2004). Patients with *CEBPA* mutations were found in cluster 4 and 15. Elevated *TRIB2* expression was observed in a subset of samples in cluster 4 which did not harbour any mutations including *CEBPA*, indicating that *CEBPA* dysregulation was through a different mechanism in these patients (Keeshan et al., 2006). Further analysis of cluster 4 patient samples revealed that as expected *CEBPA* expression was very high in the samples which carried *CEBPA* mutations, but in those without mutations its expression was silenced, and this group also showed overexpression of T-lymphoid genes including *NOTCH1* and *CD7*, as well as *CD34* indicating an immature disease phenotype (Wouters et al., 2007). The authors explored a link between TRIB2 expression and NOTCH1 activation by treating NOTCH1-dependent murine cell lines, T6E and Scid.adh, with  $\gamma$ -secretase inhibitors to block NOTCH signalling and this led to down-regulation of *Trib2* expression suggesting that *Trib2* is a downstream target of NOTCH1. Conversely overexpression of intracellular notch (ICN1) in U937 cells resulted in an increase in *Trib2* expression. ICN1 binds the transcriptional repressor CSL to activate it and ChIP analysis of the ICN1/CSL complex revealed direct binding to two sites upstream of the *Trib2* transcriptional start site. These data demonstrate that

*Trib2* is a direct *Notch1* transcriptional target and that AML cases with elevated *TRIB2* expression may be due to dysregulated *NOTCH1* signalling.

Recently gene expression analysis has revealed that *TRIB2* expression levels, while generally low in AML, are higher in *PML-RARa* positive leukaemia (cluster 12) than *PML-RARa* negative leukaemia (Liang et al., 2013). As described in 1.2.2.2.5 *PML-RARa* is frequently associated with *FLT3* mutations. Within this cluster samples with increased *TRIB2* expression were observed in the *FLT3*-TKD positive group of *PML-RARa* positive leukaemia but not *FLT3*-ITD positive group. It was been shown that *FLT3*-ITD overexpression induces a myeloproliferative disease, whereas *FLT3*-TKD induced lymphoid disease (Grundler et al., 2005).

#### 1.3.4.1.2 T-ALL

*Trib2* expression is highest in T cells and there are several studies which implicate *TRIB2* in T-ALL pathogenesis. As outlined in 1.1.5 *NOTCH1* activation is essential for driving early T cell differentiation, and activating *NOTCH1* mutations are found in over 50% of T-cell acute lymphoblastic leukaemia (T-ALL) (Weng et al, 2004). As discussed above in section 1.3.4.1.1, gene expression profiling of 285 AML patient samples identified a subset of patients with high *TRIB2* expression that also displayed aberrant *NOTCH1* activation coupled with a mixed myeloid-lymphoid phenotype, and *Trib2* was shown to be a direct transcriptional target of *NOTCH1* (Wouters et al., 2007).

More recently *TRIB2* has been identified as a target of *PITX1* (Nagel et al., 2011) a gene which is regularly activated in T-ALL. *PITX1* was overexpressed in Jurkat cells, an immortalized human T lymphocyte cell line, and gene analysis revealed activation of *TRIB2* expression. Aberrant *TAL-1* activation is present in up to 60% of T-ALLs (Ferrando et al., 2002) and *TRIB2* has also been identified as a downstream target of the transcriptional complex controlled by *TAL-1* (Sanda et al., 2012). An inducible RNA interference screen in 2 *TAL1*-positive T-ALL cell lines revealed *TRIB2* as an essential gene for cell growth. T cell lines expressing shRNAs targeting *TRIB2* were unable to survive in culture. Silencing *TRIB2* expression in *TAL1*-positive T-ALL cell lines induced apoptosis, demonstrating that it is essential for the survival of these cells. Bioinformatic analysis of over 2000 patient samples spanning 16 different acute and chronic leukaemia

subtypes revealed that there were significantly higher levels of *TRIB2* in T-ALL and pre-B-ALL than any other leukemic subtypes (Hannon et al., 2012).

There is also data supporting a role for Trib1 and Trib3 in leukaemia. Gene expression analysis of *TRIB1* reveals it is significantly increased in M4 and M5 AMLs, and AML with inv(16) and t(16;16) (Liang et al., 2013). *Trib1* was identified as a retroviral insertion site in HOXA9/MEIS1 tumours and *TRIB1* was shown to cooperate with HOXA9/MEIS1 *in vivo* to reduce disease latency from 133 days (HOXA9/MEIS1) to 63 days (*TRIB1*/HOXA9/MEIS1) (Jin et al., 2007). Alone *TRIB1*, but not *TRIB3*, overexpression induced murine AML by C/EBP $\alpha$  degradation (Dedhia et al., 2010). A study of Down syndrome related AML revealed a mutation in the *TRIB1* gene in 1 patient at arginine 107 (R107), located in the pseudokinase domain (Yokoyama et al., 2012). Mice transplanted with *TRIB1* or mutant R107 overexpressing BM, all developed AML, but with a significantly shorter latency in the R107 transplanted cohort. While *TRIB3* overexpression is unable to induce murine AML *in vivo* (Dedhia et al., 2010), bioinformatic analysis found significant upregulation of *TRIB3* expression in AML FAB subtypes M2 and M3, as well as in AML with t(8;21) and t(15;17) (Liang et al., 2013).

#### **1.3.4.2 *TRIB2* in solid tumour cancer**

##### **1.3.4.2.1 Melanoma**

Forkhead box proteins (FOX) are a superfamily of transcriptional regulators with diverse functions, and their dysregulation is implicated in a host of human cancers including melanoma. The FOXO subfamily, comprising FOXO1, FOXO3a, and FOXO4, regulate cell proliferation, survival and stress response. They are bona fide tumour suppressors. To identify regulators of FOXO activity, a 293T cell line was generated which could measure FOXO transcriptional activity (293foxREP) and a loss-of-function screen using an RNAi library of 7914 genes was performed (Zanella et al., 2010). *TRIB2* silencing in the 293foxREP cell line resulted in the induction of FOXO transcription. *TRIB2* expression was analysed in 154 patient samples of a variety of tumour types including breast, prostate and thyroid. 70% of skin cancer tumours analysed displayed elevated *TRIB2* expression. Gene expression analysis of 43 normal and melanoma tissues revealed that *TRIB2* expression was significantly upregulated in stage III or IV

melanoma. The authors then silenced *TRIB2* expression in a luciferase reporter assay using the G-361 human melanoma cell line and showed that there was an increase in *FOXO* transactivation. *TRIB2* knockdown in the G-361 line impaired cell growth and this effect could be rescued by overexpressing *TRIB2*. *TRIB2* has also been identified as a candidate biomarker in melanoma diagnosis and progression as it exhibits low expression in healthy skin samples, and this increases in benign melanoma, with highest expression seen in malignant melanoma samples (Hill et al., 2015).

#### 1.3.4.2.2 Lung Cancer

Expression of *C/EBPα* is essential for the differentiation of lung cells and its overexpression causes cell death in lung tumour cells. Considering the established relationship between *TRIB2* and *C/EBPα* in leukaemogenesis, the role of *TRIB2* in lung cancer has been examined. Transcriptional analysis of 8 non-small cell lung cancer (NSCLC) cell lines revealed significant upregulation of *TRIB2* in all, and analysis of *TRIB2* expression in 68 human primary lung tumour samples showed an increase in *TRIB2* mRNA in almost 30% of samples tested (Grandinetti et al., 2011). Knockdown of *TRIB2* in NSCLC lines reduced their proliferation and increased apoptosis, whereas *TRIB2* depletion in normal lung fibroblasts had no effect. This also translated *in vivo* where NSCLC lines transduced with control virus lead to the rapid generation of tumours while those transduced with a short hairpin RNA (shRNA) targeting *TRIB2* remained free of tumours for up to 240 days post-transplant. The authors then demonstrated a negative correlation between *TRIB2* and *CEBPA* expression in the 68 primary samples previously examined. In a luciferase reporter assay the authors showed that the presence of *TRIB2* resulted in a 3-fold decrease in activation of the reporter by *C/EBPα*, although the level of *C/EBPα* protein remained unchanged. Knockdown of *TRIB2* resulted in a 5 to 10 fold increase in the expression of *C/EBPα* target genes *GCSFR* and *NE2*. These data show that in this context *TRIB2* is exerting its oncogenic effects by modulating *CEBPA* transactivation as opposed to *C/EBPα* protein degradation as observed in AML induction. However the authors then performed immunoprecipitation-mass spectrometry in a NSCLC line transduced with *TRIB2* and identified the E3 ubiquitin ligase *TRIM21* as a binding partner, which they confirmed by CO-IP. When *C/EBPα* and *TRIB2* were co-transfected into 293T cells in the absence of *TRIM21*, little to no *C/EBPα* degradation was observed, but in the presence of

TRIM21 there was a significant decrease in C/EBP $\alpha$  protein levels indicating that both TRIB2 and TRIM21 are required for C/EBP $\alpha$  degradation.

#### 1.3.4.2.3 Liver Cancer

The wingless-type MMTV integration site (WNT) family of 19 secreted glycoproteins comprise a diverse family that regulate a host of functions from cell proliferation and stem cell self-renewal to migration and polarity, via  $\beta$ -catenin dependent and independent mechanisms. Both activating and inhibiting mutations in WNT pathways are found in many cancer types including liver cancer. Nuclear translocation of  $\beta$ -catenin results in transcriptional activation of downstream genes via T cell factor (TCF) and the Wnt/TCF pathway has been well established in hepatocarcinogenesis. Genome-wide ChIP-seq analysis and transcriptional profiling of TCF4 was performed in liver cancer cells and the data were intersected with transcriptional profiling of the HepG2 human liver cancer cell line which had WNT activation blocked using a dominant-negative TCF4 (Wang et al., 2013). The authors identified 63 genes with unique TCF4 binding regions that required WNT/TCF for expression of which *TRIB2* was among the most highly enriched. Silencing of *TRIB2* expression in HepG2 cells resulted in decreased cell proliferation and increased apoptosis, but had no effect on hepatocytes. *TRIB2* loss also impaired HepG2 cell colony forming ability and the ability of the cells to generate tumours *in vivo* suggesting that TRIB2 is essential for human liver cancer cell survival. The authors also demonstrated that TRIB2 was exerting its effects via interaction with 2 known tumour suppressor pathways in liver cancer, the Hippo and C/EBP pathways. *TRIB2* knockdown in HepG2 cells resulted in an increase of endogenous C/EBP $\alpha$ , and ectopic C/EBP $\alpha$  expression induced apoptosis in HepG2 cells.

The same group subsequently published a study showing that TRIB2 negatively regulates WNT activity (Xu et al., 2014). Overexpression of TRIB2 on two liver cancer cell lines (Bel-7402 and SMMC-7721) decreased cell proliferation, colony formation and growth *in vivo*. The authors chose these two cell lines because they have WT  $\beta$ -catenin, unlike the HepG2 line used in their previous study which carries a dominant active  $\beta$ -catenin mutation. In these lines, the authors showed that TRIB2 overexpression reduced WNT-mediated transcriptional activity and decreased levels of  $\beta$ -catenin and TCF4 protein but not mRNA. CO-IP experiments demonstrated that the E3 ligases  $\beta$ -TrCP, COP1 and SMURF3 all

bound to TRIB2 and their knockdown resulted in upregulation of  $\beta$ -catenin and TCF4. Indeed deletion of the E3 ligase binding region of TRIB2 impaired its ability to reduce  $\beta$ -catenin and TCF4 protein expression. This study highlights a dual role for TRIB2 in liver cancer acting as both a tumour suppressor and an oncogene highlighting the complex regulatory networks through which TRIB2 exerts its function.

Studies have also linked Trib1 and Trib3 to various forms of cancer. TRIB1 expression has been shown to be essential for the survival of prostate cancer cells and is linked with an aggressive disease phenotype and poor prognosis (Lin et al., 2014). TRIB1 is also involved in the etiology of glioma (Tang et al., 2015), breast (Bhushan and Kandpal, 2011), ovarian (Puiffe et al., 2007) and follicular thyroid cancer (Puskas et al., 2005). In a study of over 200 colorectal cancer (CRC) patients *TRIB3* expression was elevated and its expression correlated with poor overall survival (Miyoshi et al., 2009). The authors showed that knockdown of *TRIB3* expression in 7 different CRC cell lines resulted in decreased cell growth. *TRIB3* expression has also been shown to correlate with poor prognosis in breast cancer patients (Wennemers et al., 2011). Elevated *TRIB3* expression was reported in 56 of 60 human lung cancer samples studied and correlated with poor prognosis in NSCLC (Zhou et al., 2013).

Together these studies highlight the importance of TRIB2, and other family members, in the biology of cancer development across multiple cancer types. This thesis aims to provide further insight into the role of TRIB2 in hematopoiesis and AML pathogenesis in order to facilitate the future development of therapeutic strategies in a targeted approach to AML treatment.

## 2 Materials & Methods

### 2.1 Plasmids and cell lines

#### 2.1.1 Plasmids

All plasmids were purified from transformed chemically competent DH5 $\alpha$  *E.coli* cells using the PureYield™ Plasmid Midiprep System (Promega) according to the manufacturers' protocol. Concentration and purity were determined using a NanoDrop spectrophotometer ND-1000 (Labtech International).

For the production of retroviral particles the MigR1 expression vector was used (Figure 2. 1). MigR1 is an MSCV based retroviral construct carrying an internal ribosome entry site (IRES) and expressing enhanced green fluorescent protein (GFP) (Pear et al., 1998). MigR1 based expression vectors were packaged by 293T cells (2.2.1.1) using the packaging plasmid pCGP which encodes for the viral polyprotein *gag* and reverse transcriptase *pol*, and the envelope plasmid pCMV-VSV-G (VSVG).

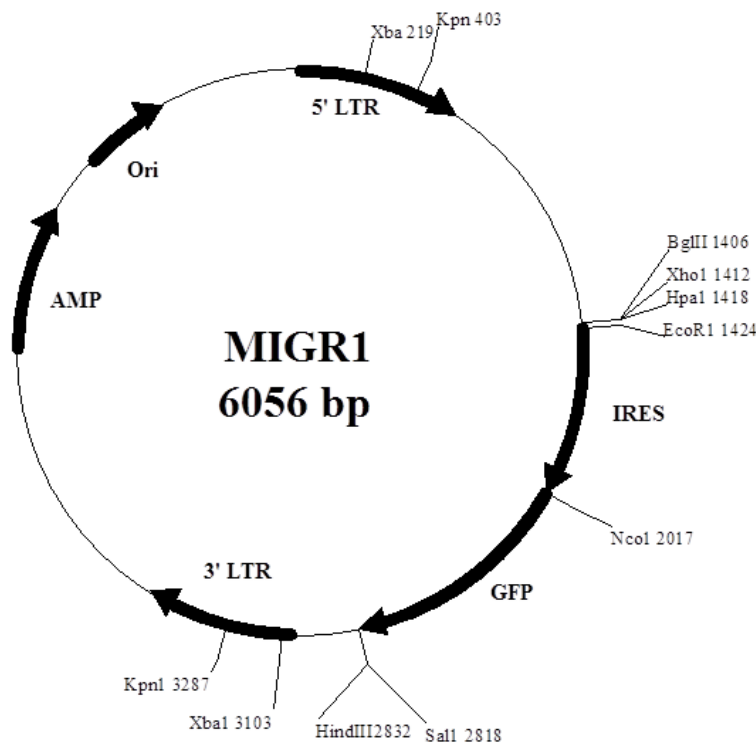


Figure 2. 1 – Plasmid map of retroviral expression vector MigR1

Rat C/EBP $\alpha$  (NM\_012524) with a C-terminus fused HA tag was cloned into either MigR1 to produce MigR1-C/EBP $\alpha$ , or pcDNA3.1-myc-HIS (PHMA) to produce HA tagged PHMA-C/EBP $\alpha$ . Rat C/EBP $\alpha$  cDNA with a C-terminus fused HA tag lacking the upstream open reading frame (ORF) was subcloned into the PHMA backbone to produce the HA tagged PHMA-p42 plasmid. C/EBP $\alpha$ -p30 expressing plasmids, which encode the p30 isoform of C/EBP $\alpha$ , were made by PCR amplification starting at the nucleotides corresponding to amino acid 118 of C/EBP $\alpha$  followed by a stop codon. The PCR product was subcloned into either the MigR1 vector to produce MigR1-p30 or the PHMA vector to produce PHMA-p30. The C/EBP $\alpha$  mutant K313R was created by Genescript in a PHMA expression vector (PHMA-K313R), and subcloned into the MigR1 backbone to produce MigR1-K313R. A 1032 base pair (bp) fragment encoding murine Trib2 cDNA (+/- N terminus FLAG tag) was subcloned into either MigR1 to produce MigR1-TRIB2, or a pcDNA3.1-myc-HIS to produce TRIB2-pcDNA3.1. For the dual-luciferase reporter assay (2.2.4) the reporter plasmid pTK-WT-G-CSFR-luciferase (*firefly*) contained 4 consensus C/EBP $\alpha$  binding sites from the G-CSFR promoter and the mutant pTK-MUT-G-CSFR-luciferase reporter construct contained 4 mutated C/EBP $\alpha$  binding sites. The pRL-TK (*renilla*) plasmid was used as a control. A 1203 bp fragment encoding the entire murine *Nfix* cDNA was subcloned (+/- N or C terminus MYC tag) into MigR1 to produce MigR1-NFIX. To date 4 murine transcriptional isoforms of NFIX have been found. The overexpression experiments outlined in chapter 5 were performed with NFIX transcript variant 2 (NM\_010906). All plasmids were available in-house.

Ubiquitin-HA, Ubiquitin/K48R-HA and Ubiquitin/K63R-HA used in ubiquitination assays (2.2.1.2) were kind gifts from Dr. R.J.Carmody, University of Glasgow.

### 2.1.2 Cell Lines

All cell lines were available in-house and were routinely tested for mycoplasma with the MycoAlert Mycoplasma Detection Kit (Lonza) in accordance with the manufacturers' protocol.

### **2.1.2.1 HEK293T Cells**

HEK293T cells (also referred to as 293tsA1609neo) are a human embryonic kidney cell line used for high efficiency transfections. They were derived from the HEK293 cell line which was engineered to stably express the SV40 large T antigen (DuBridgde et al., 1987). This permits episomal replication of plasmids that contain the SV40 origin of replication. These cells also have high expression of reverse transcriptase and envelope protein. As such they are used to produce high titre retroviruses and lentiviruses (Pear et al., 1993). HEK293T cells were cultured in Dulbecco's modified Eagles medium (DMEM) (Invitrogen) supplemented with 10% fetal bovine serum (FBS) (Invitrogen) and 1% Penicillin/Streptomycin (PS) (Invitrogen) and 1%L-Glutamine (L-Glut) (Invitrogen).

### **2.1.2.2 NIH/3T3 Cells**

NIH/3T3 cells are a mouse embryonic fibroblast cell line originally isolated from Swiss albino mouse embryo tissue (Todaro and Green, 1963). They are the gold standard in determining the efficiency of MSCV-based viruses, described in section 2.2.1.1.1. They were cultured in DMEM supplemented with 10% FBS, 1% PS and 1%L-Glut.

### **2.1.2.3 OP9 cells**

OP9 cells are a murine stromal cell line established from the calvaria of the toothless *op/op* mouse. These mice have a mutation which inhibits them from secreting M-CSF. The immunophenotype of OP9 cells has been reported to be identical to that of canonical mouse mesenchymal stem cells (Gao et al., 2010). OP9 cells are routinely used in different systems to study differentiation of stem and progenitor cells into myeloid, lymphoid and erythroid cells. In the presence of Flt3 and interleukin 7 (IL-7), OP9 cells support the differentiation of stem cells into B cells. OP9 cells were cultured in  $\alpha$ MEM media (Invitrogen) supplemented with 20% FBS, 1% PS, 1% L-Glut, 1% 100 mM sodium pyruvate (Invitrogen), 1% 1M HEPES (Invitrogen), 0.1% 2-mercaptoethanol (BME) (Sigma-Aldrich).

#### **2.1.2.4 WEHI-3B cells**

WEHI-3B cells are a murine myelomonocytic leukaemia cell line derived from the BALB/c mouse which underwent paraffin injections to induce tumour development in plasma cells (Warner et al., 1969). These cells produce very high levels of IL-3 due to retroviral integration close to the IL-3 gene locus.

Conditioned media from these cells are frequently used as a source of IL-3.

WEHI-3B cells were maintained in RPMI1640 (Invitrogen), 10% FBS, 1%PS and 1%L-Glut.

##### **2.1.2.4.1 WEHI conditioned media production**

WEHI-3B cells were seeded in T175 flasks at a concentration of  $10^5$  cells/ml to a final volume of 150 mls. After 3-4 days of incubation at 37°C, cell expansion results in the pH indicator causing a colour change. The conditioned media, now yellowish in colour, was removed and centrifuged at 300g for 10 mins.

Supernatant was filtered through a 0.45 µm minisart® syringe filter (Dutscher Scientific), and then stored in 10 or 50 ml aliquots at -20°C.

#### **2.1.2.5 BHK/MKL cells**

The BHK/MKL cell line was originally established by transfecting baby hamster kidney (BHK) cells with an expression vector encoding for SCF. BHK/MKL cells secrete SCF and conditioned media from these cells is used as a source of SCF. BHK/MKL cells were maintained in DMEM, 10% FBS, 1% PS and 1%L-Glut. BHK/MKL conditioned media was produced by the method outlined in section 2.1.2.4.1.

#### **2.1.2.6 Ba/F3 cells**

Ba/F3 cells are an IL-3 dependent immortalized pro B cell line derived from a C3H mouse (Palacios et al., 1987). Withdrawal of IL-3 induces apoptosis in Ba/F3 cells. They were cultured in RPMI1640, 10% FBS, 10% WEHI conditioned media (2.1.2.4.1), 1% PS and 1% L-Glut.

#### **2.1.2.7 32D cells**

32D cells are a murine myeloblastic cell line established from long-term murine BM cultures (Greenberger et al., 1983). Grown in the presence of IL-3 they remain undifferentiated, but removal of IL-3 induces apoptosis. 32D cells can be

induced to terminal granulocytic differentiation by replacing IL-3 with G-CSF. Thus they are useful for assessing the ability of a gene to induce or inhibit myeloid differentiation (described in section 2.2.3.1). 32D cells were maintained in RPMI1640, 10% FBS, 10% WEHI conditioned media (2.1.2.4.1), 1% PS and 1% L-Glut.

#### **2.1.2.8 C/EBP $\alpha$ <sup>-/-</sup> cells**

The C/EBP $\alpha$ <sup>-/-</sup> ( $\alpha$ <sup>-/-</sup>) cell line were originally derived from the fetal liver of *Cebpa* deficient mice (Zhang et al., 2002) and were maintained in Iscove's modified Dulbecco's medium (IMDM) (Invitrogen) supplemented with 15% FBS, 2% WEHI and 2% BHK/MKL conditioned media.

#### **2.1.2.9 Human leukaemia cell lines**

U937 cells are a human leukemic monocyte lymphoma suspension cell line isolated from a 37 year old male patient (Sundstrom and Nilsson, 1976). NB4 cells were isolated from leukaemia blast cells taken from an APL patient with t(15;17) that were cultured on bone-marrow stromal fibroblasts for 3 months before establishment of an immortalised line (Lanotte et al., 1991). The K562 suspension cell line was derived from a 53 year old female blast crisis phase BCR/ABL<sup>+</sup> chronic myeloid leukaemia (CML) patient. They do not express C/EBP $\alpha$  at the protein (Scott et al., 1992) or the mRNA (Radomska et al., 1998) level. Kasumi1 cells are a leukemic cell line established from an AML patient with t(8;21) resulting in the formation of the AML1-ETO fusion oncogene (Asou et al., 1991). As outlined in section 1.2.2.2.1, AML1-ETO downregulates *CEBPA* mRNA thus Kasumi1 cells do not express C/EBP $\alpha$  protein (Pabst et al., 2001). U937, NB4, K562 and Kasumi1 cells were all cultured in RPMI1640, 10% FBS, 1% PS and 1% L-Glut.

## **2.2 Tissue culture**

All tissue culture was performed in laminar air flow hoods (Biosafety Class II). Aseptic technique was adhered to throughout to ensure sterile work practices.

## 2.2.1 Transfection

HEK293T cells were used for efficient transfection of DNA to produce retrovirus, and for transient protein expression.

### 2.2.1.1 Production of retrovirus by calcium phosphate transfection

$5 \times 10^6$  HEK293T cells were seeded in a 10 cm dish at least 6 hrs in advance of transfection (Figure 2. 2). 2x transfection buffer (Table 2. 2) was freshly prepared in a 15 ml falcon tube. A DNA cocktail was prepared by combining 15  $\mu\text{g}$  of expression plasmid (MigR1), 10  $\mu\text{g}$  of pCGP and 6  $\mu\text{g}$  of VSVG with 50  $\mu\text{l}$  of 10x NTE (Table 2. 2) and 62.5  $\mu\text{l}$  of 2M  $\text{CaCl}_2$ , made up to 500  $\mu\text{l}$  with double distilled water (ddH<sub>2</sub>O). Media was removed from the plates and 3mls of fresh culture media was added gently to the plates without disrupting the adhered cells. 500  $\mu\text{l}$  of 2x transfection buffer was added dropwise to the DNA cocktail. A 1 ml pipette was used to blow bubbles slowly through the solution for 30 seconds (secs). The solution was then added drop by drop to the HEK293T cells evenly dispersing the drops across the plate. The plate was gently swirled before returning to incubator to ensure even distribution of the transfection solution. Cells were incubated at 37°C for 6-16 hrs before the media was removed and replaced with 4.5 mls of fresh culture media. Viral supernatants were harvested at 24, 36 and 48 hrs post-transfection. Supernatants were spun at 300 g for 5 minutes (mins) at room temperature (RT) before being aliquoted into 1 ml aliquots and snap frozen on dry ice then stored at -80°C.

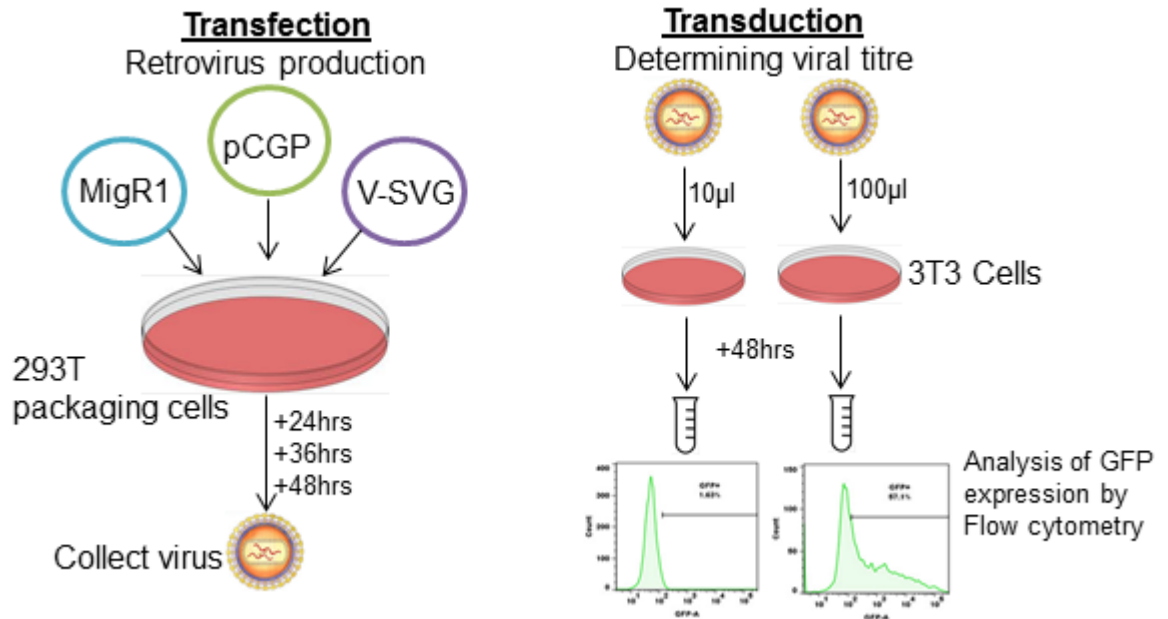


Figure 2. 2- Overview of retroviral production and titration process

#### 2.2.1.1.1 Titration of viruses using 3T3 cells

$2 \times 10^5$  NIH/3T3 cells were seeded in a 6 cm dish in 3mls of culture media and incubated at 37°C overnight (Figure 2. 2). For each virus to be titred 2 dishes were prepared. 24 hrs later the culture media was removed and replaced with 1ml of media supplemented with 4 µg/ml of polybrene (Sigma-Aldrich). Polybrene, also known as hexadimethrine bromide, is a positively charged cationic polymer which increases the efficiency of viral infection. It works by neutralising the charge repulsion between the viral particle and the cell surface. 10 µl of freshly thawed virus was added to one plate, and 100 µl to another allowing a linear range of transfection efficiency to be determined. The plates were gently swirled before overnight incubation. 24 hrs later 2 mls of fresh media were added to each plate. 24 hrs after this the media was removed, plates washed and cells were trypsinised and analysed for GFP expression by flow cytometry to determine the viral titre. The amount of virus needed was calculated as follows:

$$(X / \% \text{ titre}) \times (\text{Tested volume in } \mu\text{l} / 100) = \text{Volume of virus (mls) needed in final volume of 4mls where X is the desired \% titre}$$

For BMT experiments a 40% efficiency of transduction is optimal to avoid high titre virus resulting in multiple viral integrations *in vivo*. Thus to achieve equal transduction efficiencies using the above calculation:

If 60% of 3T3 cells expressed GFP with 100 µl of virus (and thus ~6% with 10 µl)

then:

$(40/60) \times (100/100) = 0.667$  mls or 667  $\mu$ l in a final volume of 4 mls

If 25% of 3T3 cells expressed GFP with 10  $\mu$ l of virus (and thus ~100% with 100  $\mu$ l)

then:

$(40/25) \times (10/100) = 0.16$  mls or 160  $\mu$ l in a final volume of 4 mls

### **2.2.1.2 TurboFect transfection for ubiquitination assays**

Transfections for ubiquitination assays (2.5.2) were performed using TurboFect Transfection Reagent (Fisher Scientific) as follows.  $1.5 \times 10^6$  HEK293T cells were seeded in a 6 cm dish 24 hrs before transfection. 0.5  $\mu$ g of Ub-HA (or K48-HA or K63-HA), 0.1  $\mu$ g of HA tagged PHMA-C/EBP $\alpha$  (or PHMA-p42, PHMA-p30 or PHMA-K313R) and 0.5  $\mu$ g of Trib2-pcDNA3.1 were diluted to a final volume of 400  $\mu$ l in serum free media (SFM). 8  $\mu$ l of TurboFect reagent were added to the tube, mixed gently by pipetting and incubated for 20 mins at RT. The transfection mix was added to the cells in a dropwise manner and plates swirled to ensure even distribution before being returned to the incubator. Cells were harvested for downstream processing 24 hrs later.

## **2.2.2 Retroviral transduction**

### **2.2.2.1 Suspension cell transduction**

Cells were passaged the day before transduction to ensure they would be in the log phase of growth when transduced.  $3-4.5 \times 10^6$  cells were centrifuged at 300 g and resuspended in 3 mls of culture media supplemented with 4  $\mu$ g/ml polybrene. Retrovirus was thawed rapidly and the appropriate volume, based on predetermined titre (2.2.1.1.1) was added to the cells. Cells were plated in a 6 well dish and centrifuged at 1000 g for 90 mins at RT. Cells were incubated at 37°C for 3-6 hrs. Cells were then transferred to a T75 flask with the addition of 20 mls of warmed media.

### **2.2.2.2 Primary cell transduction**

BM or FLCs were pre-stimulated overnight in DMEM supplemented with 15% FBS, 1% PS, 1% L-Glut, 10 ng/ml recombinant murine (rm) IL-3 (Peprotech), 10 ng/ml rmlL-6 (Peprotech) and 100 ng/ml rmSCF (Peprotech) at a final concentration of

2-5 x 10<sup>6</sup> cells/ml. The following morning cells were washed from plates and centrifuged at 300 g for 10 mins at 4°C. Cells were resuspended in DMEM and counted. 40-60% loss of cells was expected. Cells were resuspended in pre-stimulation cocktail without virus (3 mls per well with 4 ml volume of cytokines and polybrene). Cell concentration was 5-12 x 10<sup>6</sup> cells per well in 6 well plate. 3 mls of cell suspension were transferred to the well at which point the virus was thawed rapidly and added to the appropriate well. Where the volume of virus required was less than 1 ml, the remaining volume was made up with SFM. Plates were centrifuged at 1000 g for 90 mins at RT. Cells were incubated at 37°C overnight before a second spinoculation was performed the following morning. 1ml of cells from each well was transferred to a 1.5 ml Eppendorf tube and centrifuged at 300 g for 10 mins at 4°C. The supernatant was removed, pellet loosened by flicking, and resuspended in the appropriate volume of virus made up to 1 ml, and cytokines and polybrene (enough for 4 mls). The cell suspension was added back to the corresponding well and the plates were centrifuged at 1000 g for 90 mins at RT. Cells were incubated at 37°C until required.

## **2.2.3 Differentiation Assays**

### **2.2.3.1 32D Differentiation Assay**

32D cells were transduced with retrovirus expressing the gene of interest as per 2.2.2.1. 24 hrs post-transduction, cells were washed twice with WEHI free 32D culture media. Cells were then plated at 0.1 x 10<sup>6</sup> cells per well in either 10% WEHI (or 5 ng/ml rmlL-3) or 25 ng/ml recombinant human (rh) G-CSF (Peprotech). Cells were analysed for up to 7 days. Flow cytometry was performed to determine percentage GFP expression, and expression of the mature myeloid markers CD11b, Gr1 and F4/80. Control 32D cells stimulated with G-CSF will differentiate and display increased expression of mature myeloid markers when compared to control 32D cells maintained in IL-3.

### **2.2.3.2 Colony forming unit assay**

Colony-forming unit (CFU) assays are used to study HSPC activity *in vitro*. Single stem and progenitor cells can proliferate and differentiate into colonies in a semi-solid methylcellulose media supplemented with cytokines (Figure 2. 3). The number of colonies produced, indicates the proliferative capacity of a given cell.

The morphology of the colonies and surface marker expression of the cells indicates the differentiation state of the cells. The ability of the cells to self-renew can be assessed by serially replating cells i.e. WT HSPCs will exhaust by the 2<sup>nd</sup> replating (P) producing few or no colonies by P3. Cells that have been transformed by an oncogene will continuously replate in the CFU assay. Methocult GF M3434 (Stem Cell Technologies) methylcellulose media is optimised for use with murine BM and FL derived HSPCs. It is supplemented with rmSCF, rmlL-3, rhIL-6 and rhEPO. Aliquots of M3434 were thawed approximately 30 mins before use at RT. During this time the primary murine cells were prepared. The number of cells required for triplicate 35 mm dishes was calculated ( $5\text{-}20 \times 10^4$ ), and transferred to a sterile tube. Cells were centrifuged at 300 g for 5 mins. Cells were resuspended in 400  $\mu\text{l}$  of culture media, added to the thawed methylcellulose and mixed by pipetting up and down using a 16 gauge blunt end needle (Stem Cell Technologies) fitted with a 3 ml luer slip syringe (Terumo). Methylcellulose was allowed to rest for approximately 10 mins to allow air bubbles to dissipate. Using the blunt end needle and syringe, 1.1 ml of the final cell mixture was transferred to 3 x 35 mm culture dishes. Up to 6 dishes were placed in a 150 mm dish with 2 uncovered 35 mm dishes containing ddH<sub>2</sub>O to maintain humidity for optimal colony development. Cells were incubated for 7-14 days before colonies were counted, scored and cells analysed by flow cytometry. To assess transformation of stem and progenitor populations, cells were continuously replated to P5.

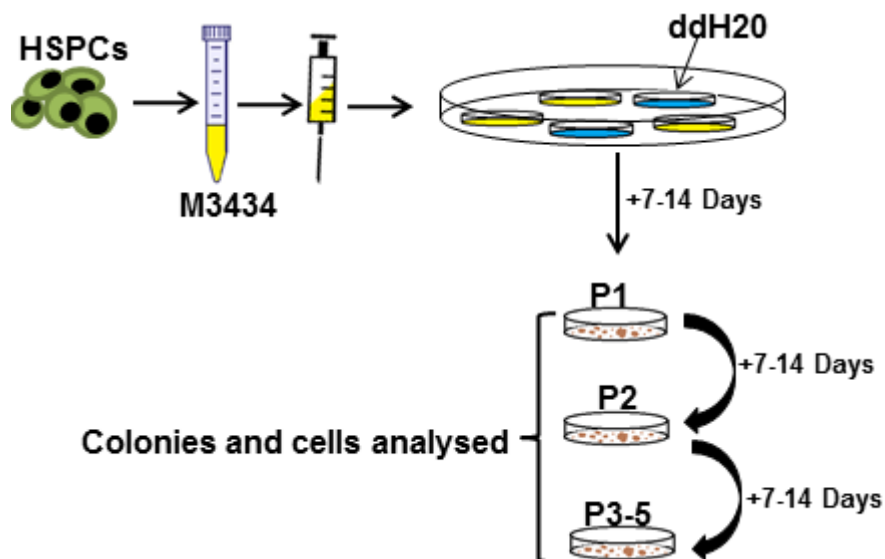


Figure 2. 3 – Schematic depiction of CFU assay

M3434 permits the growth of multipotential granulocyte, erythroid, macrophage, megakaryocyte colonies (CFU-GEMM) and granulocyte-macrophage colonies (CFU-GM), as well as the more restricted macrophage (CFU-M), granulocyte (CFU-G) and erythroid (BFU-E) colony types. These 5 colony types can be identified and counted based on their morphology using an inverted microscope and gridded scoring dish. GEMM colonies are typically very large with a dense core and a “cauliflower” shape. Granulocytic cells are round and bright and much smaller than cells of the monocytic lineage which are large and appear to have a grey centre permitting discrimination between CFU-GM which will contain both cell types, and CFU-G and CFU-M. BFU-E colonies contain erythroid cells which are hemoglobinised and thus appear red/brown in colour.

### **2.2.3.3 OP9 B cell differentiation assay**

OP9 cells were seeded at  $3 \times 10^4$  per well of a 6 well dish. 24 hrs later E14.5 FLCs or BM cells were co-cultured on OP9 cells in the presence of 1 ng/ml of rmlL-7 (Peprotech) and 5 ng/ml of rmlt3 (Peprotech) (Figure 2. 4). Every 2 days the media was removed from the dish, centrifuged and the pellet was resuspended in fresh culture media supplemented with fresh cytokines (after day 8, Flt3 was no longer added) and returned to the plates. Every 4 days the cells were passed to a fresh sub-confluent feeder layer of OP9 cells which had been seeded the previous day. The spent OP9 cells were also maintained and fresh supplemented media was added to these plates to maximise cell recovery as stem cells tended to burrow beneath the stromal layer. Cells were assessed by flow cytometry at different time points for up to 16 days of co-culture.

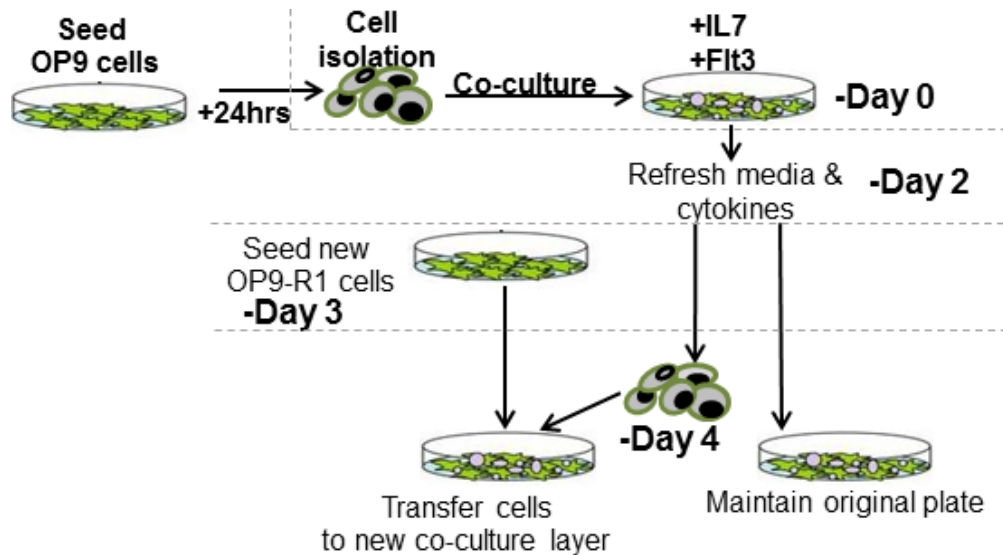


Figure 2. 4 – Diagram depicting OP9 co-culture system used to differentiate B cells

### 2.2.4 Dual-luciferase reporter assay

This assay uses 2 types of luciferase to study gene expression at the transcriptional level. *Firefly* luciferase (61kD) and *renilla* luciferase (36kD) emit light in a chemical reaction whereby the luciferase enzyme catalyses the conversion of luciferin to oxyluciferin. *Firefly* produces yellow/green light in the 550-570 nm range, while *renilla* produces blue light of 480 nm in length. The regulatory element (e.g. gene promoter) of interest is cloned into a vector upstream of the *firefly* luciferase gene. Cells are co-transfected with the *firefly* reporter vector and a control *renilla* reporter vector. A luciferase detection reagent is added to measure the amount of *firefly* luminescence - which is dependent on the response of the regulatory element to experimental conditions. Subsequently a *renilla* detection reagent is added to measure *renilla* luciferase activity which is independent of experimental modulation.

$5 \times 10^4$  293T cells per well were seeded in a 24 well dish. 24 hrs later they were co-transfected with 100 ng of G-CSFR promoter *firefly* luciferase constructs, containing either C/EBP $\alpha$  WT (pTK-WT-G-CSFR-luciferase) or mutant (pTK-Mut-G-CSFR-luciferase) binding sites, and 400 ng of either an empty PHMA vector or PHMA-C/EBP $\alpha$  or PHMA-K313R, along with 10 ng of pRL-TK Renilla luciferase internal control plasmid. Luciferase activity was measured 24 hrs post-transfection using the Dual-Luciferase Reporter Assay System (Promega). Cells were lysed using the passive lysis buffer in accordance with the manufacturers'

protocol. Growth medium was removed and the cells washed carefully once with phosphate buffered saline (PBS) (Table 2. 2) and lysed in 100  $\mu$ l of 1x lysis buffer. Luciferase detection was carried out in accordance with the manufacturers' protocol using a GloMax 20/20 luminometer (Promega). 10  $\mu$ l of cell lysate was added to 50  $\mu$ l of *firefly* luciferase assay buffer and mixed thoroughly by pipetting before luciferase reading was taken. 50  $\mu$ l of *renilla* luciferase assay buffer was then added and mixed by pipetting before luciferase reading was taken. *Firefly* luminescence readings were normalised to *renilla* values.

### 2.2.5 Magnetic-activated cell sorting

Magnetic-activated cell sorting (MACS) is a method for isolating cell populations based on their cell surface antigen expression. Positive selection (described in section 2.2.5.1) involves magnetic nanoparticles coated with antibodies against the antigen of interest being incubated with the cell population (Figure 2. 5), whereas negative selection (described in section 2.2.5.2) sees the cells of interest incubated with antibody coated magnetic particles directed against antigens that are not present on the cell of interest. Following incubation of the cells with the magnetic beads, cells are applied to a column held within a magnetic field and either the unbound cells that run through are collected (negative selection), or following the suspension passing through the column, the column is removed from the magnetic field and the cells that were bound to the beads are collected (positive selection). MS columns (Miltenyi Biotec) which can bind a maximum of  $10^7$  magnetically labelled cells were used where the maximum cell number did not exceed  $2 \times 10^8$ . LS columns (Miltenyi Biotec) which can bind a maximum of  $10^8$  magnetically labelled cells were used where the maximum cell number did not exceed  $2 \times 10^9$ .

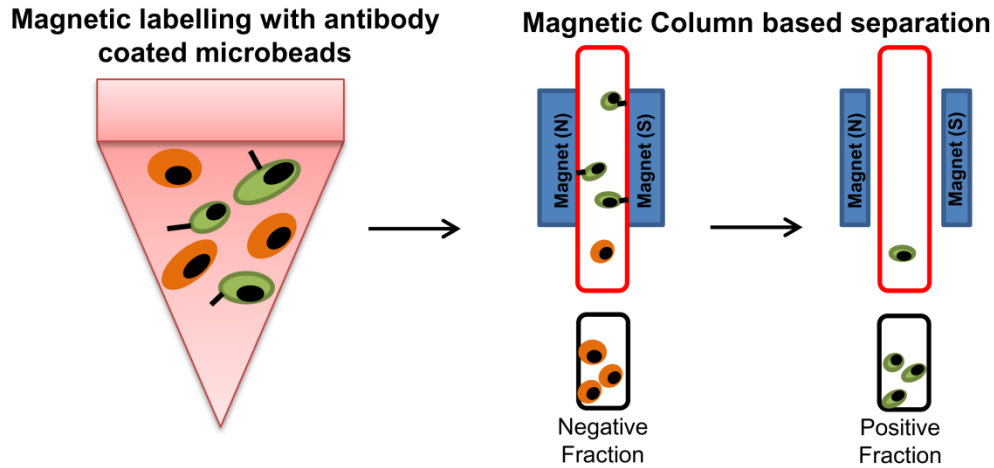


Figure 2. 5 - Schematic diagram depicting MACS cell sorting

### 2.2.5.1 cKit Purification

Murine BM cells were isolated and red blood cells (RBCs) lysed as per 2.3.2. Cells were enumerated and centrifuged at 300 g for 10 mins at 4°C. Supernatant was aspirated completely and the pellet was resuspended in 80µl of MACS buffer (Table 2. 2) per  $10^7$  cells. To this, 20 µl of cKit (CD117) microbeads (Miltenyi Biotec) were added per  $10^7$  cells. Cells were mixed well and incubated for 15 mins on ice. Cells were washed with 1 ml of buffer per  $10^7$  cells and centrifuged at 300 g for 10 mins. Pellet was resuspended up to  $10^8$  cells in 500 µl of buffer before proceeding with magnetic separation (2.2.5.3).

### 2.2.5.2 Lineage Depletion

Murine BM cells were isolated and RBCs lysed as per 2.3.2. Cells were enumerated and centrifuged at 300 g for 10 mins at 4°C. Supernatant was aspirated completely and the pellet was resuspended in a biotin-labelled lineage cocktail comprising CD3, CD4, CD8, B220, Ter119, CD11b (omitted for FLCs) and Gr1 (affymetrix eBioscience) (Table 2. 4). The cocktail was made with .07 mg/ml of each antibody per  $10^7$  cells at a final dilution of 1:50. Cells were incubated on ice for 15 mins then washed with 1 ml of MACS buffer per  $10^7$  cells and centrifuged for 10 mins at 300 g. The pellet was resuspended in 80 µl of MACS buffer per  $10^7$  cells and 30 µl of anti-biotin microbeads (Miltenyi Biotec) per  $10^8$  cells. Cells were mixed well and incubated for 15 mins on ice. Cells were washed with 1 ml of MACS buffer per  $10^7$  cells and centrifuged for 10 mins. The

pellet was resuspended up to  $10^8$  cells in 500  $\mu$ l of MACS buffer before proceeding with magnetic separation (2.2.5.3).

### 2.2.5.3 Magnetic separation

An MS or LS MACS column was placed in the magnetic field of the MACs Separator (Miltenyi Biotec). The column was equilibrated for 5 mins by adding 500  $\mu$ l (MS Column) or 3 mls (LS Column) of MACS buffer to the column. The cell suspension was then applied to the column and the flow-through was collected. The column was washed 3 times with the appropriate volumes of buffer -500  $\mu$ l for MS column or 3 ml for LS column- and washes were collected with the flow-through. This fraction contained cells unbound to the beads (i.e. for 2.2.5.1 cKit<sup>-</sup> cells, and for 2.2.5.2 for lineage<sup>-</sup> cells). To collect the bound fraction (i.e. for 2.2.5.1 cKit<sup>+</sup> cells, and for 2.2.5.2 lineage<sup>+</sup> cells), the column was removed from the separator and immediately placed on a 15ml collection tube. Either 1 ml (MS column) or 5 mls (LS column) of MACS buffer were added to the column and the cells were flushed out by inserting the plunger into the column.

## 2.3 Animal Work

Animal work was carried out in accordance with the guidelines outlined in the Animals Scientific Procedures Act 1986. WT C57BL/6 mice were purchased from Harlan UK or Charles River UK. WT B6.SJL-*Ptprc<sup>a</sup>*/BoyAiTac mice were kindly donated by Dr. Kamil Kranc and subsequently bred in house. All animals were maintained at the University of Glasgow, University College Cork and the University of Copenhagen, housed in accordance with their respective institutional guidelines. All work was carried out under the approval of the Home Office of the United Kingdom, Department of Health and Children Ireland, and Danish Ethical Committee.

### 2.3.1 BMT

The murine BMT is a powerful model for the study of hematopoietic stem and progenitor cell function, and when combined with retroviral transduction permits the study of the effects of a gene of interest on hematopoiesis and differentiation. The BMT model was used to transplant BM cells isolated from normal or fluorouracil (5-FU) treated donor mice transduced with a retrovirus of

interest (see 2.2.2.2) into donor mice whose hematopoietic compartment had been fully ablated through exposure to  $\gamma$ -irradiation (Figure 2. 6). 5-FU is a commonly used chemotherapeutic agent and when administered enriches for stem and progenitor cells in the BM. Where specified, in experiments where donor mice were treated with 5-FU, mice received intraperitoneal (IP) injections of injectable 5-FU 50 mg/ml solution (Accord Healthcare Limited) diluted in PBS to a final dose of 150-250 mg/kg. Following retroviral transduction  $0.2\text{-}1.5 \times 10^6$  cells were transplanted. When donor mice were not treated with 5-FU a total of  $3 \times 10^6$  cells were transplanted following retroviral transduction. The BMT model was also used to transplant leukemic cells or cells expanded in a CFU assay into mice whose hematopoietic compartment had been partially ablated by  $\gamma$ -irradiation. In this case  $1\text{-}6 \times 10^6$  donor cells were transplanted into recipient mice. Where specified, congenic transplants were performed (i.e cells from a CD45.2<sup>+</sup> mouse strain were transplanted into a CD45.1<sup>+</sup> recipient strain) allowing CD45.2 to be used to identify donor cells. Where syngeneic transplants were performed, GFP expression was used to monitor donor cells and disease progression.

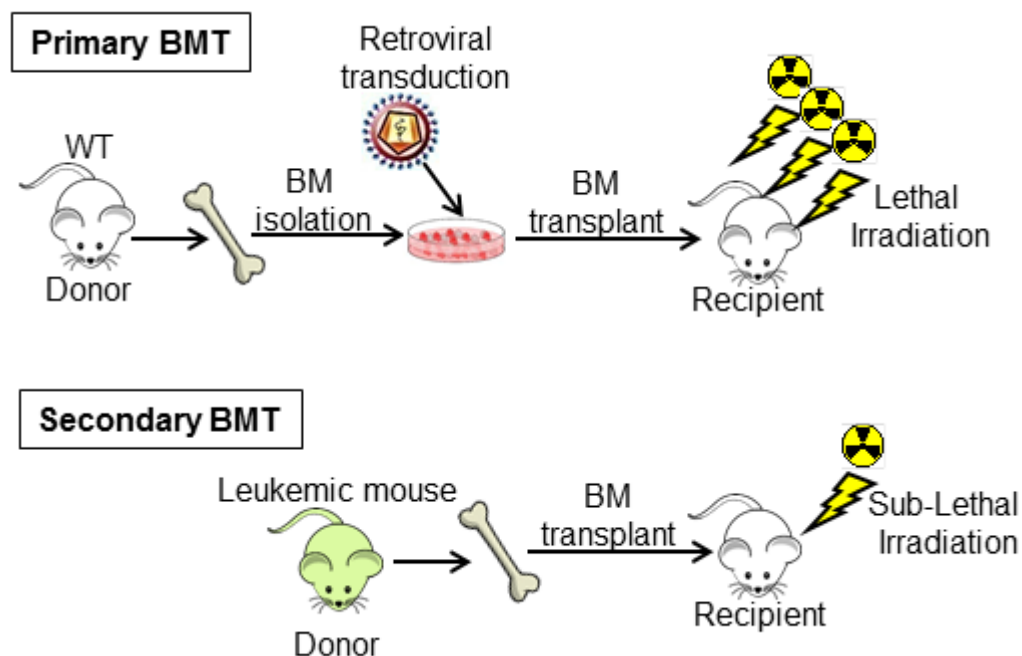


Figure 2. 6 – Experimental outline of a primary and secondary BMT.

Recipient mice were subjected to either lethal (either 1 x 9 Grays (Gy) or 2 x 4.5 Gys administered 4 hrs apart) or sublethal (1 x 6 Gys) whole body  $\gamma$ -irradiation. 4

hrs later mice received an intravenous (IV) injection of the appropriate number of donor cells in a final volume of 200ul of PBS supplemented with 2% FBS. Tail vein injections were performed using a 1ml insulin syringe with a 25g x 5/8” needle (VWR) after vasodilation stimulation under a heat lamp. Mice were maintained on 80 mg/L enrofloxacin (Baytril® injectable solution) supplied in the drinking water for 10-14 days post-transplant. Mice were monitored closely for signs of disease and blood samples taken every 2-4 weeks. For blood collection mice were first placed underneath a heat lamp to encourage vasodilation. The lateral tail vein was nicked with a lancet or the tip of a 25g needle and blood (15-50 µl) was collected in a Microvette® capillary blood collection tube (Sarstedt). Mice were euthanized according to approved Schedule 1 killing methods.

### **2.3.2 Harvesting tissues**

Immediately following confirmation of death, a cardiac puncture was performed using a 25G x 5/8” needle to remove blood for analysis. The femur, tibia and pelvic girdle were dissected out and cleaned carefully ensuring bones remained intact to maintain sterility of BM cells. Cleaned bones were dipped in 70% ethanol (EtOH) and rinsed in sterile PBS before crushing in PBS/2%FBS with a mortar and pestle to isolate BM cells. Cells were passed through a 40 µm cell strainer (Fisher Scientific). The spleen, thymus and lymph nodes were excised, and a single cell suspension was made by homogenising tissues through a 40 µm cell strainer in PBS/2%FBS using the plunger from a sterile 3 ml syringe (Terumo). For all tissues, cells were spun at 300 g for 10 mins at 4°C and RBCs were lysed by resuspending the pellet in RBC lysis buffer (Table 2. 2) and incubating on ice for 5 mins, before quenching the reaction with PBS.

### **2.3.3 Transgenic mouse models**

#### **2.3.3.1 *Trib2*<sup>-/-</sup> mice**

*Trib2*<sup>-/-</sup> mice (B6; 129s5-*Trib2*<sup>tm1Lex</sup>) were generated by Lexicon Genetics Ltd by targeting the coding and noncoding regions of exon 1. Mice were backcrossed to a C57BL/6 background for more than 10 generations.

##### **2.3.3.1.1 Genotyping and evaluation of *Trib2* excision**

Genomic DNA was isolated from tail or ear tissue of mice. Genotyping of *Trib2* WT and deleted alleles was performed using the following sets of primers: 5'-CACAATAGCGAGATATGGGAG-3', 5'-GCAATGCGACAAGTTCCGGAG-3' and 5'-GCAGCGCATCGCCTTCTATC-3' which amplified a 145bp WT allele and a 245bp deleted allele. PCR reactions were performed on a thermal cycler as follows: 5 mins at 94°C, followed by 40 cycles of 30 secs at 94°C, 30 secs at 40°C and 1 min at 72°C, followed by 5 mins at 72°C before cooling to 4°C.

### 2.3.3.2 *Cebpa* conditional model

*Cebpa<sup>fl/fl</sup>;Mx1cre* mice were crossed to *Cebpa<sup>+ / p30</sup>* (Kirstetter et al., 2008) (p30, also known as 'L' allele) to yield 4 genotypes - *Cebpa<sup>fl/+</sup>; Mx1Cre*, *Cebpa<sup>fl/p30</sup>;Mx1cre*, *Cebpa<sup>fl/+</sup>* and *Cebpa<sup>fl/p30</sup>*. 8-14 week old *Cebpa<sup>fl/fl</sup>*, *Cebpa<sup>fl/fl</sup>;Mx1Cre*, *Cebpa<sup>fl/+</sup>*, *Cebpa<sup>fl/p30</sup>* and *Cebpa<sup>fl/p30</sup>; Mx1Cre* mice were poly I:C treated to excise the *Cebpa* allele (Figure 2. 7). Animals received 3 injections every second day with 300 µg poly I:C. Resultant genotypes were *Cebpa<sup>fl/fl</sup>* (expressing solely p42 alleles which can give rise to p30), *Cebpa<sup>Δ/Δ</sup>* (null for p42 and p30), *Cebpa<sup>fl/+</sup>* (expressing solely p42 alleles which can give rise to p30), *Cebpa<sup>fl/p30</sup>* (expressing one p42 and one solely p30 allele), and *Cebpa<sup>fl/p30</sup>; Mx1Cre* referred to as *Cebpa<sup>Δ/p30</sup>* - solely expressing one p30 allele (Figure 2. 7).

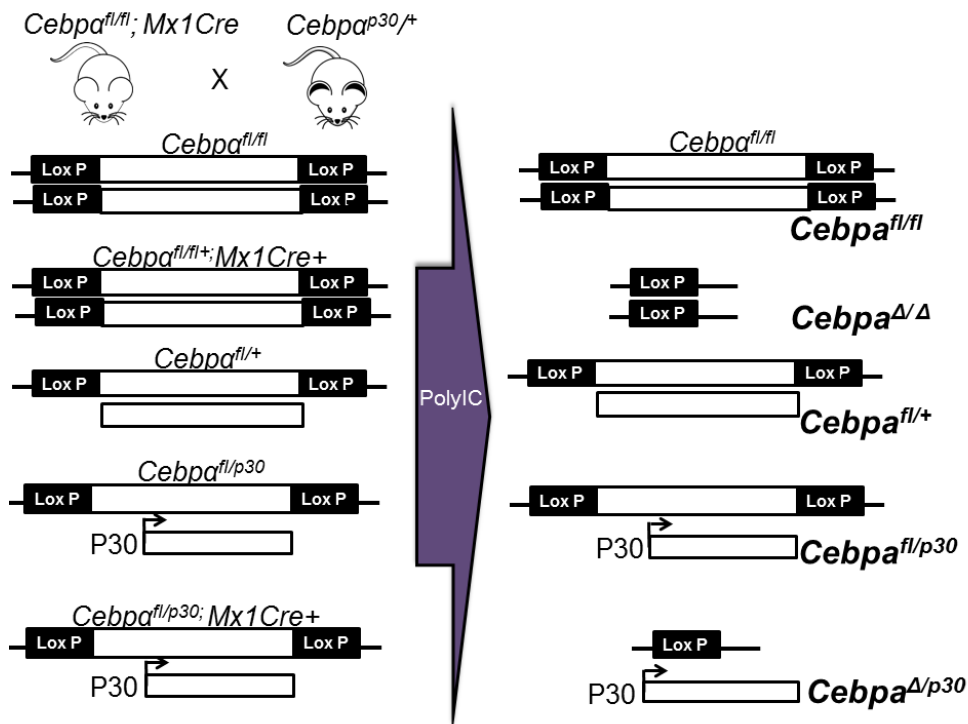


Figure 2. 7 - Schematic depiction of the generation of *Cebpa<sup>fl/fl</sup>*, *Cebpa<sup>Δ/Δ</sup>*, *Cebpa<sup>fl/+</sup>*, *Cebpa<sup>fl/p30</sup>* and *Cebpa<sup>Δ/p30</sup>* mice

### 2.3.3.2.1 Genotyping and evaluation of C/EBP $\alpha$ excision

Genomic DNA was isolated from tail or ear tissue of mice. Genotyping of floxed *Cebpa* allele was performed using the following sets of primers: 5'- CCACTCACCGCCTTGAAAGTCACA-3', 5'- CCGCGGCTCCACCTCGTAGAAGTCG-3' and 5'- GTCCTGCAGCCAGGCAGTGTCC-3' amplifying the 355 bp floxed allele and 560 bp deleted allele. Genotyping of the *Cebpa<sup>p30</sup>* allele was performed using the following sets of primers: 5'-GAC TCC ATG GGG GAG TTA GAG-3' and 5'- GCCTTGAAAGTCACAGGAG-3' amplifying a 270 bp WT allele and a 330 bp floxed allele. Confirmation of the presence or absence of *Mx1Cre* was performed using the following primers 5'- GCCTGCATTACCGGTCGATGCAACGA-3' and 5'- GTGGCAGATGGCGCGGCAACACCATT-3' amplifying the 706 bp Cre allele. PCR reactions were performed on a thermal cycler as follows: 4 mins at 94°C, followed by 35 cycles of 30 secs at 94°C, 30 secs at 55°C and 30 secs at 72°C, followed by 10 mins at 72°C before cooling to 4°C.

## 2.4 Flow Cytometry

Flow cytometry was performed using either a FACSCANTO, FACSCalibur or LSRII cell analyser (all BD Biosciences). For flow cytometry antibody information see

Table 2. 4. Unless otherwise stated samples were stained and analysed in FC Buffer (Table 2. 2), kept on ice throughout and compensation was carried out using unstained cells and single stained UltraComp Beads (affymetrix eBioscience). All data analysis was performed with FlowJo V7.6.5 or V10 (Treestar Inc). All analysis was performed on single cells gated through FSC-A versus FSC-H. Apart from the apoptosis assay, viable cells were analysed by gating through FSC and SSC, and with a DAPI dead cell exclusion dye used where the antibody panel permitted.

### **2.4.1 Determining surface antigen expression**

Cells were harvested, washed with FC buffer and stained with fluorochrome-conjugated antibodies (50  $\mu$ l per  $5 \times 10^6$  cells) at 4°C for 30 mins protected from light. Where biotinylated antibodies were used, cells were washed with FC buffer following incubation with primary antibody, and incubated with fluorochrome-conjugated streptavidin for 15 mins at 4°C protected from light. Cells were washed again with FC buffer and flow cytometric analysis was performed.

### **2.4.2 Apoptosis staining**

The tightly regulated process of programmed cell death is known as apoptosis. When cells enter apoptosis a phospholipid membrane protein normally bound internally, called phosphatidylserine, flips to the external membrane acting as a signal to macrophages. The cells then break apart and the fragments are engulfed by macrophages. To examine apoptosis by flow cytometry annexinV, which binds to phosphatidylserine, was used in conjunction with DAPI (Figure 2. 8). Neither annexinV nor DAPI will stain healthy intact cells (Q1). Cells undergoing early apoptosis will stain positively for annexinV and negatively for DAPI (Q2). Cells in late apoptosis, when the cell membrane has broken apart, will stain positively for both annexinV and DAPI (Q3) and dead cells will only stain positively for DAPI (Q4).

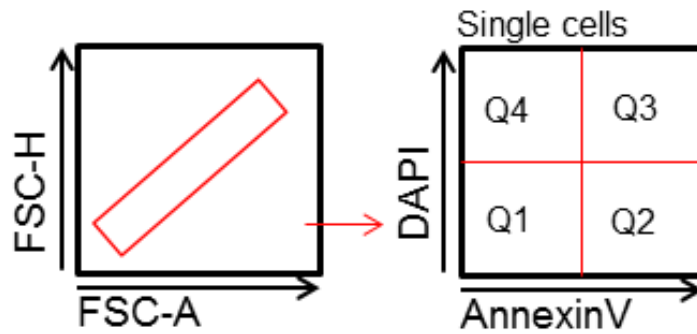


Figure 2. 8 – Gating strategy for detecting stages of apoptosis using flow cytometry

Cells of interest were centrifuged for 5 mins at 300 g and washed once with PBS before centrifuging as before. The cell pellets were resuspended in 50  $\mu$ l of annexinV at a 1:100 dilution in Hank's balanced salt solution (HBSS) (Sigma-Aldrich). The cells were incubated for 15 mins at RT protected from light. 400  $\mu$ l of HBSS was added to each tube along with DAPI to a final concentration of 1:1000. Samples were analysed by flow cytometry according to the gating in Figure 2. 8.

### 2.4.3 Proliferation assay

CellTrace™ Violet (CTV) (Invitrogen) is a fluorescent cell permeable dye that covalently binds to intracellular amine molecules allowing it to be retained inside the cell for long periods of time. Each time the cells divide the fluorescent CTV halves allowing cell division to be measured by flow cytometry. CTV was prepared to a 5 mM concentration by adding 20  $\mu$ l of DMSO to one vial of CTV reagent. The solution was stored at 4°C. Up to  $1 \times 10^6$  cells were pelleted at 300 g for 5 mins and washed once in PBS/2%FBS. Cells were resuspended in 1 ml of PBS/2%FBS to which 1  $\mu$ l of 5 mM CTV was added. Cells were incubated for 20 mins at 37°C protected from light. 4 ml of PBS/2%FBS were added to the cells and incubated for 5 mins at RT protected from light. The cells were then pelleted by centrifugation and washed once with complete media. The cells were seeded in the desired tissue culture dish with a sample taken to analyse by flow cytometry to confirm successful staining and to provide a day 0 control. Cells were subsequently assessed by flow cytometry at 24 hr intervals.

## 2.4.4 Fluorescence activated cell sorting

Fluorescence activated cell sorting or FACS uses the principles of flow cytometry to sort populations of cells on the basis of surface marker expression. When isolating primary stem and progenitor populations, total BM cells or FLCs were first MACS purified by cKit<sup>+</sup> selection (2.2.5.1) or lineage depletion (2.2.5.2). Cells of interest were harvested and washed with FC buffer and incubated with the appropriate antibodies. Cells were washed and resuspended in 400 - 600 µl of FC buffer and passed through a 40 µm cell strainer prior to sorting. Sorting was performed using a BD FACSAriaII (BD Biosciences). Schematic diagram of gating strategies used for the isolation of HSCs, MPPs, CLPs, CMPs, GMPs and MEPs is provided in Figure 1. 2.

## 2.5 Protein Assays

### 2.5.1 Western Blotting

Western blotting refers to the process of protein isolation, gel separation and subsequent transfer to a membrane to permit detection by blotting with a specific antibody.

#### 2.5.1.1 Preparation of cell lysates

##### 2.5.1.1.1 Tris or RIPA lysis

Cells were pelleted in a 1.5 ml Eppendorf tube at 300 g for 5 mins at 4°C. The media was aspirated from the cell pellet and the pellet was washed once with ice-cold PBS, supplemented with protease inhibitors - 1 mM phenylmethylsulfonyl fluoride (PMSF) (Sigma-Aldrich), 2 µg/ml aprotinin (Sigma-Aldrich), 2 µg/ml leupeptin (Sigma-Aldrich), 1 µg/ml pepstatin A (Sigma-Aldrich), 1 mM sodium orthovanadate (Na<sub>3</sub>VO<sub>4</sub>) (Sigma-Aldrich) and 1 mM sodium fluoride (NaF) (Sigma-Aldrich). Cells were lysed by adding Tris or RIPA lysis buffer (Table 2. 2) to cells and incubating on ice for 30 mins with gentle vortexing every 5 mins. Cells were then centrifuged at 14,000 g for 10 mins at 4°C. The supernatant was transferred to a fresh tube and stored at -80°C for future use, or protein concentration was determined using Bradford Reagent (Bio-Rad) according to manufacturers' protocol. The appropriate volume of protein was then resuspended in 2x SDS loading buffer (Table 2. 2)

supplemented with 4% BME and boiled for 5 mins at 95°C. Tubes were placed on ice to cool and then centrifuged for 30 secs. Sodium dodecyl sulphate-polyacrylamide gel electrophoresis (SDS-PAGE) and membrane transfer were then carried out as described in 2.5.1.2.

#### **2.5.1.1.2 Direct lysis**

For detecting C/EBP $\alpha$  expression, the direct lysis method was used. Cells were counted in duplicate to ensure accurate cell number.  $1.5 \times 10^5$  cells were centrifuged in a 1.5ml Eppendorf tube for 5 mins at 300 g at 4°C. All media was aspirated from pelleted cells, and cells were washed once with PBS. Cells were pelleted as before and all PBS was aspirated, with great care taken not to disrupt the pelleted cells. Cells were directly resuspended in 20  $\mu$ l of 2x SDS supplemented with 4% BME. The tube was vortexed and boiled for 3 mins at 95°C. Tubes were placed on ice and stored at -80°C or if loading directly they were snap frozen on dry ice or in liquid nitrogen, before thawing and carrying out SDS-PAGE gel electrophoresis and transfer as described in 2.5.1.2.

#### **2.5.1.2 SDS-PAGE and membrane transfer**

Proteins were separated using an 8-12% separating gel depending on the size of the proteins being visualised. Gels were hand cast using the Mini-PROTEAN Tetra Cell casting system (Bio-Rad). Glass plates were cleaned thoroughly before assembling with spacers in the casting frame and fixing in the casting stand. 10mls of desired percentage separating gel were prepared by mixing the appropriate volume of 30% Acrylamide/Bis-acrylamide (Sigma-Aldrich) (3.3 mls for 10% gel) with the corresponding volume of ddH<sub>2</sub>O (4.1 mls for 10% gel), 2.5 mls of 1.5 M Tris-HCl (ph 8.8), 100  $\mu$ l of 10% w/v SDS (Sigma-Aldrich), 100  $\mu$ l of 10% ammonium persulfate (APS) (Sigma-Aldrich) and 5  $\mu$ l of tetramethylethylenediamine (TEMED) (Sigma-Aldrich). The acrylamide was allowed to polymerise before 5 mls of stacking gel was prepared by mixing 830  $\mu$ l of 30% Acrylamide/Bis-acrylamide, 3.4 mls of ddH<sub>2</sub>O, 630  $\mu$ l of 1 M Tris-HCl (ph 6.8), 50  $\mu$ l of 10% w/v SDS, 50  $\mu$ l of 10% APS and 5  $\mu$ l of TEMED. The stacking gel was applied on top of the polymerised separating gel and the appropriate comb (10 or 15-well) was inserted between the plates. Once the stacking gel had polymerised the plates were fixed into the electrode assembly of the mini-tank (Bio-Rad) filled to the appropriate volume with running buffer (Table 2. 2),

samples were loaded and run at 100 volts until the gel had sufficiently resolved. Samples were run alongside a Precision Plus Protein Dual Colour Standards protein ladder (Bio-Rad). Gels were transferred onto a Protran nitrocellulose membrane (Whatman) using a 1x solution of transfer buffer (Table 2. 2). The membrane was first immersed in 1x transfer buffer along with gel blotting paper and sponges, before the gel/membrane sandwiches were assembled (as outlined in Figure 2. 9) in a Mini Trans-Blot cassette (Bio-rad). Cassettes were run at 100 volts for 1 hr in the Mini Trans-Blot cell (Bio-rad).

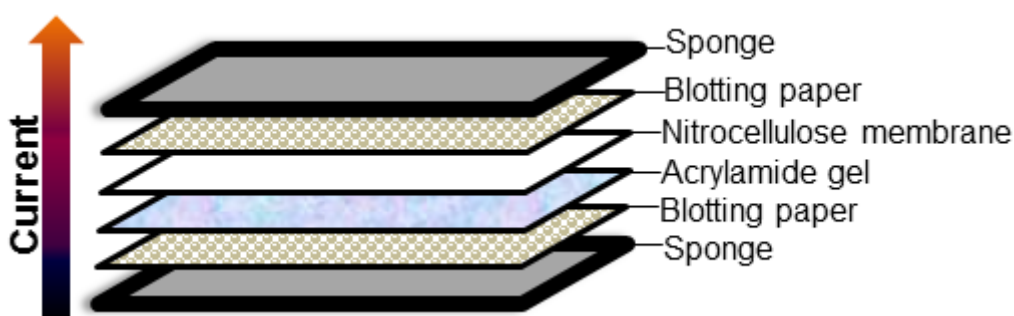


Figure 2. 9 – Diagram of the gel/membrane transfer sandwich

### 2.5.1.3 Antibody labelling and detection

All antibody incubation and washing steps were performed on an orbital shaker. All washes were done with 0.1% PBS-Tween (PBS-t). Membrane was stained with Ponceau S (Table 2. 2) to evaluate the efficiency of transfer. Stain was removed by washing 3 times in 0.1% PBS-t for 3 mins. Membrane was blocked in 0.1% PBS-t containing 5% non-fat milk for 30 mins at RT. Membrane was washed 3 times for 5 mins in 0.1% PBS-t. Blot was then incubated with the appropriate concentration of primary antibody for either 2 hrs at RT, or overnight at 4°C. Membrane was washed 3 times for 5 mins. The blot was then incubated with the appropriate secondary horse radish peroxidase (HRP) antibody for 1 hr at RT. The blot was washed 3 times for 10 mins at RT. The membrane was then visualised on CL Exposure Film (Life Technologies) using Signal West Pico or Femto (Life Technologies) ECL reagent. Details of antibodies used for western blotting are provided in Table 2. 5.

### 2.5.1.4 Stripping for re-probing

When necessary the nitrocellulose membranes were stripped to remove primary and secondary antibodies to permit re-probing with another antibody.

Membranes were incubated at RT on an orbital shaker in 10 mls of 1x Restore Western Blot Stripping Buffer (Sigma-Aldrich) for 10-15 mins. Membranes were washed three times with 0.1% PBS-t before blocking in 5% non-fat milk for 1 hr. Membranes were then re-probed with the appropriate primary and secondary antibodies as described in 2.5.1.3.

## 2.5.2 Ubiquitination assay

Ubiquitination (also known as ubiquitylation) is a post-translational modification which attaches ubiquitin (Ub) to a lysine (K) residue of a protein (Figure 2. 10). Briefly, Ub is activated in an ATP-dependent reaction by the E1 Ub-activating enzyme, the E2 Ub-conjugating enzyme transfers the Ub molecule from E1 to an active site on E2, and finally the Ub molecule is ligated with the target substrate via the E3 protein ligase. If subsequent Ub molecules are added in the same fashion then the substrate is described as polyubiquitinated. Ub molecules have 7 lysine residues (K6, 11, 27, 29, 33, 48 and 63) and so several different types of Ub chains can be formed depending on which lysine residue of the bound Ub the additional molecules bind to. K48-Ub chains signal the protein for proteasomal degradation. Whereas K63-Ub chains protect the protein from degradation, instead its function is linked with DNA repair and receptor endocytosis.

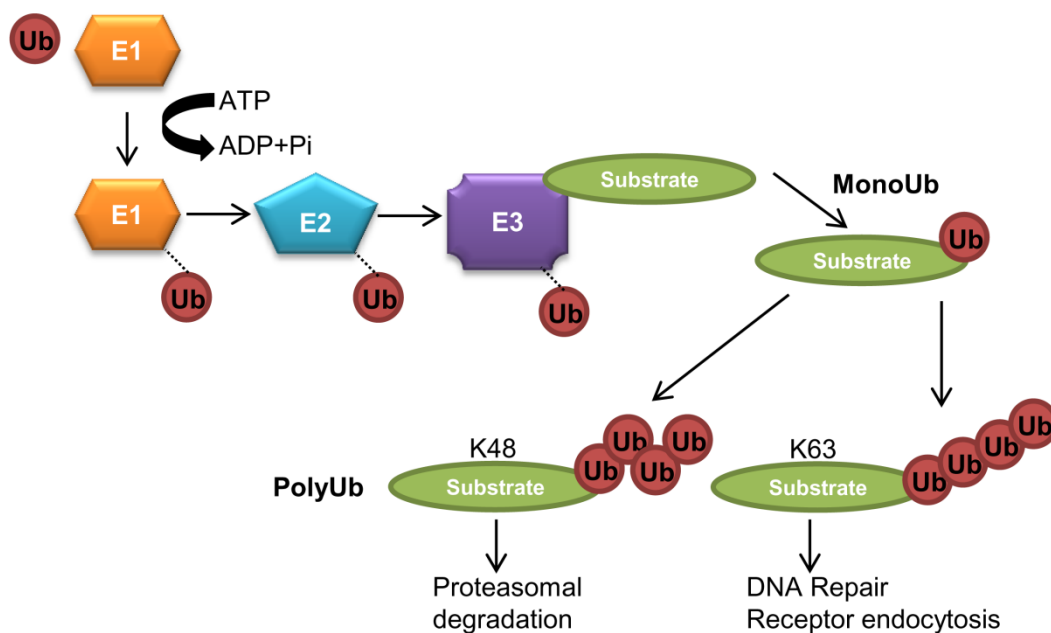


Figure 2. 10 – Diagram of the process of ubiquitination

### 2.5.2.1 Setting up the Ubiquitination IP

Cells were transfected as described in 2.2.1.2. 24 hrs post transfection cells were harvested. Plates were first incubated with 10 mM *N*-Ethylmaleimide (NEM) (Sigma-Aldrich), which inhibits deubiquitinases, for 30 secs before supernatant was aspirated and each plate was washed with 1 ml of ice-cold PBS supplemented with 10 mM NEM. Cells were removed from the plate with 1 ml of ice-cold PBS supplemented with 10 mM NEM using a cell scraper, and transferred to a 1.5 ml Eppendorf tube. Cells were centrifuged at 300 g at 4°C for 3 mins to pellet the cells. The supernatant was aspirated and cells were lysed with the addition of 100 µl of 1% SDS. Cells were then boiled at 95°C for 5 mins. Following boiling the cells were placed on ice and sonicated at 30% amplitude for 10-20 secs (at 1 sec intervals) using an EpiShear™ probe sonicator (Active Motif). Lysates were centrifuged at 14,000 g at 4°C for 10 mins. The cleared lysate was transferred to a clean Eppendorf tube. For the input sample, 10 µl of the lysate was taken and boiled with 10 µl of 2x SDS loading buffer, supplemented with 4% BME, for 5 mins at 95°C. These were either stored at -20°C until ready to use or run on a gel as described in 2.5.1.2. 900 µl of RIPA buffer (Table 2. 2) supplemented with 20 mM NEM and protease inhibitors (see 2.5.1.1.1) were added to the remaining 90 µl of protein lysate, along with 20 µl of Protein G Fast Flow Sepharose Beads (GE Lifesciences). Samples were incubated on a tube rotator (Stuart) at 4°C for 30 mins. Tubes were centrifuged for 1 min at 14,000g at 4°C. The supernatant was then transferred to a new 1.5 ml Eppendorf with 20 µl of fresh beads and 2 µl of concentrated (2 mg/ ml) C/EBPα antibody (Santa Cruz Biotechnology). Samples were incubated overnight at 4°C on a tube rotator.

### 2.5.2.2 Elution

Tubes were centrifuged for 30 secs at 14,000 g at 4°C. Pelleted beads were washed three times with supplemented RIPA (see above) by inverting the tube 10 times, and centrifuged for 30 secs at 14,000 g at 4°C. After the final wash, all supernatant was removed using a 26 gauge needle until beads were dry. 25 µl of 2x SDS loading buffer (with 4% BME) was added to each tube, tubes were vortexed, briefly centrifuged and then boiled at 95°C for 5 mins. Tubes were then vortexed, centrifuged and the sample was transferred to a fresh tube using

an insulin syringe with a 25g x 5/8” needle (VWR) taking care not to transfer any beads. Samples were then run on a gel as described in 2.5.1.2.

## **2.6 Gene Expression Analysis**

### **2.6.1 RNA extraction**

Total RNA was extracted using either the RNeasy Mini kit (Qiagen) for >50,000 cells, or for smaller cell numbers the Arcutus PicoPure kit (Fisher Scientific) was used, in accordance with the respective manufacturers protocol. Eluted samples were quantified on a Nanodrop ND1000 spectrophotometer (Labtech International). RNA was stored at -80°C until required.

### **2.6.2 cDNA synthesis**

RNA was reverse transcribed using the High Capacity cDNA Reverse Transcription kit (Applied Biosystems). RNA samples were prepared with ddH<sub>2</sub>O to a concentration of 500 ng to 1 µg of RNA per 20 µl reaction and mixed with 2 µl of 10x RT buffer, 0.8 µl of 100 mM dNTP mix, 2 µl of 10x RT random primers, 1 µl of RNase Inhibitor and 1 µl of MultiScribe Reverse Transcriptase (all Applied Biosystems). Samples were run in a Mastercycler thermal cycler (Eppendorf UK) with the following cycle - 10 mins at 25°C, 120 mins at 37°C, and 5 secs at 85°C. Synthesised cDNA was kept at 4°C in the short-term until ready for use or stored at -20°C for longer term storage.

### **2.6.3 qRT-PCR**

qRT-PCR was performed on the ABI Prism 7900 sequence detection system (Applied Biosystems). 2 µl of cDNA were used per 20 µl PCR reaction containing 10 µl of SYBR Green-PCR Master Mix (Applied Biosystems), 0.5 µl each of 10 µM forward and reverse primer and 7 µl of ddH<sub>2</sub>O. Samples were amplified on the thermal cycler for 40 cycles as follows: 2 mins at 50°C, followed by cycle of 10 mins at 95°C, 15 sec at 95°C and 1 min at 60°C, before cooling to 4°C. All reactions were performed in technical triplicates and the  $2^{-\Delta\Delta CT}$  method was used to calculate the relative level of gene expression in each sample. A list of primer sequences is provided in Table 2. 3.

## 2.6.4 Fluidigm™ high-throughput qPCR

Fluidigm™ is a high-throughput qPCR system to analyse large numbers of genes in a chip format (48.48 or 96.96). Samples are first pre-amplified and the resultant cDNA is used to examine 48 (or 96) genes across 48 (or 96) samples. The chip contains an integrated fluidic circuit (IFC) which combines the samples and primer-probe sets (also known as assays) in individual PCR reactions.

### 2.6.4.1 Preamplification and exonuclease treatment

Before use on the array, cDNA samples were first pre-amplified to enrich for loci of interest, and then treated with Exonuclease I (ExoI) to digest unincorporated primers. Forward and reverse primers were combined to a final concentration of 20 mM each. Then 5 µl of each primer pair were combined to a total of 500µl with 1x DNA suspension buffer (Fluidigm™). Pre-amplification samples were prepared in a 96 well plate by combining 1.25 µl of the pooled primer mix with 1.25 µl of cDNA and 2.5 µl of TaqMan PreAmp Master Mix (Applied Biosystems). Plates were sealed and amplified as follows: 10 mins at 95°C, 15 cycles of 15 secs at 95°C followed by 4 mins at 60°C, then cooled to 4°C. To perform ExoI treatment, ExoI (New England Biolabs) was diluted to 4 U/µl in water with ExoI Reaction Buffer (New England Biolabs). 2 µl of diluted ExoI was added to each 5µl preamplified sample, vortexed, centrifuged and placed in a thermal cycler for 30 mins at 37°C followed by 15 mins at 80°C before cooling to 4°C. Pre-amplified samples were diluted 5-fold in TE buffer and used immediately or stored at -20°C until ready to use.

### 2.6.4.2 Loading the chip

The 48.48 dynamic array was used with scope for up to 43 assays (with 5 housekeeping genes) and up to 16 triplicate samples. 96 well plates were used to prepare the assays and samples before loading the chip. To prepare the assays, first, primer pairs were prepared by combining forward and reverse primers to a final concentration of 20 mM each. Next 3 µl of 2x Assay Loading Reagent (Fluidigm™) was combined with 0.3 µl of 1x DNA suspension buffer and 2.7 µl of the pre-mixed primer pair in a well of a 96 well plate. Samples were prepared by mixing together 3 µl of 2x TaqMan Gene Expression Master Mix (Applied Biosystems) with 0.3 µl of 20X DNA Binding Dye Sample Loading Reagent

(Fluidigm™), 0.25 µl of 20X EvaGreen DNA binding dye (Biotium) and 2 µl of the pre-amplified Exol treated cDNA sample (2.6.4.1) in a well of a separate 96 well plate. Plates were vortexed for 30 secs and centrifuged for 30 secs. Before use, the chip was primed as per the manufacturers' protocol to prevent premature mixing of the samples and assays. 5µl from each well on the assay plate were loaded into the appropriate assay inlets on the left of the chip, and 5µl from each well on the sample plate were loaded into the appropriate sample inlets on the right of the chip (Figure 2. 11). The chip was placed in the IFC Controller MX system (Fluidigm™) where the integrated software initiated on-chip mixing of the components. The chip was then transferred to the BioMark HD system (Fluidigm™) to carry out qRT-PCR reactions, scanning and data collection. Fluidigm Real-Time PCR Analysis software (Fluidigm™) was used to perform data analysis and raw data were exported to Microsoft Excel where gene expression was calculated using the  $2^{-\Delta\Delta CT}$  method. A list of primer sequences is provided in Table 2. 3.

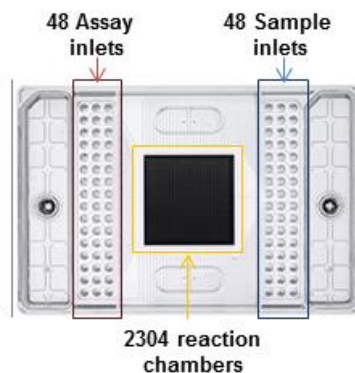


Figure 2. 11 – Fluidigm™ 48.48 Dynamic Array

## 2.7 Statistical analysis

Unless otherwise stated data represents mean value +/- standard deviation (SD). For statistical analysis comparing 2 groups an unpaired, two-tailed, Students t-test was used. For analysis of multiple groups a two-way ANOVA was applied. For comparison of survival curves a Log-rank test was used. Analysis was performed using GraphPad Prism 5 software (GraphPad Software Inc.). Significance was attained when the p-value  $\leq 0.05$  (\*),  $< 0.005$  (\*\*),  $< 0.001$  (\*\*\*) .

Table 2. 1 -Suppliers

<b>Name of Company</b>	<b>Address</b>
Accord Healthcare Limited	Durham, NC 27703, USA
Active Motif	Carlsbad, CA 92008, USA
affymetrix eBioscience	Hatfield AL10 9NA, UK
Applied Biosystems	Warrington, WA3 7QH, UK
BD Biosciences, Oxford UK	Oxford, OX4 4DQ, UK
BioRad	West Sussex, HP2 7DX, UK
Biotium	Hayward, CA 94545, USA
Charles River UK	Tranet, EH33 2NE, UK
Drew Scientific	Dallas, TX 75237, USA
Dutscher Scientific	Essex, CM13 3FR, UK
Eppendorf UK	Stevenage, SG1 2FP, UK
Fisher Scientific	Leicestershire, LE 1 5RG, UK
Fluidigm™	San Francisco, CA 94080, USA
GE Life Sciences	Buckinghamshire, HP7 9NA, UK
Genescript	Piscataway, NJ 08854, USA
GraphPad Software Inc.	La Jolla, CA 92037, USA
Harlan UK Ltd.	Blackthorn, UK
Integrated DNA technologies	B-3001 Leuven, Belgium
Invitrogen	Paisley, UK
Labtech International Ltd.	Milton Keynes, MK5 8LB, UK
Lexicon Genetics Ltd	Basking Ridge, NJ 07920, USA
Life Technologies	Gent 9050, Belgium
Lonza	Basel, Switzerland
Millipore	West Lothian, EH54 7BN, UK
Miltenyi Biotec	Surrey, GU24 9DR, UK
New England BioLabs	Ipswich, MA 01938, USA
PeproTech Ltd	London, W6 8LL, UK
Promega	Madison, WI 53711, USA
Qiagen	West Sussex, RH10 9NQ, UK
Santa Cruz Biotechnology	69115 Heidelberg, Germany
Sarstedt	51588 Numbrecht, Germany
Sigma-Aldrich	Dorset, SP8 4XT, UK
Stemcell Technologies	38000 Grenoble, France
Stuart	Staffordshire, ST15 0SA, UK
Terumo	Lakewood, CO 80215, USA
Tree Star, Inc.	Ashland, OR 97520, USA

VWR	Wayne, PA 19087, USA
Whatman plc	Kent, ME14 2LE, UK

Table 2. 2 -Recipes

<b>Solution</b>	<b>Ingredient</b>	<b>Concentration</b>
<b>PBS</b> Diluent : ddH2O	NaCl KCl Na <sub>2</sub> HPO <sub>4</sub> KH <sub>2</sub> PO <sub>4</sub>	137 mM 2.7 mM 10 mM 1.8 mM
<b>2 x Transfection Buffer</b> Diluent : ddH2O	HEPES NaCl Na <sub>2</sub> HPO <sub>4</sub>	42 mM 274 mM 1.4 mM
<b>10xNTE</b> Diluent : ddH2O	EDTA (ph8) Tris-HCl (ph7.5) NaCl	10 mM 100 mM 5 M
<b>RBC Lysis Buffer</b> Diluent : ddH2O	NH <sub>4</sub> AC KHCO <sub>3</sub> EDTA	150 mM 10 mM 0.1 mM
<b>MACS Buffer</b> 1xPBS	EDTA FBS	2 mM 2%
<b>FC buffer</b> Diluent : 1x PBS	HEPES NaN <sub>3</sub> BSA	10 mM 0.02% 0.20%
<b>Tris lysis buffer</b> Diluent : ddH2O	Tris pH7.4, NaCl, EDTA NP-40 Glycerol	50 mM 150 mM 1 mM 0.50% 5%
<b>RIPA lysis buffer</b> Diluent : ddH2O	Tris-HCl ph7.4 NaCl Triton x-100 Sodium deoxycholate SDS EDTA	50 mM 150 mM 1% 1% 0.10% 1 mM
<b>2XSDS</b> Diluent : ddH2O	Tris-HCl (ph6.8) SDS Bromophenol blue Glycerol	125 mM 4% 0.01% 20%
<b>Running buffer</b> Diluent : ddH2O	Trizma base Glycine SDS	25 mM 190 mM 0.10%

<b>Transfer buffer</b> Diluent : ddH2O	Trizma base Glycine Methanol	25 mM 190 mM 20%
<b>Ponceau S</b> Diluent : ddH2O	Ponceau S Glacial acetic acid	0.20% 5%

Table 2. 3 -DNA primer sequences

<b>Gene Symbol</b>	<b>Oligonucleotide sequence (5'-3')</b>	
<b><i>Abl</i></b>	<i>forward</i>	TGGAGATAAACTCTAAGCATAACTAAAGGT
	<i>reverse</i>	GATGTAGTTGCTTGGGACCCA
<b><i>Gusb</i></b>	<i>forward</i>	GGGACAAAAATCACCCCTGCG
	<i>reverse</i>	GCGTTGCTCACAAAGGTCAC
<b><i>B2M</i></b>	<i>forward</i>	TGCTATCCAGAAAACCCCTCA
	<i>reverse</i>	TTTCAATGTGAGGCGGGTGG
<b><i>Tbp</i></b>	<i>forward</i>	GCA GTGCC CAGCATCACTAT
	<i>reverse</i>	GCCCTGAGCATAAGGTGGAA
<b><i>Hprt1</i></b>	<i>forward</i>	GAGAGCGTTGGGCTTACCTC
	<i>reverse</i>	ATCGCTAATCACGACGCTGG
<b><i>Rnf20</i></b>	<i>forward</i>	ACCATCAATGCCCGGAAGTT
	<i>reverse</i>	GCA GCGATACTCTGGGGTTT
<b><i>Enox2</i></b>	<i>forward</i>	CGGCTGTTTAAGGAGTAGCG
	<i>reverse</i>	AGCTGGTTCAATCCTGGAACAT
<b><i>Nfix</i></b>	<i>forward</i>	AAACCAGCAAGGAGATGCGG
	<i>reverse</i>	TGATGCAGTCGCAACTGGAG
<b><i>Blink</i></b>	<i>forward</i>	GGTAAGCCCTGGTATGCTGG
	<i>reverse</i>	CTAGGGTGTACGGCTGCTTG
<b><i>E2a</i></b>	<i>forward</i>	GCCTGGATACTCAGCCGAAG
	<i>reverse</i>	TAGAAGGGGGAGGGGTAAGC
<b><i>Pax5</i></b>	<i>forward</i>	GAC ATC TTC ACC ACC ACG GAA
	<i>reverse</i>	AGGACTGTGGGCCTGGAAC
<b><i>Ikaro s</i></b>	<i>forward</i>	AGGGTCAAGACATGTCCCAAG
	<i>reverse</i>	GCTGTGCTCCAGAGGTAGTG
<b><i>CD19</i></b>	<i>forward</i>	AAACCTGACCATCGAGAGGC
	<i>reverse</i>	GGGTCAGTCATTGCTTCCTT
<b><i>Flt3</i></b>	<i>forward</i>	TTGGCCTTTGTGTCTTCCGT
	<i>reverse</i>	TTGCGAGCTGGTAGCGTTTA
<b><i>Ebf1</i></b>	<i>forward</i>	CCATGTCCTGGCAGTCTCTGA
	<i>reverse</i>	TCCATCCTTCACTCGGGCT
<b><i>Id1</i></b>	<i>forward</i>	GAACCGCAAAGTGAGCAAGG
	<i>reverse</i>	AACACATGCCGCTCGG
<b><i>Id2</i></b>	<i>forward</i>	CCTGGACTCGCATCCCACTA
	<i>reverse</i>	AGGGAATTCAGATGCCTGCAA
<b><i>Id3</i></b>	<i>forward</i>	CCTCTTAGCCTCTTGACGAC
	<i>reverse</i>	CAGCTGTCTGGATCGGGAGAT
<b><i>Pu1</i></b>	<i>forward</i>	CGCACGAGTATTACCCCTAT
	<i>reverse</i>	GAGCTCCGTGAAGTTGTTCT
<b><i>Mpo</i></b>	<i>forward</i>	CCCAGGCATAAAAACCCGT

	<i>reverse</i>	TGAATTCTCCACTTCCCCCAG
<b>Mmp9</b>	<i>forward</i>	ACGACATAGACGGCATCCAG
	<i>reverse</i>	TGGGACACATAGTGGGAGGT
<b>C/ebpe</b>	<i>forward</i>	GAGGCAGCTACAATCCCCTG
	<i>reverse</i>	CACAGGGGCCTTGAGGACA
<b>Notch1</b>	<i>forward</i>	ATCAAGCGCTCTACAGTGGG
	<i>reverse</i>	AAACCTGACCATCGAGAGGC
<b>Gata3</b>	<i>forward</i>	GGGTCAGTCATTGCTTCCTT
	<i>reverse</i>	GTTACACACTCCCTGCCTT
<b>CD3delta</b>	<i>forward</i>	GGAACACAGCGGGATTCTGG
	<i>reverse</i>	ACCATCCTTCCACCGTTCCA
<b>CD3gamma</b>	<i>forward</i>	TCTCATTGCGGGACAGGATG
	<i>reverse</i>	TATTCCCGGTCCTTGAGGGG
<b>CD7</b>	<i>forward</i>	CACCTGGATTTGGGCGTCAT
	<i>reverse</i>	ACTGGTGTACGTCTTGGGC
<b>Rictor</b>	<i>forward</i>	GAGGTGGAGAGGACACAAGC
	<i>reverse</i>	CCGGACCATTCTGTCTCGTT
<b>Gata1</b>	<i>forward</i>	CTCCCCAGTCTTTCAGGTGT
	<i>reverse</i>	CAGGGTAGAGTGCCGTCTTG
<b>Gata2</b>	<i>forward</i>	TCACCCCTAAGCAGAGAAGC
	<i>reverse</i>	CATTGCACAGGTAGTGGCC
<b>Fog1</b>	<i>forward</i>	CAAACCTCCTCCAGACAGCC
	<i>reverse</i>	CTCTGGTCTCTCCGTTGGTG
<b>Klf1</b>	<i>forward</i>	CTAAGAGGCAGGCGGCACAT
	<i>reverse</i>	CTGAGCGAGCGAACCTCC
<b>Fli1</b>	<i>forward</i>	ATCTGAAGGGGCTACGAGGT
	<i>reverse</i>	ACCACAGACAGAGCCTCCTTA
<b>Mpl</b>	<i>forward</i>	AACAAGACCGCACTAGCTCC
	<i>reverse</i>	GCGGTTCCCTCCTTTCACAT
<b>Trfr1</b>	<i>forward</i>	TCCGCTCGTGGAGACTACTT
	<i>reverse</i>	ACATAGGGCGACAGGAAGTG

Table 2. 4 -Flow cytometry antibodies

Name of antibody	Reactive species	Clone	Source
AA4.1 (CD93)	Mouse	AA4.1	affymetrix eBioscience
B220 (CD45R)	Mouse	RA3-6B2	affymetrix eBioscience
CD3	Mouse	CD3e	affymetrix eBioscience
CD4	Mouse	RM4.5	affymetrix eBioscience
CD8	Mouse	53-6.7	affymetrix eBioscience
CD11b (Mac1)	Mouse	M1/70	affymetrix eBioscience
CD11c	Mouse	N418	affymetrix eBioscience
CD16/32	Mouse	2.4G2	affymetrix eBioscience
CD19	Mouse	eBIO1D3	affymetrix eBioscience
CD34	Mouse	ram34	affymetrix eBioscience
CD41	Mouse	MWReg30	affymetrix eBioscience
CD43	Mouse	eBioR2/60	affymetrix eBioscience
CD45	Mouse	30-F11	affymetrix eBioscience
CD45.1	Mouse	A10	affymetrix eBioscience
CD45.2	Mouse	104	affymetrix eBioscience
CD48	Mouse	HM48-1	affymetrix eBioscience
CD71	Mouse	R17217	affymetrix eBioscience
CD105	Mouse	Mj7/18	affymetrix eBioscience
CD150	Mouse	TC15-12F12.2	affymetrix eBioscience
cKit (CD117)	Mouse	2B8	affymetrix eBioscience
F4/80	Mouse	BM8	affymetrix eBioscience
Flt3 (CD135)	Mouse	A2F10	affymetrix eBioscience
Gr1 (Ly-6G)	Mouse	RB6-8CS	affymetrix eBioscience
IL7Ra (CD127)	Mouse	A7R34	affymetrix eBioscience
MHCII	Mouse	AF6-120.1	affymetrix eBioscience
NK1.1	Mouse	PK136	affymetrix eBioscience
Sca1	Mouse	D7	affymetrix eBioscience
sIgM	Mouse	III41	affymetrix eBioscience
TCRB	Mouse	H57-597	affymetrix eBioscience
Ter119	Mouse	Ter119	affymetrix eBioscience

Table 2. 5 -Western blot antibodies

<b>Name of antibody</b>	<b>Reactive species</b>	<b>Dilution</b>	<b>Source</b>
Actin	Mouse	1/1000	Sigma
C/EBP $\alpha$	Rabbit	1/1000	Santa Cruz
HA	Mouse	1/1000	Sigma
K48	Rabbit	1/1000	Millipore
K63	Rabbit	1/1000	Millipore
Trib2 (b-06)	Mouse	1/1000	Santa Cruz

### **3 Results: C/EBP $\alpha$ in TRIB2 mediated AML induction**

Part of this chapter has been published in O'Connor et al, Oncogene, 2016, details provided in section 0.

## 3.1 Introduction

The p30 isoform of C/EBP $\alpha$  was first identified by western blot in 3T3 cells when a C-terminal specific C/EBP $\alpha$  antibody detected 42kD and 30kD proteins (Birkenmeier et al., 1989). Further 3T3 cell protein analysis at different stages of adipocyte differentiation revealed a change in the p42/p30 ratio as cells differentiated with no change in *Cebpa* mRNA levels (Lin et al., 1993). In healthy individuals, translation from the alternate ATG start site of *CEBPA* sees p30 co-expressed with p42 in some tissues, albeit at much lower levels than p42 expression. As discussed in section 1.2.2.2.1, frequently occurring N-terminal mutations in *CEBPA* result in increased levels of the p30 isoform and this shift in the p30/p42 ratio in favour of p30 is also observed with TRIB2 overexpression as outlined in section 1.3.4.1.1.

### 3.1.1 C/EBP $\alpha$ p30 targets

While p30 retains DNA binding and dimerization activity as the bZIP domain is still present, it lacks TAD1 as described previously and thus is unable to repress E2F activity. The TAD2 domain is common to both p42 and p30 and shared transcriptional targets have been identified. As discussed in section 1.1.3.3, C/EBP $\alpha$  can induce adipocyte differentiation from precursor cells, and both the p42 and p30 isoforms of C/EBP $\alpha$  have been shown to interact with the SWI/SNF complex in adipocyte maturation (Pedersen et al., 2001). The remodelling of chromatin to permit access of highly condensed DNA (wound around histones) to transcriptional machinery in order to control gene expression is performed by large multiprotein complexes. SWI/SNF describes a group of proteins derived from the *SWI* and *SNK* genes which can destabilise histone-DNA interactions and facilitate nucleosome (chromatin subunit) remodelling in an ATP-dependent manner. SWI/SNF complexes contain either the BRG1 or BRM ATPases. SWI/SNF is a bona fide tumour suppressor and has been shown to be mutated in over 20% of all human cancers (Kadoch and Crabtree, 2015). To investigate the ability of the C/EBP $\alpha$  isoforms to interact with SWI/SNF, a CO-IP was performed in C33A cells which lack *BRM* - one of the ATPase subunits of SWI/SNF. C33A cells were transfected with either p42, p30 or a p30 mutant lacking TAD2 (D1-215), along with BRM, and a CO-IP revealed that p42 and p30 but not D1-215 associated with BRM confirming that TAD2 was the site of SWI/SNF interaction. Through this

TAD2 mediated interaction p42 and p30 were both shown to act as lineage-instructive transcription factors directing differentiation in adipocytes.

Other studies reveal that p42 and p30 bind the same transcriptional targets but confer different effects. Chemokine receptors are a family of receptors which can induce cell migration towards a gradient of chemotactic cytokines. C-X-C chemokine receptor type 4 (CXCR4) is upregulated in many types of cancer and is the receptor for stromal cell-derived factor-1 (CXCL12), a ligand important for HSC homing and quiescence (Burger and Burkle, 2007). In AML, CXCR4 induces leukemic cells to migrate beneath the stromal layer of the BM, allowing them to evade chemotherapy. Unsurprisingly, CXCR4 expression in AML is correlated with poor prognostic outcome. A study of 220 *de novo* AML patient samples revealed that high CXCR4 expression was inversely correlated with *CEBPA* mutations, and positively correlated with WT *CEBPA* expression (Kuo et al., 2014). 293T cells were transfected with expression vectors carrying WT C/EBP $\alpha$ , or p30 or a C-terminal mutated (CTM) C/EBP $\alpha$ . WT C/EBP $\alpha$  increased CXCR4 expression at the mRNA and protein level, whereas p30 decreased CXCR4 transcription. Thus the N-terminal *CEBPA* mutation resulting in increased p30 would cause repression of CXCR4 activity and this might contribute to the favourable outcome of patients with biallelic *CEBPA* mutations, by increasing sensitivity to chemotherapy. In another study of C/EBP $\alpha$  target gene promoters it was observed that p30 had a 5-7 fold higher affinity than p42 for some promoters, namely *Pu1* and *Gcsfr* and equal affinity for neutrophil elastase (Cleaves et al., 2004). The authors subsequently show that, unlike p42 which positively regulates *Gcsfr*, p30 represses its expression, and so increased p30 expression in AML with N-terminal *CEBPA* mutations may result in competition with p42 for specific target gene promoters to exert opposing effects.

It is unclear how many target genes are shared between p42 and p30 but these studies outline both a complementary and competitive role for p30 on shared p42 target gene promoters. Several studies have also identified unique p30 target genes.

### 3.1.1.1 C/EBP $\alpha$ p42

Constructs of 5 different *CEBPA* N-terminal mutations were designed based on mutations identified in human AML samples. When WT and any of the 5 mutants, or WT and p30 vectors were *in vitro* translated at a 1:1 ratio, the resultant proteins reduced DNA binding activity compared to WT alone by over 80% (Pabst et al., 2001). Nuclear extracts were next isolated from 4 patients with N-terminal mutations and 2 patients without *CEBPA* mutations and it was shown that there was a reduction in binding to the gene which encodes for G-CSFR (*CSF3R*) in all 4 mutants compared with the patients without *CEBPA* mutations. Considering the heterozygous nature of the vast majority of bi-allelic *CEBPA* mutations, the authors investigated whether the presence of p30 would affect the transactivation ability of the WT protein. Increasing amounts of each of the 5 N-terminal mutant plasmids were transfected into CV1 cells, alongside a constant amount of WT plasmid in a luciferase reporter assay. The authors showed that the presence of any of the 5 mutants decreased the promoter activity, with a 2:1 ratio of mutant to WT sufficient to reduce the promoter activity to that seen with just the mutant plasmid. Interestingly when p30 was co-transfected with WT, a 1:1 ratio was sufficient to abrogate promoter transactivation from WT. These data suggest that p30 acts as a dominant negative regulator of p42, and that this function may contribute to leukaemogenesis in AML with N-terminal *CEBPA* mutations.

### 3.1.1.2 Ubiquitin conjugating enzyme 9

In order to elucidate the mechanism by which increased p30 can abrogate the DNA binding and transactivation potential of WT C/EBP $\alpha$ , the inducible K562C/EBP $\alpha$ p30-ER cell line was used to induce p30 expression through estradiol (ER) treatment, and samples were prepared for mass spectrometry to identify p30 target proteins (Geletu et al., 2007). The authors cross-referenced their results with proteins that were more than 2-fold upregulated in AML patients with an N-terminal mutation and identified 16 proteins common in both. Ubiquitin conjugating enzyme (*Ubc9*), which is upregulated in many cancers, was one of the novel p30 targets identified. Sumoylation is a post-translational protein modification in which 12kD small ubiquitin-like modifier (SUMO) proteins are added to or removed from proteins. Similar to ubiquitination, this process

occurs in 3 enzyme dependent steps with Ubc9 being the only E2 conjugating enzyme required for sumoylation. In a CO-IP, co-expression of WT C/EBP $\alpha$  and p30 in the presence of SUMO-1 enhanced sumoylation whereas no sumoylation was observed when p30 was co-expressed with the SUMO-deficient C/EBP $\alpha$  mutant K161R. Co-expression of p30 and SUMO with WT C/EBP $\alpha$  significantly reduced its ability to transactivate the *Cebpa* promoter in a luciferase reporter assay, while there was no change to the transactivation activity of K161R. The authors then showed using a Ubc9 siRNA that knockdown of *Ubc9* could overcome the p30 mediated increase in sumoylation and transactivation block of WT C/EBP $\alpha$ . These data provide a novel mechanism for the observed dominant negative regulation of p42 by p30, with p30 negatively regulating p42 expression by inducing its sumoylation.

### 3.1.1.3 Peptidyl-prolyl cis/trans isomerase

Peptidyl-prolyl cis/trans isomerase (PIN1) was also one of the 16 p30 target proteins identified by Geletu et al. PIN1 activity regulates cell proliferation and survival through interaction with kinase signalling pathways (e.g. MAPK). *PIN1* was shown to be overexpressed in many human cancers including brain, cervical, lung, ovary and prostate. Analysis of *PIN1* in human leukaemia samples showed higher levels of *PIN1* expression in AML samples compared with controls, and higher *PIN1* mRNA levels in *CEBPA* mutated AML compared with AML without *CEBPA* mutations (Pulikkan et al., 2010). *PIN1* is an E2F1 target gene and carries 3 E2F1 binding sites (Ryo et al., 2002), so the authors assessed *PIN1* promoter activity by E2F1 in the presence and absence of p30. Co-transfection of p30 with E2F1 significantly increased the activation of the *PIN1* promoter. Silencing of *PIN1* using an inhibitor (PiB) in the myeloid leukaemia cell line Kasumi-6, which endogenously express both p42 and p30, induced myeloid differentiation. Thus the authors hypothesise that p30, which lacks the E2F repression domain of p42, synergises with E2F1 to enhance the transcription of *PIN1*. As outlined in the introduction, a similar feedback loop was described for *TRIB2* whereby E2F1 binds the *TRIB2* promoter increasing *TRIB2* translation, which in turn degrades p42 and increases p30 which synergises with E2F1 to activate the *TRIB2* promoter (Rishi et al., 2014).

### 3.1.1.4 WD repeat-containing protein 5

MLL is a histone methyltransferase which mediates H3K4 methyltransferase activity via its SET protein domain. WDR5 is a core subunit of MLL/SET1 H3K4 methyltransferase complexes which are global regulators of gene transcription. It has been recently identified as a binding partner of p30 but not p42. Protein complexes were purified from cell lines overexpressing p42 and p30 and then mass spectrometry has identified 64 proteins that associated with p42, and 52 with p30, with only 14 in common to both (Grebien et al., 2015). Of the 52 identified p30 associated proteins, only 3 were related with transcription, and 2 of those 3 involved in histone modification/chromatin remodelling. One was SMARCD2 which is a component of the SWI/SNF complex discussed in 3.1.1, the other was WDR5. CO-IP confirmed that p30 but not p42, associated with WDR5 in 32D cells. Because WDR5 is required for H3K4 methylation by SET/MLL, and this methylation mark is associated with actively transcribed promoters, the authors performed H3K4me3 ChIP on p42 or p30 expressing cells. The results revealed a strong correlation between p30 binding and H3K4me3 marks on chromatin with 53% of p30 binding regions positive for the methylation marks, compared with just 18% of p42 binding regions. 2606 p30 target genes were shown to be actively transcribed with more than 10% of these genes showing significant changes in mRNA expression. Those upregulated were related with cell cycle control and mitosis, where as those downregulated were related with endoplasmic reticulum stress and suppression of transcription. Knockdown of *Wdr5* in p30 but not p42 expressing 32D cells resulted in upregulation of genes associated with myeloid differentiation as well an increase in Gr1 and CD11b expression in response to G-CSF stimulation.

These studies show that while p30 lacks a pivotal C/EBP $\alpha$  transactivation domain (TAD1), it not only retains some overlapping function with p42 through TAD2, but also has unique binding partners which mediate an array of functions.

### 3.1.2 Experimental mouse models of p30 in AML

As described in 1.2.2.2.1, up to 15% of AML patients have mutations in the *CEBPA* gene. The mutations are primarily found in patients with a normal karyotype and classified as M1 or M2 under the FAB classification system

(1.2.1.1). *CEBPA* mutations can be categorised as either N-terminal frame-shift mutations which result in a truncation of the p42 isoform with p30 remaining intact or C-terminal in-frame insertions or deletions which impede the DNA binding ability by disrupting the basic zipper domain. The N-terminal frame-shift mutation resulting in increased levels of p30 protein occurs most frequently. However it has been reported that most AML patients have more than one *CEBPA* mutation (>70%) and of those, the vast majority (>90%) have biallelic N-terminal and C-terminal mutations (Pabst and Mueller, 2007). As outlined earlier, perinatal lethality in the *Cebpa*<sup>-/-</sup> mouse results from hypoglycaemia (Wang et al., 1995). The first conditional *Cebpa* knockout (KO) mouse was developed by Dan Tenens' laboratory. They generated the *Cebpa*<sup>fl/fl</sup> strain, crossed them with *Mx1-Cre* transgenic mice and treated them with poly I:C thus producing the *Cebpa*<sup>Δ/Δ</sup> conditional KO. Analysis of the hematopoietic system of the *C/EBPα*<sup>Δ/Δ</sup> mouse revealed while the adult BM was filled with immature myeloblasts, the loss of *Cebpa* and resultant block in myeloid differentiation was not enough to induce AML *in vivo* (Zhang et al., 2004). Considering that the nature of *CEBPA* mutations indicates that *CEBPA* expression is rarely completely silenced, several murine models have been developed to facilitate the study of *CEBPA* mutations in AML.

### 3.1.2.1 The BRM2 knock-in murine model

*C/EBPα* is considered a tumour suppressor because it directly represses E2F activity (Slomiany et al., 2000) as outlined earlier. The p30 isoform of *C/EBPα* lacks the E2F repressor domain, thus in patients with N-terminal mutations, the excess p30 levels lead to dysregulation of E2F1 repression. To examine how *C/EBPα*-mediated E2F repression contributes to AML development, Claus Nerlovs' group generated a mouse with a homozygous knock-in mutation called BRM2 which abrogates E2F repression (Porse et al., 2005). The BRM2 point mutation preserves the ability of *C/EBPα* to bind DNA and activate promoters but it prevents the complex between *C/EBPα* and E2F from forming thus preventing E2F repression. By 36 weeks, the BRM2 mice develop a myeloproliferative disease overtime exhibiting splenomegaly and an increase in CD11b<sup>+</sup>Gr1<sup>+</sup> cells. However BRM2 mice did not succumb to full-blown AML. In addition to confirming the tumour suppressor function of E2F repression by

C/EBP $\alpha$ , this model demonstrates that disrupting this function alone is not sufficient to mimic the pathology of *CEBPA* mutated AML.

### 3.1.2.2 The L/+ and L/L knock-in murine model

In order to more accurately recapitulate the commonly occurring *CEBPA* mutations found in humans, Nerlov's group then generated a knock-in mouse where translation of p42 is specifically ablated (Kirstetter et al., 2008). Translation of p42 was disrupted by placing a Lox-P flanked cassette between the p42 and p30 initiation codons so that cre-mediated deletion of this cassette resulted in termination of p42 translation from the AUG, while maintaining p30 translation (termed the 'L' allele). Mice carrying the L allele were crossed with *MxCre* mice producing mice heterozygous for the allele (*Cebpa*<sup>Lp30/+</sup> also known as L/+), which were subsequently crossed to form the homozygous L/L mice which only expressed the p30 isoform. After 18 months L/+ mice displayed no disruption in any hematopoietic tissues and no perturbations to granulocytic differentiation being virtually indistinguishable from +/+ controls. L/L mice uniformly succumbed to AML after 9-14 months exhibiting excessive Cd11b<sup>+</sup>Gr1<sup>lo</sup> blasts in the BM, massive splenomegaly and infiltration of blast cells into the liver. Mimicking the most prevalent *CEBPA* mutation *in vivo* the authors here showed that p30 alone drives efficient transformation of granulocytes in the absence of p42.

### 3.1.2.3 The K/L and K/K knock-in murine model

Nerlov's group subsequently developed a mouse model to recapitulate the incidences of both the N-terminal and C-terminal mutations in *CEBPA* mutated AML. A knock-in allele was generated which mimicked one of the most commonly occurring C-terminal mutations i.e. the K313 duplication (K313dup) termed the K allele. The K313dup was first identified in CD7<sup>+</sup> M1 AML and it was shown to have lower protein stability than WT C/EBP $\alpha$  (Carnicer et al., 2008). The mutation may represent up to 10% of all *CEBPA* mutations. By combining the K allele (C-terminal mutation) with the aforementioned L allele (N-terminal mutation) to produce +/+, K/K, K/L and L/L mice (CD45.2<sup>+</sup>) the authors could recapitulate the spectrum of biallelic patient mutations (Bereshchenko et al., 2009). The authors transplanted FLCs from each genotype into CD45.1/2<sup>+</sup> recipient mice

with CD45.1<sup>+</sup> competitor BM cells. Analysis at 4.5 weeks post-transplant revealed expansion of the LSK compartment, primarily ST-HSCs and LMPPs, in K/L and K/K transplanted mice but not +/+ or L/L. K/L, K/K and L/L transplanted cells all induced lethal AML in recipient mice with the most aggressive disease arising from the K/L transplanted disease, and the longest latency from the K/K transplanted cells. The K/L and L/L leukaemia were granulocytic with myeloid blasts detected in the PB and infiltration into the spleen. However, only 25% of K/K leukaemias resembled this phenotype (myeloid with maturation). The remainder contained very few differentiated myeloid cells and instead were characterised by an increase in immature erythroid cells. The authors determined the reduced ability for K/K cells to induce myeloid AML with maturation was due to an inability to form committed myeloid progenitors. GMPs were detected at normal levels in L/L and +/+ mice, slightly lower in K/L mice and drastically reduced in K/K mice. This model demonstrates that the most aggressive AML was induced when the C-terminal and N-terminal mutations were combined and the ability of excess p30, arising from the N-terminal mutation, to induce myeloid differentiation was needed to form a myeloid leukaemia with maturation.

#### **3.1.2.4 The C/EBP $\alpha$ -N<sup>m</sup> and C/EBP $\alpha$ -C<sup>m</sup> overexpression murine model**

In another study 244 samples from patients with myelodysplastic syndrome (MDS) or AML were analysed and it was found that the biallelic heterozygous *CEBPA* mutations occur primarily in *de novo* AML whereas single N or C-terminal *CEBPA* mutations occur in therapy-related AML or MDS (Kato et al., 2011). The authors then generated an N-terminal mutant producing p30 only (C/EBP $\alpha$ -N<sup>m</sup>) which carried a T60fsX159 mutation between the p42 and p30 translational start sites, and a C-terminal mutant (C/EBP $\alpha$ -C<sup>m</sup>) carrying a 304\_323 duplication in the bZIP region. BM cells transduced with either mock, C/EBP $\alpha$ -N<sup>m</sup> or C/EBP $\alpha$ -C<sup>m</sup> retrovirus were transplanted into lethally irradiated recipients and it was shown that all C/EBP $\alpha$ -C<sup>m</sup> transplanted mice developed AML within 4-12 months characterised by CD11b<sup>+</sup>Gr1<sup>+</sup>cKit<sup>int/hi</sup> BM and splenic leukemic cells and splenomegaly. Less than half C/EBP $\alpha$ -N<sup>m</sup> transplanted mice developed disease, and in those that did a B-cell acute lymphoblastic leukaemia (B-ALL) was generated in most, characterised by accumulation of B220<sup>+</sup>CD19<sup>+</sup>cKit<sup>int/hi</sup> leukemic cells which infiltrated the spleen and liver. The authors then co-

transduced BM cells with C/EBP $\alpha$ -N<sup>m</sup> and C/EBP $\alpha$ -C<sup>m</sup> retrovirus, and transplanted cells expressing both into lethally irradiated recipient mice. These mice succumbed to disease with a shorter latency (3-5 months) than mice transplanted with one or the other mutant. They also exhibited an increased number of leukemic cells, and these cells were of a more immature CD11b<sup>int</sup>Gr1<sup>lo</sup>B220<sup>lo</sup>cKit<sup>lo</sup> myeloid blast phenotype when compared with the C/EBP $\alpha$ -C<sup>m</sup> transplanted mice. Contrary to observations made by Bereshchenko et al, the authors here conclude that it is the C-terminal mutation of *CEBPA* which affects differentiation, while the N-terminal mutation (i.e. excess p30) is responsible for expansion of the preleukemic cells.

## 3.2 Aims and objectives

The transcription factor C/EBP $\alpha$  is essential for granulocytic differentiation and while both isoforms p42 and p30 are commonly dysregulated in AML as well as other cancers, complete loss of C/EBP $\alpha$  expression rarely occurs. The oncogene TRIB2 drives AML *in vivo* by selectively degrading p42 but it remains to be shown whether or not C/EBP $\alpha$  expression is required for TRIB2 mediated AML. Indeed with TRIB2 mediated loss of p42, there is a marked increase in p30 expression in the resultant AML. TRIB2 has been shown to cooperate with other oncogenes (1.3.4.1.1) and it is unclear if p30 and TRIB2 cooperate in leukaemia induction. In fact the role of the p30 is not well understood in either normal hematopoiesis or AML. There is limited data available on the effect of p30 expression on steady state hematopoiesis and as outlined in 3.1.2 contradictory evidence exists implicating p30 in either a differentiation role in AML (Bereshchenko et al., 2009) or promoting proliferation of leukemic blasts (Kato et al., 2011). As such the specific aims of this chapter were:

- i. To determine the effect of enforced p30 expression on steady state hematopoiesis using an *in vivo* transplantation technique
- ii. To examine the proteolytic relationship between TRIB2 and C/EBP $\alpha$  isoforms p42 and p30
- iii. To address the role of p42 and p30 in TRIB2 mediated AML induction by utilising a conditional animal model to
  - a. Determine if C/EBP $\alpha$  is required for TRIB2 leukaemia pathogenesis
  - b. Examine if p30 cooperates with TRIB2 to drive AML

### 3.3 Results

#### 3.3.1 C/EBP $\alpha$ -p30 disrupts myelopoiesis *in vivo*

To address the effect of excess p30 on hematopoiesis a BM transduction and transplantation experiment was performed. In this model, donor mice were treated with 5-FU to deplete differentiated cells and enrich stem and progenitor populations. 5-FU also stimulates HSPCs into cycling supporting better retroviral transduction efficiency. The donor derived BM cells were isolated and transduced with titre-matched control MigR1 or p30 overexpressing retrovirus and transplanted into lethally irradiated recipients (Figure 3. 1A). The mice were sacrificed at 8-14 weeks post-transplant. Upon examination there was no difference in the number of circulating WBCs (Figure 3. 1B) nor in the spleen weights (Figure 3. 1C) between control MigR1 and p30 transplanted mice. A previously published attempt at transplanting p30 overexpressing cells into recipient mice was unsuccessful (Schwieger *et al.*, 2004). The authors used a C/EBP $\alpha$  mutant, mut10, which expressed p30 but not p42 and transplanted BM cells overexpressing control or mut10 into lethally irradiated recipients. After 12 weeks the authors were unable to detect GFP in either the blood or BM of 93% of mice transplanted with p30 overexpressing cells, whereas all mice receiving control transduced cells expressed GFP (range 2%-79%). The authors deduced that high expression of p30 impaired stem and progenitor cell survival. It should also be noted that upon analysis of the small percentage of mice which successfully engrafted the donor p30 expressing cells (<10%), the authors reported no effect of p30 overexpression on lineage distribution.

With this in mind GFP expression in the BM, spleen, PB and thymus of the MigR1 and p30 chimeric mice was first analysed. While the GFP expression detected in p30 mice was lower overall than in MigR1 controls, there were moderate levels of chimerism achieved in most tissues for most mice (Figure 3. 2). Any tissues with lower than 5% GFP expression were omitted from further flow cytometric analysis. The BM, spleen, PB and thymus were next analysed for markers of mature myeloid (CD11b, Gr1), B (B220, CD19) and T (CD4, CD8) cells. Contrary to the findings of Schwieger *et al*, there was a significant increase in the percentage of CD11b<sup>+</sup>Gr1<sup>+</sup> myeloid cells in the GFP<sup>+</sup> compartment of the BM and spleen of p30 chimeric mice (Figure 3. 3) when compared with MigR1 controls.

This correlates well with previously published observations in the L/L model (discussed in section 3.1.2.2). Before leukemic transformation, the authors noted that the L/L mice exhibited a CD11b<sup>+</sup>Gr1<sup>+</sup> phenotype (the L/L-2 phenotype) between 2 and 6 months.

This was coupled with a significant decrease in the percentages of B220<sup>+</sup>CD19<sup>+</sup> B cells in the BM and spleen, and also in the PB (Figure 3. 4). There was a small but significant increase of CD4<sup>+</sup> cells in the BM of the p30 mice (Figure 3. 5A), but no significant differences in CD4 and CD8 expression in the other tissues (Figure 3. 5). These data suggest overexpression of the p30 disrupts myelopoiesis *in vivo*.

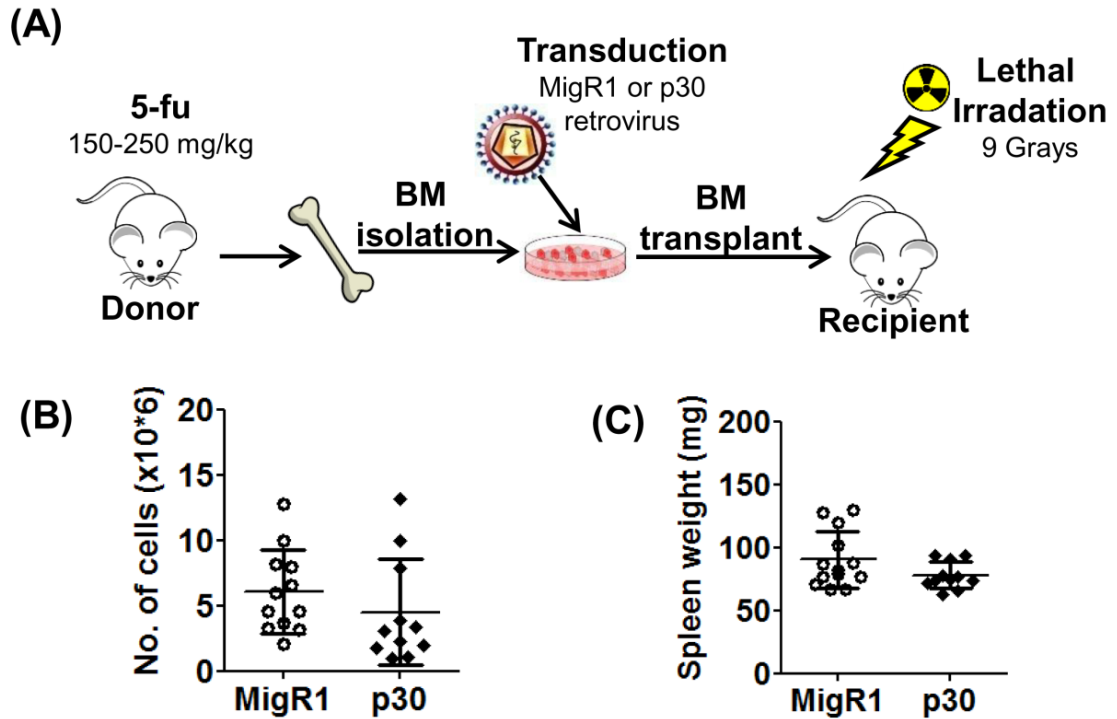


Figure 3. 1 - BMT model to determine the effect of p30 overexpression on hematopoiesis

BM isolated from 5-FU treated donor mice was transduced with control MigR1 or p30 overexpressing retrovirus and transplanted into 6-10 week old lethally irradiated recipient mice. Mice were sacrificed 8-14 weeks post-transplant and analysed. (A) Schematic overview of BMT. (B) Graph of the number of WBCs in PB of MigR1 (n=12) or p30 (n=11) transplanted mice. (C) Graph of the spleen weights of MigR1 (n=13) or p30 (n=11) transplanted mice. Scatter plots display mean  $\pm$  SD and data represents mice from 2 independent transplants.

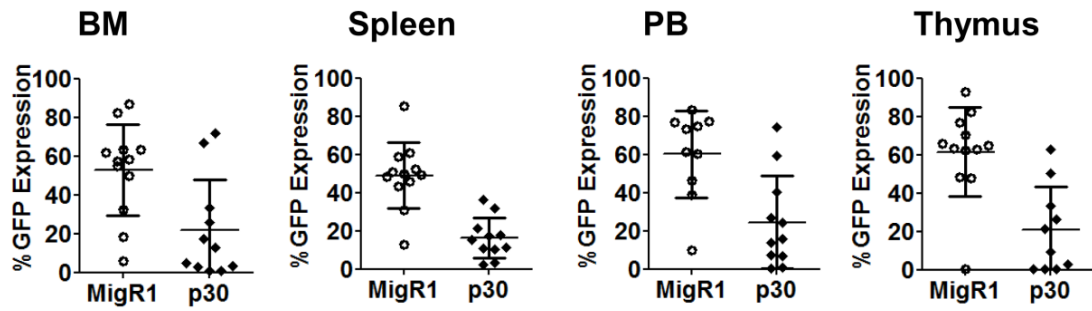


Figure 3. 2 - Analysis of GFP expression in MigR1 and p30 transplanted mice

Mice transplanted with MigR1 (n=10-12) or p30 (n=10-11) expressing BM were sacrificed 8-14 weeks post-transplant and percentage GFP expression was determined in the BM, spleen, PB and thymus by flow cytometry. Scatter plots display mean +/- SD and data represents mice from 2 independent transplants.

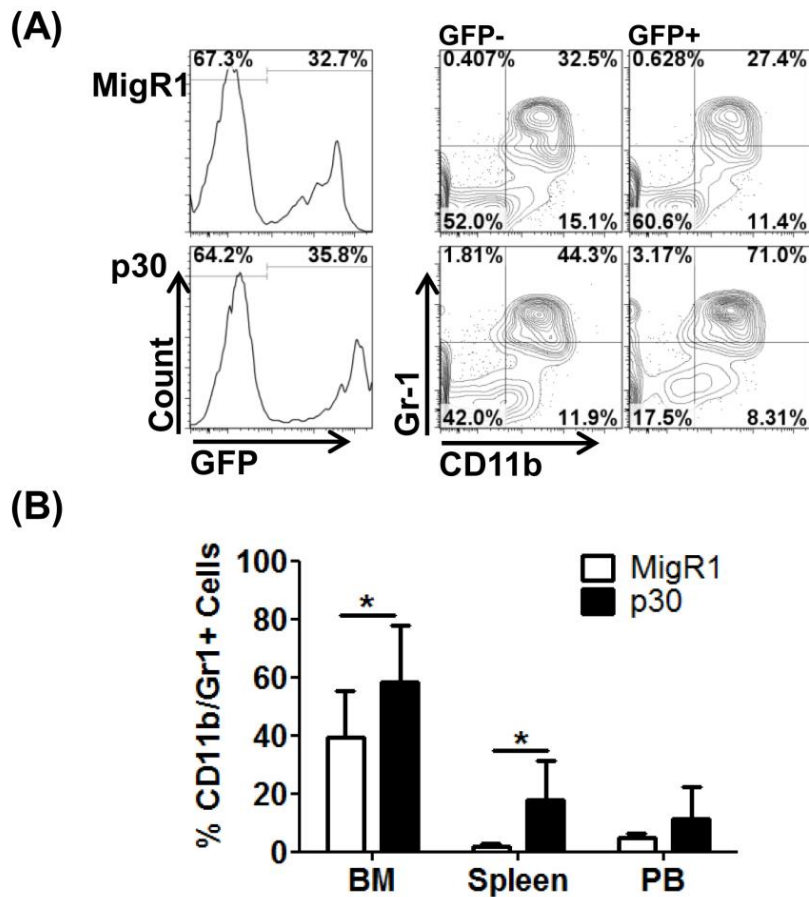


Figure 3. 3 - Overexpression of p30 enhances myelopoiesis *in vivo*.

(A) Representative flow cytometric analysis of BM cells from mice reconstituted with BM cells transduced with MigR1 or p30 retrovirus, showing engraftment of GFP (left panel) and CD11b and Gr1 expression in the GFP<sup>-</sup> and GFP<sup>+</sup> fractions.

(B) Graph of percentage number of GFP<sup>+</sup> myeloid cells (CD11b<sup>+</sup>Gr1<sup>+</sup>) in the BM, spleen and PB of MigR1 (n=6-13) and p30 (n=6-9) transplanted mice. Tissues with <5% GFP expression were omitted from analysis. Results are representative of 2 independent virus transduction and transplantation experiments, +/-SD. \*p≤0.05

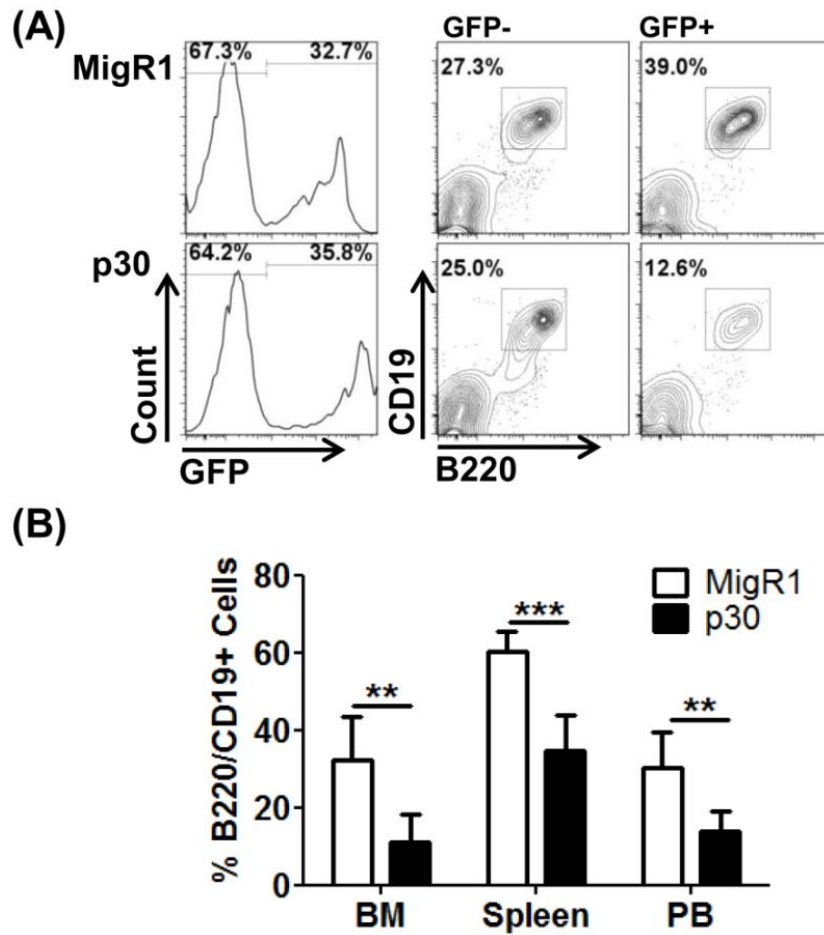


Figure 3. 4 - Overexpression of p30 results in a decrease in mature B cells *in vivo*.

(A) Representative flow cytometric analysis of BM cells from mice reconstituted with BM cells transduced with MigR1 or p30 retrovirus, showing engraftment of GFP (left panel) and B220 and CD19 expression in the GFP<sup>-</sup> and GFP<sup>+</sup> fractions.

(B) Graph of percentage number of GFP<sup>+</sup> myeloid cells (B220<sup>+</sup>CD19<sup>+</sup>) in the BM, spleen and PB of MigR1 (n=6-13) and p30 (n=6-9) transplanted mice. Tissues with <5% GFP expression were omitted from analysis. Results are representative of 2 independent virus transduction and transplantation experiments, +/-SD.

\*\*p<0.005, \*\*\*p<0.001.

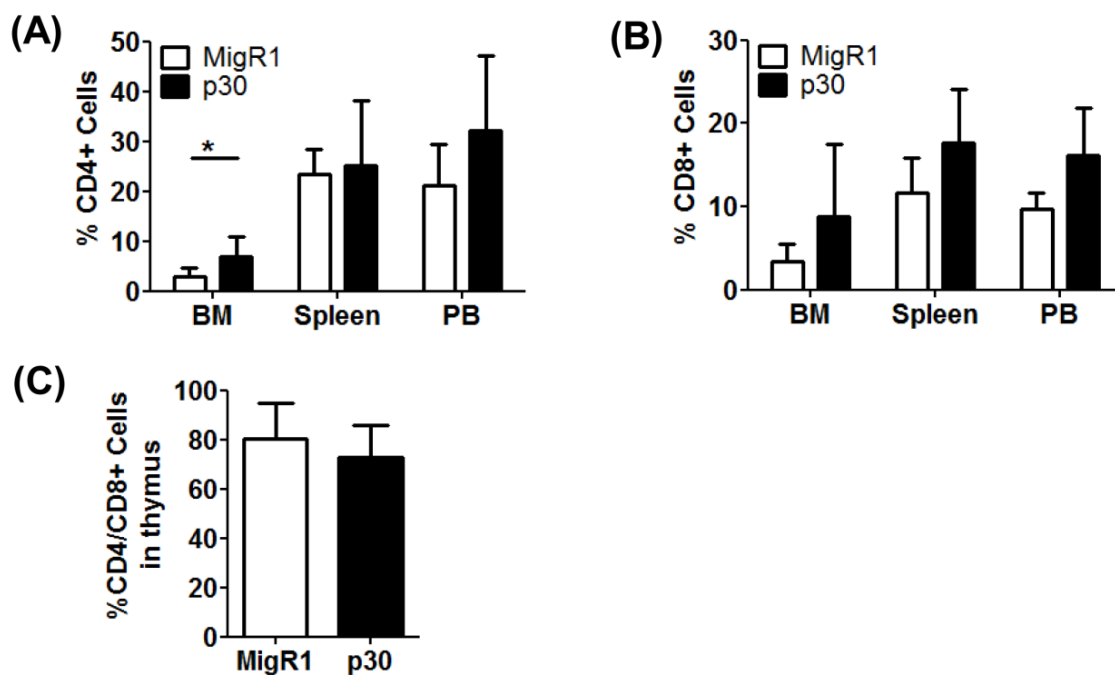


Figure 3. 5 - The effect of p30 overexpression on CD4 and CD8 expression *in vivo*.

(A) Graph of percentage number of GFP<sup>+</sup> CD4<sup>+</sup> cells in the BM, spleen and PB of mice reconstituted with BM cells transduced with MigR1 (n=6-13) or p30 (n=6-9) retrovirus. (B) Graph of percentage number of GFP<sup>+</sup> CD8<sup>+</sup> cells in the BM, spleen and PB of MigR1 (n=6-13) and p30 (n=6-9) transplanted mice. (C) Graph of percentage number of GFP<sup>+</sup> CD4<sup>+</sup> CD8<sup>+</sup> cells in the thymus of MigR1 (n=7) and p30 (n=4) transplanted mice. Tissues with <5% GFP expression were omitted from analysis. Results are representative of 2 independent virus transduction and transplantation experiments, +/-SD. \*p≤0.05

### 3.3.2 Overexpression of C/EBP $\alpha$ -p30 induces AML *in vivo*

As described in section 3.1.2 the oncogenic effects of N-terminal mutations resulting in excess p30 are well established. Unlike those models, in the overexpression transplant model discussed in 3.3.1 excess p30 is present with physiological levels of p42. Under these conditions excess p30 was shown to disrupt myelopoiesis. However, it was unclear whether the observation of increased CD11b<sup>+</sup>Gr1<sup>+</sup> cells in the p30 chimeric mice was the result of p30 promoting myeloid differentiation or p30 causing aberrant proliferation of mature cells. To evaluate this it was decided to extend the time-line of the transplant model in a small number of animals. Of 5 mice transplanted with p30 overexpressing BM cells, 2 succumbed to disease at 26 (M1) and 36 (M2) weeks respectively, while a third mouse (M3) did not develop disease (Figure 3. 6A). The remaining 2 mice from the experiment have been omitted from analysis as due to unexpected premature death it could not be determined if they had succumbed to disease. Upon examination, the mouse which did not develop disease did display engraftment of donor cells in the BM but no signs of disruption to myelopoiesis (Figure 3. 6B). Analysis of the leukemic mice, M1 and M2, revealed elevated WBC counts and splenomegaly (Figure 3. 7A and B) and distinct GFP clones in each disease (Figure 3. 7C). M1 carried 2 clones - the predominant GFP<sup>lo</sup> clone and very low expression of a GFP<sup>hi</sup> clone, with M2 almost exclusively carrying a GFP<sup>hi</sup> clone. Upon flow cytometric analysis, the BM cells of the M1 GFP<sup>hi</sup> clone had a myeloproliferative phenotype with a very high percentage of CD11b<sup>+</sup>Gr1<sup>+</sup> cells present and virtually no lymphocytes. However BM cells of the predominant M1 GFP<sup>lo</sup> clone were almost completely bereft of myeloid and B cell markers with virtually all cells aberrantly expressing CD8 with over 40% co-expressing CD4 (Figure 3. 8). On the other hand in the BM of M2, the predominant clone was GFP<sup>hi</sup> and this had virtually identical surface marker expression to the GFP<sup>hi</sup> clone in M1 with an elevated percentage of CD11b<sup>+</sup>Gr1<sup>+</sup> cells and an almost complete absence of B and T cell markers (Figure 3. 9). In contrast in M2 the GFP<sup>-</sup> (25.6%) and GFP<sup>lo</sup> (1.44%) populations were virtually indistinguishable from one another, with normal myeloid and T cell marker expression, and lower than normal B cell marker expression.

To determine if these diseases with 2 distinct phenotypes induced by p30 overexpression represented overt transplantable leukaemia, secondary

transplants were performed with cells from the primary p30 diseases (Figure 3. 10). In 2 independent experiments,  $6 \times 10^6$  leukemic spleen cells or  $4 \times 10^6$  leukemic BM cells from M1 were transplanted into a total of 6 recipient mice. After 10 weeks there was no detectable GFP in the PB of all transplanted mice. Cells transplanted from M2 however were able to generate leukaemia in secondary hosts with all transplanted mice succumbing to disease with a mean latency of 27 weeks (Figure 3. 11A). They had very high WBC counts and splenomegaly (Figure 3. 11B and C). Flow cytometric analysis of the leukemic BM cells showed that the secondary disease resembled the GFP<sup>hi</sup> clone from the parent AML, but with aberrant B220 expression (Figure 3. 12) and a more immature myeloid phenotype. Thus in an overexpression BMT model in the presence of physiological levels of p42, p30 was able to induce a transplantable AML *in vivo* in 1 out of 3 cases. Thus it was hypothesised that the increased proliferation of myeloid cells observed in the short-term BMT in section 3.3.1 could weakly (33%) transform to full blown leukaemia.

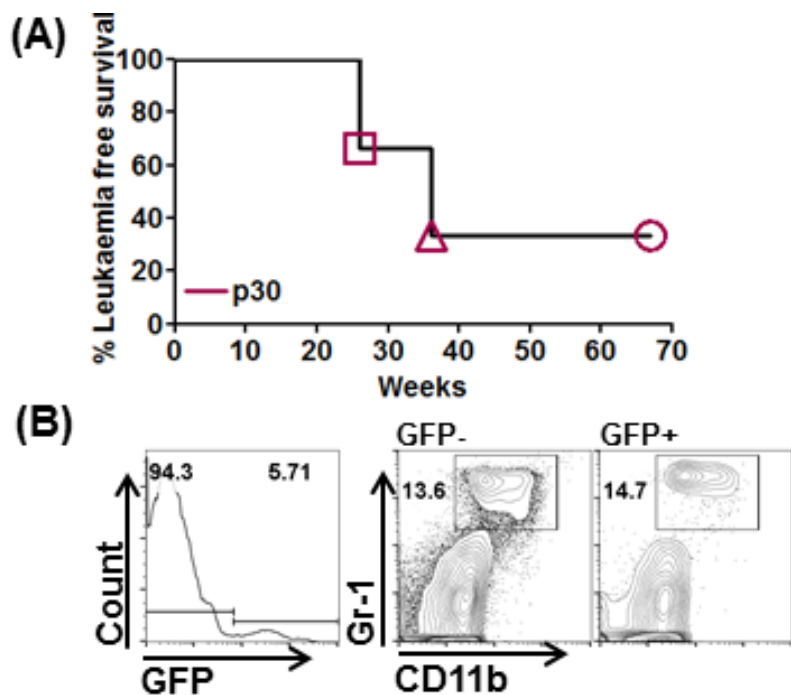


Figure 3. 6 - Overexpression of p30 induces leukaemia *in vivo*

(A) Kaplan-Meier survival curve of mice reconstituted with BM cells transduced with p30 expressing retrovirus, with 2 of 3 mice succumbing to disease at 26 and 36 weeks respectively. (B) Flow cytometric analysis of BM from the surviving mouse showing engraftment of GFP<sup>+</sup> p30 expressing donor cells (left panel) and normal levels of CD11b and Gr1 expression in the GFP<sup>-</sup> and GFP<sup>+</sup> compartments of the BM.

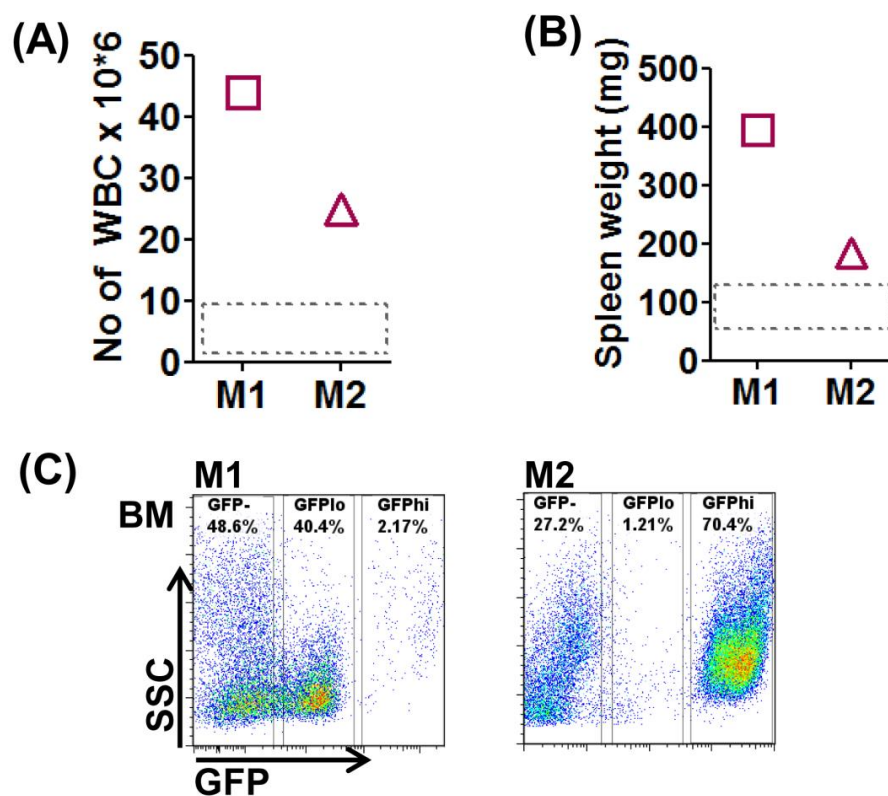


Figure 3. 7 - Analysis of p30 leukemic mice

Graph of (A) WBC counts and (B) spleen weights of p30 leukemic mice. Grey dashed line represents normal range from a healthy mouse. (C) Scatter plots of GFP expression in BM of M1 (left panel) and M2 (right panel).

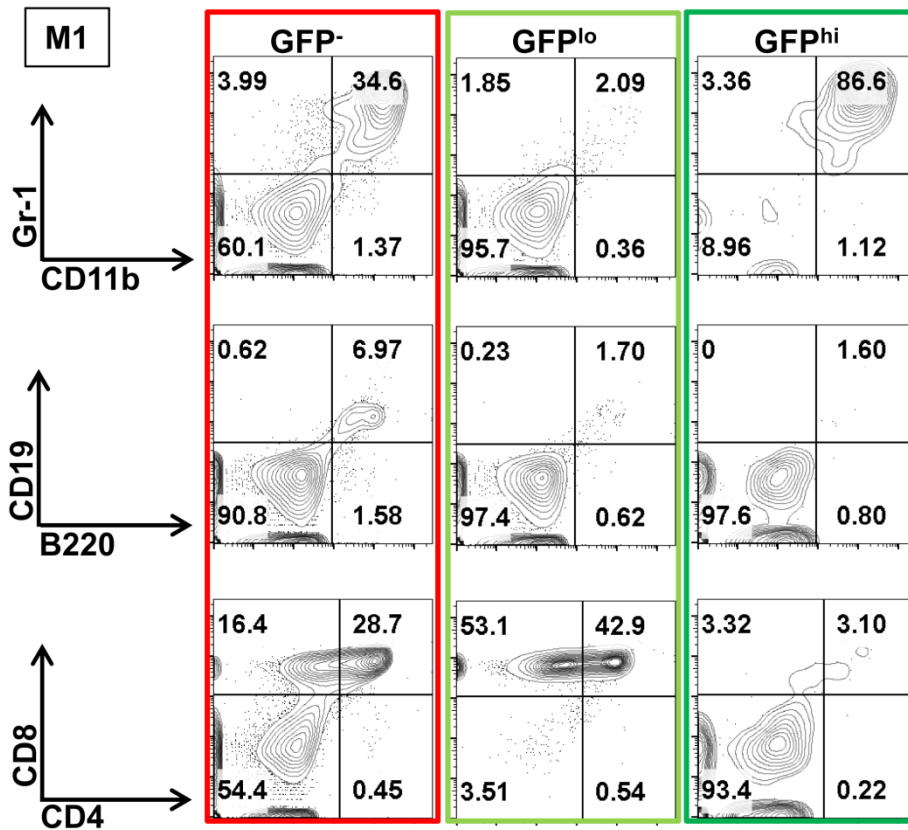


Figure 3. 8 - Flow cytometric analysis of GFP clones of M1 leukemic BM cells

Flow cytometric analysis of the expression of markers of mature myeloid (CD11b, Gr1), B (B220, CD19), and T (CD4, CD8) cells on BM cells from M1 through GFP<sup>-</sup> (left panel), GFP<sup>lo</sup> (middle panel) and GFP<sup>hi</sup> (right panel).

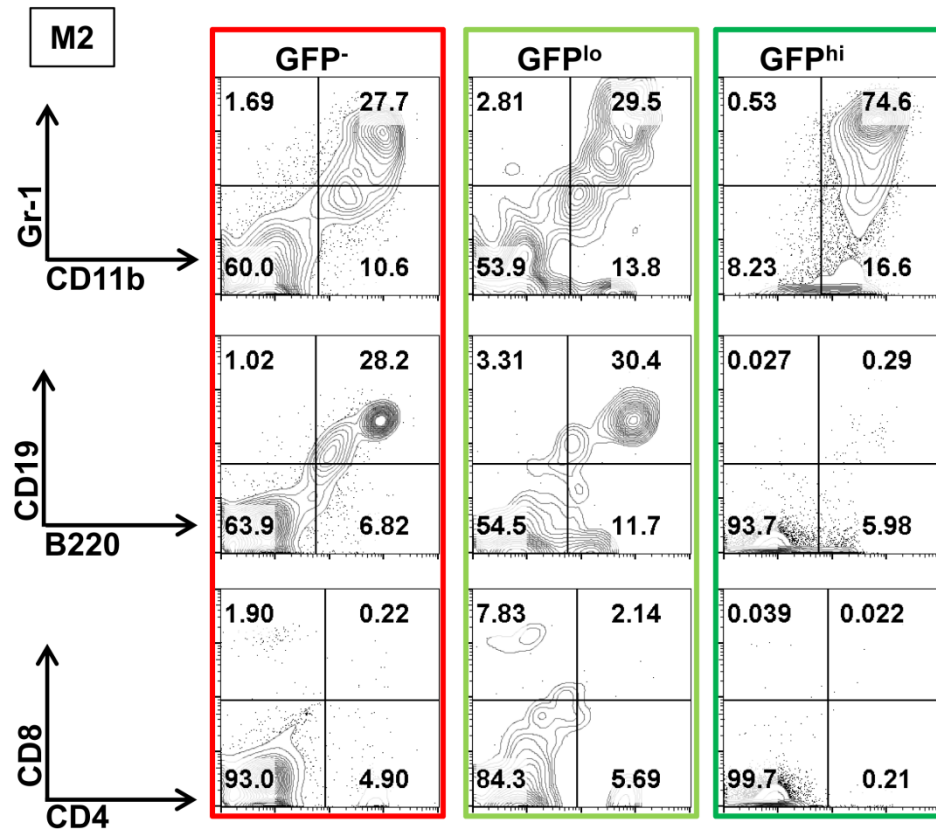


Figure 3. 9 - Flow cytometric analysis of GFP clones of M2 leukemic BM cells

Flow cytometric analysis of the expression of markers of mature myeloid (CD11b, Gr1), B (B220, CD19), and T (CD4, CD8) cells on BM cells from M2 through GFP<sup>-</sup> (left panel), GFP<sup>lo</sup> (middle panel) and GFP<sup>hi</sup> (right panel).

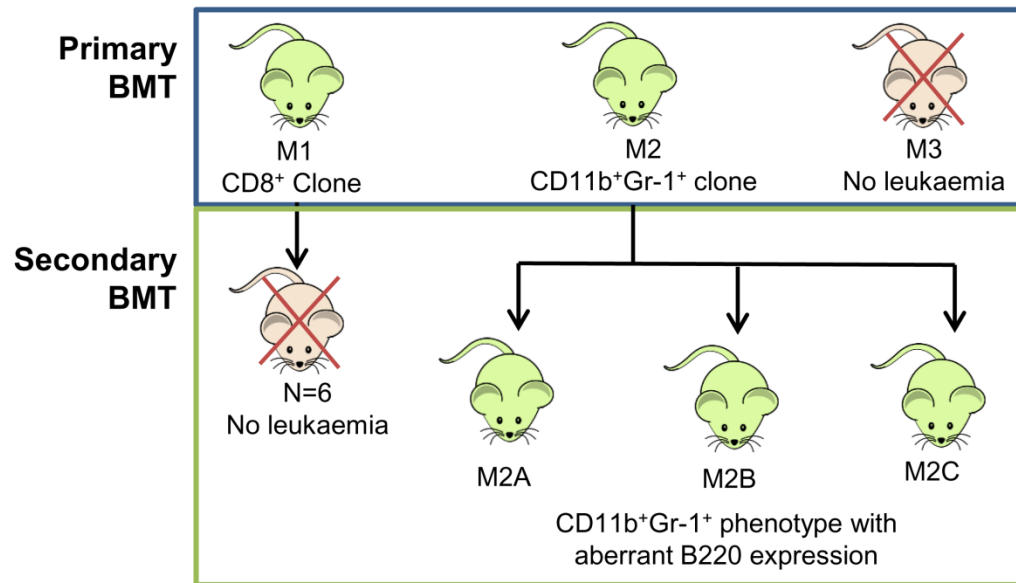


Figure 3. 10 - Schematic overview of secondary and tertiary p30 overexpression transplants

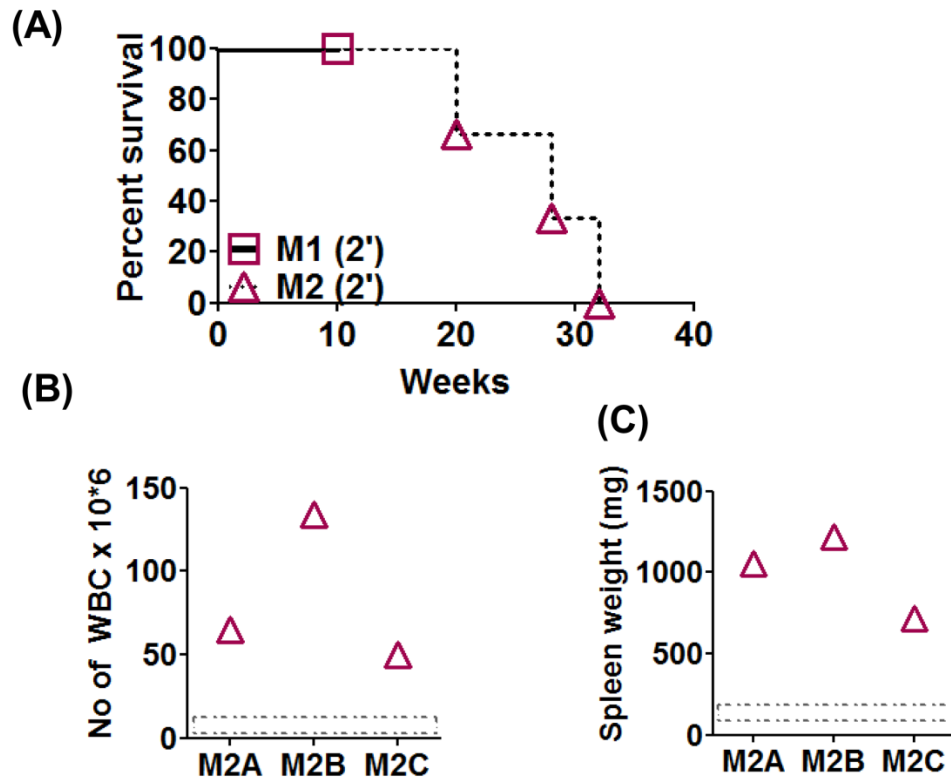


Figure 3. 11 - M2 but not M1 transplanted cells induce AML in secondary recipients

(A) Kaplan-meier survival curve of sub-lethally irradiated mice transplanted with primary leukemic cells from M1 (n=6) or M2 (n=3). M1 transplanted cells failed to engraft in secondary hosts. M2 transplanted mice succumbed to disease with a median latency of 27 weeks. Graph of (B) WBC counts and (C) spleen weights of leukemic mice transplanted with M2 primary p30 leukemic cells. Grey dashed line represents normal range from a healthy mouse.

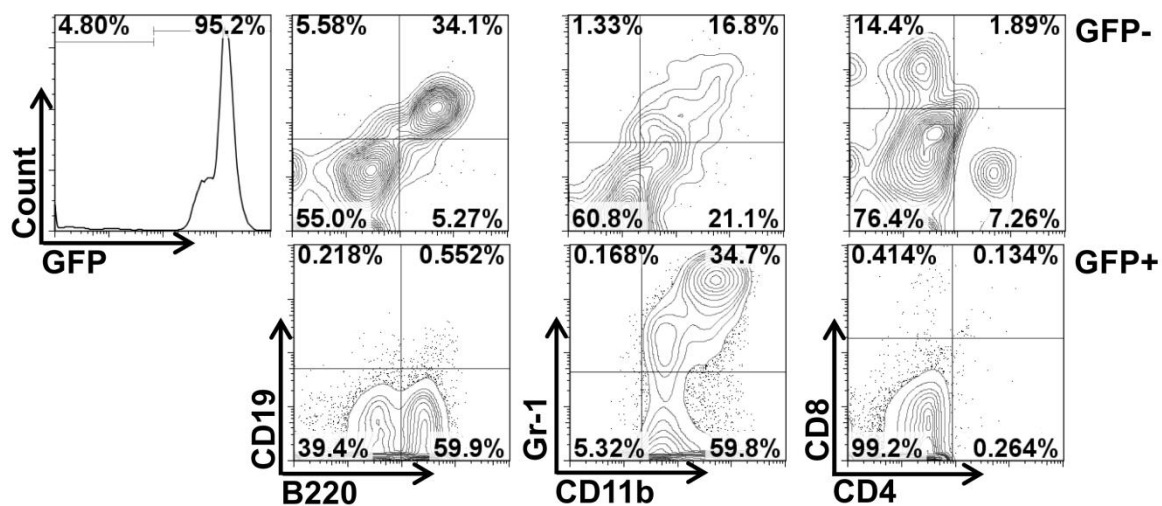


Figure 3. 12 - Flow cytometric analysis of BM of p30 (M2) secondary leukaemia.

Representative flow cytometric analysis of BM from p30 (M2) secondary leukaemia. Percentage GFP expression in the BM (histogram) and analysis of B cells (B220, CD19), myeloid cells (CD11b, Gr1) and T cells (CD8, CD4) in the GFP<sup>-</sup> and GFP<sup>+</sup> compartment of the BM are shown.

### 3.3.3 Trib2 degrades p42, but not p30, via K48 mediated ubiquitination

Given that above it was determined that p30 overexpression could induce a transplantable AML *in vivo* and considering the ability of TRIB2 to cooperate with other oncogenes as previously outlined, the question remains if TRIB2 and p30 cooperate to induce AML. As outlined in 1.3.4.1.1, TRIB2 induces AML by causing proteasomal degradation of p42 and an increase in p30. As previously discussed it has been shown that the degradation of p42 by TRIB2 is proteasome dependent (Keeshan et al., 2006) and TRIB2 has a COP1-binding domain which is essential for C/EBP $\alpha$  degradation (Keeshan et al., 2010). COP1 is an E3 ubiquitin ligase which forms a complex with TRIB2 and C/EBP $\alpha$  that is necessary for p42 degradation. Ubiquitination, as described in 2.5.2, is a process whereby proteins are modified by being tagged at a K residue with 8.5kD molecules of the Ub protein, which may act as a signal for their degradation via the proteasome. It occurs in three steps - activation, conjugation and ligation, with each step being catalysed by a separate class of enzyme - E1 ubiquitin-activating enzymes, E2 ubiquitin-conjugating enzymes and E3 ubiquitin ligases. In order to determine if TRIB2 was inducing Ub specific degradation of C/EBP $\alpha$ , an *in vitro* ubiquitination assay was performed. Briefly 293T cells were transfected with C/EBP $\alpha$ , TRIB2 and UB, cells lysed 24 hrs later and ubiquitination was detected by CO-IP of the target protein followed by anti-UB blotting. It was shown that in the presence of TRIB2 there is a dramatic increase in C/EBP $\alpha$  ubiquitination (Figure 3. 13 - top panel)

As outlined earlier, Ub molecules have 7 lysine residues themselves, K6, 11, 27, 29, 33, 48 and 63, and successive addition of Ub molecules to a substrate is called polyubiquitination. Several different types of Ub chains can be formed depending on which lysine residue of the previous Ub molecule they attach to. K48-Ub chains signal the protein for proteasomal degradation while K63-Ub chains protect the protein from degradation. Using K48 and K63 specific antibodies it was shown that ubiquitination of C/EBP $\alpha$  by TRIB2 was not via the non-degradative K63 polychain pathway (Figure 3. 13 middle panel) but the K48 polychain degradative pathway (Figure 3. 13 bottom panel). These data would suggest that inhibiting the proteasome could negate the function of TRIB2 by preventing the degradation of p42. To test this hypothesis, U937 cells which

endogenously express TRIB2 and C/EBP $\alpha$ , were transduced with control MigR1 or MigR1-TRIB2 retrovirus. GFP<sup>+</sup> cells were sorted after 16-24 hrs and treated with 10nM Bortezomib, a proteasome inhibitor developed for treating multiple myeloma. Cells expressing TRIB2 displayed increased sensitivity to Bortezomib treatment (Figure 3. 14A). Conversely U937 cells overexpressing C/EBP $\alpha$  showed decreased sensitivity to Bortezomib induced proteasome inhibition indicating that enforced C/EBP $\alpha$  expression was able to rescue Bortezomib induced cell death (Figure 3. 14B). Two *CEBPA* null leukemic cell lines, K562 (Radomska et al., 1998) and Kasumi1 (Pabst et al., 2001), were also transduced with MigR1 or MigR1-TRIB2 and in the absence of C/EBP $\alpha$  expression, increased TRIB2 levels had no effect on Bortezomib induced toxicity (Figure 3. 14C and D). These data demonstrate that the TRIB2 mediated K48-specific ubiquitination of C/EBP $\alpha$  can be targeted by proteasome inhibition.

Considering the selective way in which TRIB2 degrades p42 *in vivo* in AML induction it was determined whether or not TRIB2 would also induce p30 ubiquitination. Either p42 or p30 were transfected, with Ub, into 293T cells with or without TRIB2. TRIB2 was unable to ubiquitinate p30 (lane2) despite a significant increase in p42 ubiquitination in the presence of TRIB2 (lane4) (Figure 3. 15). As mentioned above, the site of ubiquitination on the substrate is a K residue. Previously outlined in 1.2.2.2.1, a common recurrent *CEBPA* mutation occurs at residue K313 that results in a duplication of the K residue, K313KK (K313dup). Thus it was hypothesised that this may be a potential site for TRIB2 mediated C/EBP $\alpha$  ubiquitination. To explore this, a *CEBPA* mutant was made by site-directed mutagenesis in which the K residue at site 313 was mutated to an arginine (R). K313R or WT C/EBP $\alpha$ , were co-transfected with UB into 293T cells with or without TRIB2. The K313R mutation resulted in loss of TRIB2 induced C/EBP $\alpha$  ubiquitination (lane 2) when compared with WT C/EBP $\alpha$  (Lane 4) (Figure 3. 16). Indeed background levels of K313R ubiquitination (lane 1) also appeared lower than WT C/EBP $\alpha$  (lane3) suggesting increased protein stability. To ensure that the results observed were not due to a mutation-related loss of function, a dual luciferase reporter assay was performed. Indeed K313R was still able to stimulate the luciferase reporter construct of *Gcsfr*, a C/EBP $\alpha$  target gene, at equivalent levels to WT C/EBP $\alpha$  (Figure 3. 17A). To confirm that the K313R mutant retained functional C/EBP $\alpha$  activity, a *Cebpa* null cell line ( $\alpha^{-/-}$ ) which

differentiates upon enforced expression of C/EBP $\alpha$  was transduced with control MigR1, MigR1-C/EBP $\alpha$  or MigR1-K313R retrovirus and analysed for Gr1 expression by flow cytometry. After 2 days in culture both WT C/EBP $\alpha$  and K313R overexpression had resulted in a comparable increase in expression of the mature granulocyte marker (Figure 3. 17B and C). Thus mutating the K313 residue did not abrogate the transcriptional or functional activity of C/EBP $\alpha$ . Together these data show that K313 represents a site of TRIB2 mediated ubiquitin conjugation on C/EBP $\alpha$  and mutation of this site abrogates ubiquitin-dependent proteasomal degradation of C/EBP $\alpha$  by TRIB2.

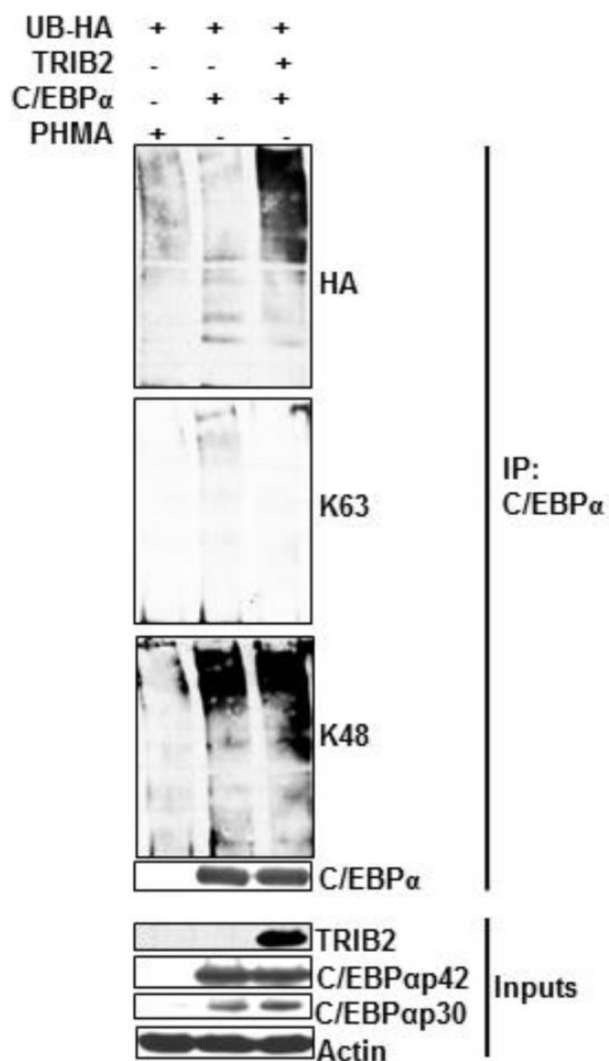


Figure 3. 13 - Analysis of TRIB2 mediated ubiquitination of C/EBP $\alpha$

293T cells were transfected with ubiquitin-HA, TRIB2, C/EBP $\alpha$  and PHMA empty vector control, and a ubiquitination assay was performed. Immunoblotting for HA detects total ubiquitination (top IP panel), K63 species of polyubiquitination (second IP panel), K48 species of polyubiquitination (third IP panel), and C/EBP $\alpha$  detects IP protein (bottom IP panel). Immunoblotting for TRIB2 and C/EBP $\alpha$  detects input levels and actin serves as a loading control (input panels).

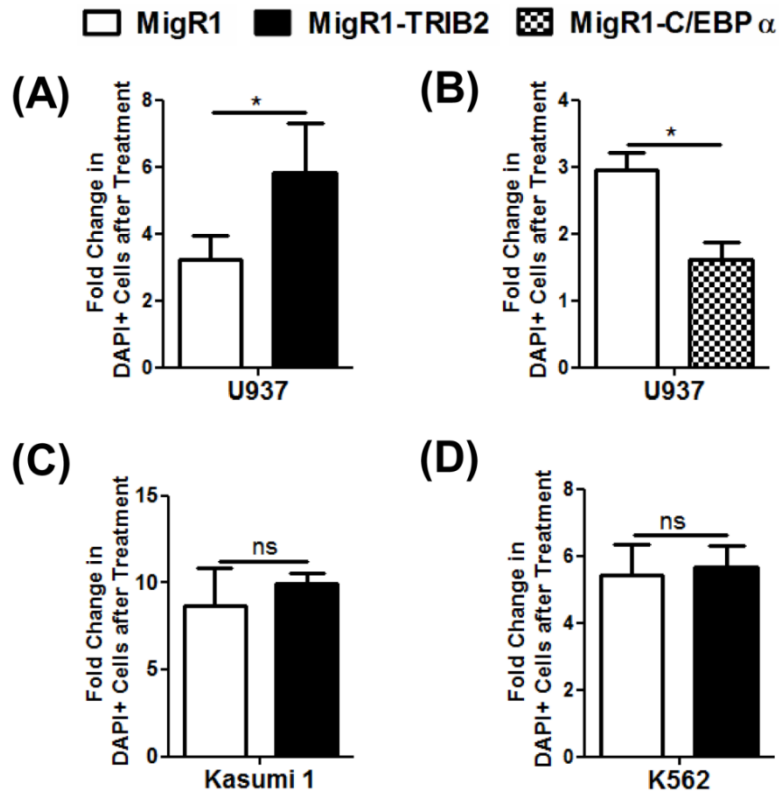


Figure 3. 14 - Degradation of p42 by TRIB2 can be targeted by Bortezomib induced proteasome inhibition in leukaemia cell lines.

Sorted GFP<sup>+</sup> cells transduced with MigR1 control, and MigR1-TRIB2 (A, C, D) or MigR1-C/EBP $\alpha$  (B) retrovirus were treated +/- 10nM Bortezomib for 16-24hrs and analysed by flow cytometry for DAPI expression. Graph of fold change in cell death as determined by DAPI positive cells. Data displayed is average of 3 technical replicates, and is representative of 2 independent experiments. ns denotes not significant, \*P $\leq$ 0.05, \*\*P<0.005 by Student's unpaired t test.

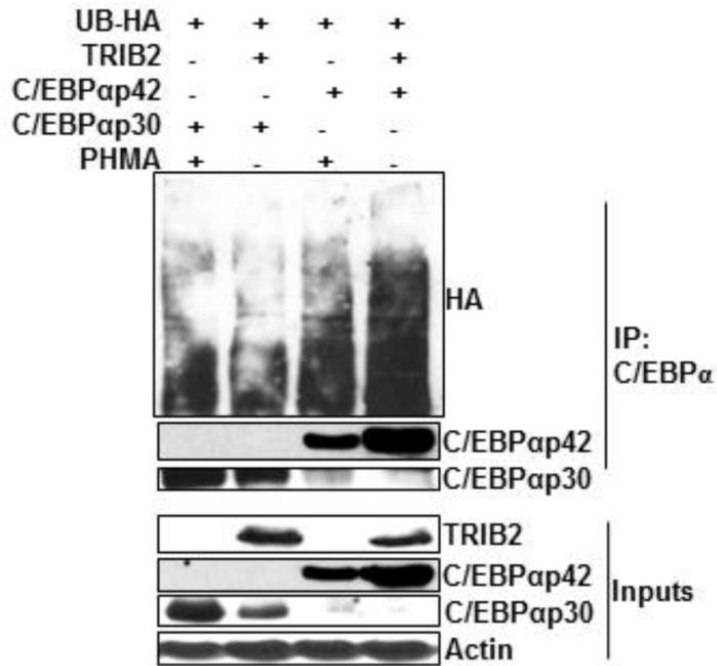


Figure 3. 15 - Analysis of TRIB2 mediated ubiquitination of C/EBP $\alpha$  isoforms p42 and p30

293T cells were transfected with ubiquitin-HA, TRIB2, p30, p42 and PHMA empty vector control, and ubiquitination assay was performed. Immunoblotting for HA detects total ubiquitination (top IP panel), and C/EBP $\alpha$  detects IP protein (bottom IP panels). Immunoblotting for TRIB2 and C/EBP $\alpha$  detects input levels and actin serves as a loading control (input panels).

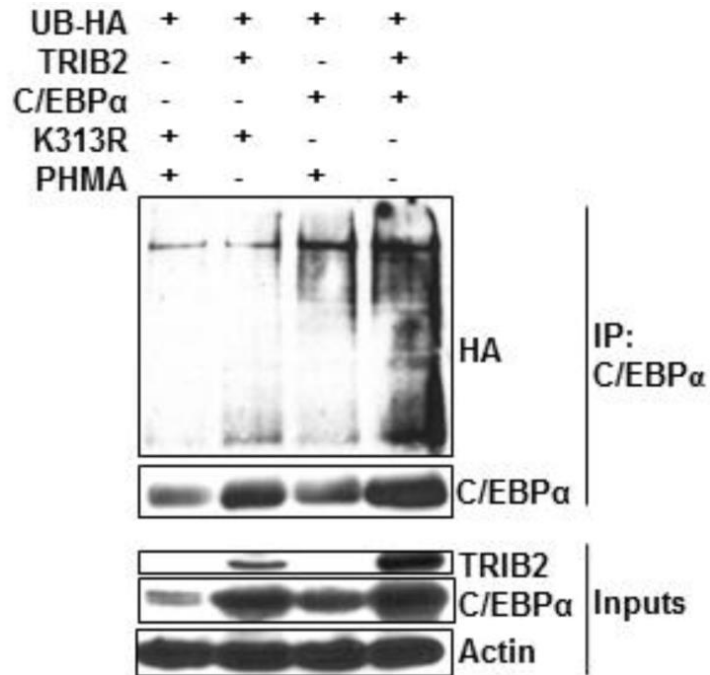


Figure 3. 16 - Analysis of TRIB2 mediated ubiquitination of K313R mutant

293T cells were transfected with ubiquitin-HA, TRIB2, C/EBP $\alpha$ , K313R and PHMA empty vector control, and ubiquitination assay was performed. Immunoblotting for HA detects total ubiquitination (top IP panel), and C/EBP $\alpha$  detects IP protein (bottom IP panel). Immunoblotting for TRIB2 and C/EBP $\alpha$  detects input levels and actin serves as a loading control (input panels).

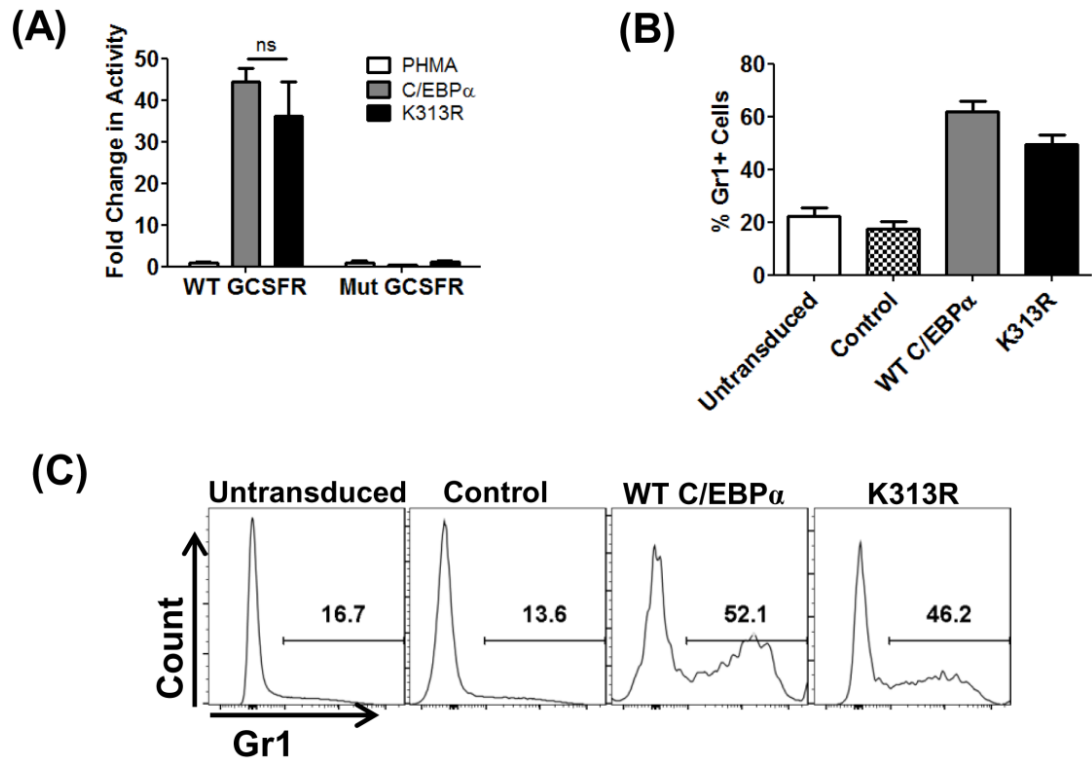


Figure 3. 17 - C/EBP $\alpha$  mutant K313R retains transcriptional and differentiation activity

(A) 293T cells were co-transfected with the *Gcsfr* promoter *firefly* luciferase constructs containing either the WT C/EBP $\alpha$  (WT GCSFR) or mutant binding sites (Mut GCSFR), and either an empty PHMA vector or vector containing C/EBP $\alpha$  or K313R, along with a pRL-TK Renilla luciferase internal control plasmid. Luciferase activity was measured 24 hrs post-transfection. Bar chart represents reporter luciferase activity for each sample normalised for *renilla* values, and graphed relative to the control sample. Results analysed using two-tailed unpaired t-test and representative of 3 independent experiments. The *Cebpa* null cell line ( $a^{-/-}$ ) were transduced with control MigR1, MigR1-C/EBP $\alpha$  or MigR1-K313R retrovirus and analysed for Gr1 expression after 48 hrs. (B) Graph of average percentage Gr1 expression  $\pm$  SD and (C) representative histograms of Gr1 expression. Data represents 1 experiment with 3 technical replicates.

### 3.3.4 Degradation of p42 is the key driver of TRIB2-induced AML

The data thus presented has demonstrated that p30 overexpression can induce transplantable AML *in vivo* and that TRIB2 degrades p42 by ubiquitination but cannot degrade p30. As previously discussed, *CEBPA* mutations rarely result in complete loss of C/EBP $\alpha$  expression and there is evidence to suggest that some oncogenes require a threshold of C/EBP $\alpha$  expression for AML initiation (Ohlsson et al., 2014, Collins et al., 2014) as outlined in 1.2.2.2.1. In order to evaluate a cooperative relationship between p30 and TRIB2 in AML induction, it was first investigated whether or not the presence of C/EBP $\alpha$  was essential for the oncogenic effects of TRIB2. A BMT was performed using the previously described conditional *Cebpa<sup>fl/fl</sup>; Mx1Cre* mouse model, where poly I:C treatment facilitates ablation of *Cebpa* in the hematopoietic compartment. Two weeks post deletion, cKit<sup>+</sup> HSPCs isolated from the BM of poly I:C treated control *Cebpa<sup>fl/fl</sup>* and *Cebpa $\Delta/\Delta$*  animals were transduced with MigR1-TRIB2 retrovirus. The transduced cells were then transplanted into lethally irradiated recipient mice, and monitored for disease progression. As expected, all mice reconstituted with *Cebpa<sup>fl/fl</sup>* cells expressing TRIB2 developed lethal AML with a median latency of 33 weeks, but in striking contrast, TRIB2 transduced *Cebpa $\Delta/\Delta$*  HSPCs failed to give rise to AML (Figure 3. 18A). The BM of *Cebpa $\Delta/\Delta$*  transplanted mice was examined 14 months after transplantation, and GFP<sup>+</sup> cells were detected suggesting that the TRIB2 expressing *Cebpa $\Delta/\Delta$*  cells are able to properly home to the BM but were not able to initiate leukaemia (Figure 3. 18B). Thus, despite TRIB2 functioning to degrade C/EBP $\alpha$  to induce AML, the complete absence of C/EBP $\alpha$  abrogates TRIB2 oncogenicity, suggesting that a certain threshold of C/EBP $\alpha$  (p42 or p30) expression is necessary for TRIB2 to initiate AML.

Considering the necessity of C/EBP $\alpha$  expression for TRIB2 to induce AML, it was next determined whether p42 degradation or p30 accumulation was the key driver of this pathway, and whether p30 could cooperate with TRIB2 to accelerate disease progression. In order to investigate this, a transplant model was designed which utilised donor cells from an established *Cebpa* conditional knockout model (described in 3.1.2.2) that either only expressed the p30 isoform (previously L/L, referred to here as *Cebpa $\Delta/p30$* ), or were heterozygous for this allele still expressing p42 on one allele (previously L/+, referred to here as *Cebpa<sup>fl/p30</sup>* cells). CD45.2<sup>+</sup> donor cells from poly I:C treated 8-14 week old

*Cebpa*<sup>fl/+</sup>, *Cebpa*<sup>fl/p30</sup> and *Cebpa*<sup>fl/p30</sup>; *Mx1Cre* (i.e. *Cebpa*<sup>Δ/p30</sup>) mice were harvested two weeks post deletion, transduced with MigR1 or MigR1-TRIB2 retrovirus and transplanted into CD45.1<sup>+</sup> lethally irradiated recipients (Figure 3. 19). *Cebpa*<sup>fl/+</sup> mice carried full-length *Cebpa* on both alleles and thus had WT levels of p42 and p30, therefore MigR1 transplanted mice were expected to remain disease free, while TRIB2 transplanted mice were expected to develop AML as previously published (Keeshan et al., 2006) (Figure 3. 20). *Cebpa*<sup>fl/p30</sup> mice carry 1 allele with full-length *Cebpa* and one p30 only allele and as such had lower levels of p42 and excess p30, thus MigR1 transplanted mice were expected to remain disease free as previously reported (Kirstetter et al., 2008). However it was not known if the excess p30 would cooperate with TRIB2 and affect the disease latency as TRIB2 has been shown to cooperate with other oncogenes (Keeshan et al., 2008). *Cebpa*<sup>Δ/p30</sup> mice which carried p30 on one allele only expressed p30 and were null for p42. As outlined in 3.1.2.2, mice only expressing p30 (also known as L/L) have been shown to uniformly develop leukaemia therefore the MigR1 transplanted mice were expected to develop leukaemia within 9-14 months as previously published. Following transduction, a fraction of the donor cells were kept in *in vitro* culture for 3 days post transplantation and assessed for GFP expression to ensure comparable levels of transduction were achieved between samples (Figure 3. 21A). Following transplantation, CD45.2 and GFP expression were monitored at 7 weeks post-transplant (Figure 3. 21B and C) in peripheral blood and every 2-3 weeks thereafter (Figure 3. 22) showing recipient reconstitution with donor cells.

Control cohorts of mice transplanted with *Cebpa*<sup>fl/+</sup> and *Cebpa*<sup>fl/p30</sup> cells transduced with MigR1 did not develop any disease, as expected. Analysis of these mice showed completely normal hematopoiesis as evidenced by normal WBC counts (Figure 3. 23A), spleen weights (Figure 3. 23B) and distribution of peripheral blood cells (Figure 3. 23C-E). Indeed flow cytometric analysis also showed that mice from both of these groups displayed normal BM, peripheral and splenic hematopoiesis (Figure 3. 24). The mice transplanted with TRIB2 transduced *Cebpa*<sup>fl/+</sup> cells developed AML, with a median latency of 49 weeks, also as expected. However, mice transplanted with TRIB2 transduced *Cebpa*<sup>fl/p30</sup> cells developed a much more aggressive AML with an accelerated latency of 29 weeks (Figure 3. 25A) as evidenced by elevated white blood cell counts and

splenomegaly (Figure 3. 25B and C). This supports our hypothesis that p30 could cooperate with TRIB2 to accelerate AML. Mice transplanted with MigR1 transduced *Cebpa*<sup>Δ/p30</sup> cells developed AML with a median latency of 40 weeks, as previously published for *Cebpa*<sup>L/L</sup> mice (“L” refers to p30). However no significant acceleration of the disease was seen in mice transplanted with TRIB2 transduced *Cebpa*<sup>Δ/p30</sup> cells (median latency of 35 weeks) (Figure 3. 26A) indicating that the presence of p42 was important for the cooperativity of TRIB2 and p30. Indeed, comparing TRIB2 induced AML in *Cebpa*<sup>fl/p30</sup> and *Cebpa*<sup>Δ/p30</sup> background, the excess p30 accelerated AML only in the presence of p42 (Figure 3. 26B). Flow cytometric analysis of leukemic cells from *Cebpa*<sup>fl/+</sup>-TRIB2, *Cebpa*<sup>fl/p30</sup>-TRIB2, *Cebpa*<sup>Δ/p30</sup>-MigR1 and *Cebpa*<sup>Δ/p30</sup>-TRIB2 AML cells confirmed a predominantly cKit<sup>+</sup> disease (Figure 3. 27). Protein analysis of C/EBPα expression between the *Cebpa*<sup>fl/+</sup>-TRIB2, *Cebpa*<sup>fl/p30</sup>-TRIB2, *Cebpa*<sup>Δ/p30</sup>-TRIB2 and *Cebpa*<sup>Δ/p30</sup>-MigR1 AML cells groups verified the expected p42 and p30 expression levels in leukaemic BM cells (Figure 3. 28). In the *Cebpa*<sup>fl/+</sup>-TRIB2 cohort (lane 1) there was a shift in the leukemic ratio of p42:p30 with a decrease in p42 and increase in p30 when compared with control (lane 6). As expected, increased p30 expression was also observed in the *Cebpa*<sup>fl/p30</sup>-MigR1 (lane 2) and *Cebpa*<sup>fl/p30</sup>-TRIB2 (lane 3) samples, with a clear reduction in p42 expression with TRIB2 (lane 3 versus lane 2). Comparable levels of p30 were present in the absence of p42 in *Cebpa*<sup>Δ/p30</sup>-MigR1 (lane 4) and *Cebpa*<sup>Δ/p30</sup>-TRIB2 (lane 5) samples. Taken together these data show that despite TRIB2 functioning to degrade p42, C/EBPα is essential for the initiation of TRIB2 mediated AML and only in the presence of p42 is there a cooperative effect seen with p30.

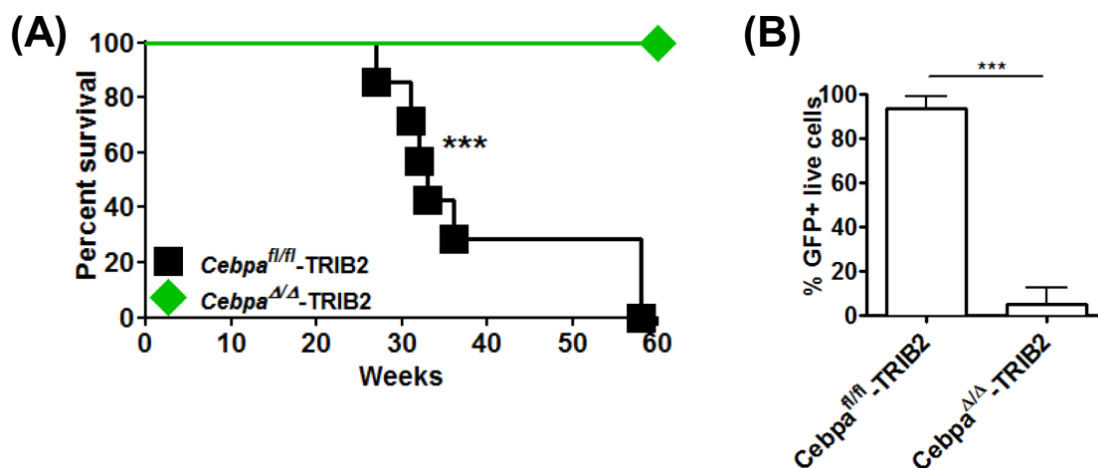


Figure 3. 18 - C/EBP $\alpha$  is required for TRIB2 mediated AML induction

**(A)** Kaplan-Meier survival curve of mice reconstituted with either  $Cebpa^{fl/fl}$  or  $Cebpa^{\Delta/\Delta}$  bone marrow cells transduced with TRIB2 expressing retrovirus. The median survival of mice reconstituted with  $Cebpa^{fl/fl}$ -TRIB2 cells was 33 weeks (n=12), none of the mice reconstituted with  $Cebpa^{\Delta/\Delta}$ -TRIB2 cells developed leukaemia within 60 weeks (n=10). \*\*\*P<0.0001 by Log-rank test. **(B)** Fraction of cells expressing GFP in bone marrow of leukemic mice ( $Cebpa^{fl/fl}$ -TRIB2) or when the experiment was terminated 60 weeks post transplantation ( $Cebpa^{\Delta/\Delta}$ -TRIB2). Data are represented as mean +/- SD, \*\*\*P<0.0001 by Student's t-test. This experiment was performed by Dr. Ewa Ohlsson, in a collaboration with Professor Bo Porse, University of Copenhagen.

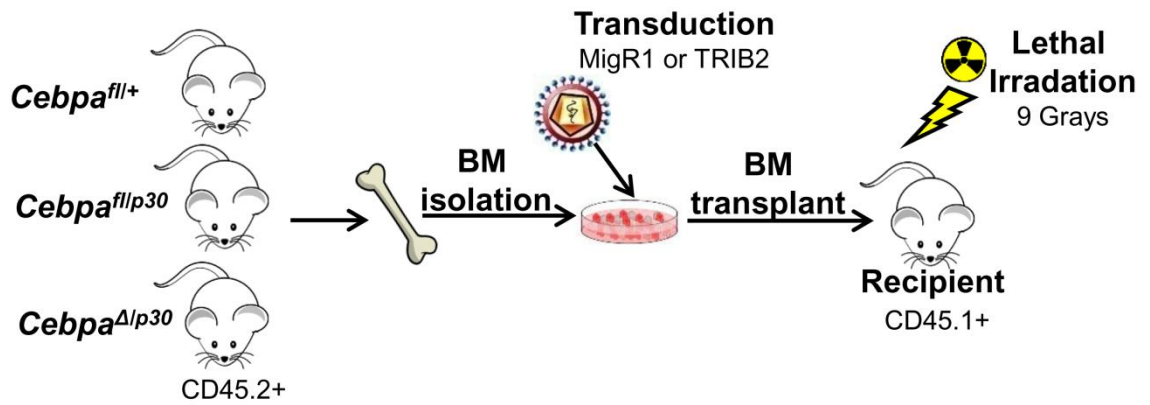


Figure 3. 19 - Schematic overview of BM transplantation experiment

CD45.2<sup>+</sup> donor cells from poly I:C treated 8-14 week old *Cebpa*<sup>fl/+</sup>, *Cebpa*<sup>fl/p30</sup> and *Cebpa*<sup>Δ/p30</sup> mice were harvested two weeks after deletion, transduced with MigR1 or MigR1-TRIB2 retrovirus and transplanted into lethally irradiated CD45.1<sup>+</sup> recipient mice.

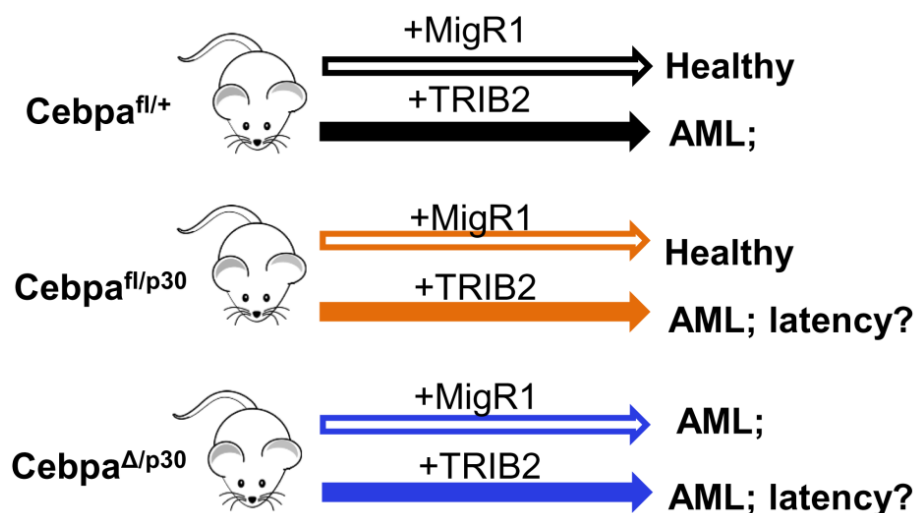


Figure 3. 20 - Schematic overview of predicted outcomes of bone marrow transplant experiment

Mice transplanted with MigR1 transduced *Cebpa*<sup>fl/+</sup> cells (full-length C/EBPα translated from both alleles) were expected to remain disease free while those transplanted with TRIB2 expressing *Cebpa*<sup>fl/+</sup> should develop AML. Mice transplanted with MigR1 transduced *Cebpa*<sup>fl/p30</sup> cells (1 allele from which full-length CEBPA is translated and 1 allele from which p30 is translated) were expected to remain disease free but it was not known if excess p30 would cooperate with TRIB2 in mice transplanted with TRIB2 expressing *Cebpa*<sup>fl/p30</sup> cells. Mice transplanted with MigR1 expressing *Cebpa*<sup>Δ/p30</sup> cells (p30 translated from both alleles) were expected to uniformly develop leukaemia within 9-14 but it was not known if TRIB2 and p30 would cooperate in the absence of its substrate p42.

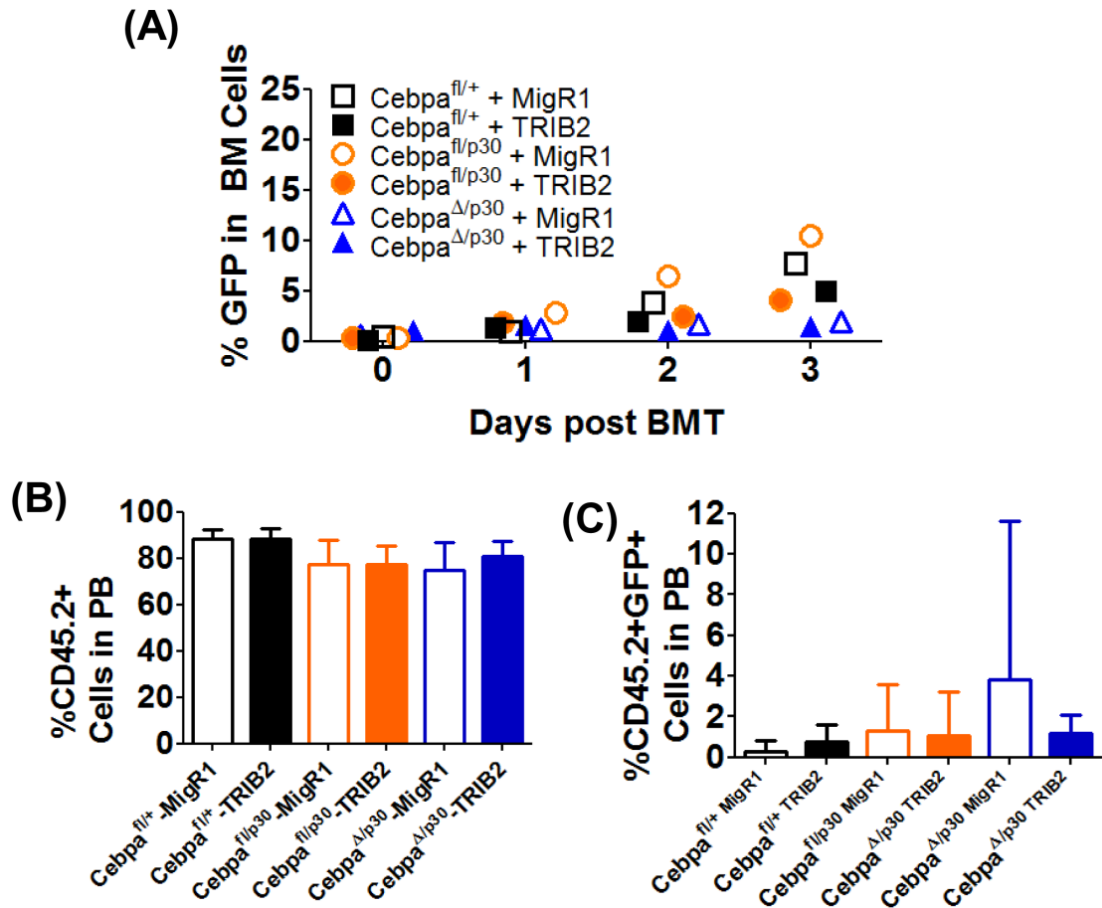


Figure 3. 21 - Engraftment of donor cells in recipient mice.

(A) Graph of percentage of GFP expression in donor BM cells, tracked *in vitro* for 3 days post BMT. (B) Engraftment of transplanted cells is shown as average percentage of CD45.2<sup>+</sup> cells in peripheral blood at 7 weeks post BMT +/- SD, and (C) average percentage of CD45.2<sup>+</sup>GFP<sup>+</sup> cells in the peripheral blood at 7 weeks post BMT +/- SD.

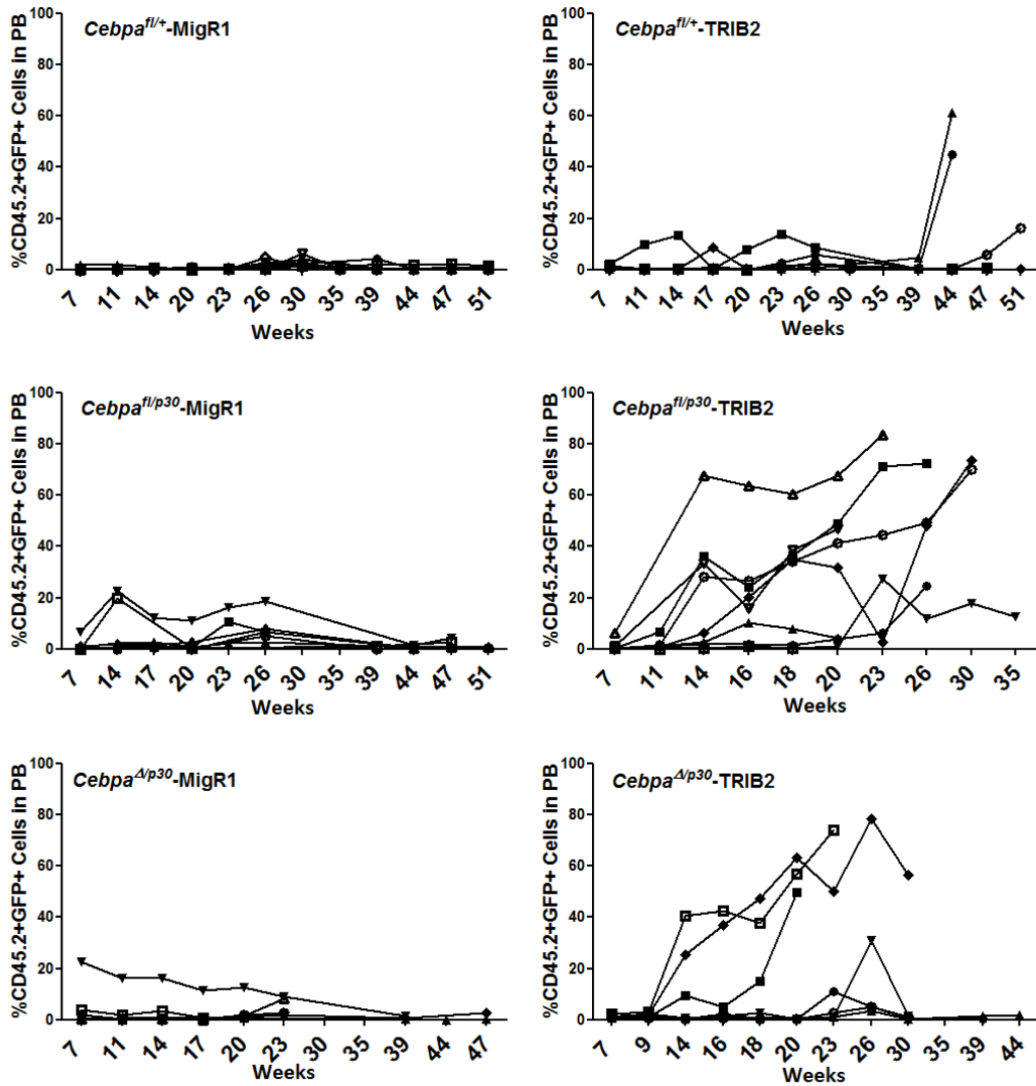


Figure 3.22 - Analysis of GFP expression in CD45.2<sup>+</sup> cells in the PB over time

Representation of disease progression as an increase in CD45.2<sup>+</sup>GFP<sup>+</sup> cells detected over time in the PB of *Cebpa*<sup>fl/+</sup>-MigR1 and *Cebpa*<sup>fl/+</sup>-TRIB2 mice (top panel), *Cebpa*<sup>fl/p30</sup>-MigR1 and *Cebpa*<sup>fl/p30</sup>-TRIB2 mice (middle panel), and *Cebpa*<sup>Δ/p30</sup>-MigR1 and *Cebpa*<sup>Δ/p30</sup>-TRIB2 mice (bottom panel).

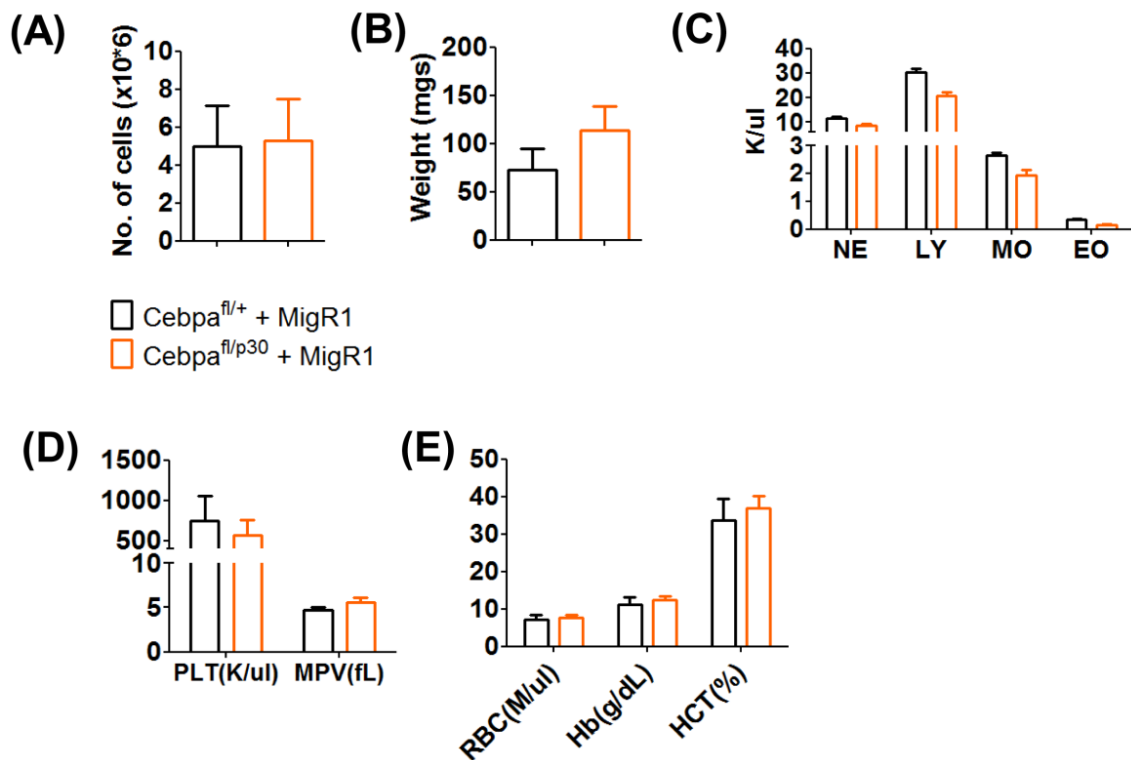


Figure 3. 23 - Analysis of PB cells and spleen weights in control groups

Evidence of normal hematopoiesis in *Cebpa*<sup>fl/+</sup>-MigR1 (n=9) and *Cebpa*<sup>fl/p30</sup>-MigR1 (n=6) control groups is shown as (A) average WBC count +/- SD, (B) average spleen weights +/- SD, (C) average number (K/ul) of neutrophils (NE), lymphocytes (LY), monocytes (MO) and eosinophils (EO) +/- SD, (D) average number of platelets (PLT) and mean platelet volume (MPV) +/- SD, and (E) average number of RBCs, amount of hemoglobin (Hb) and percentage hematocrit (HCT) in the PB +/- SD.

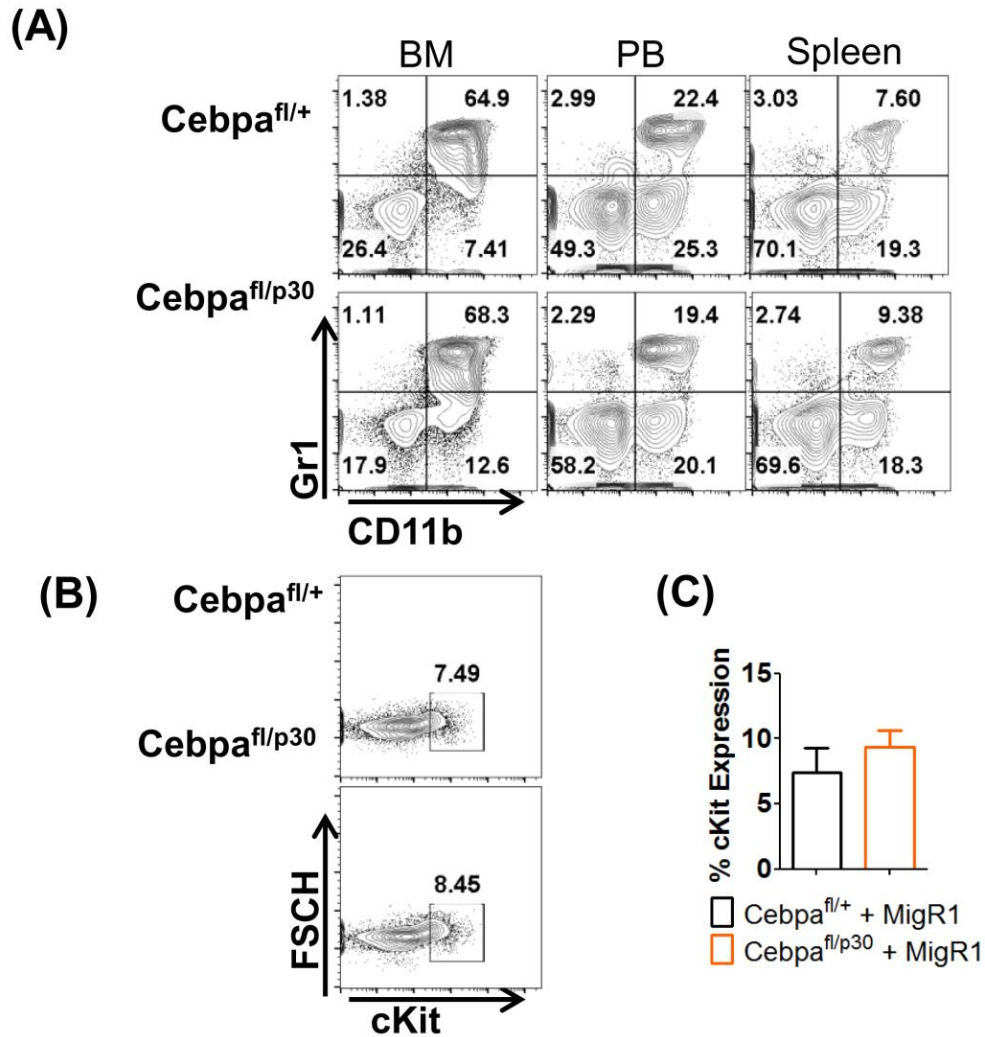


Figure 3. 24 - Flow cytometric analysis of tissues from control mice

**(A)** Representative flow cytometric of CD11b and Gr1 expression in BM, PB and spleen cells isolated from *Cebpa<sup>fl/+</sup>-MigR1* (n=9) and *Cebpa<sup>fl/p30</sup>-MigR1* (n=6) control mice. **(B)** Representative flow cytometric analysis of cKit expression on BM cells isolated from *Cebpa<sup>fl/+</sup>-MigR1* and *Cebpa<sup>fl/p30</sup>-MigR1* control mice. **(C)** Graph of average percentage cKit expression on BM of control mice +/- SD

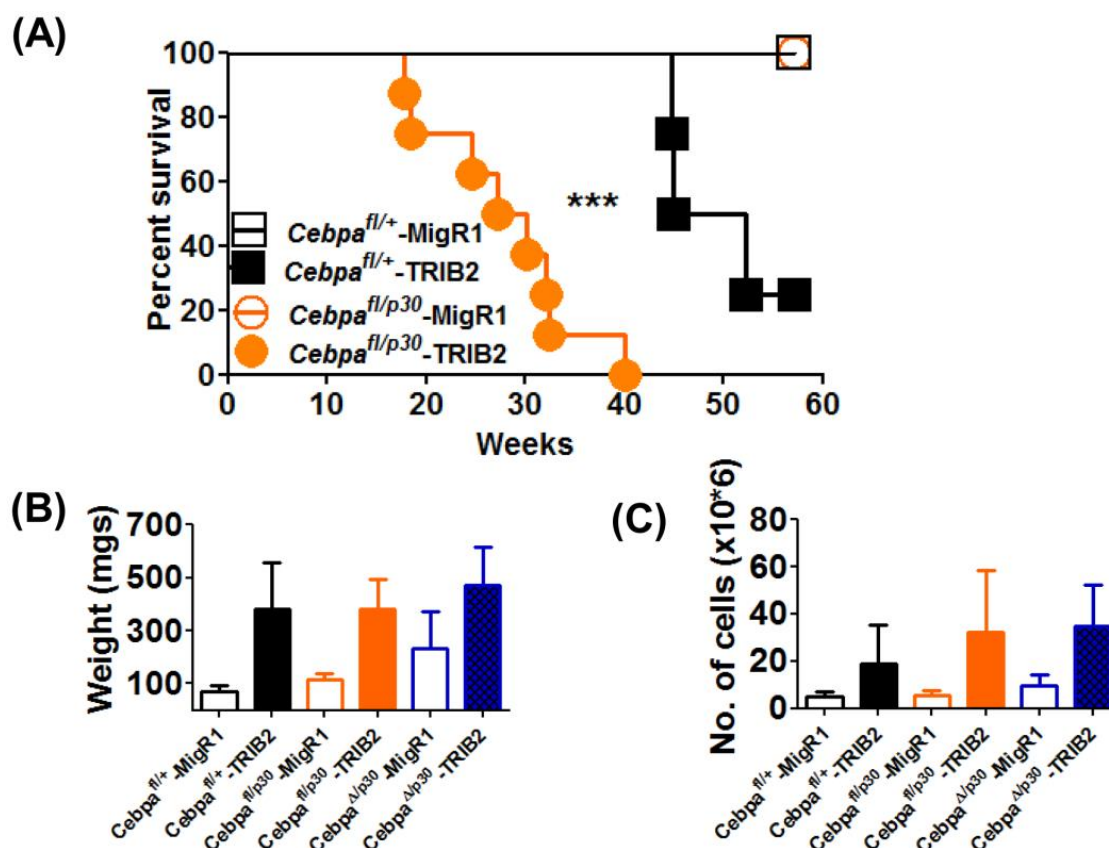


Figure 3. 25 - Survival curve of *Cebpa*<sup>fl/+</sup> and *Cebpa*<sup>fl/p30</sup> transplanted mice

(A) Kaplan-Meier survival curve of mice reconstituted with either *Cebpa*<sup>fl/+</sup> or *Cebpa*<sup>fl/p30</sup> BM cells transduced with MigR1 or TRIB2 expressing retrovirus. None of the mice reconstituted with *Cebpa*<sup>fl/+</sup>-MigR1 (n=9) or *Cebpa*<sup>fl/p30</sup>-MigR1 (n=6) developed leukaemia within 60 weeks. The median survival of mice reconstituted with *Cebpa*<sup>fl/+</sup>-TRIB2 cells was 49 weeks (n=4), while the median survival of mice reconstituted with *Cebpa*<sup>fl/p30</sup>-TRIB2 was 29 weeks (n=8). \*\*\*P<0.0001 by Log-rank test. (B) Average spleen weights +/-SD and (C) average WBC +/- SD of each cohort of transplanted mice depicting normal hematopoiesis in the *Cebpa*<sup>fl/+</sup>-MigR1 (n=9) or *Cebpa*<sup>fl/p30</sup>-MigR1(n=6) groups, and leukaemia in the *Cebpa*<sup>fl/+</sup>-TRIB2 (n=4), *Cebpa*<sup>fl/p30</sup>-TRIB2 (n=8), *Cebpa*<sup>Δp30</sup>-MigR1 (n=6) and *Cebpa*<sup>Δp30</sup>-TRIB2 (n=8) groups.

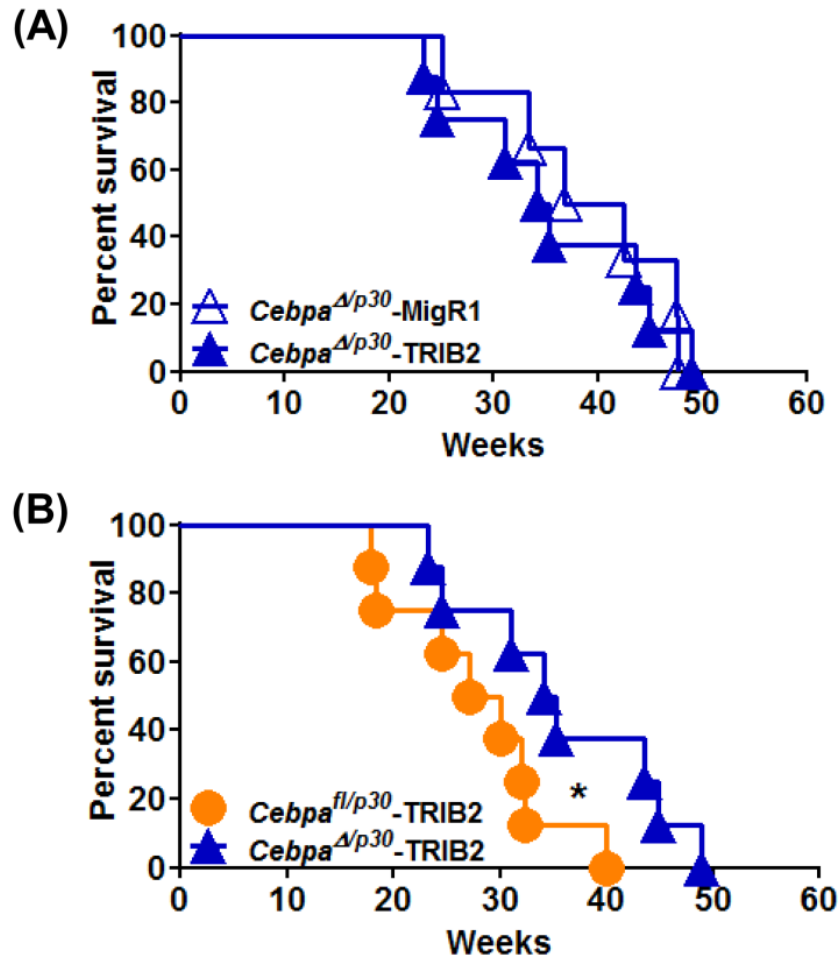


Figure 3. 26 - Survival curve of *Cebpa*<sup>Δ/p30</sup> transplanted mice

(A) Kaplan-Meier survival curve of mice reconstituted with *Cebpa*<sup>Δ/p30</sup> BM cells transduced with MigR1 or TRIB2 expressing retrovirus. The median survival of mice reconstituted with *Cebpa*<sup>Δ/p30</sup>-MigR1 cells was 40 weeks (n=6), while the median survival of mice reconstituted with *Cebpa*<sup>Δ/p30</sup>-TRIB2 cells was 35 weeks (n=8). P=0.8111 by Log-Rank test. (B) Kaplan-Meier survival curve comparing mice reconstituted with *Cebpa*<sup>fl/p30</sup>-TRIB2 or *Cebpa*<sup>Δ/p30</sup>-TRIB2 BM cells. \*P≤0.05 by Log-rank test.

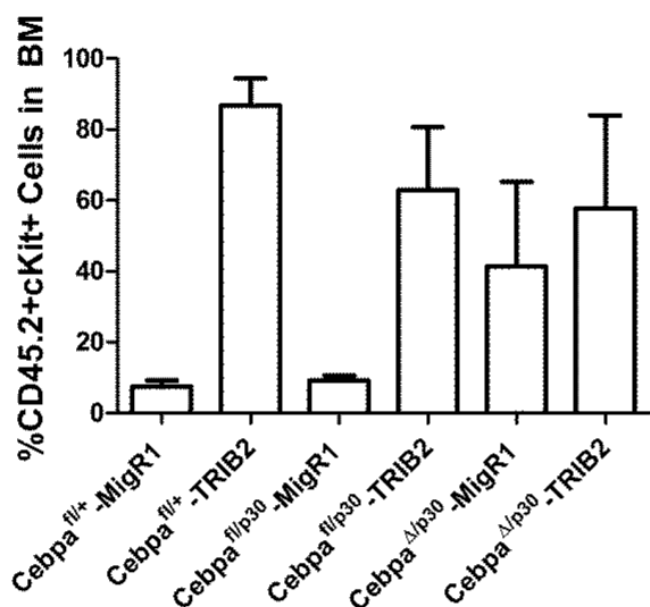


Figure 3. 27 - Expression of cKit in BM cells of transplanted mice

Graph of average percentage cKit expression in CD45.2<sup>+</sup> BM cells of mice transplanted with *Cebpa*<sup>fl/+</sup>-MigR1 (n=9), *Cebpa*<sup>fl/+</sup>-TRIB2 (n=4), *Cebpa*<sup>fl/p30</sup>-MigR1 (n=6), *Cebpa*<sup>fl/p30</sup>-TRIB2 (n=8), *Cebpa*<sup>Δ/p30</sup>-MigR1 (n=6) and *Cebpa*<sup>Δ/p30</sup>-TRIB2 (n=8) expressing cells +/- SD.

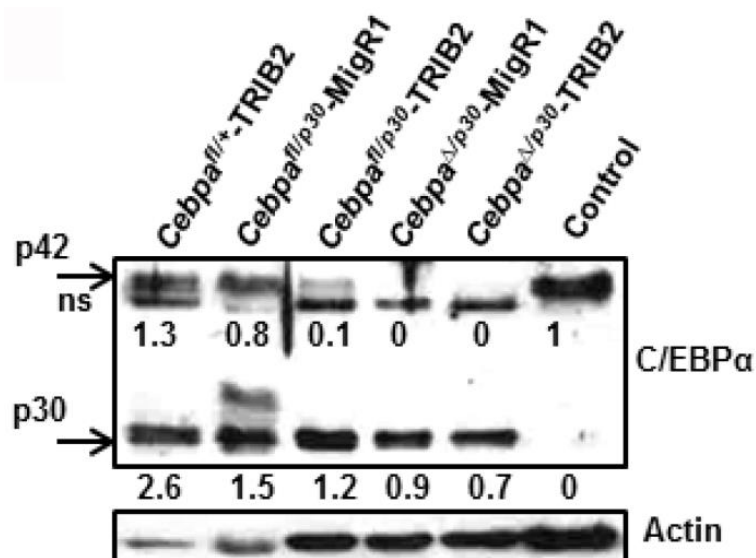


Figure 3. 28 - Western blot analysis of C/EBP $\alpha$  expression in BM cells from transplant cohorts

CD45.2<sup>+</sup>DAPI<sup>-</sup> leukemic BM cells were sorted for by FACS and directly lysed in SDS buffer as described in 2.5.1.1.2. Western blot analysis was performed. ns denotes non-specific band, and actin serves as a loading control.

### 3.4 Discussion

The data show that overexpression of p30 induced myeloid differentiation *in vivo* which, in a small-scale study, resulted in a weakly penetrant transplantable AML. It was found that TRIB2 selectively degrades p42 by K48 mediated proteasome dependent ubiquitination but was not able to ubiquitinate the p30 isoform. Degradation of p42 by TRIB2 could be targeted using the proteasome inhibitor Bortezomib. Mutation of residue K313 abrogated this function indicating that this site which is frequently found mutated in AML, is required for TRIB2 mediated C/EBP $\alpha$  ubiquitination. It was determined by BMT that, despite functioning to degrade C/EBP $\alpha$ , C/EBP $\alpha$  is essential for TRIB2 induced AML. The data also show that in the presence of p42, TRIB2 and p30 cooperate to accelerate AML induction. Together these data reveal important insights into the degradative relationship between TRIB2 and C/EBP $\alpha$  and support a dichotomous role for C/EBP $\alpha$  in the pathogenesis of TRIB2 induced AML.

Contrary to previously published data (Schwieger et al., 2004), p30 overexpressing BM cells engrafted in a murine BMT and provided long-term reconstitution of the hematopoietic system in recipient mice. It is unclear why the p30 overexpressing cells in the study by Schwieger *et al* failed to engraft. The authors used an FMEV based retroviral vector and showed that BM cells were efficiently transduced by control and mut10 retrovirus (range 32%-69%). The discrepancy may relate to the expression vector itself, or differences in experimental conditions. Overexpression of p30 resulted in an increase in the number of mature CD11b<sup>+</sup>Gr1<sup>+</sup> myeloid cells observed in the GFP<sup>+</sup> compartment of p30 chimeric mice. There is evidence to support a role for p30 to promote myeloid differentiation as it shares with p42 a transactivation domain (TAD2) and thus there is overlap of transcriptional targets between p42 and p30. Indeed the observed ability for p30 to mediate the CMP to GMP transition in the absence of p42 as described in section 3.1.2.2 (Kirstetter et al., 2008) would also support the idea that p30 overexpression can induce myeloid differentiation. However, other studies show that increased p30 expression decreases expression of *Gcsfr* which would inhibit maturation of myeloid cells (Cleaves et al., 2004). Unlike p42, p30 was also unable to induce differentiation in the IL-3 dependent cell line 32D (Keeshan et al., 2003). The fact that p30 induced myeloproliferation of CD11b<sup>+</sup>Gr1<sup>+</sup> mature cells in the short-term which transformed into a mature

myeloid leukaemia in the long-term, albeit weakly penetrant, suggests that instead of inducing myeloid cell maturation p30 overexpression may induce cell proliferation.

In a recent publication, genome-wide transcriptome analysis was performed on K562 cells carrying Tet-inducible p42 or p30 (Hughes et al., 2015). Expression of urothelial carcinoma associated 1 (UCA1), a long non-coding RNA, was significantly upregulated in p30 expressing cells, compared with control. In human AML patient samples, high UCA1 expression correlated with CN-AML carrying *CEBPA* mutations and it has been shown to promote tumour cell growth in solid tumours. The authors demonstrated that p30 bound to and activated UCA1 expression. Knockdown of UCA1 in K562 cells, a myeloid leukaemia cell line, induced a block at the G1-S phase transition of the cell cycle by increasing expression of the CDK inhibitor p27<sup>kip1</sup>. Thus it is possible that p30 overexpression in the presence of physiological levels of p42 could cause aberrant proliferation of mature myeloid cells via activating transcription of UCA1, inhibiting expression of p27<sup>kip1</sup> and promoting proliferation.

When the primary p30 AML cells were transplanted into a secondary recipient they produced a B220<sup>+</sup> disease. There is some evidence suggesting that p30 overexpression may affect the B cell lineage. In the aforementioned study from Kato *et al* (3.1.2.4), the authors generated retrovirus overexpressing a C/EBP $\alpha$  N-terminal mutant (C/EBP $\alpha$ -N<sup>m</sup>) which only expressed p30. BM cells overexpressing C/EBP $\alpha$ -N<sup>m</sup> were transplanted into lethally irradiated recipient mice with less than half developing disease, which correlates with the weak penetrance observed in the p30 driven AML (1 out of 3 mice). Most of the mice that did develop disease were phenotypically akin to B-ALL characterised by the accumulation of B220<sup>+</sup>CD19<sup>+</sup>cKit<sup>int/hi</sup> leukemic cells which infiltrated the spleen and liver.

Ubiquitination analysis demonstrated that TRIB2 degrades p42 by K48 mediated proteasomal ubiquitination. This was supported by the observation that leukaemic U937 cells transduced with TRIB2 were more sensitive to proteasome inhibition than controls. Indeed enforced C/EBP $\alpha$  expression was shown to rescue cells from Bortezomib induced cellular toxicity. The specificity of proteasome inhibition on the Trib2-C/EBP $\alpha$  axis was demonstrated with the use

of C/EBP $\alpha$  null leukaemia cell lines (K562 and Kasumi 1), where overexpression of TRIB2 had no effect on sensitivity to Bortezomib. The ubiquitin proteasome system (UPS) is a highly regulated mechanism for protein degradation and turnover and targeting the UPS has recently emerged as a novel therapeutic route in cancer treatment. Activity of the UPS has been shown to be elevated in AML, ALL and MDS patient samples and combination therapy incorporating drugs targeting the UPS system represents a novel therapeutic development for hematological disorders (Salome et al., 2015). Bortezomib was the first proteasome inhibitor used successfully in a clinical trial. In multiple myeloma it was shown to reversibly inhibit the 26S proteasome preventing the breakdown of the NF $\kappa$ B inhibitor I $\kappa$ B thus stabilising NF $\kappa$ B stopping it from translocating to the nucleus inactivating key cell signalling pathways integral to myeloma cell function (Field-Smith et al., 2006). It has also proven effective in treating mantle cell lymphoma and is being used in a clinical trial in combination with other chemotherapeutics (daunorubicin and cytarabine) in AML (Attar et al., 2013). As outlined in section 1.3.4.1.1, *TRIB2* is elevated in a subset of human AML cases with WT *CEBPA* and targeting the TRIB2-C/EBP $\alpha$  axis by proteasome inhibition may represent a potential therapeutic avenue in these AML cases.

The K313KK (K313dup) mutation is found in up to 10% of AML patients and leads to C/EBP $\alpha$  instability (Carnicer et al., 2008). As described in 3.1.2.3, the C-terminal K313dup mutation was shown to cooperate with the N-terminal mutation (Bereshchenko et al., 2009). The data presented show that mutation of K313 to K313R abrogated TRIB2 mediated C/EBP $\alpha$  ubiquitination while retaining its DNA binding, transcriptional activation and downstream differentiation function, suggesting that K313 is a site of TRIB2 ubiquitination on C/EBP $\alpha$ . In the study of 285 AML patient samples organised into 16 clusters based on gene expression analysis discussed in section 1.3.4.1.1, elevated TRIB2 expression (cluster 4) was shown to correlate with CD7 expression and TCR rearrangement (Wouters et al., 2007). It has also been shown that patients with K313dup are positive for CD7 and have TCR rearrangements (Carnicer et al., 2008). In light of these findings it is possible that the K313dup mutation may increase the susceptibility of C/EBP $\alpha$  to be ubiquitinated by TRIB2 by providing an additional lysine residue for ubiquitin conjugation, resulting in increased C/EBP $\alpha$  degradation. However the K313 site is present in both p42 and p30, yet TRIB2

was unable to ubiquitinate p30. It is unclear why TRIB2 selectively degrades p42 and in the absence of a crystal structure for TRIB2, one can only hypothesise that the TRIB2-p42 and TRIB2-p30 protein complexes are structurally different. It is tempting to speculate that the conformation of the TRIB2-p30 complex inhibits the binding of COP1 to TRIB2 which has been shown to be essential for p42 degradation (Keeshan et al., 2010).

The *Cebpa*<sup>Δ/Δ</sup> BM transduction and transplant data show definitively that the presence of C/EBPα is essential for TRIB2 mediated AML induction. This correlates with the aforementioned studies of HOXA9/MEIS1 (Collins et al., 2014) and MLL rearranged leukaemia (Ohlsson et al., 2014) which as described in section 1.2.2.2.1, also demonstrate the necessity for C/EBPα in leukaemia initiation. A recent publication has suggested that it is not C/EBPα, but rather granulocytic differentiation which is required for leukaemogenesis (Ye et al., 2015). The authors demonstrated that in a *Cebpa* null background MLL-AF9 and MOZ-TIF2 were unable to initiate leukaemia, but pharmacological induction of granulopoiesis by GM-CSF administration returned the leukaemogenic potential of these oncogenes in the absence of *Cebpa* expression. Under normal physiological conditions the protein levels of p42 are greater than p30 protein levels, and when this balance changes toward higher p30 expression it is considered leukemic, as observed in leukaemia cell lines and AML patients (Leroy et al., 2005). The use of the *Cebpa*<sup>fl/p30</sup> model, which carries one WT allele and one p30 only allele, with TRIB2 overexpression, demonstrated that expression of the p42 isoform from one *Cebpa* allele was necessary and sufficient for TRIB2 to cooperate with p30 in AML. In the absence of p42, *Cebpa*<sup>Δ/p30</sup>, the addition of TRIB2 did not further accelerate AML induced by p30 itself, unlike the accelerated AML observed when p42 is present. It is possible that the cooperation observed in the presence of p42 is the result of TRIB2 converting p42 to p30 but the mechanism by which TRIB2 increases p30 expression remains to be elucidated. In light of the recent publication from Ye *et al*, it is also possible that the presence of p42 in the *Cebpa*<sup>fl/p30</sup> model influenced the latency of TRIB2 mediated AML through more efficient induction of granulocytic differentiation from the CMP to the GMP than p30 could provide alone.

Collectively these data show that TRIB2 mediated AML relies on the expression of C/EBP $\alpha$ . It degrades p42 through K48-specific ubiquitination at K313. While the mechanism by which TRIB2 overexpression upregulates p30 in AML induction is unknown, we show that unlike p42, TRIB2 is unable to ubiquitinate p30. Overexpression of p30 in the presence of physiological levels of p42 resulted in enhanced proliferation of mature myeloid cells with weak transformation ability. Using a conditional murine model TRIB2 was shown to cooperate with p30 in leukaemogenesis only in the presence of p42. These data highlight the molecular interplay between TRIB2 and C/EBP $\alpha$  in AML pathogenesis and present a novel therapeutic window for the use of proteasome inhibition in a subset of AML with high TRIB2 expression.

Some of the data presented here have been published in O'Connor et al, 2016, details provided in section 0.

## **4 Results: Identifying the TRIB2 leukaemia initiating cell**

Part of this chapter has been published in Liang et al, Cell Discovery, 2016, details provided in section 0.

## 4.1 Introduction

As described in 1.1, the entire hematopoietic system is generated by a small pool of long-lived HSCs. Like all stem cells in the body, HSCs are characterised by both their ability to self-renew, and to give rise to more differentiated cells. While AML cells within a given disease often appear to be morphologically homogeneous, there is now a large body of evidence showing that leukemic cells comprise a heterogeneous population and these cells also contain a small number of leukaemia stem cells (LSCs) responsible for generating and maintaining the disease.

### 4.1.1 Modelling tumour development

There are 2 mutually exclusive models describing the way in which tumours develop - namely the stochastic model and the hierarchy or cancer stem cell (CSC) model (Figure 4. 1).

#### 4.1.1.1 The stochastic model

The stochastic model of tumour development assumes that within a given tumour all cells have the potential to initiate tumours, but that each cells' behaviour is affected randomly by intrinsic (e.g. levels of transcription factors) or extrinsic (e.g. microenvironment) influences. Central to this model is the idea that all tumour cells have the potential to be affected by these factors, and the effects are reversible. This has been expanded to include clonal evolution whereby new mutations accumulating within given cells will result in clonal diversity, further increasing the heterogeneity observed within tumours. Indeed some cancer types do appear to adhere to this model. It has been shown in melanoma that up to 50% of cells within a tumour are capable of forming secondary tumours in xenograft transplants (Quintana et al., 2010). The authors also tested 16 markers that were heterogeneously expressed on melanoma tumour cells including CD44 and cKit, as putative markers of tumour initiating cells, but expression or exclusion of any one marker failed to affect the tumour initiating activity of that cell. Furthermore the tumours that arose from each marker-defined fraction produced secondary tumours that were phenotypically similar to the parent tumour, regardless of the phenotype of the transplanted starting cells. These experiments show that melanoma tumours are not arranged

hierarchically, and contain a high number of tumorigenic cells that can initiate a disease in a secondary recipient which is phenotypically similar to the parent disease.

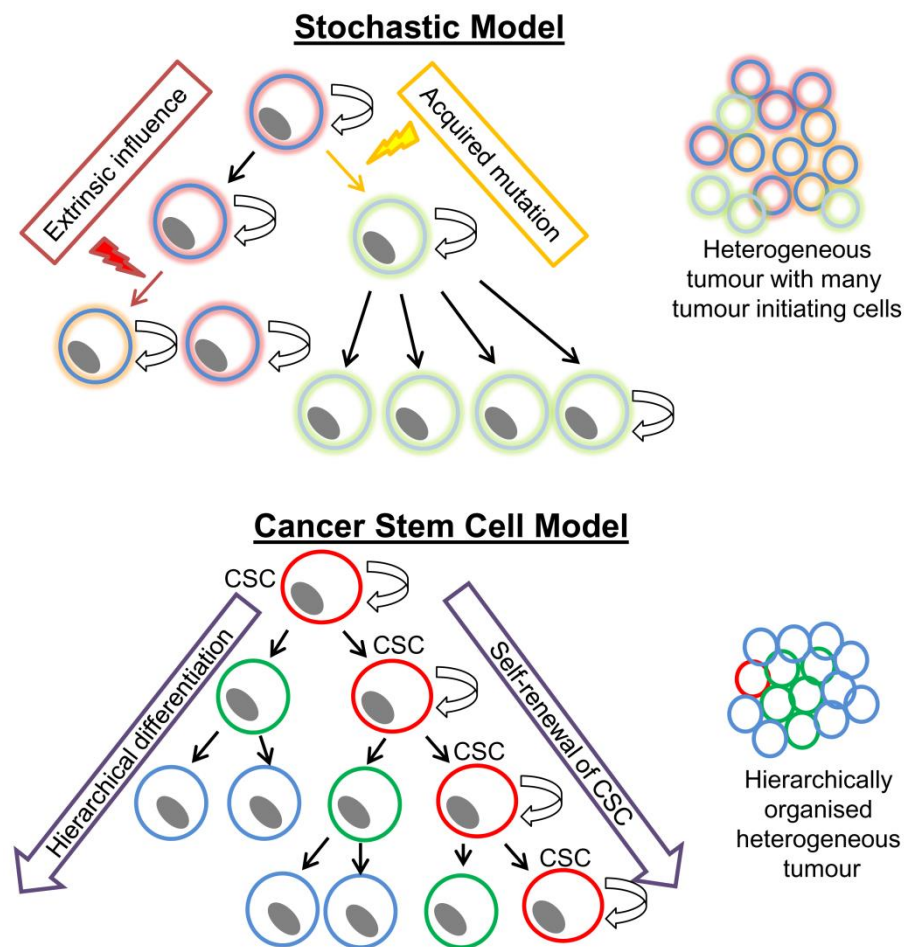


**Figure 4. 1– Schematic diagram of the stochastic and cancer stem cell models of tumour development**

#### 4.1.1.2 The cancer stem cell model

The cancer stem cell or hierarchy model proposes that CSCs exist which share characteristics of normal HSCs in their ability to self-renew and to differentiate into more mature progeny. The concept centres on a hierarchical tumour arrangement which mimics normal development, with only a biologically distinct subset of CSCs responsible for disease initiation and propagation. Therefore in order to therapeutically eradicate a disease, the CSCs must be targeted. The first CSCs were identified in AML, following the development of the xenograft transplant model. In 1995 the non-obese diabetic/severe combined immune-deficient (NOD/SCID) mouse model was produced, by crossing the Nod mouse which has impaired NK and antigen-presenting cell function, with the Scid mouse

which lacks T and B cell function (Shultz et al., 1995). This permitted the transplantation of purified populations of cells from human AML samples into the immunocompromised mice, to determine if the cells were able to generate disease *in vivo*. In seminal work performed by John Dick and colleagues, human AML samples from a variety of FAB subtypes with different bulk populations of blast cells were fractionated based on their CD34 and CD38 expression. CD34 is a cell surface marker present on human stem and progenitor populations, while CD38 is expressed on more committed progenitor cells (Figure 4. 2). CD34<sup>+</sup>CD38<sup>-</sup> cells are therefore the most primitive type of leukemic cell. Only these cells, comprising a mere 0.2% of the bulk AML population, were able to generate disease when transplanted into NOD/SCID mice (Bonnet and Dick, 1997, Lapidot et al., 1994). As few as 5000 cells were able to initiate leukaemia in the recipient mice. However even with 100 times as many cells transplanted, neither CD34<sup>+</sup>CD38<sup>+</sup> nor CD34<sup>-</sup> leukemic cells could generate leukaemia *in vivo*. Furthermore in addition to proliferating and differentiating in primary transplants, the CD34<sup>+</sup>CD38<sup>-</sup> leukemic cells were also able to re-establish AML in secondary transplants demonstrating self-renewal ability.

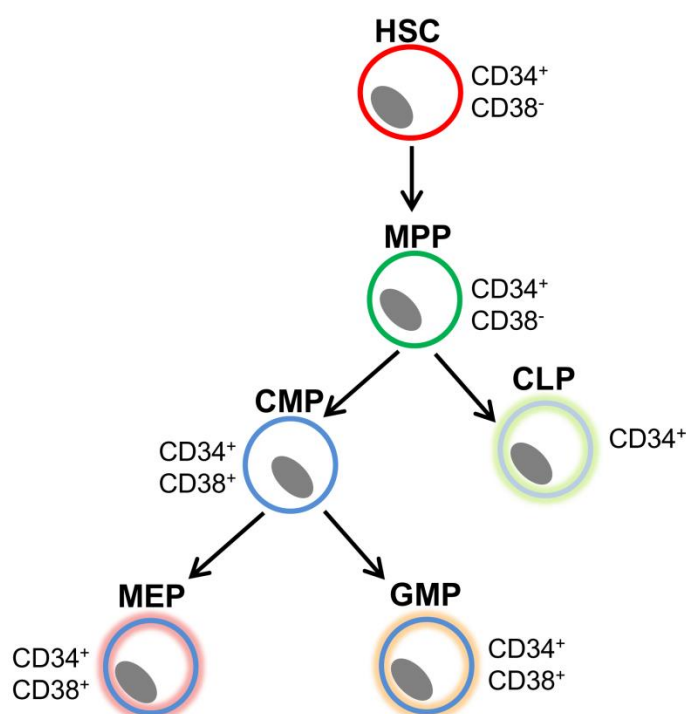


**Figure 4. 2 – Schematic representation of CD34 and CD38 expression on human stem and progenitor cells**

Following these discoveries the NOD/SCID mouse model has been used to identify CSCs in solid tumour cancers. Using a modified NOD/SCID model where breast cancer tumours were generated in the recipients' mammary fat pad, only Lin<sup>-</sup>CD44<sup>+</sup>CD24<sup>-/low</sup> breast tumour cells were able to generate tumours *in vivo* (Al-Hajj et al., 2003). CSCs have been identified based on their surface marker expression in a variety of other tumour models, including CD133<sup>+</sup> CSCs in colon (O'Brien et al., 2007), brain (Singh et al., 2004) and lung cancer (Eramo et al., 2008). These studies demonstrate that many forms of cancer, including AML, adopt the cancer stem cell model, with heterogeneous tumours containing a small population of CSCs that have the ability to induce and maintain tumour growth *in vivo*, as well as produce non CSCs, supporting a hierarchical arrangement of cells within the tumour.

#### **4.1.2 Leukaemia stem cell heterogeneity and plasticity**

The idea that LSCs are exclusively restricted to the CD34<sup>+</sup>CD38<sup>-</sup> compartment has been challenged with the development of new xenograft models. There are several limitations to using NOD/SCID mice to study the LSC in AML. NOD/SCID mice have a short lifespan and are prone to the spontaneous development of thymic lymphomas (Shultz et al., 1995). In addition there is a relatively low

frequency of engraftment of primary human AML cells in NOD/SCID mice ranging from between 0.1% to 10% detection in BM of transplanted mice (Ailles et al., 1999). To overcome these issues the NOD/SCID/IL2R $\gamma$ <sup>null</sup> (NSG) mouse was generated which has a deletion in the  $\gamma$ -common chain, eliminating residual NK cell activity (Shultz et al., 2005). These mice are not prone to spontaneous thymic lymphomas, they have a longer lifespan and they engraft human cells better than NOD/SCID mice.

NSG mice have been used to extend our understanding of the AML LSC. In one study, CD34 expression in 19 AML samples from different subtypes with different karyotypes was shown to be highly variable among samples, with 32% lacking CD34 expression, yet all samples were able to engraft (range 10.4%-43.0%) in NSG recipient mice (Sarry et al., 2011). This suggested that the earlier characterisation of AML LSCs as CD34<sup>+</sup>CD38<sup>-</sup> in NOD/SCID transplants may have been too restrictive. The authors also assessed the ability for the Lin<sup>-</sup> and Lin<sup>dim</sup> fractions of leukemic cells to initiate leukaemia *in vivo*, and surprisingly cells from both fractions could generate disease. Indeed most intriguing was the observation that the LSCs displayed a certain amount of plasticity. As expected, when primitive Lin<sup>-</sup>CD38<sup>-</sup> leukemic cells were transplanted they produced Lin<sup>-</sup>CD38<sup>-</sup> and Lin<sup>-</sup>CD38<sup>+</sup> cells *in vivo* as well as Lin<sup>+</sup> cells. However when the more mature committed Lin<sup>dim</sup>CD38<sup>+</sup> cells were transplanted, they too produced both Lin<sup>dim</sup>CD38<sup>+</sup> and the immature Lin<sup>-</sup>CD38<sup>-</sup> cells. The authors also showed that LSCs were indeed enriched in the Lin<sup>-</sup>CD38<sup>-</sup> cell fraction (1 in 3.8x10<sup>4</sup>), yet also present with the lowest frequency in the Lin<sup>dim</sup>CD38<sup>+</sup> fraction (1 in 1.0x10<sup>6</sup>).

LSC heterogeneity and plasticity has been demonstrated many times with different models. Using the HOXA9/MEIS1 mouse model, leukemic cells were fractionated into 4 subpopulations - Lin<sup>-</sup>cKit<sup>+</sup>, Lym<sup>+</sup>cKit<sup>+</sup> (where Lym represents a cocktail of lymphoid markers including B220, CD19, CD3 $\epsilon$ , CD4, CD8a, and TCR- $\beta$ ), Gr1<sup>+</sup>cKit<sup>+</sup> and Gr1<sup>+</sup>cKit<sup>lo</sup> cells. Each population was assessed for their ability to initiate disease by limiting dilution transplant and the authors showed that all populations were able to initiate AML *in vivo* (Gibbs et al., 2012). However the frequency with which they initiated disease varied substantially. As few as 100 Lin<sup>-</sup>cKit<sup>+</sup> and Lym<sup>+</sup>cKit<sup>+</sup> initiated a secondary disease, while 1000 Gr1<sup>+</sup>cKit<sup>+</sup> and 10,000 Gr1<sup>+</sup>cKit<sup>lo</sup> were required in order to generate AML in the secondary recipient. As with the aforementioned study, the secondary diseases represented

the parent disease fully regardless of the transplanted cell phenotype, meaning that even the more mature Gr1<sup>+</sup>cKit<sup>lo</sup> transplanted cells were able to produce cells of a less differentiated phenotype *in vivo*.

Thus while LSCs are certainly far more commonly found in the most immature sub-fraction of leukemic cells, they can also be detected in mature subsets which are equally capable of recapitulating the heterogeneity of the parent disease.

### 4.1.3 The leukaemia initiating cell

The LSC is a cell which is capable of initiating and propagating leukaemia *in vivo*. As described in 4.1.2, cellular heterogeneity exists within the LSC fraction, and LSCs also exhibit plasticity. Thus characterising the LSC population does not identify the original cell that gave rise to the leukaemia. The cell of origin or LIC refers to the cell from which a specific leukaemia normally arises, and it is hypothesised that the LIC may influence the progression or phenotype of a disease, as well as its response to therapy. It is unclear whether the LIC is a HSC or a more committed progenitor cell, and it is likely dependent on the transforming event. In general terms the HSC is the most obvious candidate for the LIC of a given disease considering their shared self-renewal characteristics. Indeed gene expression analysis has revealed many shared pathways between HSCs and LSCs. In a 2011 study, 4 subpopulations were sorted from 16 human AML samples based on CD34 and CD38 expression, and each fraction was tested for LSC enrichment using a xenograft transplant assay (Eppert et al., 2011). As expected, LSCs were identified primarily in the CD34<sup>+</sup>CD38<sup>-</sup> fraction, but also in the CD34<sup>+</sup>CD38<sup>+</sup> fraction. Global gene expression analysis was performed on each fraction and compared with HSC, progenitor cell and differentiated cell samples. The HSC gene signature was enriched in LSCs. The LSCs were also compared with previously generated data sets from stem, progenitor and mature cell populations, and here too LSC gene expression correlated positively with that of primitive cells, and negatively with mature populations. However, considering the heterogeneity and plasticity of the LSC compartment committed progenitor cells may also represent the LIC.

Several studies have explored the LIC of specific oncogenes mostly using either a methylcellulose-based serial replating assay and/or a retroviral-mediated murine BMT, and these studies are outlined below and summarised in Table 4-1. The use of the serial replating assay for investigating oncogenicity became popular following a publication by Lavau et al in 1997. To determine if the fusion protein HRX-ENL would affect self-renewal and differentiation, Lin<sup>-</sup> BM cells transduced with the oncogene or control MSCV retrovirus and serially replated in methylcellulose medium supplemented with IL-3, IL-6, GM-CSF and SCF (Lavau et al., 1997). The authors observed that unlike the primary colonies which were similar for both control and HRX-ENL transduced BM and of a mature myeloid phenotype, the secondary colonies differed greatly. Control cells produced very small and diffuse colonies indicating limited self-renewal and proliferative capacity, whereas secondary colonies from HRX-ENL expressing cells were much larger and of 3 distinct phenotypes. Type I colonies contained immature myeloid precursor cells and were compact in size, Type II colonies contained more mature cells and had a compact centre surrounded by a diffuse halo of cells, while type III colonies were the most differentiated and comprised dispersed cells with no core. By the third replating control cells had exhausted their proliferative potential and were unable to generate colonies, whereas the HRX-ENL expressing cells showed enhanced potential, with further increases observed at the fourth replating. This model is now frequently used to determine if an oncogene confers self-renewal and proliferative potential to BM stem and progenitor cells *in vitro*.

#### **4.1.3.1 MLL rearranged AML**

##### **4.1.3.1.1 MLL-ENL**

As described in section 1.2.2.2.3, translocations resulting in MLL fusion proteins are commonly found in myeloid and lymphoid leukaemia. Over-expression of certain MLL fusion proteins, including MLL-ENL, induces AML *in vitro* (Lavau et al., 2000). The MLL-ENL translocation was assessed for its ability to transform different progenitor compartments (Cozzio et al., 2003). MLL-ENL transduced HSC, CMP and GMP cells produced identical compact colonies in an *in vitro* serial replating assay with a blast-like morphology, while the control transduced cells produced a range of colony types from undifferentiated to differentiated. MEPs transduced with MLL-ENL were not able to serially replat, or grow in culture.

HSC, CMP and GMP cells transduced with MLL-ENL retrovirus were transplanted into lethally irradiated recipients and all mice developed AML with the same latency (90-100 days). Titration of the injected number of MLL-ENL expressing cells revealed that HSCs were more efficient than CMPs, and CMPs more efficient than GMPs at inducing AML *in vivo*.

#### 4.1.3.1.2 MLL-GAS7

In a similar study the fusion protein MLL-GAS7 was assessed. 5-FU treated BM transduced with control or MLL-GAS7 retrovirus serially replated in a CFU assay producing cells with a cKit<sup>+</sup>Sca1<sup>+</sup> phenotype with low levels of B220 and CD11b expression but no other lineage markers, typical of an MPP (So et al., 2003). These cells generated 3 types of leukaemia upon transplantation: a cKit<sup>+</sup>CD11b<sup>+</sup>Gr1<sup>+</sup>B220<sup>-</sup>CD19<sup>-</sup> AML, a cKit<sup>+</sup>CD43<sup>+</sup>B220<sup>+</sup>BP-1<sup>+</sup>CD19<sup>+</sup>CD11b<sup>-</sup>Gr1<sup>-</sup> ALL and a cKit<sup>+</sup>CD11b<sup>+</sup>B220<sup>+</sup>CD19<sup>-</sup>Gr1<sup>-</sup> acute biphenotypic leukaemia (ABL). Purified HSCs, CLPs, CMPs, GMPs and MEPs were then transduced with MLL-GAS7 and serially replated in methylcellulose medium supplemented with myeloid or lymphoid cytokines. HSC, CMP and GMP transduced cells formed third round colonies under myeloid conditions producing primarily ckit<sup>+</sup>Gr1<sup>+</sup>CD11b<sup>+</sup> cells, but unlike CMP and GMP transduced cells, the HSCs also had a small proportion of CD11b<sup>+</sup>B220<sup>+</sup> bi-phenotypic cells. Only MLL-GAS7 transduced HSCs replated in lymphoid conditions producing 3 distinct subpopulations expressing either CD11b, B220 and CD19, or CD11b and B220. The HSC was the only subpopulation susceptible to multi-lineage transformation by MLL-GAS7 overexpression, giving rise to the MPP-like LSC.

#### 4.1.3.1.3 MLL-AF9

In another study LSKs, HSCs and GMPs were transduced with the MLL fusion oncogene MLL-AF9 (Krivtsov et al., 2013). In a CFU assay single MigR1 transduced cells exhausted after 1-3 replatings, while MLL-AF9 transduced cells continuously formed colonies. However when transplanted, the transformed LSK induced AML with a shorter latency and much higher penetrance than the GMP. A limiting dilution experiment from MLL-AF9 transformed HSC and GMP single cell clones determined a much higher LIC frequency in the HSC (1 in 29388) compared to the GMP (1 in 168,427). Indeed the authors demonstrated that these 2 LICs also exhibit differences in gene expression. Leukemic GMPs isolated from an MLL-AF9 leukaemia originating from the HSC (LGMP<sup>HSC</sup>) or GMP (LGMP<sup>GMP</sup>) were analysed

for expression of *Evi1*. It had been previously documented that MLL-AF9 overexpression maintains *Evi1* expression in the HSC, but does not activate *Evi1* expression in committed myeloid progenitor cells. The authors found that *Evi1* expression levels were 200-fold higher in the LGMP<sup>HSC</sup> than the LGMP<sup>GMP</sup>. Thus while both the LGMP<sup>HSC</sup> and LGMP<sup>GMP</sup> outwardly exhibit the characteristics of a GMP cell, there are significant differences in gene expression. Indeed the authors also showed that HSC-derived MLL-AF9 AML was less responsive to standard chemotherapeutics than GMP-derived AML.

#### **4.1.3.2 AML fusion proteins from other common chromosomal rearrangements**

##### **4.1.3.2.1 MOZ-TIF2 and BCR-ABL**

MOZ-TIF2 is a fusion oncoprotein generated by inv(8) and is associated with M4/5 AML by FAB classification, while BCR-ABL is a fusion gene caused by a t(9;22) and is found in most patients with CML, and some ALL and AML patients. In a comparative study of the ability of the MOZ-TIF2 and BCR-ABL oncogenes to transform stem and progenitor cells, MOZ-TIF2 was shown to be able to transform the HSC, CMP and GMP populations *in vitro* with the transduced cells exhibiting serial replating ability, whereas BCR-ABL could only transform the HSC (Huntly et al., 2004). Subsequently CMP, GMP or whole BM mononuclear cells (MNC) were transduced with either MOZ-TIF2 or BCR-ABL and transplanted into recipient mice. All mice receiving MOZ-TIF2 transduced cells developed AML with comparable latencies (113-240 days) and a virtually identical disease phenotype, while only the BCR-ABL transduced BM MNCs generated disease *in vivo*. The authors hypothesise that the differences observed may be in part due to the oncogenes themselves whereby BCR-ABL can provide the self-renewal signals to cells but fails to impair differentiation unlike MOZ-TIF2, which would lead to an expansion of mature myeloid cells, insufficient to generate leukaemia in mice.

##### **4.1.3.2.2 CALM/AF10**

The CALM/AF10 fusion protein is formed from a reciprocal translocation between chromosomes 10 and 11. The translocation is primarily associated with T-ALL but has also been observed in many myeloid leukaemias (Salmon-Nguyen et al., 2000) and CALM/AF10 transduced stem and progenitor cells induce AML in mice (Deshpande et al., 2006). The phenotype of the disease showed that most cells

expressed CD11b and Gr1 but not B220 (B220<sup>-</sup>/MM<sup>+</sup>), but an additional 2 populations of cells existed which were either CD11b<sup>+</sup> or Gr1<sup>+</sup> with B220 expression (B220<sup>+</sup>/MM<sup>+</sup>) or were B220<sup>+</sup> but lacked myeloid markers (B220<sup>+</sup>/MM<sup>-</sup>). All 3 populations displayed DJ rearrangements suggesting that the leukaemia originated from a DJ rearranged cell. Transcriptionally the B220<sup>+</sup>/CD11b<sup>-</sup> cells displayed significant upregulation of cell cycle, translation and DNA repair and replication genes, compared with B220<sup>-</sup>/CD11b<sup>+</sup> where genes involved in cell death and communication were increased. A limiting dilution assay revealed, as expected, a very high frequency of leukaemia cell propagation from the B220<sup>+</sup>/CD11b<sup>-</sup> cells (1 in 36), compared with an extremely low frequency for the B220<sup>-</sup>/MM<sup>+</sup> cells (1 in 19,717). Further characterisation of the CALM/AF10 LIC revealed a B220<sup>+</sup>CD43<sup>+</sup>AA4.1<sup>+</sup>CD24<sup>+</sup>CD11b<sup>-</sup>Gr1<sup>-</sup>Sca1<sup>-</sup> phenotype. Here, unlike with MLL-GAS7 which transforms a HSC and directs a multi-lineage leukaemia, the CALM/AF10 LIC is a progenitor cell with lymphoid characteristics which can generate a myeloid leukaemia *in vivo*.

#### 4.1.3.2.3 DEK/CAN

In AML t(6;9) is characterised by the formation of the DEK/CAN fusion protein and is associated with early clinical onset and poor prognosis. DEK/CAN overexpression in Lin<sup>-</sup>Sca1<sup>+</sup> BM cells had no effect on the replating efficiency of the cells when compared to controls with both unable to form colonies beyond the third replating (Oancea et al., 2010). However it did result in a higher number of colonies produced. To determine the effect of DEK/CAN on the potential of early progenitors/ST-HSCs the authors used a CFU-S12 assay where the DEK/CAN expressing cells from the first plating were injected into lethally irradiated recipient mice whose spleens were then analysed after 12 days for the number of splenic colonies present. DEK/CAN significantly increased the ability of the cells to generate splenic colonies *in vivo*. In a transplantation experiment the authors then demonstrate that DEK/CAN overexpressing long term (Lin<sup>-</sup>Sca1<sup>+</sup>cKit<sup>+</sup>Flk2<sup>-</sup>) but not short term (Lin<sup>-</sup>Sca1<sup>+</sup>cKit<sup>+</sup>Flk2<sup>+</sup>) HSCs were able to generate leukaemia *in vivo*. This study demonstrates that the DEK/CAN LIC resides within the HSC compartment, but is restricted to the LT-HSC.

#### 4.1.3.2.4 PML-RAR $\alpha$

As discussed in section 1.2.2.2.5, APL is characterised by a chromosomal translocation on chromosome 15 which results in the fusion of RAR $\alpha$  and PML

genes. To study the APL LIC, human PMLRARA was expressed in transgenic mice. This induced a high level of mortality caused by the development of cutaneous tumours, thus leukaemic spleen cells were harvested and transplanted into sublethally irradiated recipient mice, to generate *in vivo* APL (Guibal et al., 2009). From these mice LSKs, cKit<sup>-</sup>CD34<sup>+</sup>CD16/32<sup>+</sup>Gr1<sup>high</sup>, cKit<sup>+</sup>CD34<sup>+</sup>CD16/32<sup>+</sup>Gr1<sup>int</sup> cells were sorted and transplanted into sublethally irradiated tertiary recipients. Neither LSKs nor CD34<sup>-</sup>CD16/32<sup>+</sup>Gr1<sup>high</sup> leukaemic cells were able to initiate APL *in vivo*. However cKit<sup>+</sup>CD34<sup>+</sup>CD16/32<sup>+</sup>Gr1<sup>int</sup> transplanted mice all developed APL with a very short latency (median survival of 34.5 days). A limiting dilution transplant demonstrated that the cKit<sup>+</sup>CD34<sup>+</sup>CD16/32<sup>+</sup>Gr1<sup>int</sup> cells induced a dose-dependent leukaemia with as few as 30 cells being able to initiate disease, albeit it with a much longer latency (120 days). These data suggest that unlike the aforementioned models of AML, the APL LIC may reside in a more mature cell population.

#### 4.1.3.2.5 NUP98/HOXA9

The NUP98/HOXA9 fusion protein forms as the result of a relatively rare t(7;11) translocation found most often in AML patients. NUP98-HOXA9 was able to confer serial replating ability in a CFU assay to transduced CMPs, GMPs and MEPs (Kvinlaug et al., 2011). NUP98-HOXA9 transformed CMP, GMP and MEPs were also able to generate AML *in vivo* when transplanted into recipient mice. The same study also evaluated AML1-ETO and FLT3-ITD (see section 1.2.2.2.6).

Overexpression of FLT3-ITD was unable to induce replating ability in CMPs, GMPs or MEPs. AML1-ETO transduced CMPs and GMPs but not MEPs continuously replated, however, neither FLT3-ITD nor AML1-ETO transduced CMP, GMP or MEPs could initiate AML *in vivo*.

#### 4.1.3.2.6 MN1

While MN1 is a frequent fusion partner with the transcription factor TEL in AML or MDS patients with t(12;22), alone its overexpression also induces AML *in vivo*. In an investigation of the MN1 LIC, single HSCs, CMPs, GMPs, MEPs and granulocytes were sorted and transduced with MN1. The authors showed that only the CMP was susceptible to transformation by MN1 with MN1 expressing CMP clones able to serially replate to P5 (Heuser et al., 2011). Transplanted MN1 transduced CMP clones were also able to drive an aggressive leukaemia with an immature immunophenotype, which included some B220 expression. Gene

expression analysis revealed that healthy CMP cells when compared with bulk MN1 leukemic cells shared a large degree of overlap including *Meis1* and *Flt3* expression. The authors theorised that it was the gene expression signature of the CMP which lent itself to MN1 transformation. This study demonstrates that CMPs are the MN1 LIC and their susceptibility to MN1 transformation is due in part to the gene expression profile of these cells.

#### 4.1.3.3 C/EBP $\alpha$

Conditional mouse models have been generated to mimic *CEBPA* mutations, as discussed in section 3.1.2. L/L mice are homozygous for the p30 allele and these mice develop AML with a 9-14 month latency (Kirstetter et al., 2008). The authors identified 3 age-dependent BM phenotypes in the L/L mice. Mice less than 2 months old had very few BM neutrophils, with normal cKit levels (L/L-1). This progressed to an intermediate stage with high levels of CD11b<sup>+</sup>Gr1<sup>+</sup> mature granulocytes (L/L-2) which uniformly transitioned into granulocytic transformation with a block in differentiation and an accumulation of myeloblasts, as well as an increase in cKit<sup>+</sup> cells by 6 months (L/L-3). C/EBP $\alpha$  is essential for the CMP to GMP transition in granulocytic transformation so the authors then showed that GMPs were still formed in L/L-1 mice indicating that p30 alone can mediate this transition. In a CFU assay comparing cells from L/L and L/+ mice, L/+ GMPs had a mild increase in replating capacity over +/+ GMPs, but L/L GMPs had a large increase in replating ability. The LSKs had comparable replating efficiencies until the fourth plating, but subsequently adopted the same plating efficiencies as the GMP cells. The MEPs did not serially replate from any of the genotypes. Indeed sorted CD11b<sup>+</sup> BM cells from L/L-3 mice containing few if any LSK cells were able to initiate an aggressive AML in secondary recipients. These data support the idea that the self-renewal capacity of the cells occurs once the immature stem cells reach a committed myeloid progenitor stage.

In a subsequent study, a knock-in allele was generated to introduce one of the most common C-terminal mutations - the K313dup (K allele) - into mice (Bereshchenko et al., 2009). Heterozygous K/+ mice were crossed with L/+ mice to produce KL mice. Cells from KL mice were able to generate AML in secondary recipients. To determine the KL LIC, three cell fractions were isolated from the

leukemic mice - a HSC-containing fraction I (Sca-1<sup>+</sup>), a myeloid progenitor fraction II (Sca-1<sup>-</sup>CD11b<sup>lo/+</sup>cKit<sup>+</sup>) and a mature leukemic cell fraction III (Sca-1<sup>-</sup>CD11b<sup>hi</sup>cKit<sup>lo/-</sup>), and were transplanted into recipient mice. Only fraction II (containing myeloid progenitors) drove AML in the secondary recipients. *CEBPA* mutations frequently occur with *FLT3*-ITD mutations. Mutating a single *Cebpa* allele in cooperation with *Flt3*-ITD was shown to be insufficient to initiate leukaemia *in vivo*, however the combination of biallelic *Cebpa* mutations with *Flt3*-ITD (KLI) resulted in a significant shortening of the KL disease latency (33.8 wks to 22.5 wks) (Reckzeh et al., 2012). KLI whole BM, GMPs and MPPs all induced AML in recipient mice, while KLI LT-HSCs did not generate disease *in vivo*. As expected only the KL whole BM and GMPs induced AML when transplanted. These findings support both the hierarchical ordering of leukemic cells, and similar studies which suggest that the LIC is a more committed progenitor cell which acquires self-renewal ability.

Together these data demonstrate that the LIC can affect the disease latency, biology and thus therapeutic response of a given leukaemia. Indeed the LIC varies considerably depending on the nature of the transforming event and so it is necessary to examine oncogenes individually to determine their cell of origin.

Table 4-1 - List of LIC studies

Lesion	Chromosomal Rearrangement	Populations tested	LIC	Reference
MLL-ENL	t(11;19)	HSC, CMP, GMP, MEP	HSC, CMP, GMP	Cozzio et al, 2003
MLL-GAS7	t(11;17)	HSC, CLP, CMP, GMP, MEP	HSC	So et al, 2003
MLL-AF9	t(9;11)	HSC, GMP	HSC, GMP	Krivtsov et al, 2013
MOZ-TIF2	inv(8)	Whole BM <sup>s</sup> , HSC, CMP, GMP	HSC, CMP, GMP	Huntley et al, 2011
BCR-ABL	t(9;22)	Whole BM <sup>s</sup> , HSC, CMP, GMP	HSC	Huntley et al, 2011
CALM/AF10	t(10;11)	B220 <sup>+</sup> CD11b <sup>-</sup> Gr-1 <sup>-</sup>	B220 <sup>+</sup> CD11b <sup>-</sup> Gr-1 <sup>-</sup>	Deshpande et al, 2006
		B220 <sup>+</sup> CD11b <sup>+</sup> Gr-1 <sup>+</sup>		
		B220 <sup>+</sup> CD11b <sup>-</sup>		
		B220 <sup>+</sup> Gr-1 <sup>-</sup>		
DEK/CAN	t(6;9)	LT-HSC, ST-HSC	LT-HSC	Oancea et al, 2010
PML-RAR $\alpha$	t(15;17)	LSKs	cKit <sup>+</sup> CD34 <sup>+</sup> CD16/32 <sup>+</sup> Gr-1 <sup>int</sup>	Guibal et al, 2009
		cKit <sup>+</sup> CD34 <sup>+</sup> CD16/32 <sup>+</sup> Gr-1 <sup>hi</sup>		
		cKit <sup>+</sup> CD34 <sup>+</sup> CD16/32 <sup>+</sup> Gr-1 <sup>int</sup>		
NUP98-HOXA9	t(7;11)	CMP, GMP, MEP	CMP, GMP, MEP	Kvinlaug et al, 2011
MN1	t(12;22)	HSC, CMP, GMP, MEP, Gran	CMP	Heuser et al, 2011
C/EBP $\alpha$ -KL	N/A	LT-HSC, MPP, GMP	GMP	Reckzeh et al, 2012
C/EBP $\alpha$ -KL with FLT3-ITD	N/A	LT-HSC, MPP, GMP	MPP, GMP	Reckzeh et al, 2012

## 4.2 Aims and Objectives

It was hypothesized that TRIB2 functionally targets C/EBP $\alpha$  in normal and malignant hematopoiesis. TRIB2, expressed in 5FU enriched BM cells, was shown to induce AML in a murine transplant model dependent on C/EBP $\alpha$  degradation. The role of TRIB2 in normal hematopoiesis and specifically myelopoiesis is not known, nor has the TRIB2 LIC been identified. *Cebpa* is differentially expressed in stem and myeloid progenitor cells (Hasemann et al., 2014), being present at low levels in the HSC, and increasing expression during granulocytic maturation where its expression is highest at the GMP stage, and completely absent from the MEP. Thus it was hypothesised that the levels of C/EBP $\alpha$  protein available for degradation in stem and progenitor populations may affect the ability of TRIB2 to initiate AML, or may affect the latency or phenotype of the resultant disease. As such the specific aims of this chapter were:

- i. To identify the Trib2 LIC using
  - a. an *in vitro* methylcellulose serial replating assay technique and
  - b. an *in vivo* transplantation approach
- ii. To determine if loss of Trib2 affects steady state hematopoiesis by
  - a. analysing the hematopoietic compartment of the *Trib2*<sup>-/-</sup> mouse and
  - b. assessing the effect of Trib2 loss on *in vitro* myeloid differentiation

## 4.3 Results

### 4.3.1 *Trib2* can transform all cell populations *in vitro*

To investigate the ability of the oncogene *Trib2* to transform HSCs, MPPs, CMPs, GMPs and MEPs, an *in vitro* approach was first utilised. FACS sorted stem and progenitor cells transduced with a lentiviral vector encoding *Trib2*, were seeded in methocult supplemented with cytokines that induce myeloid differentiation. Following P1, GFP<sup>+</sup> cells were sorted and serially replated. If the cells still formed colonies by the third replating this implied acquisition of self-renewal ability and increased proliferation. The cells were serially replated to the P5, and colonies and cells were analysed from P3 to P5 (Figure 4. 3). All TRIB2 transduced populations were still efficiently producing colonies at P3, and these cells still formed colonies by P5, however different efficiencies between groups were observed (Figure 4. 4A). By P5, CMP derived cells were producing very few colonies that were very small in size (Figure 4. 4B). TRIB2 transformed GMP derived cells also produced smaller sized colonies, while MPP derived cells produced the largest sized colonies. Colonies were also categorised based on their morphology as described by Lavau et al outlined in 4.1.3. Immature Type I colonies were well represented on transformed HSC, MPP, GMP and MEP plates, comprising 25-50% of colonies by P3 but much fewer on CMP plates (Figure 4. 5). The intermediate Type II colonies were rarely observed in TRIB2 transformed CMP or GMPs, being most prominent on transformed MPP plates, as well as HSC and MEP plates (Figure 4. 5). Interestingly, while type III mature colonies were present on all plates, they were predominantly on CMP and GMP plates with CMP plates being primarily composed of type III colonies. Cytospins of the cells demonstrated that TRIB2 transformed HSC, MPP, GMP and MEP derived colonies contained many undifferentiated cells with a high nucleus/cytoplasm ratio, while CMP derived colonies contained very few undifferentiated cells, with almost all cells showing evidence of granulocytic or monocytic differentiation (Figure 4. 6).

It was next determined if the differences in colony size and shape, and cellular morphology correlated with cell surface marker changes. Flow cytometric analysis of P3 cells revealed that cells from HSC, MPP, GMP and MEP derived colonies had very similar expression levels of CD11b and Gr1 (Figure 4. 7A and

B), while CMP derived cells demonstrated higher levels of Gr1 and virtually no CD11b expression. The cell surface expression of CD11b and Gr1 changed in some populations between P3 and P5. CD11b and Gr1 expression increased slightly in HSC and MPP derived cells (Figure 4. 7A and B). There was high cKit expression in almost all populations at each plating, although less than 50% of MPP derived cells expressed cKit by P5 (Figure 4. 8). Analysis of CD11b and Gr1 expression was performed through the cKit<sup>+</sup> and cKit<sup>-</sup> gates revealing no CD11b expression and low Gr1 expression on cKit<sup>+</sup> cells, while as expected the cKit<sup>-</sup> cells expressed mature myeloid markers (Figure 4. 9). By P5, only the MPP derived cells retained a significant cKit<sup>-</sup> population (>50%), and these cells had high CD11b expression and some CD11b<sup>+</sup>Gr1<sup>+</sup> cells (Figure 4. 10). Moreover by P5 the CMP derived cells had acquired significant Gr1 expression with over 65% of cells cKit<sup>+</sup>Gr1<sup>+</sup>CD11b<sup>-</sup>. The high levels of cKit expression observed in HSC, CMP, GMP and MEP derived TRIB2 transduced cells correlates well with published data showing TRIB2-induced AML are cKit<sup>+</sup> (Keeshan et al., 2006).

Together these data show that Trib2 can transform stem and progenitor populations *in vitro* with different efficiencies, and the resultant transformed colony and cell type differs depending on the cell of origin. The data shows that Trib2 has conferred both self-renewal ability and a differentiation block to HSCs, GMPs and MEPs. While TRIB2 transduced MPPs also displayed self-renewal ability, by P5 there was a large population of cKit<sup>-</sup> cells still present which express the myeloid differentiation markers CD11b and Gr1. These data indicate that the Trib2 LIC resides in either the HSC or GMP or MEP as only these populations display pre-leukemic characteristics *in vitro*.

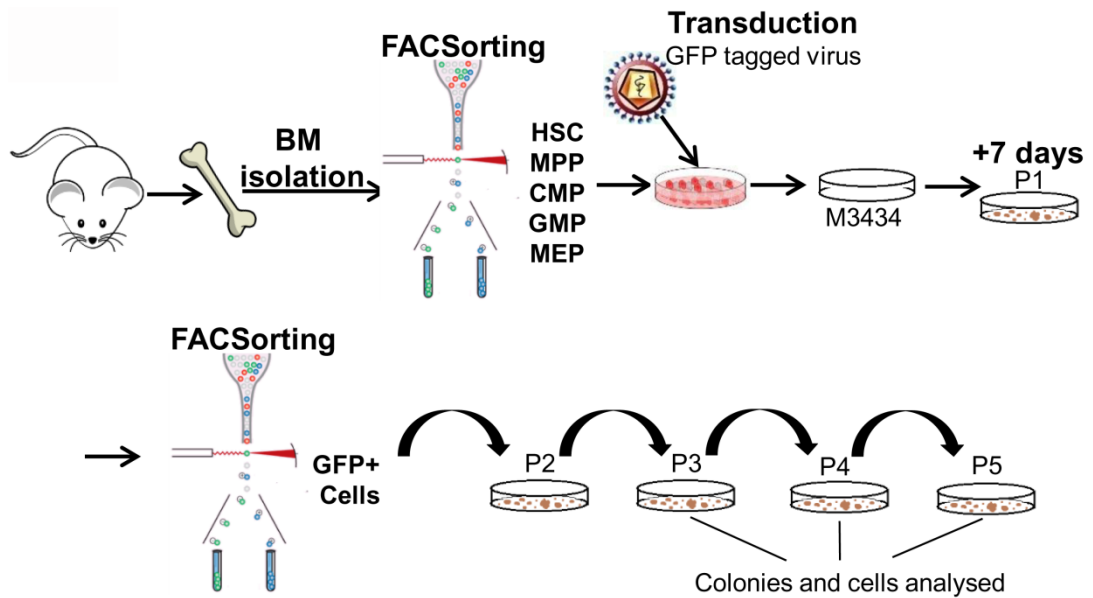


Figure 4. 3 - Schematic overview of CFU experiment used to identify the leukaemia initiating cell

Murine BM cells were isolated and sorted for HSC ( $\text{Lin}^- \text{cKit}^+ \text{Sca1}^+ \text{CD150}^+ \text{CD48}^-$ ), MPP ( $\text{Lin}^- \text{cKit}^+ \text{Sca1}^+ \text{CD150}^- \text{CD48}^-$ ), CMP ( $\text{Lin}^- \text{cKit}^+ \text{Sca1}^- \text{CD34}^+ \text{CD16/32}^{\text{lo}}$ ), GMP ( $\text{Lin}^- \text{cKit}^+ \text{Sca1}^- \text{CD34}^+ \text{CD16/32}^{\text{hi}}$ ) and MEP ( $\text{Lin}^- \text{cKit}^+ \text{Sca1}^- \text{CD34}^- \text{CD16/32}^-$ ) populations. Following transduction the TRIB2 expressing cells were plated in M3434 methylcellulose media 24hrs later. After 7 days (P1) colonies had formed, cells were then removed and sorted for GFP expression before replating in M3434. GFP<sup>+</sup> cells were serially replated to P5 and colonies and cells were analysed at P3, P4 and P5.

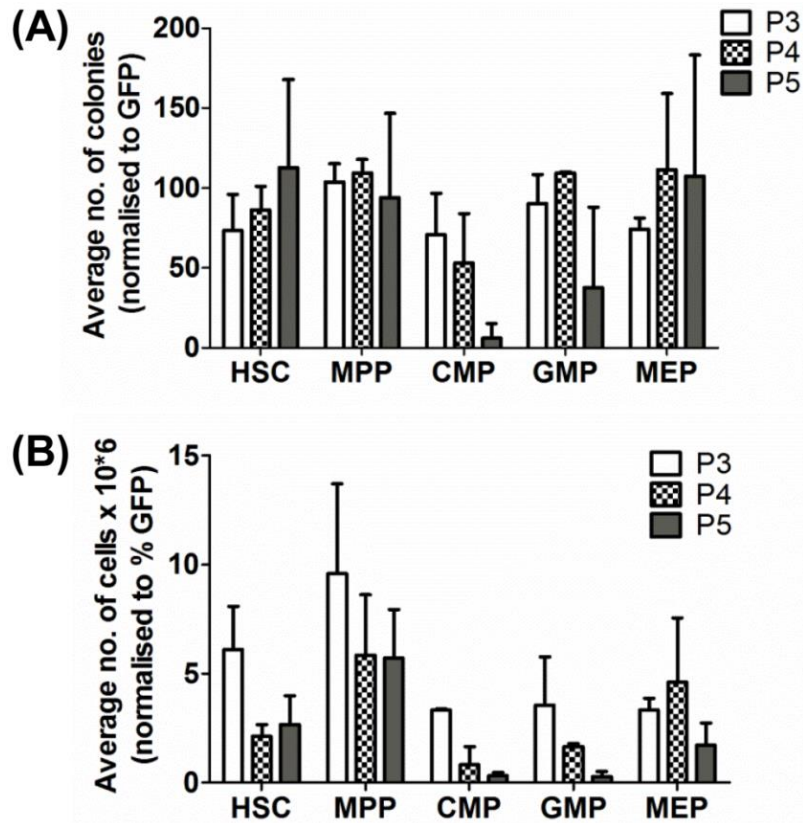


Figure 4. 4 - TRIB2 transforms stem and progenitor populations *in vitro* with different efficiencies

(A) Average number of colonies at each replating normalised to GFP expression. Averages are of 2 independent experiments each with 3 technical replicates shown +/- SD. (B) Average number of cells produced at each replating. Averages are of pooled triplicate plates from 2 independent experiments +/- SD.

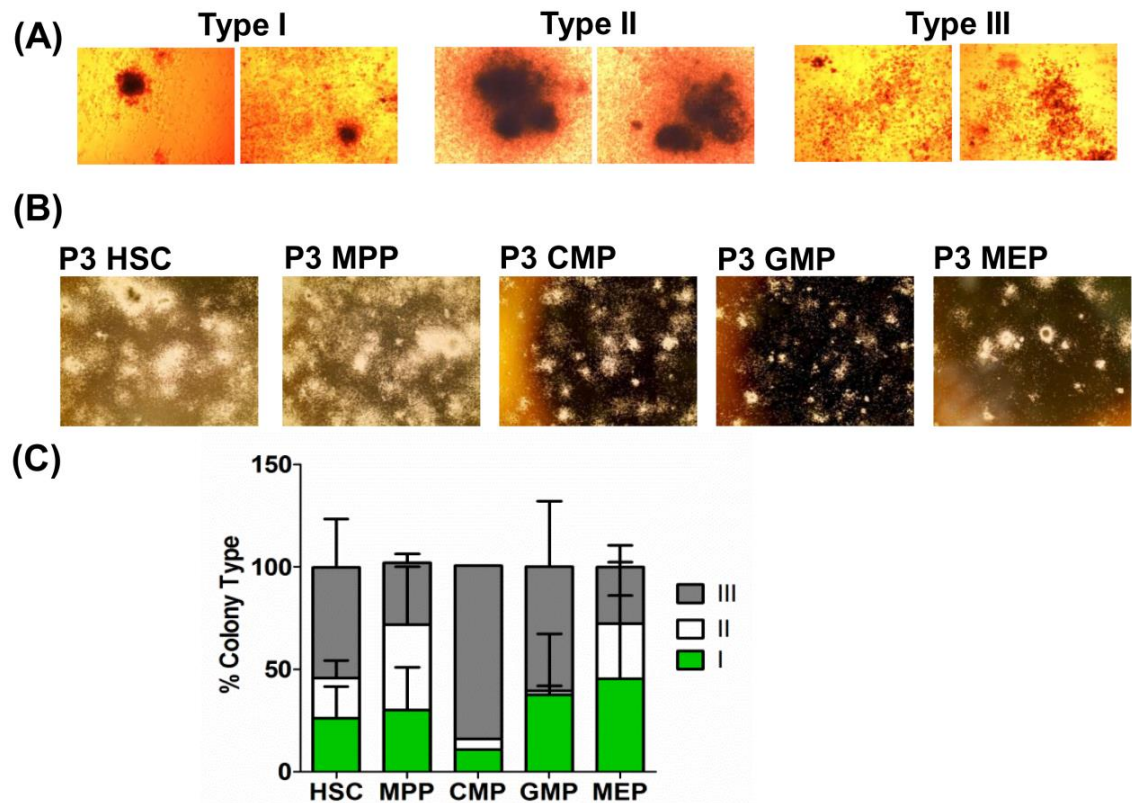


Figure 4. 5 - Colony size and type differs between TRIB2 transformed stem and progenitor groups

(A) Representative images of colony types under 4x magnification. (B) Representative images of groups of colonies taken at P3 under 2x magnification (C) Distribution of colony types at P5. Bars represent the average of 2 independent experiments each with 3 technical replicates +/- SD.

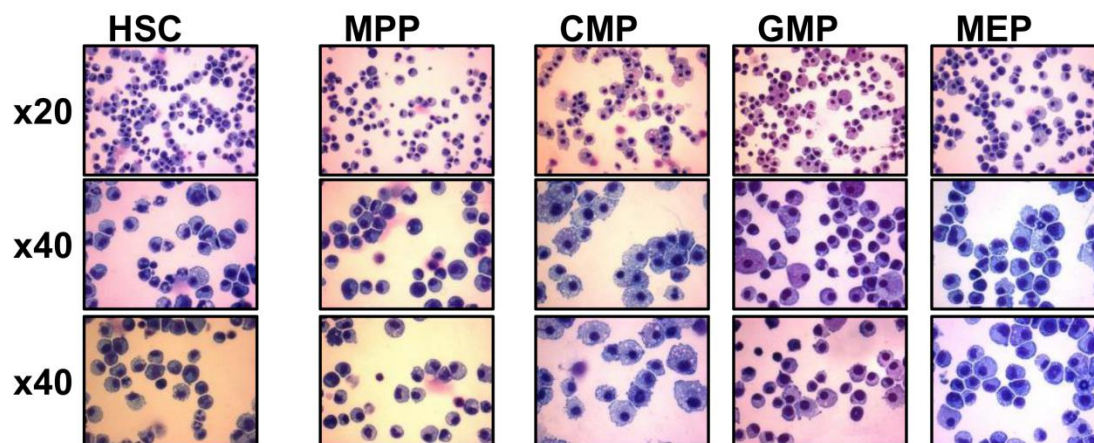


Figure 4. 6 - Cellular morphology of TRIB2 transformed stem and progenitor cells

Cells from P3 colonies were spun onto glass slides using a cytocentrifuge and stained with the KwikDiff staining system. Representative images are shown, taken under 20X (top panel) and 40X (bottom panels) magnification.

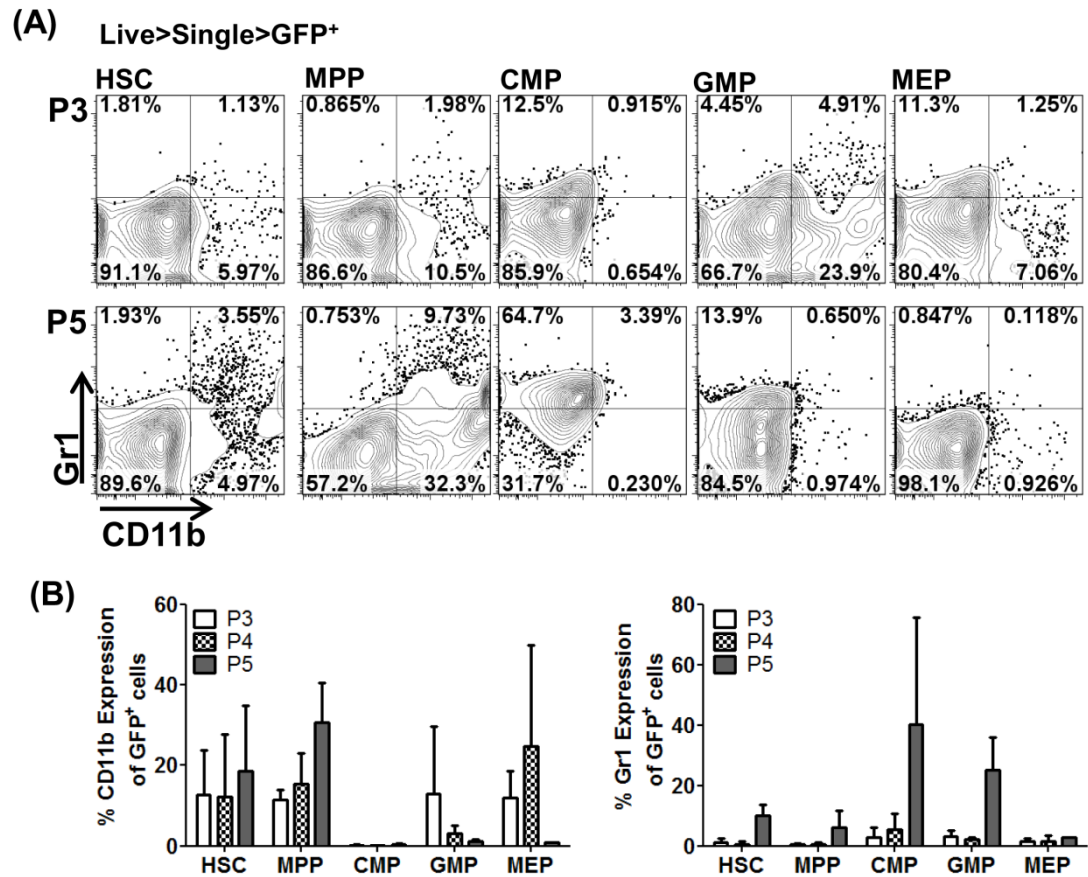


Figure 4. 7 - Comparison of CD11b and Gr1 expression in transformed stem and progenitor cells from P3, 4 and P5

Cells from each replating were stained for CD11b and Gr1 and analysed by flow cytometry. (A) Representative flow cytometric analysis of GFP<sup>+</sup> TRIB2 transformed stem and progenitor cells from P3 and P5. (B) Graphs represent the average percentage expression of CD11b (left) and Gr1 (right) of GFP<sup>+</sup> TRIB2 transformed stem and progenitor cells from P3, P4 and P5. Data represents the average of 2 independent experiments +/- SD.

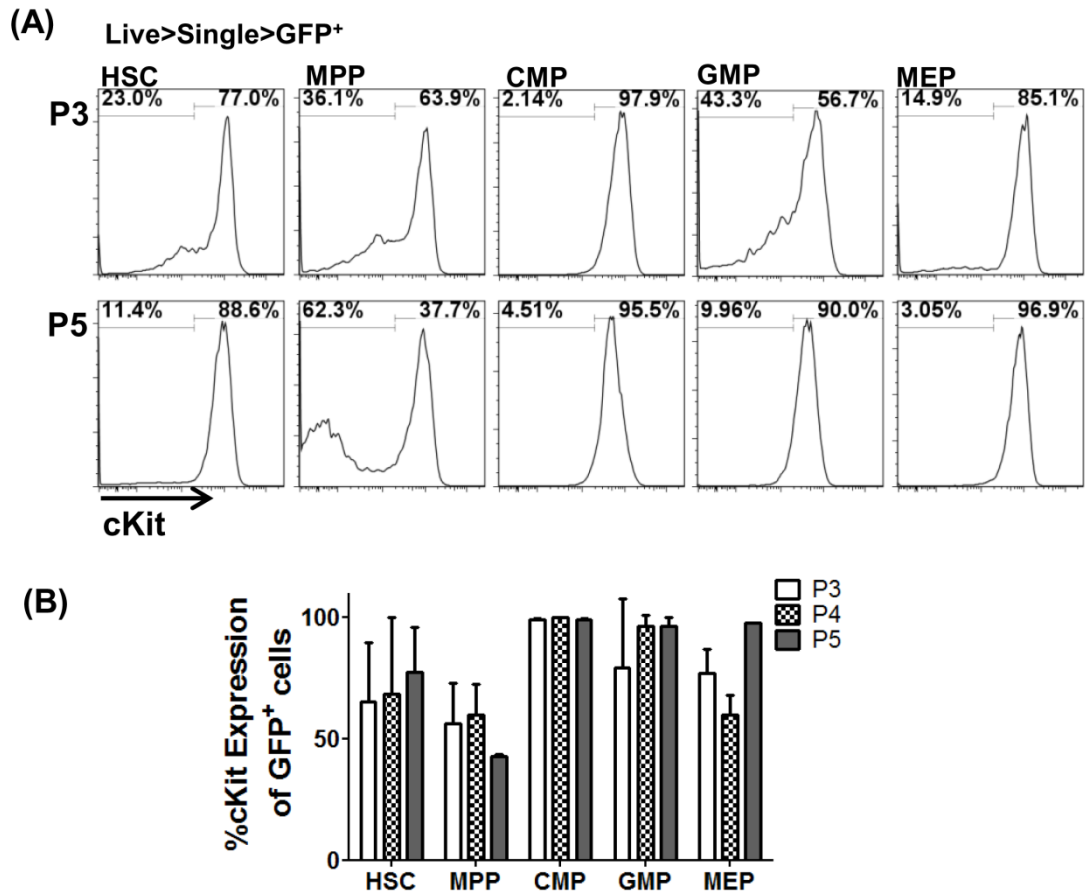


Figure 4. 8 - Comparison of cKit expression in transformed stem and progenitor cells from P3, 4 and P5

Cells from each replating were stained for cKit expression and analysed by flow cytometry. **(A)** Representative flow cytometric analysis of GFP<sup>+</sup> TRIB2 transformed stem and progenitor cells from P3 and P5. **(B)** Graphs represent the average percentage expression of cKit on GFP<sup>+</sup> TRIB2 transformed stem and progenitor cells from P3, P4 and P5. Data represents the average of 2 independent experiments +/- SD.

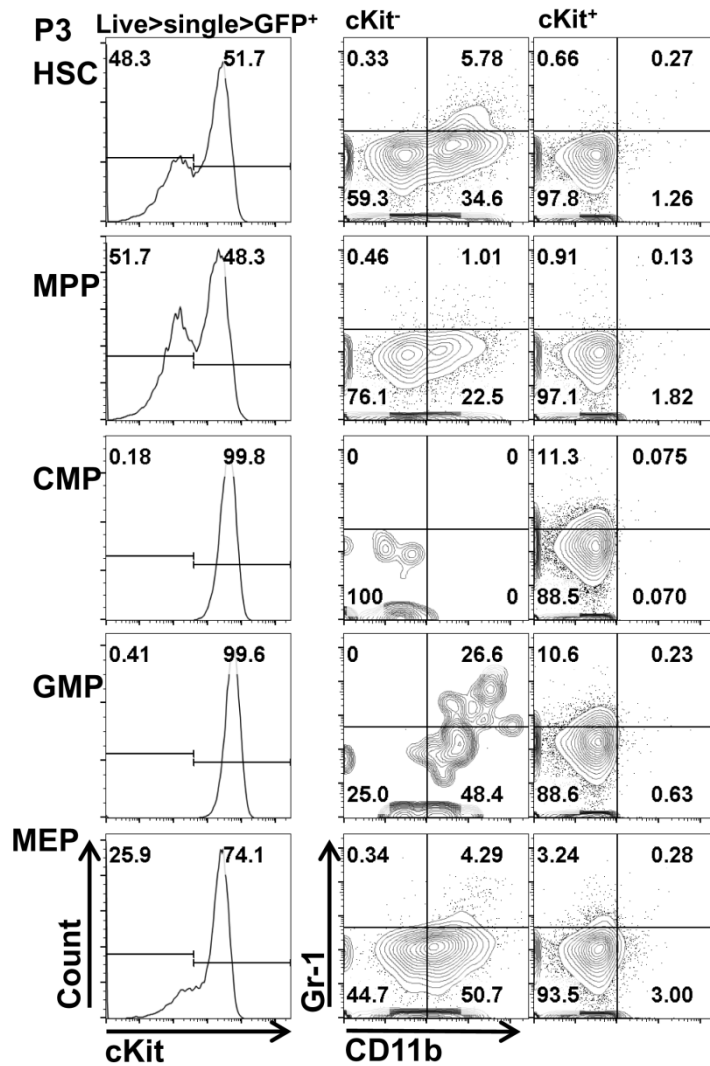


Figure 4. 9 - Differential expression of mature myeloid markers in cKit<sup>+</sup> and cKit<sup>-</sup> populations of transformed stem and progenitor cells at P3

Representative flow cytometric analysis of TRIB2 transformed P3 stem and progenitor populations showing cKit histograms (left) and CD11b and Gr1 expression through the cKit<sup>+</sup> (right) and cKit<sup>-</sup> gate (middle). Data is representative of 2 independent experiments.

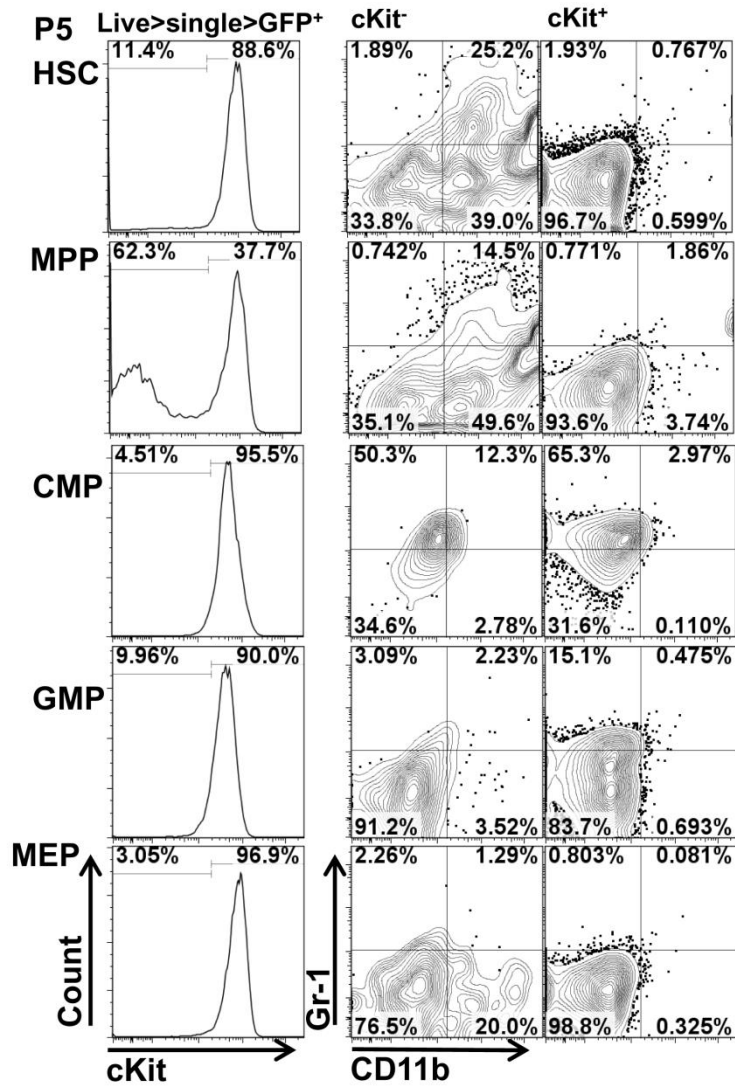


Figure 4. 10- Differential expression of mature myeloid markers in cKit<sup>+</sup> and cKit<sup>-</sup> populations of transformed stem and progenitor cells at P5

Representative flow cytometric analysis of TRIB2 transformed P5 stem and progenitor populations showing cKit histograms (left) and CD11b and Gr1 expression through the cKit<sup>+</sup> (right) and cKit<sup>-</sup> gate (middle). Data is representative of 2 independent experiments.

### 4.3.2 *Trib2* generates leukaemia *in vivo* with different latencies from the HSC and GMP, but not the MPP or CMP

The results from the serial replating assay indicated that Trib2 conferred replating and self-renewal capacity to the HSC, MPP, CMP, GMP and MEP populations. Despite this, TRIB2 was unable to efficiently block differentiation in the MPP and to fully transform the CMP derived cells. In order to resolve these observations and to elucidate the leukaemia initiating potential of the stem and progenitor populations, a BMT was performed. It was hypothesised that transplanting pre-leukemic cells from the serial replating assay would shorten the disease latency *in vivo* (~6 months with unfractionated BM). By P3 of the serial replating assay all populations were exhibiting hallmarks of pre-leukemic cells i.e. efficiently producing colonies, high cKit expression and low expression of mature myeloid markers. Thus the CD45.2<sup>+</sup> cells from P3 HSC, MPP, CMP and GMP derived colonies were selected to transplant into sublethally irradiated CD45.1<sup>+</sup> C57BL/6 recipient mice and transplanted animals were monitored for 1 year (Figure 4. 11). Attempts to culture MEPs *ex vivo* for viral transduction had failed, and thus MEPs are precluded from the analysis.

Peripheral bleeds were taken at 7 weeks post-transplant and the levels of engraftment were determined by CD45.2 expression in the blood. Cells transplanted from HSC and GMP derived colonies displayed high levels of engraftment (Figure 4. 12A). Cells transplanted from MPP-derived colonies showed no engraftment in the recipient mice, while only 1 of 5 CMP transplanted mice displayed engraftment in the PB at 7 weeks post-transplant. The MPP and CMP transplanted mice who displayed no engraftment in the PB were culled at 16 weeks post BMT (Figure 4. 12B) and all had normal white blood cell (WBC) counts, normal spleen weights, and normal percentages of circulating neutrophils, lymphocytes, monocytes, eosinophils and basophils (Figure 4. 13). Flow cytometric analysis revealed no engraftment of CD45.2<sup>+</sup> cells in the BM, spleen or PB at 16 weeks post-transplant (Figure 4. 14). All mice transplanted with GMP derived cells succumbed to disease with a median latency of just 14 weeks (Figure 4. 15). Of the cohort transplanted with HSC derived cells, only 1 of 4 mice developed disease within 1 year, with a latency of 26 weeks. Further analysis of the mice that displayed peripheral engraftment but did not develop leukaemia within 1 year showed no disruption to hematopoiesis with normal

spleen weights, WBC counts and normal percentages of circulating neutrophils, lymphocytes, monocytes, eosinophils and basophils (Figure 4. 16).

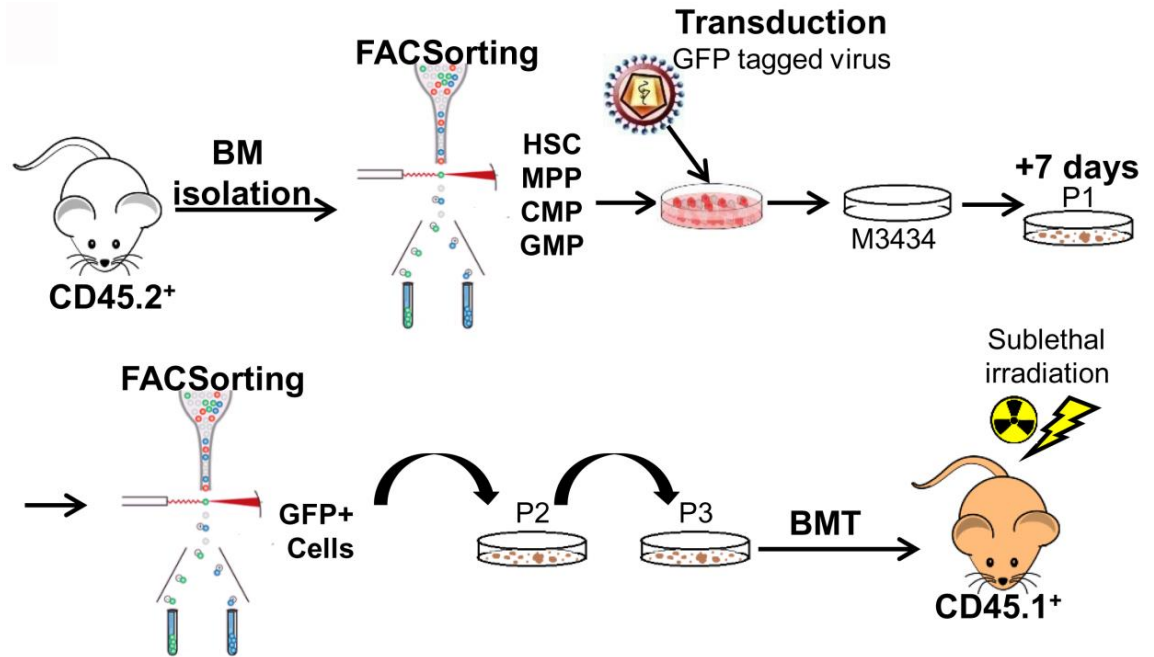


Figure 4. 11 - Schematic overview of transplantation model used to identify the TRIB2 leukaemia initiating cell

BM cells were isolated from CD45.2<sup>+</sup> mice and sorted for HSC (Lin<sup>-</sup>cKit<sup>+</sup>Sca1<sup>+</sup>CD150<sup>+</sup>CD48<sup>-</sup>), MPP (Lin<sup>-</sup>cKit<sup>+</sup>Sca1<sup>+</sup>CD150<sup>-</sup>CD48<sup>-</sup>), CMP (Lin<sup>-</sup>cKit<sup>+</sup>Sca1<sup>-</sup>CD34<sup>+</sup>CD16/32<sup>lo</sup>), and GMP (Lin<sup>-</sup>cKit<sup>+</sup>Sca1<sup>-</sup>CD34<sup>+</sup>CD16/32<sup>hi</sup>) populations. The cells were transduced with GFP tagged *Trib2* lentivirus and plated in M3434 methylcellulose media after 24hrs. After 7 days (P1) colonies had formed, cells were then removed and sorted for GFP expression before serial replating in M3434. P3 cells were transplanted into sub-lethally irradiated CD45.1<sup>+</sup> recipient mice.

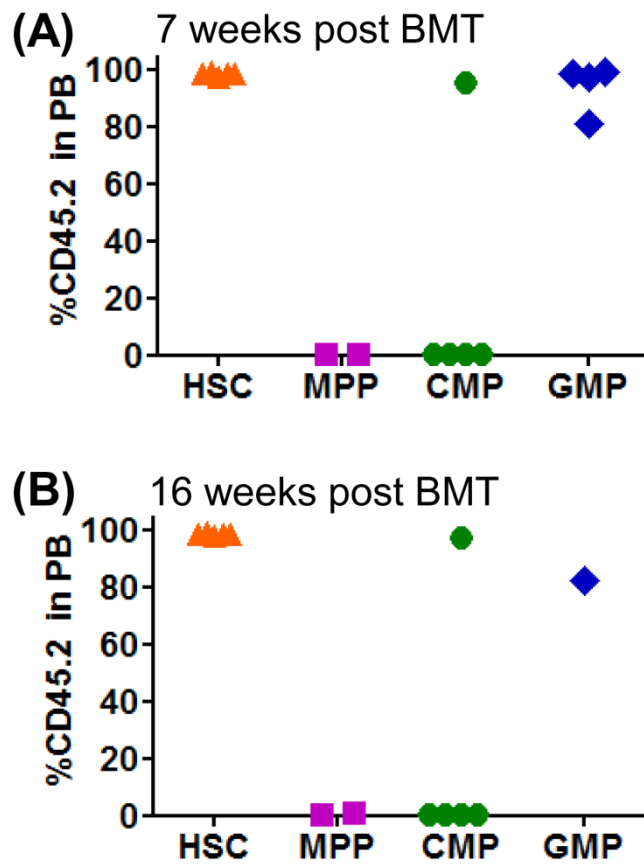


Figure 4. 12 - Varying engraftment levels in TRIB2 LIC transplanted mice

Peripheral bleeds were taken at (A) 7 weeks and (B) 16 weeks post BMT and analysed by flow cytometry for CD45.2 expression. Each dot represents percentage CD45.2 expression in the PB of an individual mouse, HSC (n=4), MPP (n=2), CMP (n=5), GMP (n=4).

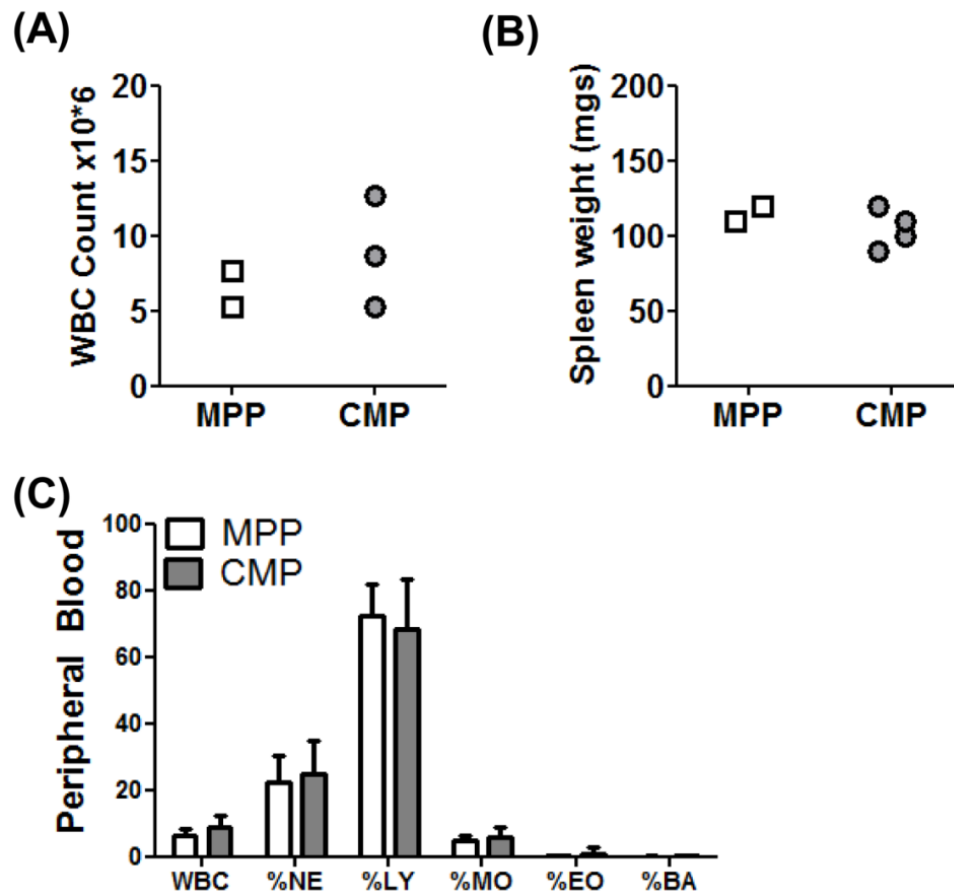


Figure 4. 13 - Normal hematopoiesis in mice that failed to engraft transplanted cells

MPP and CMP transplanted mice that demonstrated no peripheral engraftment by 16 weeks were sacrificed and analysed. (A) WBC counts and (B) spleen weights of MPP and CMP transplanted non-engrafted mice. Each dot represents an individual mouse. (C) The white cell differential of the PB was analysed using a HemaVet 950 (Drew Scientific). Average percentage neutrophils (NE), lymphocytes (LY), monocytes (MO), eosinophils (EO) and basophils (BA) plotted +/- SD. Average of n=2 MPP, n=3 CMP.

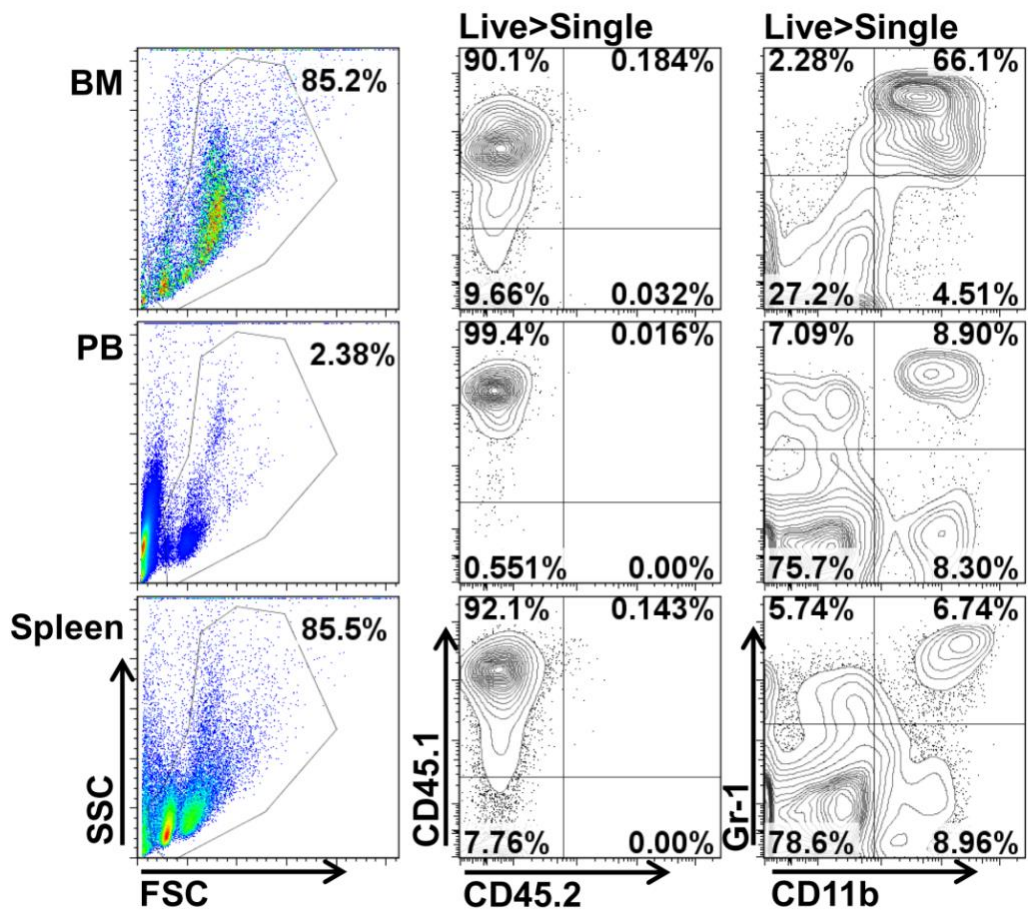


Figure 4. 14 - No BM or splenic engraftment of donor cells at 16 weeks in mice failing to display peripheral engraftment at 7 weeks post BMT

Representative flow cytometric analysis of cells from the BM, PB and spleen of mice at 16 weeks post BMT. MPP (n=2) and CMP (n=4) transplanted mice that did not display peripheral engraftment also lacked CD45.2 expression (middle panel) in the BM and spleen, and displayed normal myelopoiesis by CD11b and Gr1 expression (right panel).

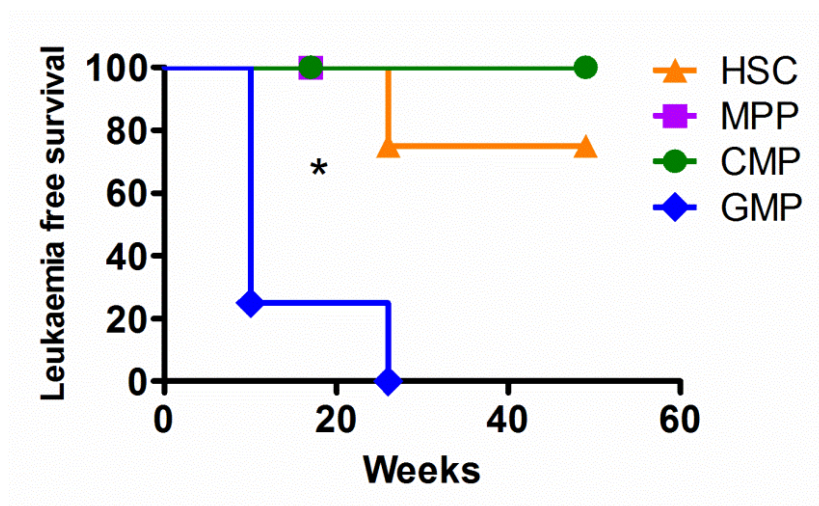


Figure 4. 15 - TRIB2 generates leukaemia from the HSC and GMP with different latencies, but not the MPP or CMP.

Kaplan-Meier survival curve of mice reconstituted with cells derived from TRIB2 transformed HSC, MPP, CMP and GMP colonies. The median survival of mice reconstituted with GMP derived cells was 14 weeks (n=4), 1 (of 4) HSC mouse developed disease within 1 year with a latency of 26 weeks, while none of the mice reconstituted with MPP (n=2) or CMP (n=5) derived cells developed leukaemia. \*P=0.0171 by Log-rank test.

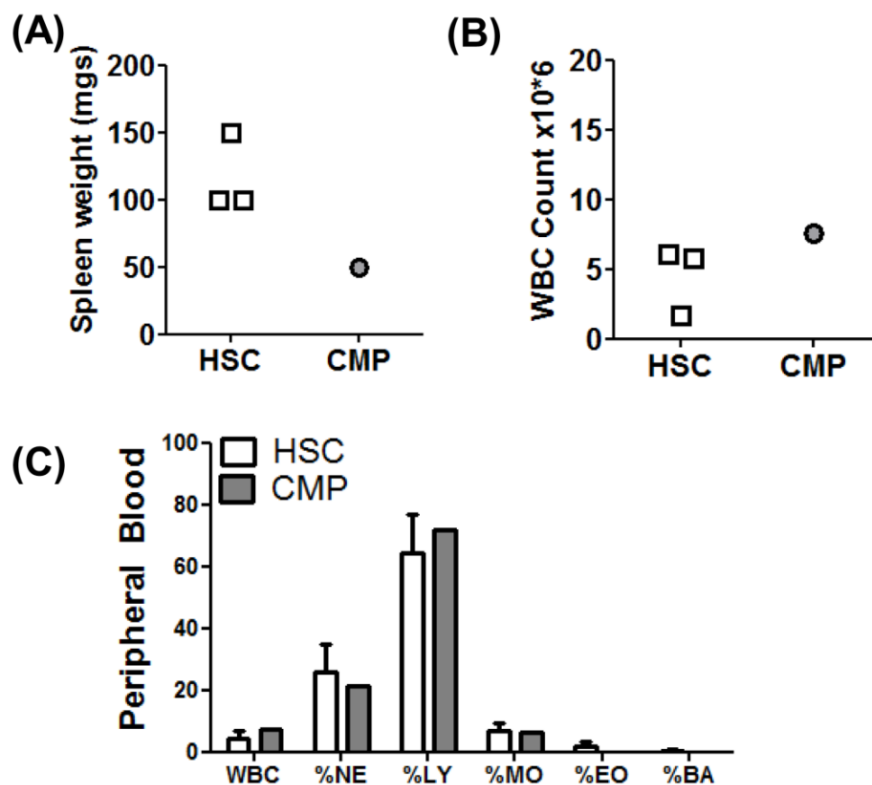


Figure 4. 16 - HSC and CMP transplanted mice that engrafted the donor cells, but did not succumb to disease displayed normal hematopoiesis after 1 year

HSC and CMP transplanted mice that demonstrated high levels of peripheral engraftment, but did not develop disease, were sacrificed and analysed after 1 year. (A) Spleen weights and (B) WBC counts of HSC and CMP transplanted mice. Each dot represents an individual mouse. (C) The white cell differential of the PB was analysed using a HemaVet 950 (Drew Scientific). Average percentage neutrophils (NE), lymphocytes (LY), monocytes (MO), eosinophils (EO) and basophils (BA) plotted +/- SD. Average of n=3 HSC, n=1 CMP.

### 4.3.3 TRIB2 propagates phenotypically different diseases from the HSC and GMP

The leukaemias generated from TRIB2 transformed HSC and GMP derived cells were morphologically distinct. The HSC-transplanted mouse presented with a very high WBC count while the WBC count of GMP mice were within the normal range (Figure 4. 17A). There was massive infiltration of leukocytes in the spleen of the HSC mouse as evidenced by splenomegaly, whereas the spleen weights of the GMP mice were within the normal range (Figure 4. 17B). Flow cytometric analysis of the BM showed a much higher than normal percentage of CD11b<sup>+</sup>Gr1<sup>+</sup> cells in the GMP derived disease coupled with a decrease in cells expressing B and T cell markers (Figure 4. 18). The HSC derived disease was wholly different from that of the GMP. BM cells of the HSC transplanted mouse had little to no Gr1 expression, with almost all cells expressing the B cell marker B220, but not CD19, and a fraction of cells expressing the T cell marker CD8 but not CD4. The patterns of expression for both the GMP and HSC diseases were also observed in the spleen (Figure 4. 19A) and PB (Figure 4. 19B). While the GMP transplanted mice did not display splenomegaly or elevated WBC, analysis of the absolute cell numbers in the BM and PB demonstrated that TRIB2 induced a myeloproliferative-like disease from the GMP (Figure 4. 20). The phenotype of neither the HSC nor GMP derived AML fully recapitulated TRIB2-induced AML from 5-FU treated BM with the bulk leukemic cells expressing cKit<sup>+</sup>CD11b<sup>int</sup>Gr1<sup>int</sup> (Keeshan et al., 2006).

Because the HSC transplanted mouse had a very unusual disease phenotype, a more extensive panel of cell surface markers were examined. As mentioned B220 was expressed on all HSC derived leukemic cells, in contrast to a complete absence of B220 expression in GMP derived leukemic cells (Figure 4. 21A). There were comparably low levels of CD19 and IL7R $\alpha$  expression in both groups, with slightly higher surface IgM expression in the HSC derived leukemic cells (Figure 4. 21A). CD43 expression was high in both GMP and HSC derived leukemic cells (Figure 4. 21B), with almost all HSC derived leukemic cells staining double positive for B220 and CD43 expression. These 2 markers are co-expressed at the early stages of B cell development, suggesting a possible phenotypic B cell leukaemia had been generated from the TRIB2 transformed HSC. However, analysis of the T cell compartment revealed that approximately 24% of HSC

derived leukemic cells were also CD8<sup>+</sup> (Figure 4. 22A), yet neither the CD8<sup>+</sup> nor CD8<sup>-</sup> fraction expressed the T cell markers CD4, CD3 or TCR $\beta$ . Levels of CD8, CD4, CD3 and TCR $\beta$  expression were all very low in the GMP derived disease (Figure 4. 22B). Analysis of markers of mature myeloid cells revealed a slight increase in CD11c expression and a large increase in MHCII expression on HSC derived leukemic cells when compared with GMP derived cells (Figure 4. 23A), but much lower CD11b expression. CD8 was not co-expressed with either CD11b or MHCII (Figure 4. 23B). CD8 and CD11c, which in normal hematopoiesis are found co-expressed on regulatory T cells (Vinay and Kwon, 2010) were expressed together at low levels in HSC derived leukemic cells. Over 40% of HSC derived leukemic cells expressed MHCII, a surface molecule found primarily on dendritic cells, but also present on some B cells. Within the MHCII<sup>+</sup> and MHCII<sup>-</sup> fraction of leukemic cells there was differential expression of CD11b and CD11c (Figure 4. 23C). Thus in addition to approximately 24% B220<sup>+</sup>CD43<sup>+</sup>CD8<sup>+</sup> cells, over 40% of the leukaemic population was comprised of B220<sup>+</sup>CD43<sup>+</sup>MHCII<sup>+</sup>CD8<sup>-</sup> cells, and 17% of these were also double positive for CD11c and CD11b expression, markers frequently co-expressed on dendritic cells.

These data show that Trib2 cannot induce leukaemia from the MPP or CMP *in vivo*. It does induce leukaemia from the HSC and GMP *in vivo*, with different efficiencies, and has the ability to generate different types of leukaemia depending on the cell of origin. A uniformly myeloproliferative disease with 100% penetrance was generated from the TRIB2 transformed GMPs, while a weakly penetrant leukaemia with highly aberrant cell surface marker expression of mixed lineage was generated from the TRIB2 transformed HSC.

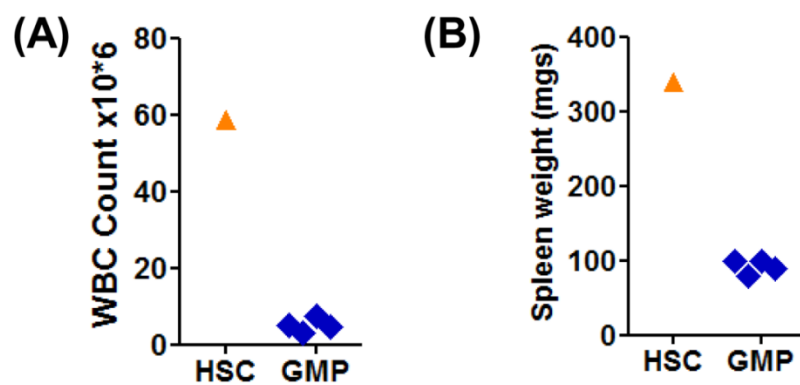


Figure 4. 17 - Physically distinct diseases arose from the TRIB2 transformed HSC and GMP

(A) WBC count and (B) spleen weights of HSC (n=1) and GMP (n=4) transplanted leukemic mice. Each dot represents an individual mouse.

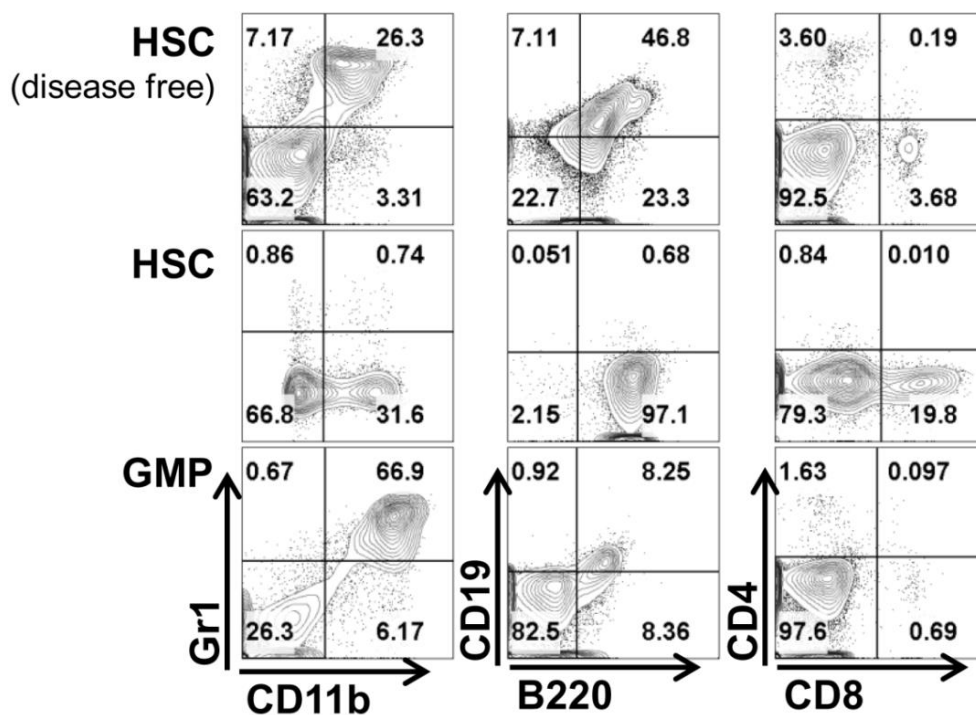


Figure 4. 18 - TRIB2 generates phenotypically different diseases from the HSC and GMP

Representative flow cytometric analysis of mature myeloid (CD11b, Gr1), B (B220, CD19) and T (CD4, CD8) cell markers in the BM of a HSC transplanted mouse that did not develop leukaemia (top) and the BM of a HSC (middle) and GMP (bottom) transplanted CD45.2<sup>+</sup> leukemic mouse. Data is representative of n=1 HSC and n=4 GMP mice.

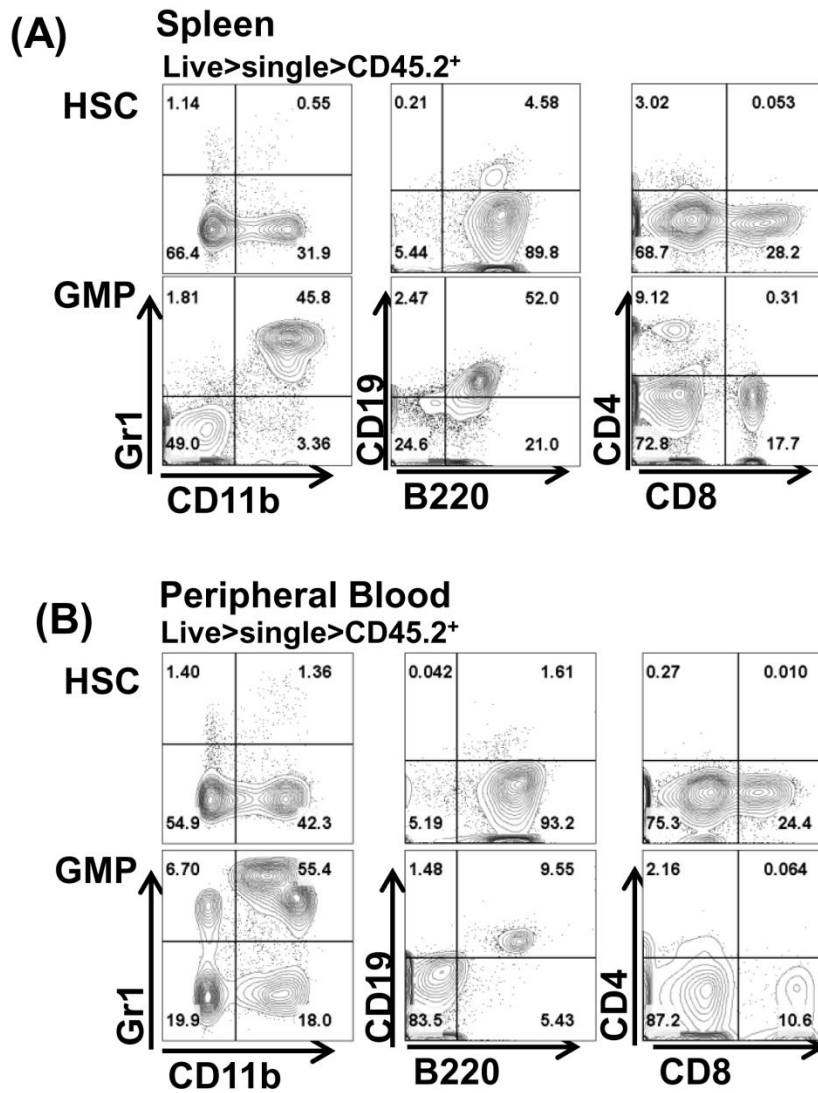


Figure 4. 19 - HSC and GMP derived leukemic cells infiltrate the spleen and peripheral blood

Representative flow cytometric analysis of mature myeloid (CD11b, Gr1), B (B220, CD19) and T (CD4, CD8) cell markers in the (A) spleen and (B) PB of HSC and GMP transplanted CD45.2<sup>+</sup> leukemic mice. Data is representative of n=1 HSC and n=4 GMP mice.

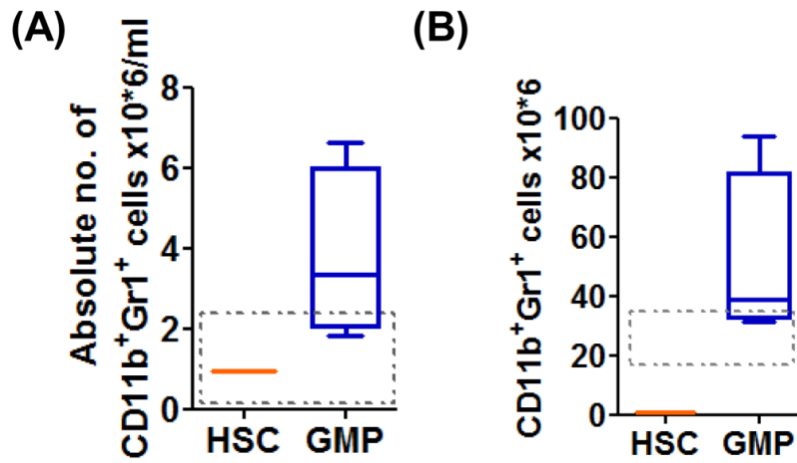


Figure 4. 20 - Absolute frequency of BM and PB CD11b<sup>+</sup>Gr1<sup>+</sup> in leukemic mice

Absolute numbers of CD11b<sup>+</sup>Gr1<sup>+</sup> cells in the (A) peripheral blood and (B) bone marrow of HSC transplanted (n=1) and GMP transplanted (n=4) leukemic mice. Box and whiskers plot with whiskers denoting min to max, and line representing mean values. Dashed box denotes normal range in healthy mice as determined by HemaVet 950FS reference intervals (PB) and previously published data (BM) (Yang et al., 2013).

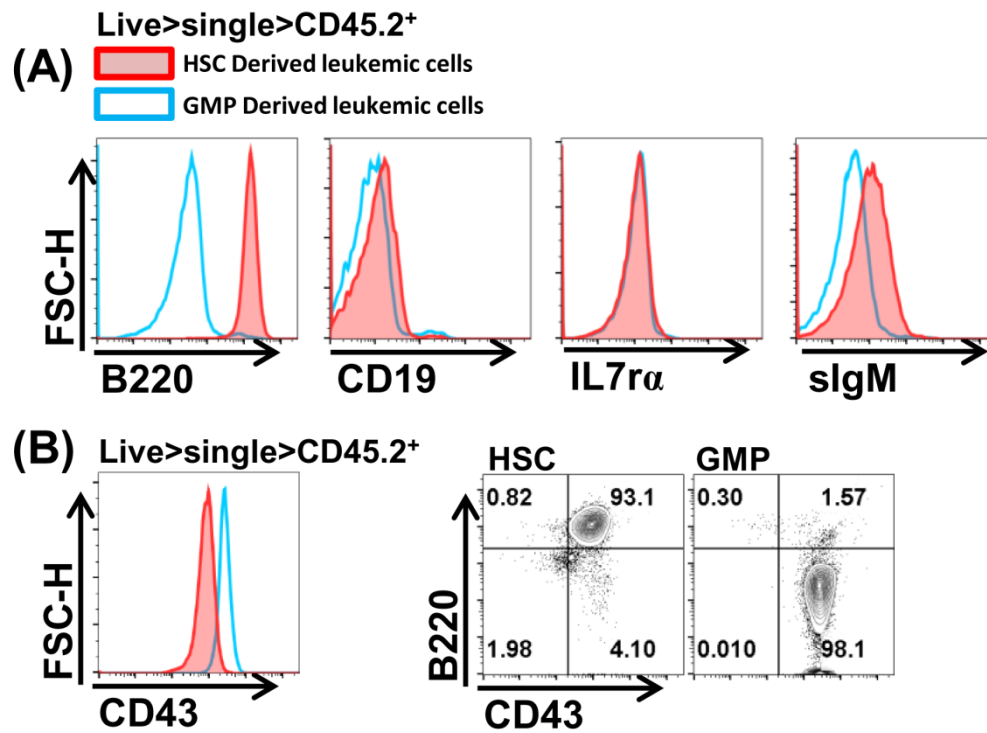


Figure 4. 21 - Distinct B cell surface marker expression patterns on HSC derived leukemic cells compared with GMP derived leukemic cells

(A) Representative histogram overlay of expression of B cell surface markers on HSC and GMP derived CD45.2<sup>+</sup> leukemic cells (B) Representative histogram overlays of expression of CD43 on HSC and GMP derived CD45.2<sup>+</sup> leukemic cells (left) and representative contour plots of B220 and CD43 co-expression on HSC and GMP derived CD45.2<sup>+</sup> leukemic cells. Data is representative of n=1 HSC and n=4 GMP mice.

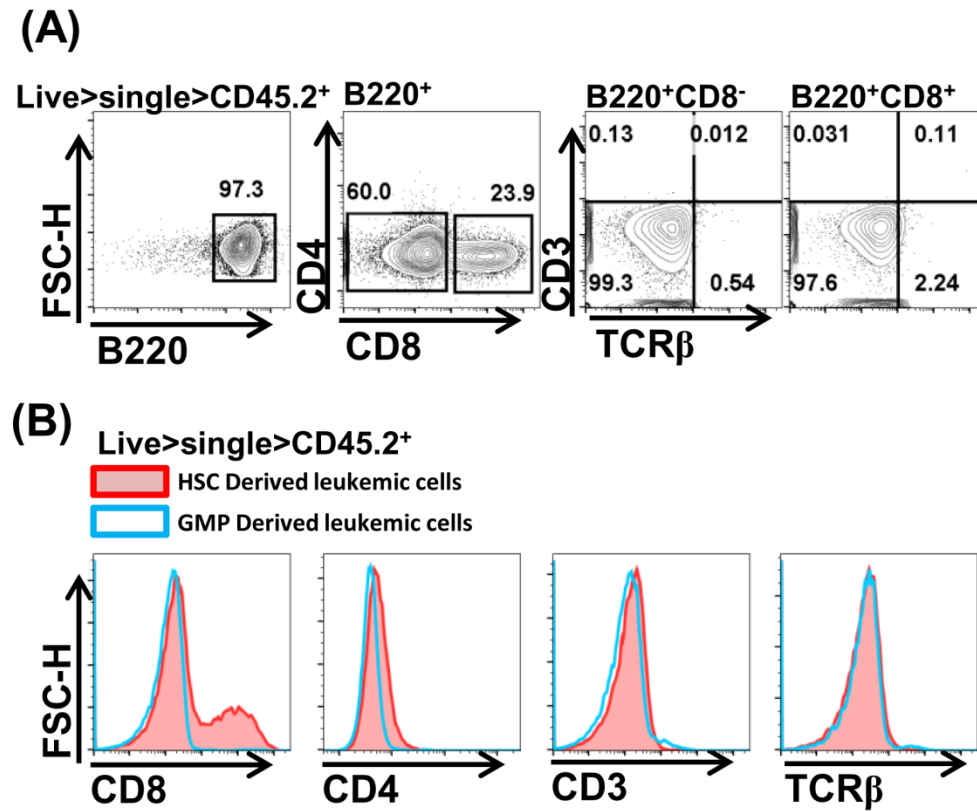


Figure 4. 22 - Aberrant T cell surface marker expression patterns on HSC derived leukemic cells compared with GMP derived leukemic cells

(A) Representative contour plots of T cell surface marker expression on HSC derived CD45.2<sup>+</sup> leukemic cells. (B) Representative histogram overlays of expression of T cell surface markers on HSC and GMP derived CD45.2<sup>+</sup> leukemic cells. Data is representative of n=1 HSC and n=4 GMP mice.

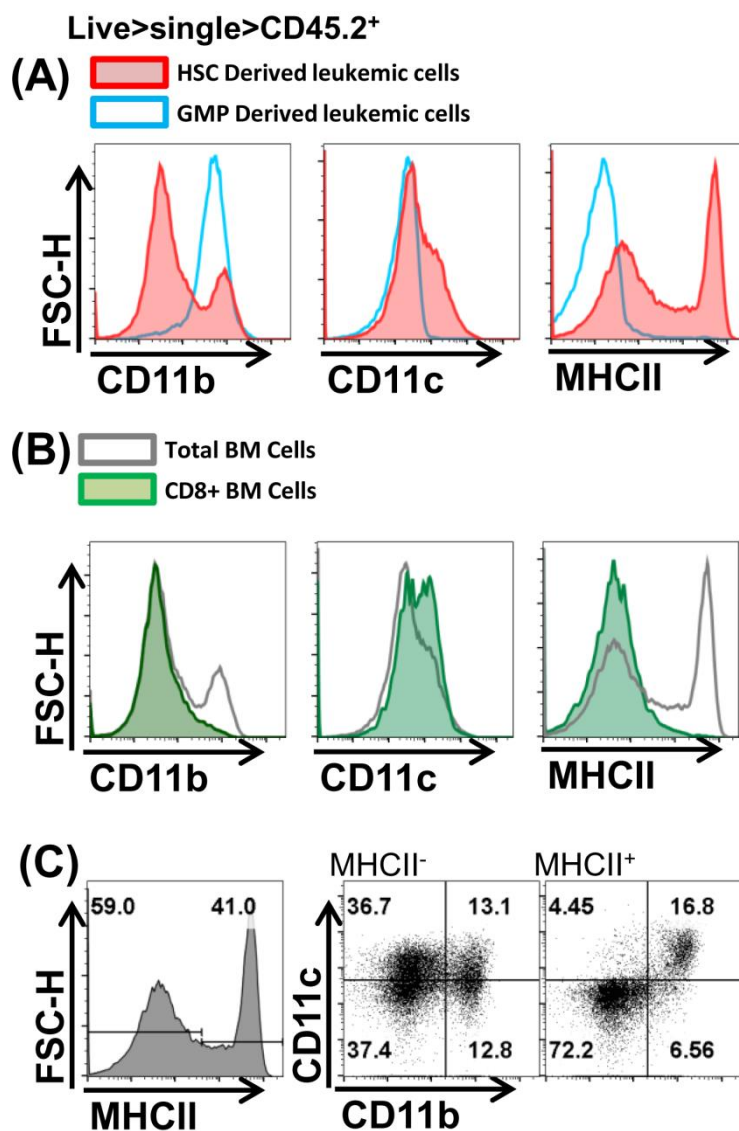


Figure 4. 23 - Differential myeloid cell surface marker expression patterns on HSC and GMP derived leukemic cells

(A) Representative histogram overlays of expression of myeloid cell surface markers on HSC and GMP derived CD45.2<sup>+</sup> leukemic cells (B) Histogram overlays of myeloid cell surface marker expression on total or CD8 expressing HSC derived CD45.2<sup>+</sup> leukemic cells (C) Representative flow cytometric analysis of CD11b and CD11c on MHCII<sup>+</sup> (right) and MHCII<sup>-</sup> (middle) HSC derived CD45.2<sup>+</sup> leukemic BM. Data is representative of n=1 HSC and n=4 GMP mice.

#### 4.3.4 Loss of *Trib2* does not perturb bone marrow hematopoiesis *in vivo*

As outlined in 1.3.3.5, *TRIB2* is differentially expressed in the hematopoietic system. Within the BM compartment its highest expression is in CD4<sup>+</sup> T cells and in the myeloid lineage *TRIB2* expression is highest in granulocytes and lowest in monocytes (Liang et al., 2013). Considering the fact that *TRIB2* generated such different disease phenotypes from the HSC and GMP, it was hypothesized that it may play a role in steady state BM hematopoiesis. To investigate this, the *Trib2* knockout mouse was studied (described in section 2.3.3.1). First the PB was analysed by flow cytometry for circulating myeloid (CD11b<sup>+</sup>Gr1<sup>+</sup>), B (B220<sup>+</sup>CD19<sup>+</sup>), CD8<sup>+</sup> T and CD4<sup>+</sup> T cells. There was no difference between the percentages of myeloid, B and T cells in *Trib2*<sup>-/-</sup> PB when compared to WT controls (Figure 4. 24). Analysis of mature leukocytes in the spleen also revealed no differences in the expression of markers of mature myeloid, B and T cells (Figure 4. 25). The BM of WT and *Trib2*<sup>-/-</sup> mice was then analysed. There was no difference between the distribution of differentiated leukocytes of WT and *Trib2*<sup>-/-</sup> BM (Figure 4. 26). The immature erythroid cells in the BM were next analysed using the cell surface markers CD71 and Ter119. These 2 markers can be used to look at the 4 main stages of erythroid maturation in the BM identifying CD71<sup>hi</sup>Ter119<sup>int</sup> pro-erythroblasts, CD71<sup>+</sup>Ter119<sup>+</sup> basophilic erythroblasts, CD71<sup>int</sup>Ter119<sup>+</sup> polychromatic erythroblasts and CD71<sup>-</sup>Ter119<sup>+</sup> orthochromatic erythroblasts. Loss of *Trib2* did not have a significant effect on the percentages of any of the erythroid progenitors in the BM (Figure 4. 27).

To ensure that loss of *Trib2* did not affect the BM stem and progenitor populations, cells were stained using CD150 and CD48, members of the SLAM family of cell surface molecules (described in section 1.1.2). There were no differences in the percentages of HSC, MPP, HPC-1 or HPC-2 cells (Figure 4. 28), nor of LSK cells. Committed myeloid progenitor cells were also identified by flow cytometry (also described in section 1.1.2), and no differences were observed between the WT and *Trib2*<sup>-/-</sup> mice in CMP, GMP or MEP cells, nor in the LK compartment (Figure 4. 29). Overall no defect in homeostatic hematopoiesis was apparent by immuno-phenotypic analysis. However because *TRIB2* has been shown to degrade C/EBP $\alpha$ , and C/EBP $\alpha$  is essential for terminal granulocytic

differentiation it was hypothesised that the absence of TRIB2 may result in increased levels of C/EBP $\alpha$ . C/EBP $\alpha$  facilitates and is essential for the CMP to GMP transition thus increased levels of C/EBP $\alpha$  could lead to accelerated differentiation. To explore this total BM isolated from WT or *Trib2*<sup>-/-</sup> mice was plated in methylcellulose. As described in section 2.2.3.2, M3434 methylcellulose media is supplemented with SCF, IL-3, IL-6 and EPO supporting the formation of myeloid and erythroid colonies. The morphology of colony types produced (E, GEMM, GM, M and G) and the criteria for their classification are outlined in section 2.2.3.2 There was no difference in the number of colonies produced from *Trib2*<sup>-/-</sup> BM cells compared with WT control cells (Figure 4. 30A) and while *Trib2*<sup>-/-</sup> BM cells generated more erythroid colonies *in vitro*, this difference was not statistically significant (Figure 4. 30B). Flow cytometric analysis of myeloid cell surface marker expression also revealed no differences in the expression of CD11b, Gr1, F4/80 or CD11c on cells from *Trib2*<sup>-/-</sup> colonies compared with WT control colonies (Figure 4. 31).

Taken together, these data indicate that TRIB2 may be dispensable for steady-state BM hematopoiesis as there was no disruption to the distribution of stem, progenitor or differentiated cell populations in the *Trib2*<sup>-/-</sup> mouse. Indeed loss of TRIB2 also did not affect the ability of BM stem and progenitor cells to form colonies and differentiate *in vitro*. As discussed in section 1.3.2, the Tribbles family of pseudokinases share a large degree of structural homology and it is likely that they may share overlapping functions in the hematopoietic system. Therefore compensation from TRIB1 or TRIB3 may account for the normal phenotype of the *Trib2*<sup>-/-</sup> mouse.

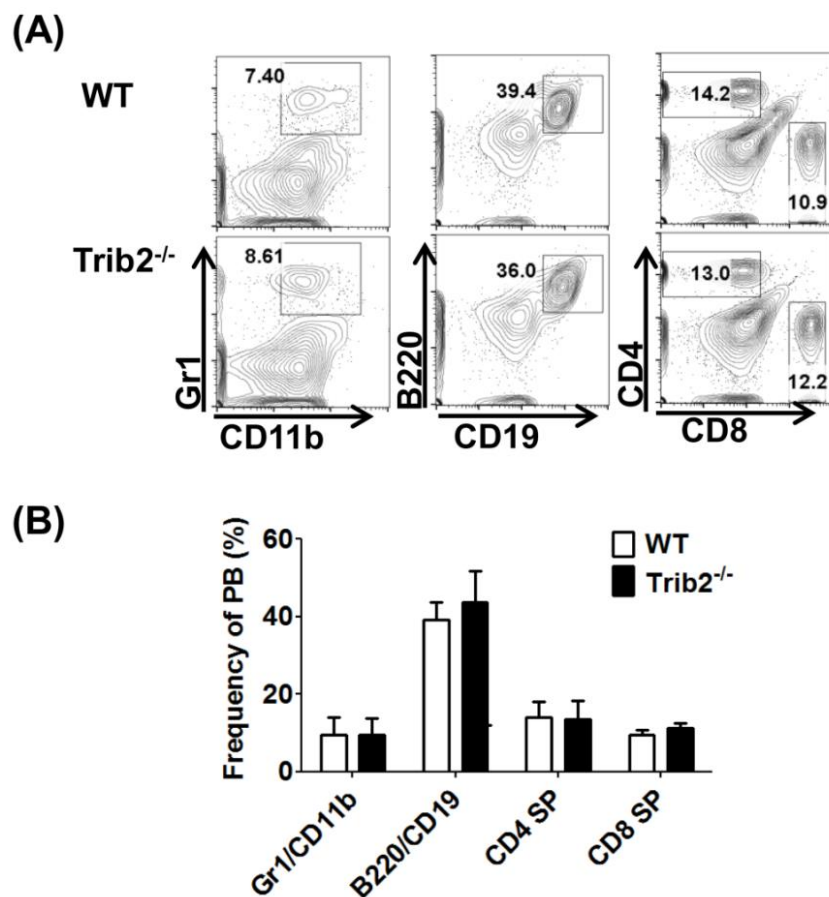


Figure 4. 24 - Normal levels of circulating leukocytes in *Trib2*<sup>-/-</sup> mice

(A) Representative contour plots of myeloid (CD11b, Gr1), B (B220, CD19) and T (CD4, CD8) cells in the PB of 6-14 week old WT and *Trib2*<sup>-/-</sup> mice. (B) Graph of average percentage expression of markers on WT (n=3) and *Trib2*<sup>-/-</sup> (n=10) PB cells +/- SD.

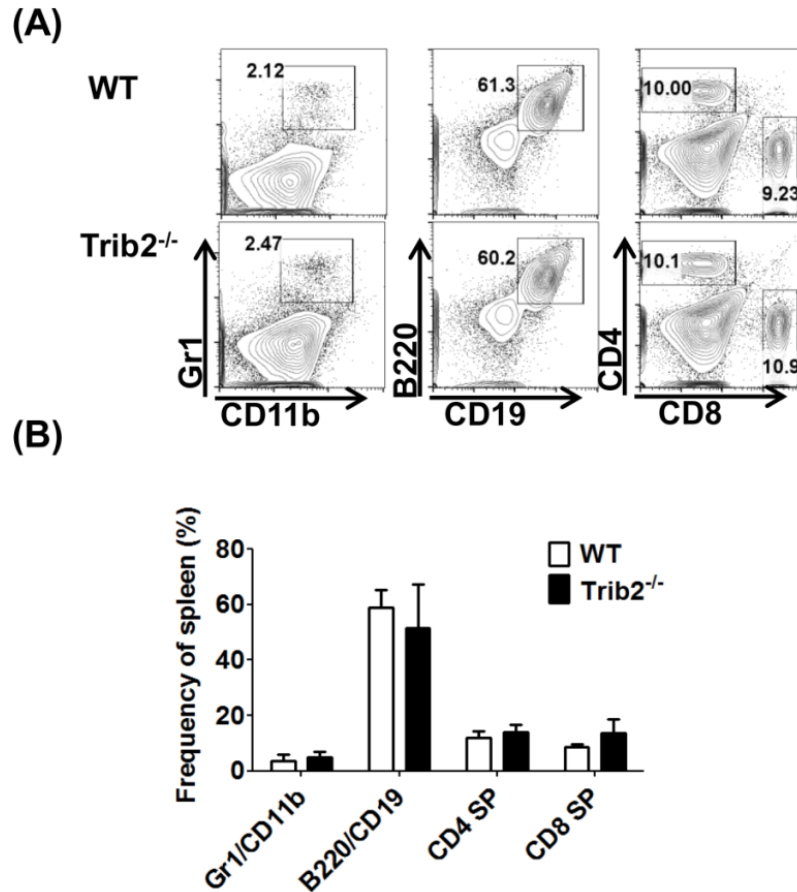


Figure 4. 25 - Normal distribution of splenic leukocytes in *Trib2*<sup>-/-</sup> mice

(A) Representative contour plots of myeloid (CD11b, Gr1), B (B220, CD19) and T (CD4, CD8) cells in the spleen of 6-14 week old WT and *Trib2*<sup>-/-</sup> mice (B) Graph of average percentage expression of markers on WT (n=3) and *Trib2*<sup>-/-</sup> (n=6) spleen cells +/- SD.

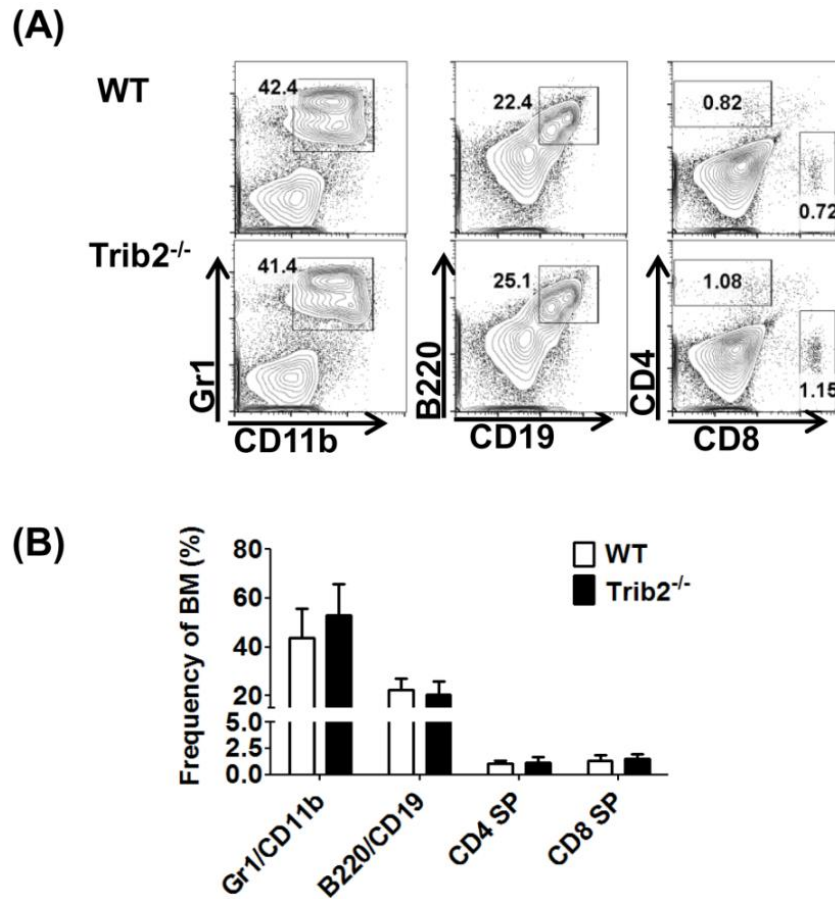


Figure 4. 26 - Normal BM hematopoiesis in *Trib2*<sup>-/-</sup> mice

(A) Representative contour plots of myeloid (CD11b, Gr1), B (B220, CD19) and T (CD4, CD8) cells in the BM of 6-14 week old WT and *Trib2*<sup>-/-</sup> mice. (B) Graph of average percentage expression of markers on WT (n=3) and *Trib2*<sup>-/-</sup> (n=9) BM cells +/- SD.

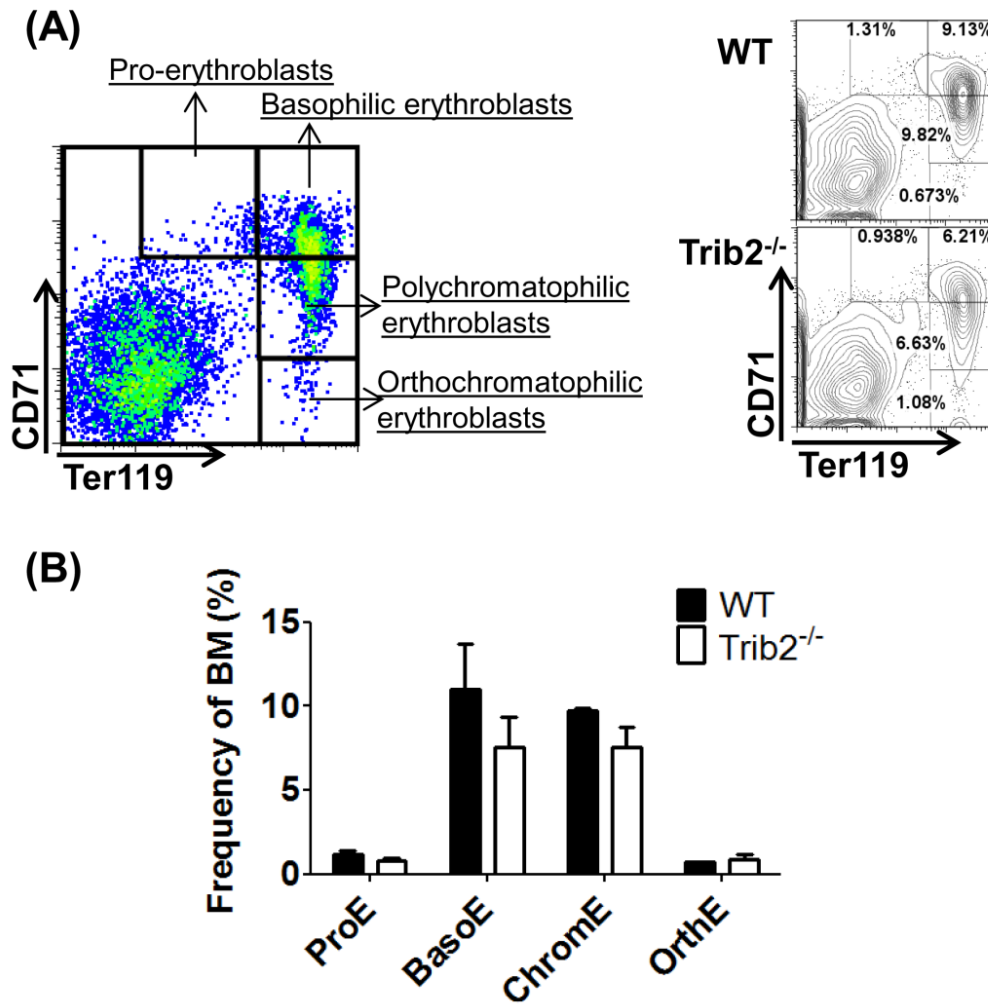


Figure 4. 27 - Normal BM erythropoiesis in *Trib2*<sup>-/-</sup> mice

(A) Gating strategy for detection of committed erythroid progenitors (left) and BM cells from WT and *Trib2*<sup>-/-</sup> mice were stained for Ter119 and CD71 (right) to isolate subpopulations of erythroblasts. (B) Graph of average percentage of each erythroid subpopulation in 6-14 week old WT (n=2) and *Trib2*<sup>-/-</sup> BM (n=2) cells +/- SD where ProE denotes proerythroblasts, BasoE denotes basophilic erythroblasts, ChromoE denotes polychromatophilic erythroblasts and OrthoE denotes orthochromatophilic erythroblasts.

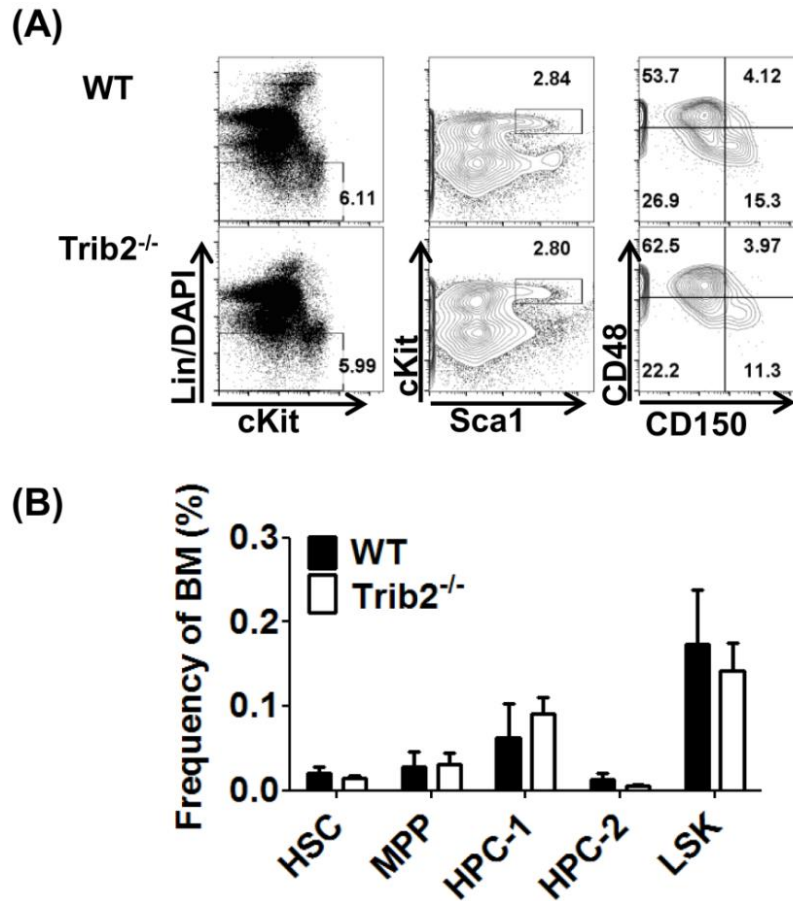


Figure 4. 28 - Normal distribution of stem and progenitor cells in *Trib2*<sup>-/-</sup> mouse

(A) Representative flow cytometric analysis of BM stem and progenitor cells from 6-14 week old WT and *Trib2*<sup>-/-</sup> mice. (B) Graph of average percentage of HSC (Lin<sup>-</sup>cKit<sup>+</sup>Sca1<sup>+</sup>CD150<sup>+</sup>CD48<sup>-</sup>), MPP (Lin<sup>-</sup>cKit<sup>+</sup>Sca1<sup>+</sup>CD150<sup>-</sup>CD48<sup>-</sup>), HPC-1 (Lin<sup>-</sup>cKit<sup>+</sup>Sca1<sup>+</sup>CD150<sup>-</sup>CD48<sup>+</sup>), HPC-2 (Lin<sup>-</sup>cKit<sup>+</sup>Sca1<sup>+</sup>CD150<sup>+</sup>CD48<sup>+</sup>) and LSK (Lin<sup>-</sup>cKit<sup>+</sup>Sca1<sup>+</sup>) cells present in WT (n=3) and *Trib2*<sup>-/-</sup> (n=3) BM.

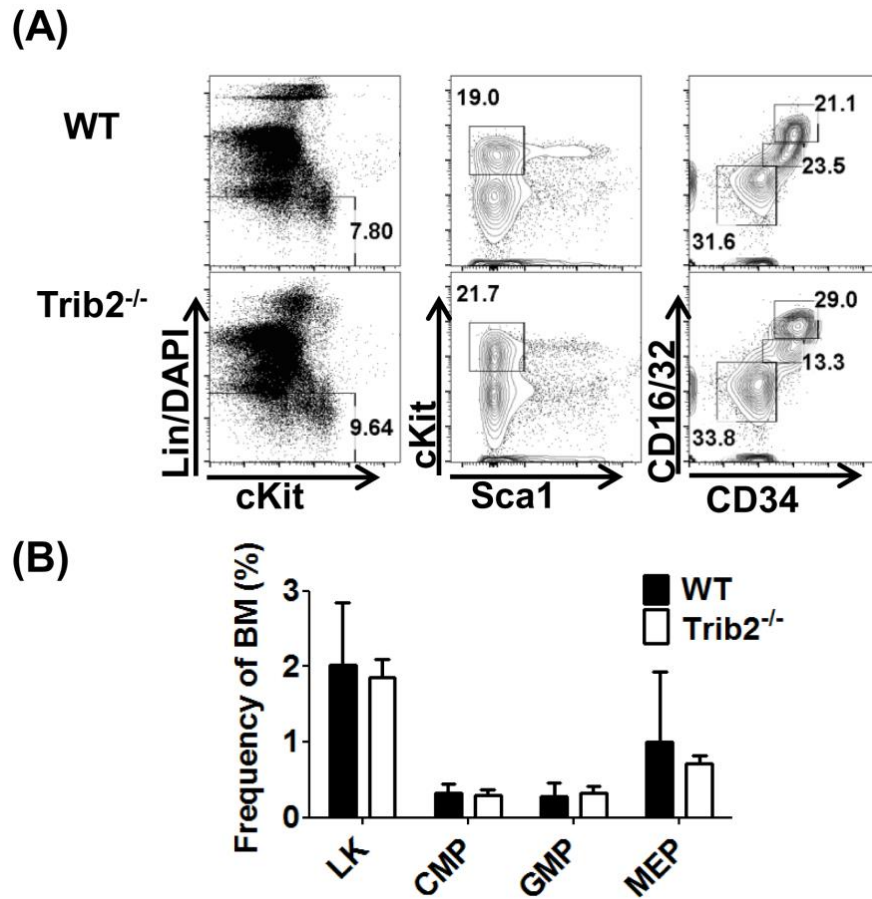


Figure 4. 29 - Normal distribution of myeloid progenitor cells in *Trib2*<sup>-/-</sup> BM

(A) Gating strategy and representative flow cytometric analysis of BM myeloid progenitor cells from 6-14 week old WT and *Trib2*<sup>-/-</sup> mice. (B) Graph of average percentage of LK (Lin<sup>-</sup>cKit<sup>+</sup>Sca1<sup>+</sup>), CMP (LK CD34<sup>+</sup>CD16/32<sup>lo</sup>), GMP (LK CD34<sup>+</sup>CD16/32<sup>hi</sup>) and MEP (LK CD34<sup>+</sup>CD16/32<sup>-</sup>) cells present in WT (n=3) and *Trib2*<sup>-/-</sup> (n=3) BM.

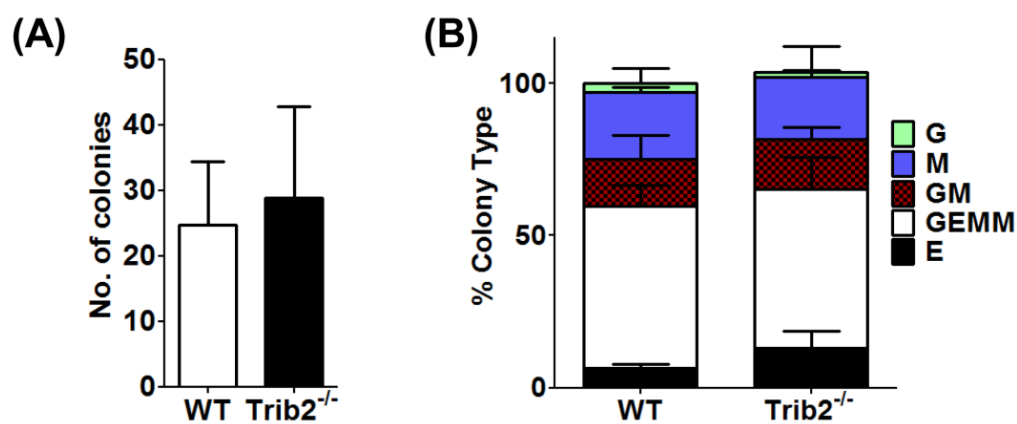


Figure 4. 30 - Absence of *Trib2* does not impair BM colony forming ability

(A) BM was isolated from litter-matched 6-8 week old WT or *Trib2*<sup>-/-</sup> mice, RBCs were lysed and 20,000 cells were plated in triplicate in methylcellulose media (M3434). Colonies with >50 cells were counted and (B) scored based on morphology. All data points correspond to the mean and the standard deviation of 3 independent experiments.

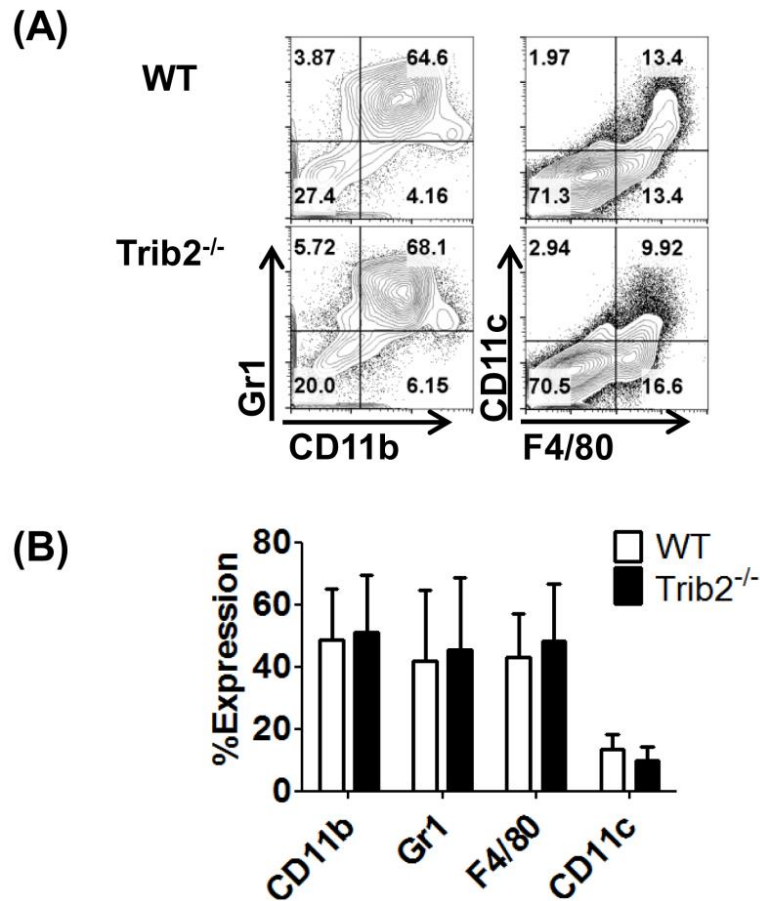


Figure 4. 31 - No differences in the expression of mature myeloid markers on cells from P1 WT and *Trib2*<sup>-/-</sup> colonies

**(A)** Representative flow cytometric analysis of myeloid cell marker CD11b, Gr1, F4/80 and CD11c expression on cells from P1 of methylcellulose assay. **(B)** Graph of average percentage expression of each marker. Bars represent averages of 3 independent experiments +/-SD.

## 4.4 Discussion

TRIB2 overexpression was able to confer self-renewal and proliferative capacity on stem and progenitor populations *in vitro* with all populations efficiently producing third round colonies in a serial replating assay. However the cell of origin affected the number, size and morphology of colonies produced, as well as the morphology and surface marker expression of cells within those colonies. Striking differences existed in the CMP derived colonies which had a predominantly mature myeloid phenotype and lost replating ability between P3 and P5. While the MPP derived cells efficiently replated to P5, the cells were comprised of mostly cKit<sup>-</sup> cells expressing markers of myeloid maturation. These differences translated *in vivo*, where TRIB2 was only able to initiate leukaemia from the HSC and GMP, and not the CMP and MPP. The TRIB2 transformed HSC and GMP diseases differed greatly in disease latency, penetrance and phenotype. TRIB2 transformed GMPs efficiently produced a mature myeloproliferative disease while *Trib2* transformed HSCs produced a weakly penetrant leukaemia with mixed myeloid and lymphoid characteristics. Despite the differential expression of *TRIB2* in the hematopoietic system and the observed ability of TRIB2 to induce leukaemias with both lymphoid and myeloid characteristics, it was determined that TRIB2 was dispensable for *in vivo* steady state hematopoiesis, and *in vitro* myeloid differentiation. These data suggest that while TRIB2 can increase proliferation and self-renewal in all tested populations *in vitro*, the *Trib2* LIC resides in the HSC and GMP. The differences in the resultant disease phenotype may be attributed to either the phenotype of the starting cell, or the mechanism of action of TRIB2 within that cell type.

The data indicate that TRIB2 overexpression confers the ability to serially replate *in vitro* to HSCs, MPPs, CMPs, GMPs and MEPs. However while all populations efficiently produced colonies to P3, the CMP derived cells lost their replating and proliferative capacity by P5. Indeed CMP derived colonies were also different to all other populations in that they were primarily of a mature type III morphology and cytopins of cells from transformed CMP derived colonies revealed an almost completely monomorphic differentiated cell type. Furthermore when transplanted at P3 into sub-lethally irradiated recipients only 1 in 5 mice engrafted the transplanted CMP derived cells. In a previous study looking at the effect of HRX-ENL transformation on BM cells, it was shown that

when type III colonies were individually selected from a plate they replated at a low frequency - with just 1 in 5 colonies successfully replating (Lavau et al., 1997), correlating with the observed frequency of CMP colony engraftment. Despite efficiently producing many large colonies in the 5<sup>th</sup> replating, the cells from the MPP derived colonies also failed to engraft and generate disease *in vivo*. By P5, more than 50% of MPP derived cells expressed CD11b and Gr1 but no cKit. Indeed by P5 over 65% of CMP derived cells were expressing Gr1. These observations suggest that the reason the MPP and CMP derived cells did not generate AML *in vivo* was that, despite conferring self-renewal ability, TRIB2 failed to block differentiation of the MPP and CMP derived cells, similar to observations made of BCR-ABL by Huntly et al outlined in 4.1.3.2.1.

The ability of TRIB2 to immortalise the MEP *in vitro* is interesting. TRIB2 induces AML by degrading the essential myeloid transcription factor C/EBP $\alpha$  thereby blocking myeloid differentiation (Keeshan et al., 2006). However *Cebpa* is not expressed in MEPs (Miyamoto et al., 2002) indicating that the *in vitro* transformation of the MEP by TRIB2 must be through a different mechanism. In mammals the evolutionarily conserved FOX proteins comprise a family of 4 transcription factors (FOXO1, FOXO3a, FOXO4 and FOXO6) which are involved in regulating genes that affect a variety of critical cell fate decisions. They are downstream effectors of the PI3K-Akt pathway (Burgering and Kops, 2002) and amongst other functions they regulate cell cycle progression and cell differentiation. They are well established as tumour suppressors and their dysregulation has been linked with numerous forms of cancer including prostate (Shukla et al., 2009), breast (Hu et al., 2004) and leukaemia (Parry et al., 1994). In a recent melanoma study, *TRIB2* was shown to repress *FOXO* activity and support the growth of melanoma cells (Zanella et al., 2010). The authors used a 293T cell line modified with a reporter construct capable of measuring *FOXO* transcriptional activity to study *FOXO* regulation. They performed a large-scale loss-of-function screen (>7500 human genes) to identify putative regulators of *FOXO* activity and showed that *TRIB2* silencing resulted in *FOXO* transcription. In a luciferase reporter assay, silencing *TRIB2* in the G-361 human melanoma cell line resulted in an increase in *FOXO*-driven luminescence. Loss of *TRIB2* from the G-361 cells also greatly impaired their growth and expansion. *FOXO1*, *FOXO3a* and *FOXO4* are all expressed in erythroid progenitor cells and during erythroid

differentiation (Mahmud et al., 2002). Indeed *FOXO3a* has been shown to induce erythroid differentiation through down-regulation of the *Id1* gene (Birkenkamp et al., 2007). Therefore inhibition of *Foxo* activity in the MEP by TRIB2 overexpression could account for the block in differentiation and acquired serial replating activity observed *in vitro*. However transplantation of TRIB2 expressing MEPs would be required to determine if the cells were fully transformed, and could generate disease *in vivo*.

Only the TRIB2 overexpressing HSC and GMP derived cells were able to generate leukaemia *in vivo*, and they did so with different penetrance and latency. The median latency of the GMP derived disease was just 10 weeks while the latency of the HSC derived disease was significantly longer at 26 weeks. It was hypothesised that transplanting preleukemic cells from the third round of serial replating would decrease the latency of the disease *in vivo* (~25.5 weeks primary AML and ~5 weeks secondary AML) (Keeshan et al., 2006). As such it is unclear as to whether the serial replating had any effect on TRIB2 mediated disease latency. A transplant of freshly transduced purified populations may result in similar disease latencies with the HSC representing the expected TRIB2 latency. It is possible that the GMP disease may have enriched for the TRIB2 LIC compared to the slower HSC derived disease. Support for this comes from previously described studies that the LIC can be enriched in the HSC (Bonnet and Dick, 1997, Sarry et al., 2011, Gibbs et al., 2012, Krivtsov et al., 2013, Cozzio et al., 2003) or a more mature myeloid progenitor population such as the GMP (Goardon et al., 2011, Bereshchenko et al., 2009, Heuser et al., 2011, Guibal et al., 2009, Reckzeh et al., 2012) and that the identity of the LIC can affect the disease latency. In addition to studies outlined in 4.1.3, a study of 100 primary AML samples showed that LSC activity was enriched in subsets which phenotypically resembled murine LMPPs and GMPs (Goardon et al., 2011). They observed that the leukemic LMPP-like (L-LMPP) cells gave rise to leukemic GMPs (L-GMP) which were the dominant cell type (~80%), but the inverse was not true, mimicking the normal hematopoietic hierarchy. When examined at the molecular level the L-LMPP and L-GMP cells resembled their normal counterparts suggesting that the LIC was a committed progenitor cell as opposed to a HSC with aberrant surface marker expression. However, the majority of these studies show that regardless of the LIC, the resultant diseases are virtually

indistinguishable from one another. Therefore, it is somewhat misleading to reconcile these observations with those of Trib2, because the Trib2 LIC resulted in striking differences in the phenotype, latency and penetrance of the disease, suggesting that distinct mechanisms of Trib2 leukaemogenesis from the HSC and the GMP exist.

The differences in expression of myeloid and lymphoid markers in Trib2 HSC and GMP derived diseases are possibly attributable to the expression levels of lineage specific genes in the given LIC. A mature myeloproliferative disease was observed from the GMP. C/EBP $\alpha$  is essential for the CMP to GMP transition and its expression is highest in the GMP. A recent study by Ye et al has put forward an interesting hypothesis which reports that myeloid differentiation is required for the formation of LSCs and for AML initiation (Ye et al., 2015). They utilised the conditional *Cebpa* KO model in conjunction with overexpression of the MLL-AF9 fusion gene. LSK and CMP cells were isolated from Poly I:C treated MxCre<sup>-</sup> *Cebpa*<sup>f/f</sup> (control) and MxCre<sup>+</sup> *Cebpa*<sup>f/f</sup> (KO) mice and transduced with MLL-AF9 virus, then transplanted into recipient mice. Transduced KO cells failed to initiate disease *in vivo* with control mice succumbing to disease within 4 months. The *Cebpa* GFP<sup>+</sup> KO LSKs successfully generated B cells, CMPs and MEPs but were unable to produce GMP cells. Gene expression analysis revealed that in *Cebpa* GFP<sup>+</sup> KO LSKs and CMPs, downstream targets of MLL-AF9 such as *HoxA9* and *Meis1* were expressed at equal or higher levels as in *Cebpa* GFP<sup>+</sup> Control LSKs and CMPs. The authors then showed that MLL-AF9 leukaemia could be restored in *Cebpa* KO cells by treating cells with GM-CSF and IL-3 to overcome the block in differentiation caused by loss of C/EBP $\alpha$ , thus demonstrating that it was not loss of C/EBP $\alpha$  itself but rather impaired myelomonocytic differentiation which prevented leukaemia initiation. This may account for the transformation of the GMP and not the CMP or MPP by Trib2.

A small proportion of acute leukaemias, known as bi-phenotypic, exhibit both myeloid and lymphoid characteristics. It has not been determined whether these diseases arise from the transformation of immature progenitors which have myeloid and lymphoid potential, or if the leukaemic cell phenotypes are due to aberrant expression of lineage related genes, and thereby lineage specific cell surface markers. While it has not been previously reported for Trib2, the transformation of the HSC by an oncogene resulting in a multi-lineage disease

phenotype is not a unique observation among LIC studies. As outlined in 4.1.3.1.2, similar results were observed using the oncogene MLL-GAS7. MLL-GAS7 overexpression induced a mixture of AML (80%), ALL (10%) and bi-lineage leukaemia (10%) *in vivo* (So et al., 2003). In a serial replating assay supplemented with myeloid cytokines, MLL-GAS7 transduced CMPs and GMPs serially produced colonies of cKit<sup>+</sup>Gr1<sup>+</sup>CD11b<sup>+</sup> cells, while cells from HSC colonies also expressed B220. In a lymphoid permissive serial replating assay only the MLL-GAS7 transduced HSC was able to replate and produce colonies of cells with both myeloid and lymphoid characteristics. This demonstrates that, despite the observed plasticity of LSCs described in 4.1.2, only the HSC is prone to multi-lineage transformation by MLL-GAS7, paralleling the observations made for TRIB2. Clearly the multi-lineage potential and transcriptional program of the HSC contributes to the myeloid, B and T cell features observed in the HSC derived TRIB2 leukaemia. What is unclear is the degree to which this phenotype can be attributed to the experimental model used. It is important to acknowledge that the methylcellulose media used favours myeloid cell growth and maturation and so lymphoid potential is hindered greatly. Despite this, cells with lymphoid characteristics were still observed in the TRIB2 transformed HSC derived disease. As described in section 1.3.3.5, *TRIB2* expression is highest in T cells, it has been shown to be a downstream target of the T cell oncogenes *NOTCH1*, *PITX1* and *TAL1* and its expression is upregulated in a subset of B cell-ALL with a t(1:19) translocation (Liang et al., 2013). Thus it is possible that under optimised experimental conditions, TRIB2 could generate a lymphoid leukaemia *in vivo*, perhaps from the HSC or CLP, instead of the observed mixed lineage leukaemia.

Differences in the expression of lineage associated transcription factors may account for the differences in the HSC and GMP derived diseases. However, the ability of TRIB2, and other oncogenes, to generate leukaemia from functionally and phenotypically distinct stem and progenitor populations also suggests that there are overlapping gene expression signatures initiated by different oncogenes which facilitate leukemic transformation. This hypothesis has been addressed in some of the aforementioned studies. In the study outlined in 4.1.3.2.5 the gene expression signature of MOZ-TIF2, NUP98-HOXA9, AML1-ETO or control transduced GMPs was examined (Kvinlaug et al., 2011). In order to

focus on genes related with self-renewal the authors first compared normal LSKs with normal GMPs, and identified a set of 167 genes which were differentially expressed including *Foxo3a* (self-renewal) and *Meis1* (leukemic transformation). Comparing this “leukaemia initiation signature” with the transduced GMPs revealed a 76% overlap (127 of 167) in expression with 14 genes differentially expressed downstream of all 3 of the oncogenes tested, confirming the existence of common transcriptional programmes of leukaemogenesis initiated from different oncogenes.

Based on the observation that TRIB2 overexpression could block myeloid development, and also induce a mixed lineage disease *in vivo* the hematopoietic compartment of the *Trib2*<sup>-/-</sup> mouse was examined. No significant differences in the percentage of mature myeloid cells, B and T cells were observed in the *Trib2*<sup>-/-</sup> mice when compared with WT controls. Indeed a normal distribution of stem and myeloid progenitor cells and erythroblasts was also observed in *Trib2*<sup>-/-</sup> BM. It was previously reported that TRIB2 is not essential for murine development (Takasato et al., 2008), and now it has been confirmed that steady state hematopoiesis also appears undisrupted in the absence of TRIB2. Indeed TRIB1 and TRIB3 have also been shown to be dispensable for development (Yamamoto et al., 2007, Okamoto et al., 2007). The 3 mammalian tribbles family members share more than 45% sequence homology, so one consideration in fully assessing a role for TRIB2 in hematopoiesis is the potential for overlapping function with other family members, in particular TRIB1. TRIB1 has been identified as a potent inducer of AML (Yokoyama et al., 2010) and this action is also driven by C/EBP $\alpha$  degradation, but TRIB3 does not possess this ability. Both TRIB1 and TRIB2 are capable of degrading CEBP $\beta$  (Naiki et al., 2007), while Trib3 is able to block the activation of *Cebpb* (Bezy et al., 2007). The overlapping functions of TRIB1 and TRIB2 appear to be dependent on cell type, as TRIB3 has functional similarities with TRIB2 in adipocytes where they are both down regulated during adipocyte differentiation (Naiki et al., 2007). The understanding of how the Tribbles family contributes to hematopoiesis would be greatly enhanced by a study of a *Trib1/2* double knockout mouse. Indeed a *Trib1/2/3* triple knockout mouse could indicate whether or not these are an essential family of pseudokinases for development. However attempts to generate the double and triple knockout mice by researchers in the field have

thus far failed (Endre Kiss-Toth, Vishva Dixit; personal communication) suggesting potential lethality. The development of conditional models would greatly facilitate our understanding of the importance of the *Tribbles* family in hematopoiesis.

In summary the data presented here show that TRIB2 overexpression leads to the immortalization of stem and progenitor populations *in vitro* regardless of their levels of *Cebpa* expression. However TRIB2 was only able to initiate disease *in vivo* from the HSC and GMP, driving a potent myeloproliferative AML from the GMP, while the HSC resulted in a weakly penetrant multi-lineage disease, suggesting that 2 distinct mechanisms of oncogenesis were involved. Together these data provide new insight into the TRIB2 LIC demonstrating that TRIB2 produces very distinct diseases from the HSC and GMP. Further exploration of the ability of TRIB2 to induce lymphoid leukaemias *in vivo* could provide a new leukaemia model, a potentially valuable resource for therapeutic approaches considering the frequency of lymphoid leukaemias with high TRIB2 expression.

Some of this work has been published in Ling Liang et al, 2016, details provided in section 0.

## **5 Results: NFIX expression critically modulates early B lymphopoiesis and myelopoiesis**

Part of this chapter has been published in O'Connor et al, 2015, provided in section 0.

## 5.1 Introduction

### 5.1.1 Nuclear factor one (NFI)

The nuclear factor one (NFI) transcription factor protein was first identified in 1982 when it was isolated from the nuclear extracts of HeLa cells (Nagata et al., 1982). The authors were studying the replication of adenovirus *in vitro*, during which a terminal protein of the virus forms a covalent bond with the 5' end of the viral genome. This complex acts as a primer for replication, but it requires 3 additional proteins from the host cell to complete replication. One of these proteins was identified as the 47kD NFI. It was shown to stimulate the formation of this complex by acting as a sequence-specific DNA binding protein that preferentially binds double stranded DNA (Nagata et al., 1983). NFI is often denoted as NFI/CTF because it was shown to be identical in polypeptide sequence to the CCAAT-binding transcription factor (CTF) (Jones et al., 1987). The CCAAT box is a conserved sequence of nucleotides (GGCCAATCT) which are found upstream of a transcription start site, in the -60/-100 region of eukaryotic gene promoters. It is one of the most common eukaryotic promoter elements, providing a binding site for a large group of transcription factors. NFI has been shown to stimulate DNA replication and transcription initiation *in vitro*, by activating RNA polymerase II transcription on a variety of promoters (Rossi et al., 1988, Mink et al., 1992).

### 5.1.2 Structure of NFI

The general structure of the *NFI* gene comprises 11 coding exons, with a highly conserved 200-220 amino acid residue N-terminal domain which is responsible for DNA binding and dimerization (Mermod et al., 1989, Gounari et al., 1990). This region is also sufficient to stimulate the initiation of DNA replication in adenovirus. The transcriptionally active domain is located in the C-terminus and consists of a 100 amino acid, proline rich (~25%) sequence (Figure 5. 1). While the C-terminus is highly variable between NFI family members, the C-terminus of each member is highly conserved across species (Kruse and Sippel, 1994). NFI binds as either hetero- or homodimers to a palindromic DNA sequence TTGGC(N<sub>5</sub>)GCCAA (Gronostajski et al., 1985). NFI proteins can also bind to consensus half sites (TTGGC and GCCAA) but with lower affinity (Meisterernst et



cells were treated with RA, which induces myeloid differentiation, NFIA was displaced and replaced with C/EBP $\alpha$ . Conversely when cells resistant to RA (and therefore unable to undergo differentiation) were treated, NFIA remained bound to the *miR-223* promoter and no C/EBP $\alpha$  binding was detected, suggesting competition between these 2 proteins for regulation of the *miR-223* promoter. A similar regulatory network was reported by Rosa et al. They demonstrated that PU.1 activates the transcription of *miR-424*, which in turn stimulates monocyte differentiation by repressing NFIA translation (Rosa et al., 2007). More recently it was shown that knocking down *Nfia* in murine BM CD11b<sup>+</sup>Gr1<sup>+</sup> cells led to their efficient differentiation into macrophages and dendritic cells *in vitro* (McClure et al., 2014).

NFIA has also been described in erythroid differentiation. When CD34<sup>+</sup> hematopoietic progenitor cells were stimulated to enter either erythropoiesis (EPO, IL-3 and GM-CSF) or granulopoiesis (IL-3, GM-CSF and G-CSF), NFIA mRNA and protein expression were significantly upregulated in cells undergoing erythroid differentiation, and dramatically reduced in those undergoing granulocytic differentiation (Starnes et al., 2009). HPCs transduced with a lentiviral shRNA targeting *NFIA* were unable to differentiate into erythroid cells. Most of the cells had died by day 8, and any remaining cells by day 12 displayed a myeloid phenotype. Furthermore, a transcriptome-wide approach revealed that in both CD34<sup>+</sup> and leukemic K562 cells, NFIA induces an erythroid transcriptional program (Starnes et al., 2010).

### 5.1.3.2 NFIB

Recently *NFIB* was identified as a novel regulator of megakaryocyte maturation. Loss of *NFIB* in CD34<sup>+</sup> PB cells, dramatically reduced their ability to differentiate towards MKs, and conversely overexpression of NFIB in CD34<sup>+</sup> cells increased cell maturation (Chen et al., 2014). It has also been implicated in polycythaemia vera (PV). PV is a rare hematopoietic malignancy involving uncontrolled proliferation of red blood cells in the BM, the molecular basis for which is unknown. Increased *NFIB* expression was detected in granulocytes and CD34<sup>+</sup> cells of certain PV patients harbouring a 9qLOH mutation compared to those without this mutation (Kralovics et al., 2002). More recently single cell gene expression analysis showed an 8 fold increase of *NFIB* expression in the MPP

compared to the HSC (Notta et al., 2011), alluding to a role for *NFIB* in stem and progenitor cells of the BM.

### 5.1.3.3 NFIC

As with *NFIB* above, loss of *NFIC* was also found to disrupt megakaryocyte differentiation from CD34<sup>+</sup> PB cells and, like *NFIB*, its overexpression promoted differentiation (Chen et al., 2014). In addition, in the BM compartment, *NFIC* is highly expressed in osteoblasts (Perez-Casellas et al., 2009). *Nfic*<sup>-/-</sup> mice display an osteoporosis-like phenotype and *Nfic* overexpression in *Nfic*<sup>-/-</sup> cells has been shown to reduce adipocyte differentiation via PPAR $\gamma$  signalling while increasing differentiation of osteoblasts (Lee et al., 2014).

### 5.1.3.4 NFIX

To date the only study of NFIX in the hematopoietic compartment was performed by the McKinney-Freeman group in 2013. Initially, *Nfix* was identified as a potential novel regulator of HSC repopulating ability in a transcriptome-wide study of HSCs, purified from more than 2500 embryonic and adult mice (McKinney-Freeman et al., 2012). They subsequently reported that *Nfix* expression increases during embryonic development with high expression of *Nfix* in murine adult HSPCs (Holmfeldt et al., 2013). They showed that loss of *Nfix* in HSPCs resulted in a greatly reduced repopulating ability when transplanted into lethally irradiated mice, which was attributed to an increase in apoptotic cell death. They also reported down-regulation of key survival genes in HSPCs with loss of *Nfix*, demonstrating that *Nfix* plays a role in HSPC survival under stress conditions.

## 5.2 Aims and Objectives

*Nfix* is differentially expressed in murine HSPCs during development with highest expression detected in the adult BM (Holmfeldt et al., 2013), and it is expressed at a much higher level than the other NFI genes. As outlined in 5.1.3.4, Holmfeldt and colleagues have demonstrated that *Nfix* regulates HSPC repopulating ability under stress conditions by modulating a number of key survival genes. However, its role in steady state hematopoiesis is unclear. In addition, there is an established role for the other NFI family members in the differentiation of hematopoietic stem and progenitor cells, but the role of *Nfix* in lineage determination is unknown. In order to assess whether *Nfix* plays a role in differentiation in the hematopoietic system, the specific aims of this chapter were:

- i. To investigate the effect of *Nfix* on hematopoiesis
  - a. Using a retroviral transduction and BMT approach to determine if ectopic expression of NFIX on stem and progenitor cells affects lineage distribution *in vivo*
  - b. Examine the role of NFIX in lineage decisions using myeloid or B cell permissive culture conditions *in vitro assays*
- ii. To determine the effect of loss of *Nfix* on hematopoietic lineage specification

## 5.3 Results

### 5.3.1 NFIX overexpression favours myelopoiesis over B cell lymphopoiesis *in vivo*

In order to determine if NFIX plays a role in hematopoiesis, BM cells were isolated from 5-FU treated C57BL/6 donor mice and transduced with either control MigR1 or NFIX expressing retrovirus. The cells were transplanted into lethally irradiated recipient mice. At 6-10 weeks post BMT, PB was taken and assessed by flow cytometry for the reconstitution of the myeloid, B and T cell compartments. There was a significant reduction in the percentage of B220<sup>+</sup> and CD19<sup>+</sup> B cells in the GFP<sup>+</sup> compartment of the PB of NFIX mice compared with the MigR1 mice (Figure 5. 2). No change in the percentage of circulating CD4<sup>+</sup> and CD8<sup>+</sup> cells was observed (Figure 5. 3). However, there was a significant increase in the percentage of circulating CD11b<sup>+</sup>Gr1<sup>+</sup> myeloid cells in the GFP<sup>+</sup> compartment of NFIX mice compared with MigR1 control mice (Figure 5. 4). These data indicate that NFIX overexpression disrupts B cell and myeloid differentiation *in vivo*. Subsequent analysis of the BM also revealed a pronounced loss of B cells, and significant increase in CD11b<sup>+</sup>Gr1<sup>+</sup> myeloid cells (Figure 5. 5). Similarly, the splenic B cells were dramatically depleted in the GFP<sup>+</sup> compartment of NFIX mice when compared with MigR1 controls. The concomitant increase in myeloid cells was also evident in the spleen (Figure 5. 6).

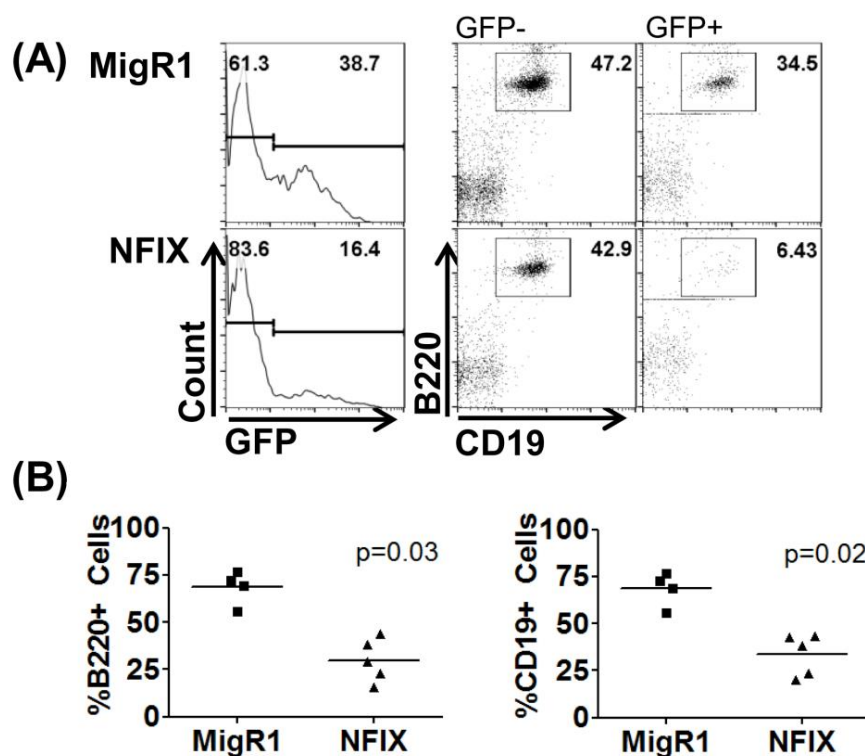


Figure 5. 2 - NFIX overexpression results in decreased B220 and CD19 expression in the PB.

C57BL/6 mice were reconstituted with BM cells transduced with MigR1 or NFIX retrovirus. **(A)** Representative flow cytometric analysis of PB cells showing engraftment of GFP (left panel), and B220<sup>+</sup>CD19<sup>+</sup> B cells in the GFP<sup>-</sup> and GFP<sup>+</sup> fractions. **(B)** Graph of percentage number of GFP<sup>+</sup> B cells (B220<sup>+</sup> left and CD19<sup>+</sup> right) in the PB at 6 weeks post BMT, MigR1 n=4, NFIX n=5. Results are representative of 2 independent experiments. For statistical analysis an unpaired, two-tailed, students t-test performed.

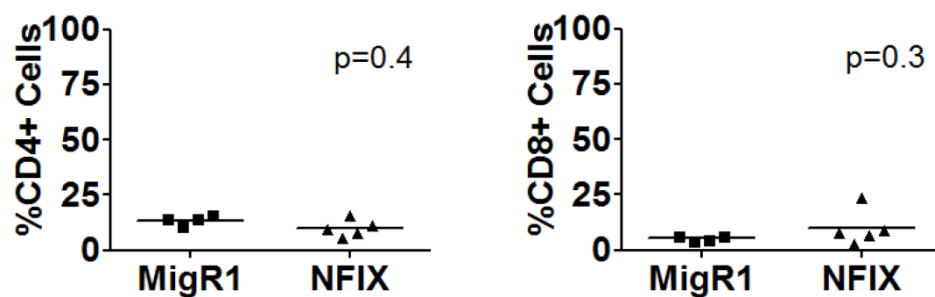


Figure 5. 3 - NFIX overexpression does not affect T cell maturation *in vivo*.

Graph of percentage number of GFP<sup>+</sup> CD4<sup>+</sup> cells (left) and GFP<sup>+</sup> CD8<sup>+</sup> cells (right) in the PB of MigR1 and NFIX chimeric mice at 6 weeks post BMT, MigR1 n=4, NFIX n=5. Data is representative of 2 independent experiments. For statistical analysis an unpaired, two-tailed, students t-test performed.

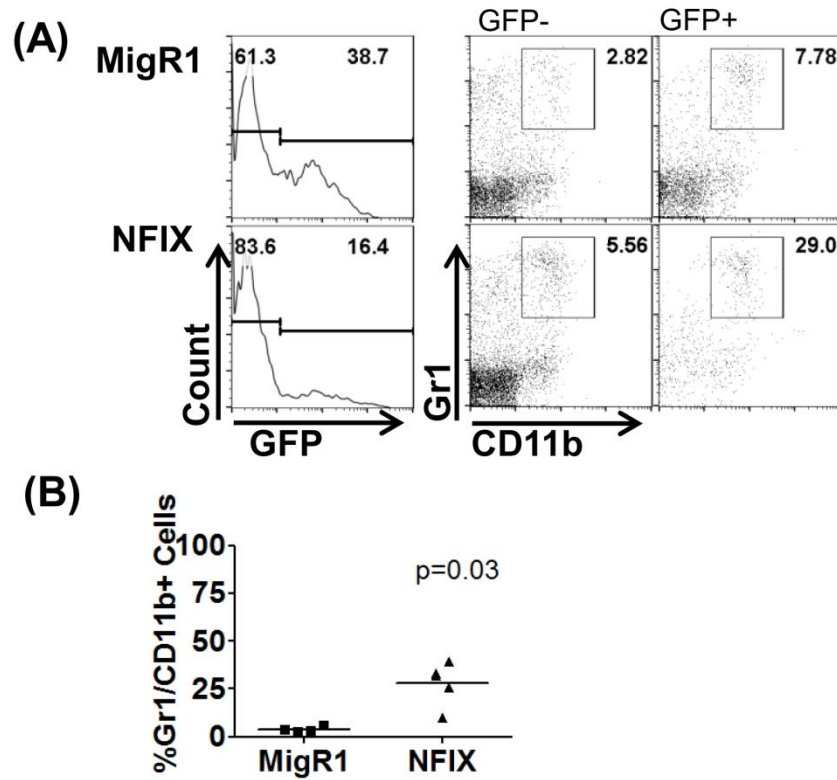


Figure 5. 4 - NFIX overexpression results in a higher percentage of peripheral myeloid cells *in vivo*.

**(A)** Representative flow cytometric analysis of PB cells showing engraftment of GFP (left panel) and CD11b<sup>+</sup>Gr1<sup>+</sup> myeloid cells in the GFP<sup>-</sup> and GFP<sup>+</sup> fractions. **(B)** Graph of percentage number of GFP<sup>+</sup> myeloid cells (CD11b<sup>+</sup>Gr1<sup>+</sup>) in the PB at 6 weeks post BMT, MigR1 n=4, NFIX n=5. Results are representative of 2 independent experiments. For statistical analysis an unpaired, two-tailed, students t-test performed.

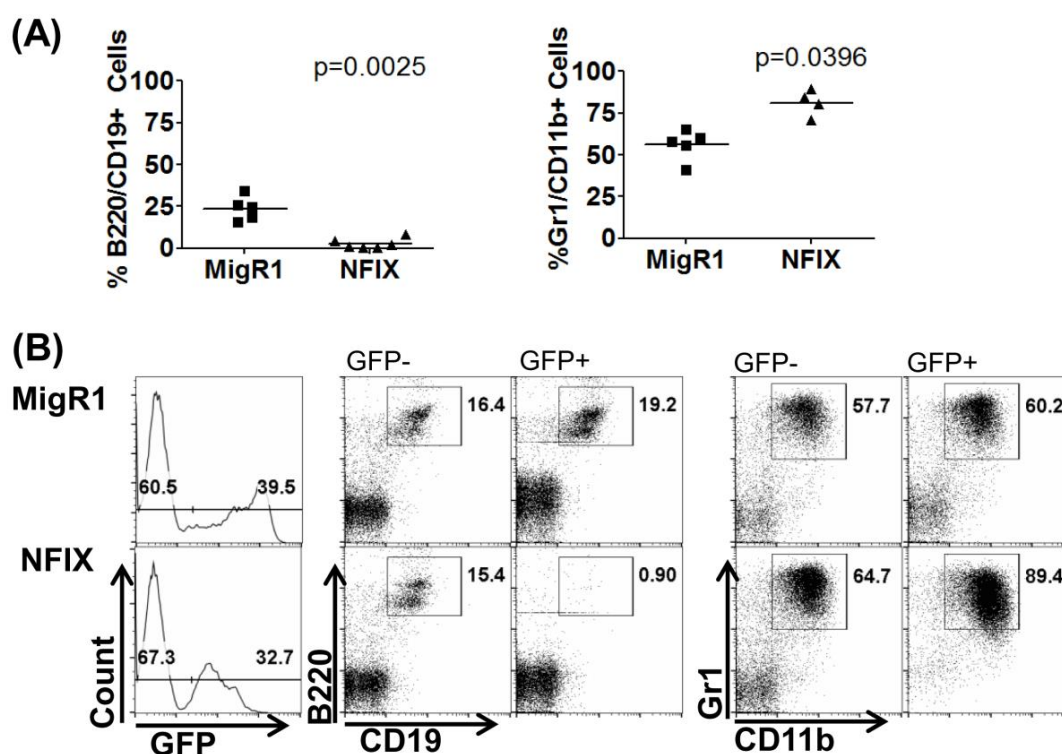


Figure 5. 5 - Disrupted hematopoiesis in the BM of NFIX mice.

C57BL/6 mice were reconstituted with BM cells transduced with MigR1 or NFIX retrovirus. **(A)** Graphs of percentage GFP<sup>+</sup> B cells (left, MigR1 n=5, NFIX n=6) and GFP<sup>+</sup> myeloid cells (right, MigR1=5, NFIX =6) in the BM of chimeric mice 10 weeks post BMT. **(B)** Representative flow cytometric analysis in MigR1 and NFIX chimeric animals 10 weeks post BMT showing GFP engraftment (left panel). Results are representative of 2 independent experiments. For statistical analysis an unpaired, two-tailed, students t-test performed.

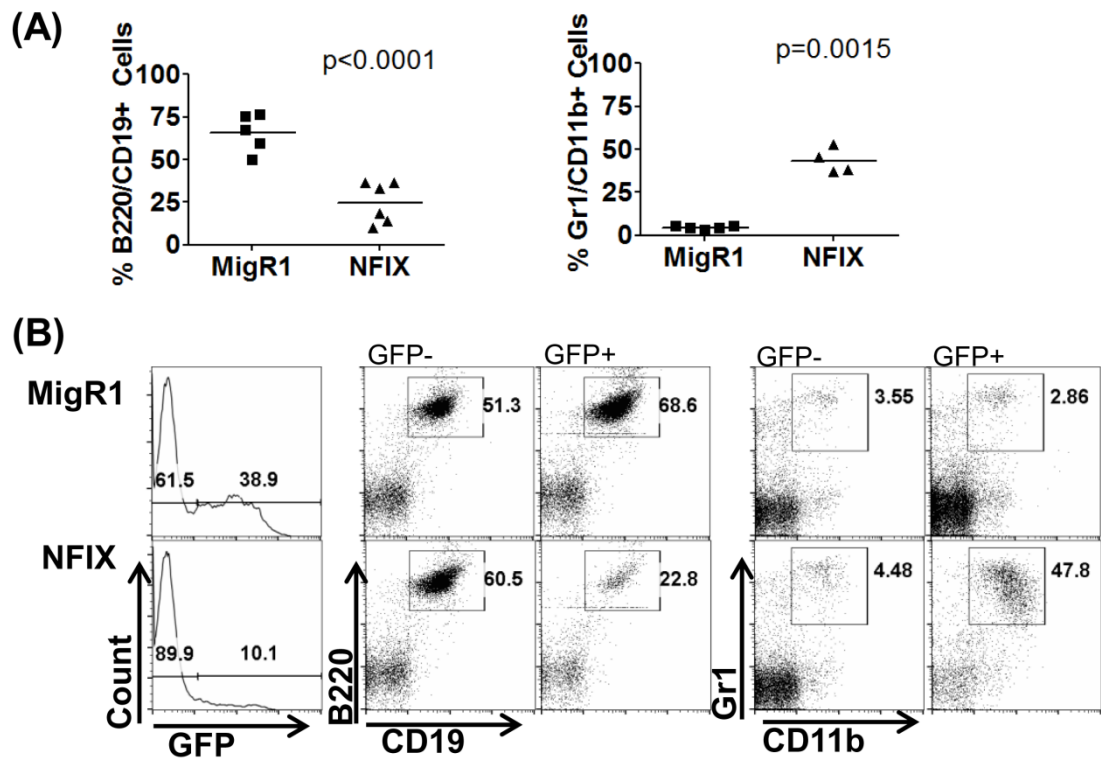


Figure 5. 6 - Disrupted hematopoiesis in the spleen of NFIX mice.

C57BL/6 mice were reconstituted with BM cells transduced with MigR1 or NFIX retrovirus. **(A)** Graphs of percentage GFP<sup>+</sup> B cells (left, MigR1=5, NFIX=6) and GFP<sup>+</sup> myeloid cells (right, MigR1=5, NFIX=4) in the spleen of chimeric mice 10 weeks post BMT. **(B)** Representative flow cytometric analysis in MigR1 and NFIX chimeric animals 10 weeks post BMT showing GFP engraftment (left panel). Results are representative of 2 independent experiments. For statistical analysis an unpaired, two-tailed, students t-test performed.

### 5.3.2 NFIX expression decreases during B cell development

Due to the disruption of the B cell compartment in the NFIX chimeric mice, endogenous levels of *Nfix* during the different stages of B cell development (described in section 1.1.4) were determined. A publically available microarray dataset of mouse B cell lineage populations was analysed through the GEO database (Mansson et al., 2008). In this dataset the CLP (Lin<sup>-</sup>B220<sup>-</sup>CD19<sup>-</sup>CD127<sup>+</sup>Flt3<sup>+</sup>Sca1<sup>low</sup>Kit<sup>low</sup>) is subdivided into hCD25<sup>-</sup> and hCD25<sup>+</sup>. hCD25 is the interleukin-2 receptor (IL-2R)  $\alpha$ -chain, a cell surface marker expressed on activated T cells, B cells and monocytes as well as progenitor populations (Kumar et al., 2008). It also included the pro-B (CD19<sup>+</sup>AA4.1<sup>+</sup>CD43<sup>low</sup>), pre-B (CD19<sup>+</sup>B220<sup>+</sup>CD43<sup>-</sup>IgM<sup>-</sup>) and mature spleen (IgM<sup>+</sup>CD19<sup>+</sup>) B cells. There was a dramatic decrease in *Nfix* expression between the CLP and the pro-B cell stage of differentiation, and *Nfix* expression continued to decrease as the cells matured into splenic B cells (Figure 5. 7A). Next qPCR was performed on sorted B cell progenitor cells from WT C57Bl/6 mice. Pre-pro-B (B220<sup>+</sup>CD43<sup>+</sup>CD19<sup>-</sup>), pro-B (B220<sup>+</sup>CD43<sup>+</sup>CD19<sup>+</sup>), pre-B (B220<sup>+</sup>CD43<sup>-</sup>CD19<sup>+</sup>IgM<sup>-</sup>) and immature B (B220<sup>+</sup>CD43<sup>-</sup>CD19<sup>+</sup>IgM<sup>+</sup>) cells were purified and *Nfix* expression determined. Consistent with the microarray data, *Nfix* expression decreased between the pre-pro-B and pro-B cell stages, and continued to decrease as the cells matured (Figure 5. 7B). Gene expression analysis of some lineage specific transcription factors (*Cebpa*, *Notch1* and *Cd19*) was performed as a control, on both the microarray dataset (Figure 5. 7C top panel) and the sorted murine B cell progenitors (Figure 5. 7C bottom panel), and revealed consistent results.

In order to evaluate this expression pattern in humans, a microarray dataset from human B cell compartments was accessed through the GEO database (Novershtern et al., 2011). *NFIX* expression was analysed in the HSC2 (Lin<sup>-</sup>CD38<sup>-</sup>CD34<sup>+</sup>), early B-cell (CD34<sup>+</sup>CD10<sup>+</sup>CD19<sup>+</sup>) and pro-B cell (CD34<sup>-</sup>CD10<sup>+</sup>CD19<sup>+</sup>) compartments. Consistent with our murine data, there was a decrease in *NFIX* expression from the human HSC2 compartment to the pro-B cells (Figure 5. 8A). To examine the *Nfix* expression pattern of the myeloid BM progenitor populations, HSC (lin<sup>-</sup>Kit<sup>+</sup>Sca1<sup>+</sup>Flt3<sup>-</sup>), LMPP (Lin<sup>-</sup>Kit<sup>+</sup>Sca1<sup>+</sup>Flt3<sup>+</sup>), CMP (Lin<sup>-</sup>Kit<sup>-</sup>CD34<sup>int</sup>CD16/32<sup>int</sup>), GMP (Lin<sup>-</sup>Kit<sup>-</sup>CD34<sup>+</sup>CD16/32<sup>+</sup>) and MEP (Lin<sup>-</sup>Kit<sup>-</sup>CD34<sup>low</sup>CD16/32<sup>low</sup>) populations were sorted and analysed by qPCR. No downregulation of *Nfix* was observed in the myeloid restricted progenitors

(Figure 5. 8B). Having observed the downregulation of *Nfix* during both human and murine B cell differentiation, a more detailed flow cytometric analysis of B cell development was performed in the NFIX chimeric mice. CD43 (leukosialin) was used in conjunction with CD19 and B220 to differentiate between the CLP, pro-B and pre-B stages of B cell differentiation (Figure 5. 9A). Compared with MigR1 controls the NFIX mice displayed a significant reduction in the percentage of pro-B cells (B220<sup>+</sup>CD43<sup>+</sup>) and the more mature populations (Figure 5. 9B and C). Consistent with the stage at which endogenous *Nfix* is downregulated, these data show, that overexpression of NFIX induces a differentiation block during the pre-pro-B to pro-B stage of early B cell development.

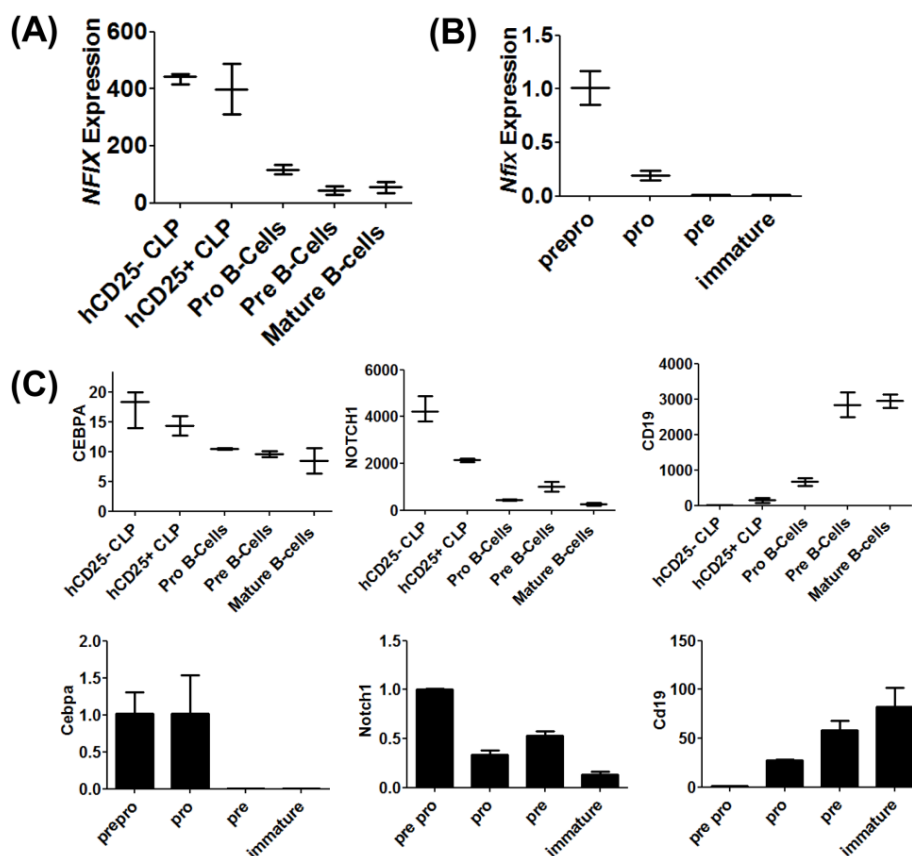


Figure 5.7 - Gene expression in murine B cell progenitor populations.

(A) Analysis of *Nfix* expression during murine B cell differentiation using the B-cell lineage microarray dataset (GSE11110). (B) qRT-PCR analysis of *Nfix* expression in murine B cell populations fractionated by flow cytometry. Data in (A) and (B) are representative of three independent experiments, performed in duplicate and error bars denote  $\pm$ SD. (C top panel) *Cebpa*, *Notch1*, and *Cd19* gene expression in the B-cell progenitor microarray data. Max gene expression data was calculated for each B-cell progenitor population from the B-cell progenitor microarray dataset (GSE11110). Microarray data was collapsed to max probe expression for each gene using the Collapse Dataset suite in GenePattern. Values for each progenitor cell type were then plotted using GraphPad. Error bars represent max and min values for each cell type. (C bottom panel) qPCR analysis of B cell and myeloid cell specific gene expression in sorted murine B cell populations fractionated by flow cytometry. Relative levels of *Cebpa*, *Notch1*, and *Cd19* expression in pre-pro-B, pro-B, pre-B and immature B cell populations. 18S was used as an endogenous control. Each gene/18s ratio in pre-pro-B cell progenitors was normalized to 1. These analyses were performed by Maura Hannon.

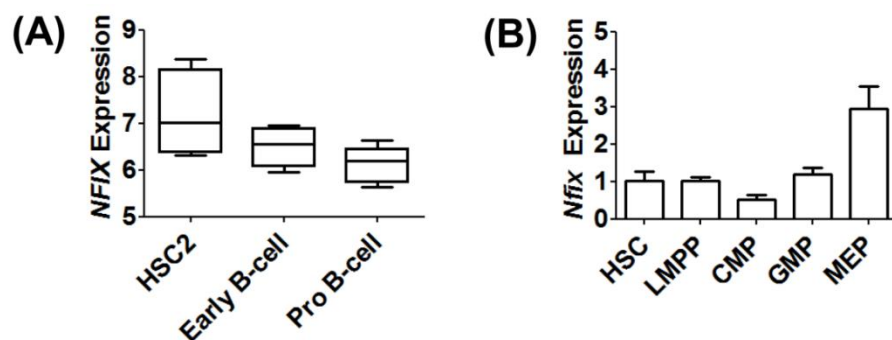


Figure 5. 8 - *NFIX* expression in stem and progenitor populations.

**(A)** Analysis of *NFIX* expression in human B cell development from the human hematopoiesis microarray dataset (GSE24759). Plots represent raw values and error bars represent max and min values- HSC2 n=4, Early B-cell n=4, Pro-B cell n=5. This analysis was performed by Maura Hannon. **(B)** Analysis of *Nfix* expression by qPCR in murine stem and progenitor cells isolated from WT adult BM. Bars represent mean values +/- SD, n=3 for each sample.

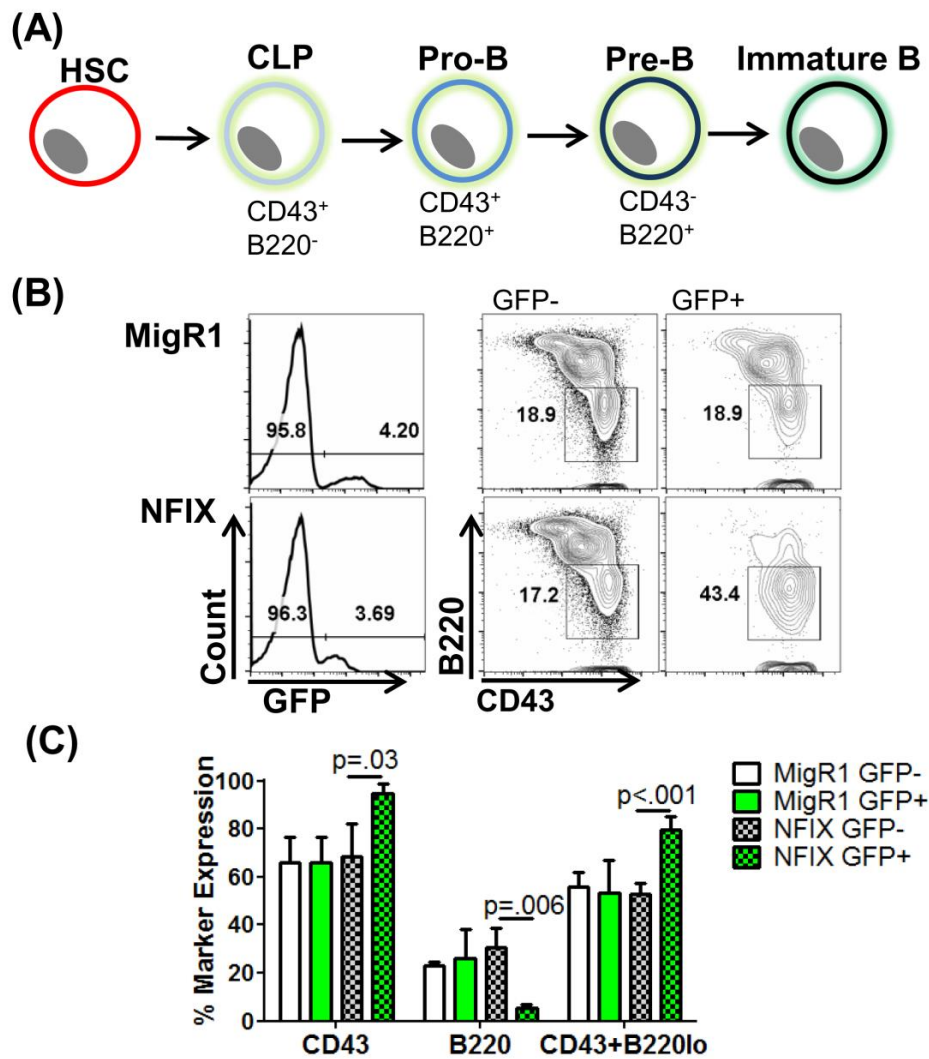


Figure 5. 9 - NFIX overexpression results in a block at the pro-B cell stage of B cell differentiation.

**(A)** Schematic depiction of the use of B220 and CD43 as markers of the stages of B cell differentiation. **(B)** Representative flow cytometric analysis, with gates and percentages showing B220<sup>lo</sup>CD43<sup>+</sup> populations (early B cells) in GFP<sup>-</sup> and GFP<sup>+</sup> populations. **(C)** Graph of percentage expression of CD43<sup>+</sup>, B220<sup>+</sup>, and B220<sup>lo</sup>CD43<sup>+</sup> populations in BM cells from chimeras established with MigR1 or NFIX progenitors 8-10 wks previously, n=3. Error bars denote +/- SD of 2 independent experiments.

### 5.3.3 NFIX expression favours myelopoiesis over B cell lymphopoiesis

*Nfix* expression was downregulated in the B cell lineage and its overexpression *in vivo* led to a block in B cell development before the pro-B cell stage of differentiation, with a concomitant increase in myeloid cell maturation. To further investigate these observed effects, an *in vitro* OP9 co-culture experiment was performed. As described in section 2.2.3.3, co-culture on OP9 stromal cells in the presence of B cell permissive cytokines, IL-7 and FLT3, induces cells to differentiate into mature B220<sup>+</sup>CD19<sup>+</sup> B cells. First, total FLCs were isolated from the FL of E14.5 C57Bl/6 embryos, transduced with MigR1 or NFIX retrovirus and co-cultured with OP9 cells supplemented with 5 ng/ml FLT3 and 1 ng/ml IL-7. After 16 days in co-culture the control MigR1 expressing FLCs had fully differentiated into mature B cells, whereas the NFIX expressing FLCs were not able to differentiate showing little to no expression of B220 or CD19 (Figure 5. 10). In fact NFIX expressing FLCs differentiated into CD11b<sup>+</sup>Gr1<sup>+</sup> myeloid cells despite the presence of B cell supportive cytokines. To determine if NFIX could block B cell development from the HSPC population, FL HSPCs (Lin<sup>-</sup>Sca1<sup>+</sup>cKit<sup>+</sup>Flt3<sup>-</sup>) were sorted and transduced with control MigR1 or NFIX retrovirus. The cells were co-cultured on OP9 cells supplemented with 5 ng/ml FLT3 and 1 ng/ml IL-7. Again the efficient differentiation of the MigR1 expressing FL HSPCs into B220<sup>+</sup>CD19<sup>+</sup> B cells was observed after 12 days in culture. However NFIX overexpression completely abrogated B cell development from the HSPC (Figure 5. 11). To determine what molecular changes were associated with NFIX overexpression gene expression analysis was performed on lineage specific targets in the BM. The upregulation of *ID* genes and E-protein inhibition, have been shown to be involved in promoting myeloid lineage commitment while suppressing lymphoid differentiation as cells leave the LMPP compartment (Cochrane et al., 2009). The BM analysis showed that NFIX expression leads to a small but significant decrease in *E2a*, and a concomitant increase in *Id2* and *Id3* (Figure 5. 12). Changes in the expression of these genes correlates with our *in vivo* and *in vitro* findings that NFIX disrupts B cell differentiation.

In order to rule out a toxic effect of ectopic NFIX expression on B cells, and to show that the observed result was indeed a block in lymphoid commitment, NFIX

was overexpressed in the committed pro-B cell line BA/F3. The NFIX expressing cells were assessed for changes in proliferation and viability. NFIX expression was retained at a steady level in transduced BA/F3 cells over a 5 day period (Figure 5. 13A). These cells also proliferated at a normal rate by trypan blue cell counts (Figure 5. 13B) and using the CTV stain on sorted MigR1 or *Nfix* expressing cells (Figure 5. 13C). The effect of NFIX overexpression on BAF/3 cell viability was then determined by analysing DAPI and annexin-V expression in cells over a 3 day period. There was no difference in cell viability between control MigR1 and NFIX expressing cells (Figure 5. 14A and B). These data demonstrate that NFIX overexpression does not have a toxic effect on B cells and the changes seen *in vivo* and *in vitro* are due to its effects on cell fate decisions.

The myeloid potential of NFIX expressing BM cells was then investigated by plating cells in methylcellulose media (M3434) which supports the growth of E, GM, G, M and GEMM colonies (see section 2.2.3.2). Total BM cells transduced with MigR1 or NFIX retrovirus were plated in M3434 and assessed after 9-11 days. NFIX expression in bulk BM cells had no effect on the number of colonies produced (Figure 5. 15A). However there was an increase in the number of mature colonies (GM, G, M) and decrease in the number of immature colonies (E, GEMM) observed, compared with MigR1 control plates (Figure 5. 15B). This correlated with flow cytometric data which showed higher CD11b and F4/80 expression in the NFIX expressing cells (Figure 5. 15C). To determine if this effect was driven from an uncommitted HSC or a more committed progenitor population, HSCs, CMPs and GMPs were FACS sorted and transduced with MigR1 and NFIX retrovirus, plated in M3434 media and assessed after 12-14 days. NFIX expression had no effect on the number of colonies produced from the HSC. However there was a significant decrease in the numbers of colonies produced from the CMP and GMP cells expressing NFIX, compared to control (Figure 5. 16A). There was also an increase in the CD11b and F4/80 expression in cells from NFIX expressing CMP and GMP derived colonies compared with the control MigR1 cells (Figure 5. 16B). These data indicate that NFIX expression drives myeloid maturation from committed myeloid progenitor cells. To further support this hypothesis NFIX was overexpressed in the 32D myeloblastic cell line and the effect on myeloid cell surface markers was assessed by flow cytometry. As outlined previously in section 2.2.3.1, 32D cells are IL-3 dependent and remain

in an undifferentiated state in its presence. When IL-3 is removed and replaced with G-CSF the cells will differentiate. In the presence of IL-3, a significant increase in the F4/80 expression of NFIX expressing 32D cells was observed, whereas the MigR1 expressing 32D cells remained in an undifferentiated state (Figure 5. 17). This increase was further enhanced when the cells were grown in the presence of G-CSF (Figure 5. 18). Gene expression analysis was then performed on 32D and BA/F3 cells which had been transduced with MigR1 and NFIX, and sorted for GFP expression. Matrix metalloproteinase 9 (*Mmp9*) and *Gcsfr* were significantly upregulated in 32D cells upon ectopic NFIX expression (Figure 5. 19A). MMP9 is involved in neutrophil functions like migration (Bradley et al., 2012), and is secreted by tumour-associated neutrophils to promote angiogenesis. As discussed in 1.1.3.1, G-CSFR is the cell surface receptor for G-CSF which initiates granulocyte proliferation and differentiation, and is expressed in myeloid progenitors, immature and mature granulocytes. A significant increase in the expression of *Cebpa*, essential for granulopoiesis, was also observed in NFIX expressing BA/F3 cells (Figure 5. 19B). These data strongly indicate that NFIX overexpression *in vitro* and *in vivo* promotes myelopoiesis while suppressing B cell lymphopoiesis.

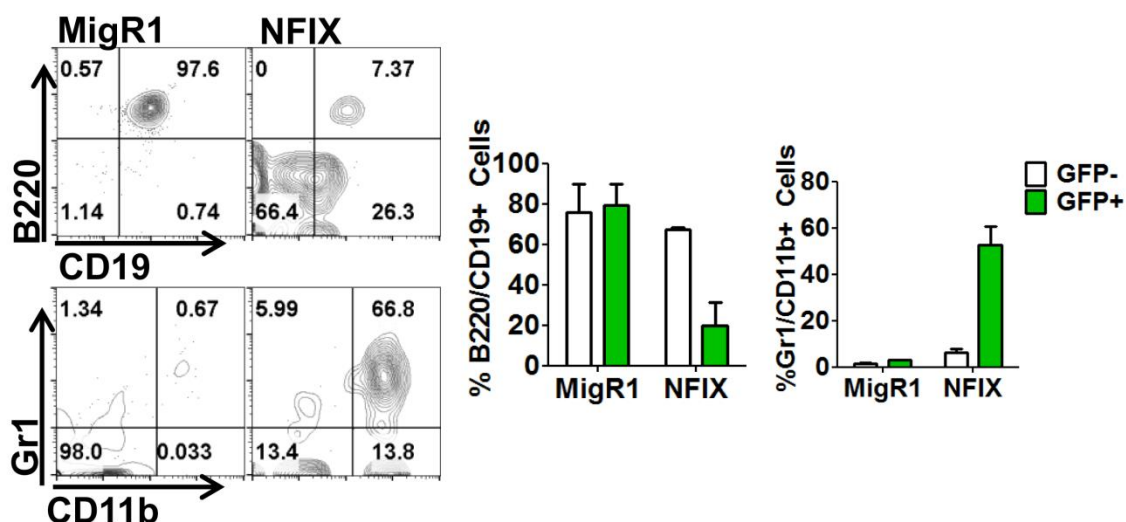


Figure 5.10 - NFIX blocks B cell differentiation *in vitro* in favour of myelopoiesis.

Total FLCs were transduced with MigR1 or NFIX retrovirus, plated on OP9 cells, and analysed by flow cytometry for 16 days. Representative flow cytometry plots of B cells (B220<sup>+</sup>CD19<sup>+</sup>, top panels) and myeloid cells (CD11b<sup>+</sup>Gr1<sup>+</sup>, lower panels). Data is representative of 3 replicates from 2 independent experiments. Graphs show the mean GFP expression in B220<sup>+</sup>CD19<sup>+</sup> cells (left) and CD11b<sup>+</sup>Gr1<sup>+</sup> cells (right). Error bars denote +/- SD of 3 technical replicates.

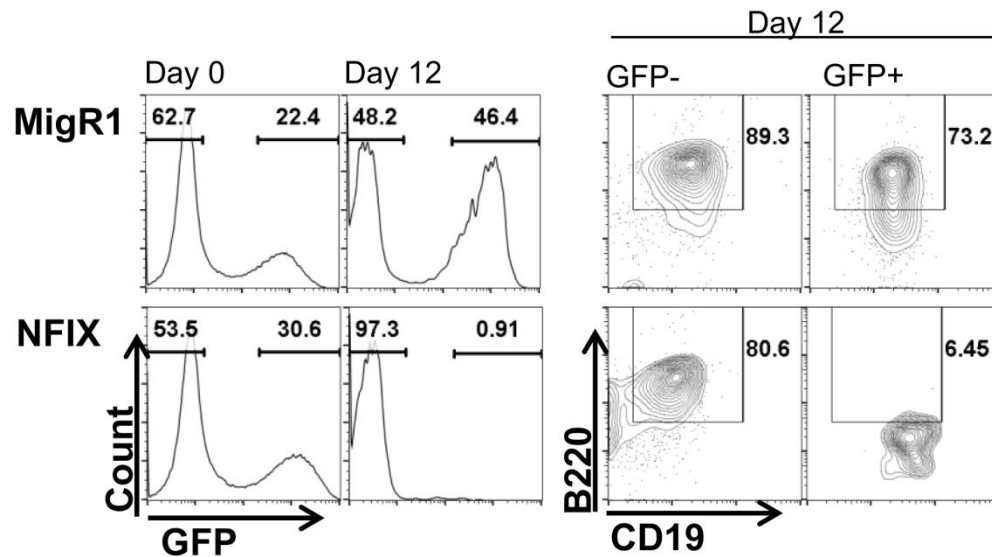


Figure 5. 11 - NFIX blocks B cell differentiation from the HSPC.

E14.5 FL HSPCs ( $\text{Lin}^{-}\text{Sca1}^{+}\text{cKit}^{+}\text{Flt3}^{-}$ ) transduced with control MigR1 or NFIX retrovirus were plated on OP9 cells (day 0) and analysed by flow cytometry on day 12. Representative flow cytometry plots of day 0 and day 12 GFP expression (left histograms), and GFP<sup>-</sup> and GFP<sup>+</sup> B220<sup>+</sup>CD19<sup>+</sup> cells at day 12 (right contour plots) representative of 2 independent experiments.

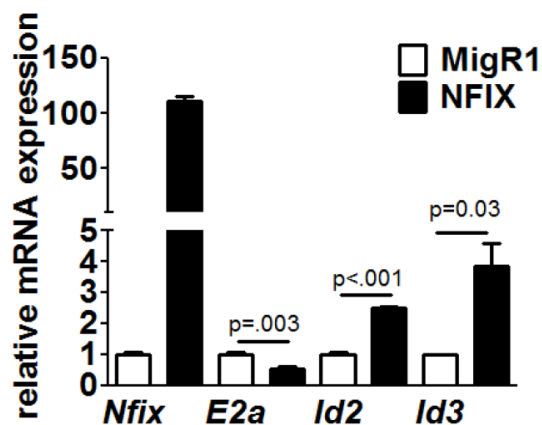


Figure 5. 12 - Gene expression analysis of NFIX expressing BM relative to MigR1 control.

Total BM cells were sorted for MigR1 and NFIX expression 24 hr post transduction and qPCR was performed. Graph represents relative mRNA expression of *Nfix*, *E2a*, *Id2* and *Id3* genes presented relative to control MigR1 cells. Error bars denote +/- SD of 3 technical replicates. Data representative of 2 biological replicates. Analysis of gene expression data was performed by Joana Campos.

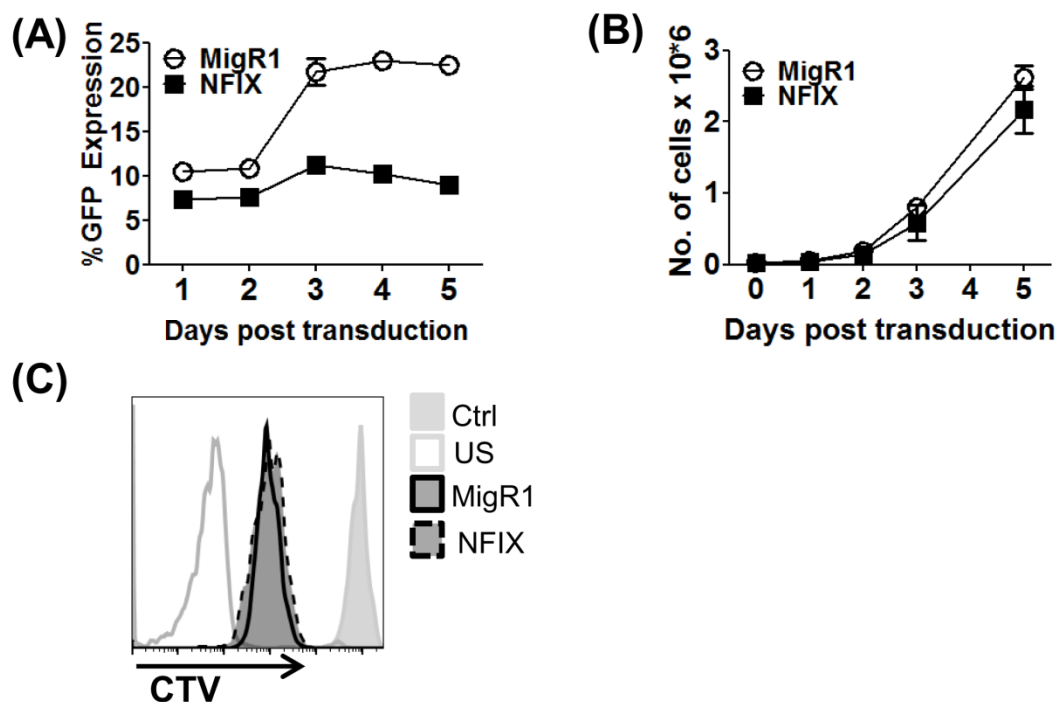


Figure 5. 13 - Ectopic NFIX expression does not affect BA/F3 cell growth.

**(A)** Tracking GFP expression in MigR1 and NFIX expressing BA/F3 cells over 5 days in culture, showing mean of 3 technical replicates  $\pm$  SD. Graph is representative of 2 independent experiments. **(B)** Graph of 5 days of cell growth of GFP<sup>+</sup> sorted BA/F3 cells transduced with either MigR1 or NFIX retrovirus. Each point represents the average number of cells from 2 independent experiments. Error bars denote  $\pm$  SD. **(C)** Tracking BA/F3 cell division after 5 days in culture as shown by dilution of CTV in GFP expressing cells. MigR1 and NFIX overexpressing cells are compared to unstained control and day 0 cells as positive and negative controls respectively. Graph is representative of 2 independent experiments.

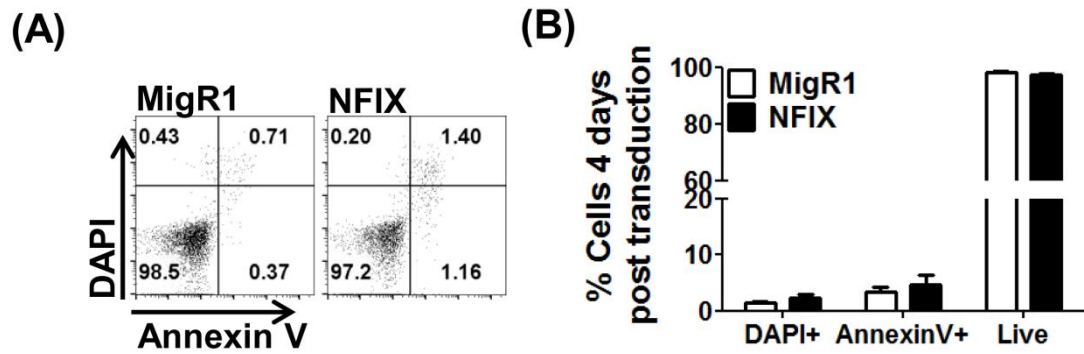


Figure 5. 14 - Ectopic NFIX expression does not affect BA/F3 cell viability.

(A) Representative flow cytometry plot of the expression of apoptotic markers AnnexinV and DAPI in MigR1 or NFIX transduced, GFP sorted BA/F3 cells, 4 days after transduction. (B) Graph of the average percentage of GFP sorted BA/F3 cells expressing DAPI, AnnexinV and live cells (double negative for DAPI and AnnexinV), from 2 independent experiments. Error bars denote +/- SD.

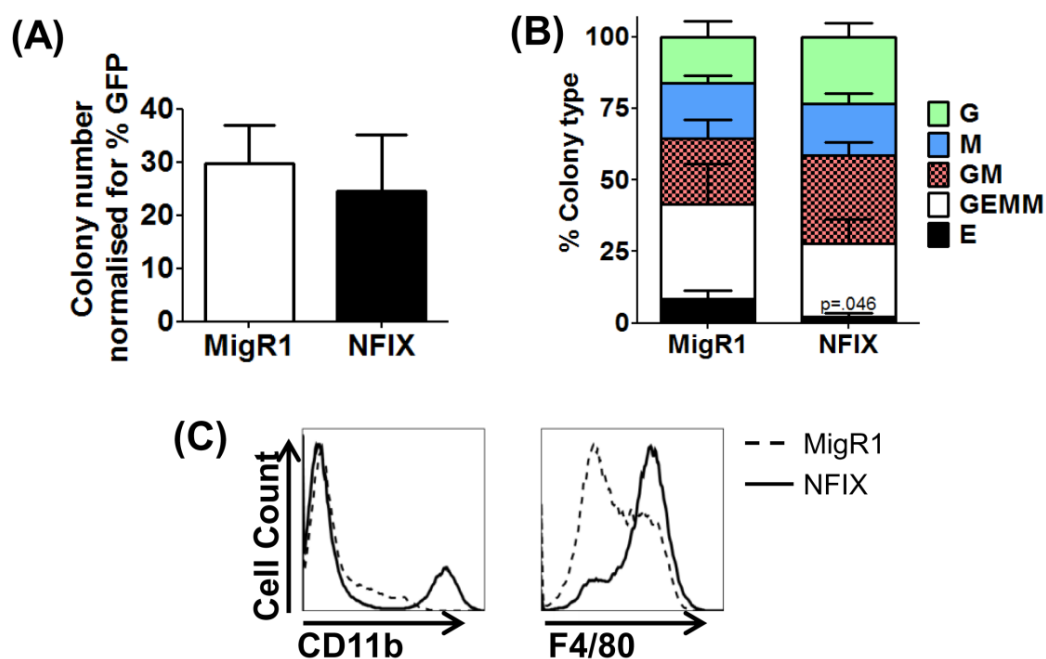


Figure 5. 15 - NFIX enhances myeloid differentiation *in vitro*.

MigR1 and NFIX transduced total BM cells were plated in methylcellulose media (M3434) and colonies counted and scored according to morphological criteria after 9-11 days. Bar charts represent **(A)** the average number of colonies normalised to GFP expression +/- SD and **(B)** the mean percentage of erythroid (E), granulocyte/erythrocyte/monocyte/megakaryocyte (GEMM), granulocyte/monocyte (GM) macrophage (M) and granulocyte (G) colonies, from 3 independent experiments +/- SEM. **(C)** Representative flow cytometric analysis of CD11b and F4/80 expression of cells from colony assay.

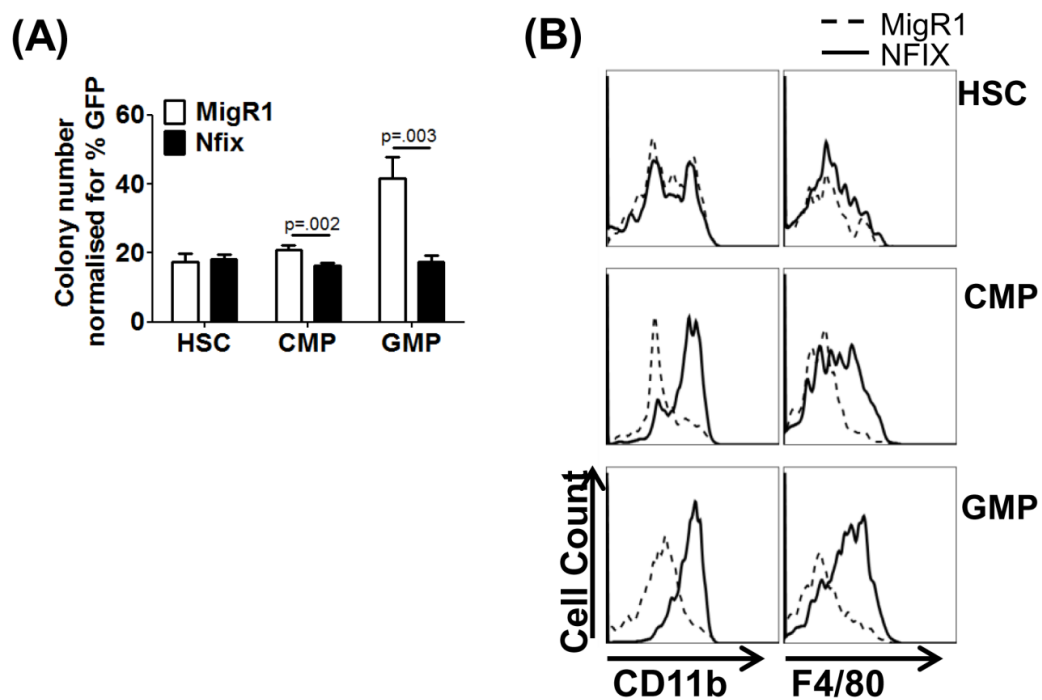


Figure 5. 16 - Differentiation of myeloid progenitor populations by NFIX *in vitro*.

**(A)** Bars represent average number of colonies from HSCs, CMPs and GMPs transduced with control MigR1 or NFIX. Colonies were counted on day 12 and graph represents mean of triplicate plates normalized to GFP expression +/- SD. Data representative of 2 independent experiments. For statistical analysis an unpaired, two-tailed, students t-test performed. **(B)** Representative flow cytometric analysis of cells from colony assay in (A).

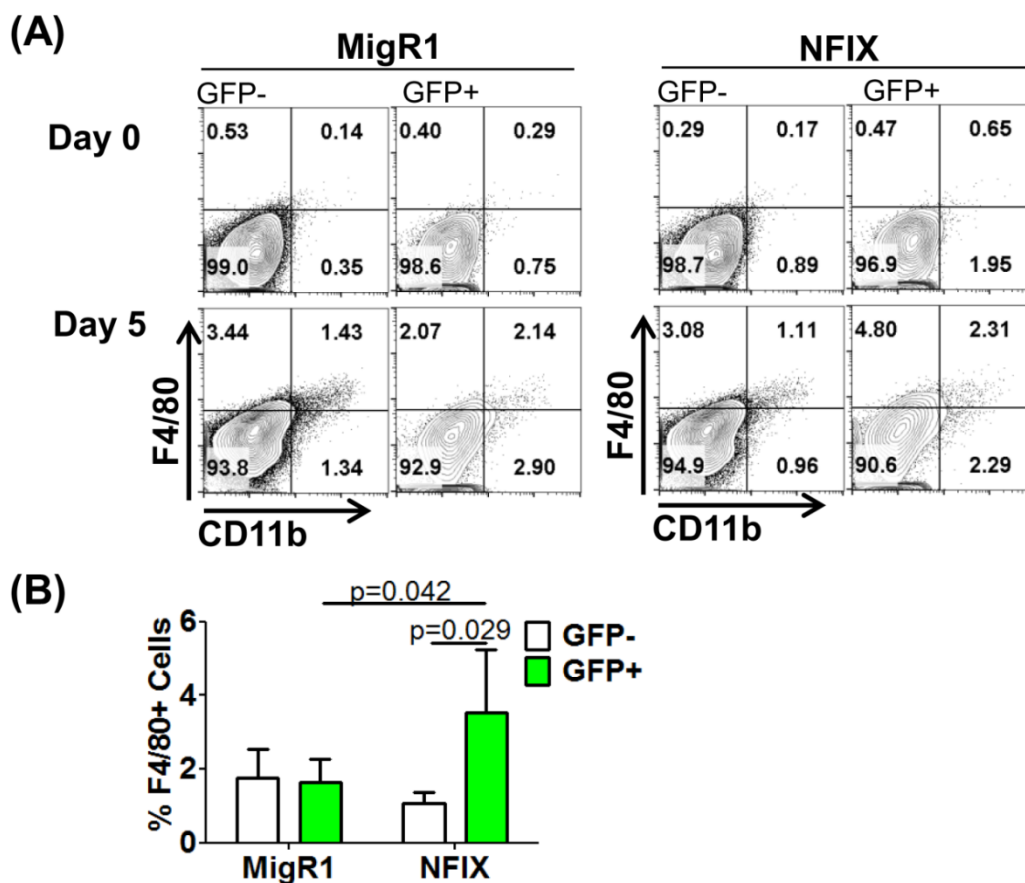


Figure 5. 17 - NFIX promotes differentiation of 32D cells in the presence of IL-3.

32D cells were transduced with MigR1 or NFIX maintained in IL-3 for 5 days, and analysed for CD11b and F4/80 expression by flow cytometry. **(A)** Representative flow cytometric analysis at day 0 and day 5. **(B)** Graph of the mean percentages of F4/80 expression. Mean of 3 independent experiments are shown +/- SD. For statistical analysis an unpaired, two-tailed, students t-test performed.

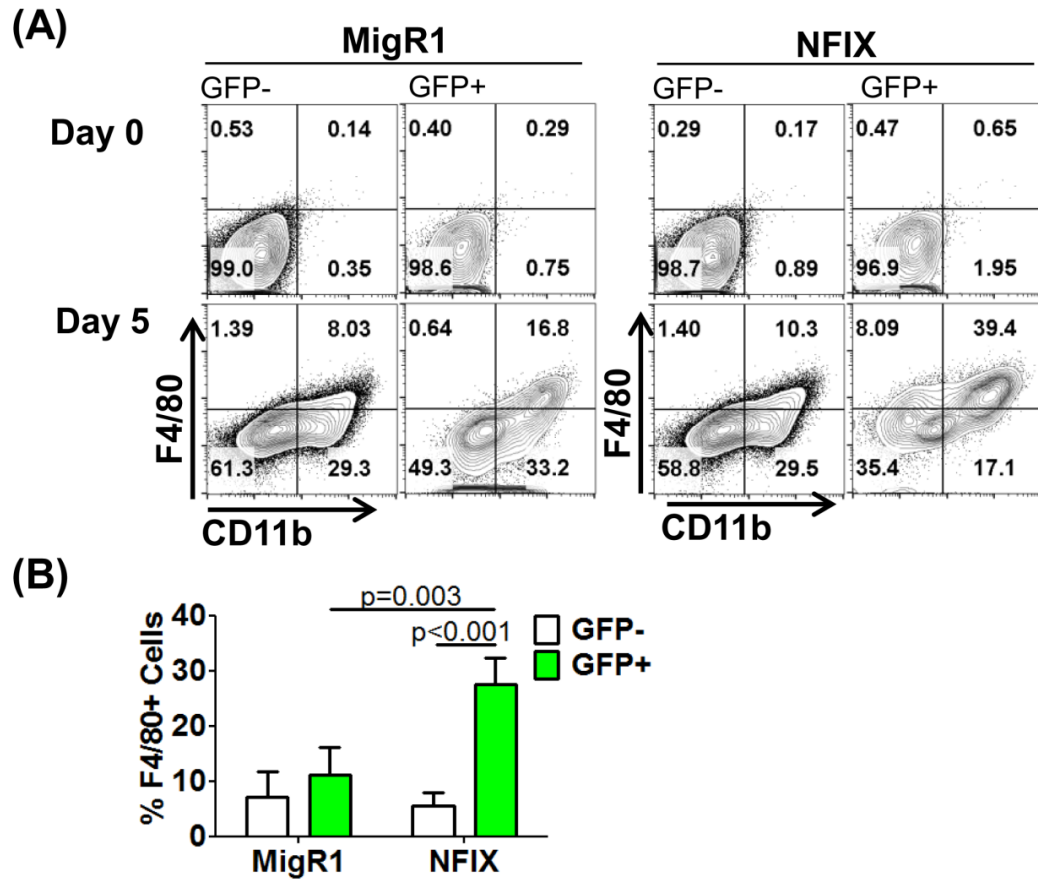


Figure 5. 18 - NFIX enhances 32D cell differentiation in the presence of G-CSF.

32D cells were transduced with MigR1 or NFIX maintained in G-CSF for 5 days, and analysed for CD11b and F4/80 expression by flow cytometry. **(A)** Representative flow cytometric data at day 0 and day 5. **(B)** Graph of the mean percentages of F4/80 expression. Mean of 3 independent experiments are shown +/- SD. For statistical analysis an unpaired, two-tailed, students t-test performed.

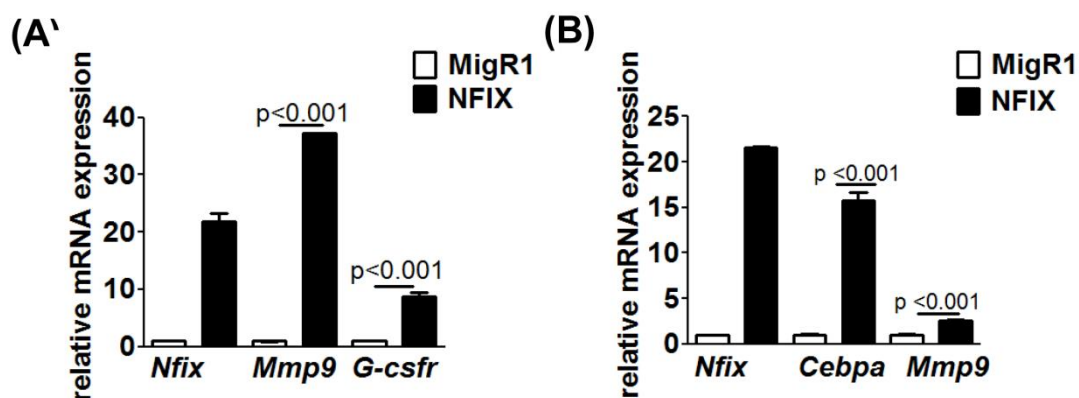


Figure 5. 19 - Gene expression changes in NFIX expressing cells.

(A) 32D cells and (B) Ba/F3 cells were transduced with MigR1 and NFIX, and qRT-PCR was performed. Graphs represent relative mRNA expression of *Nfix*, *Mmp9*, *Gcsfr* and *Cebpa* genes presented relative to control MigR1 cells. Error bars denote +/- SD of 3 technical replicates. Data representative of 2 biological replicates. For statistical analysis an unpaired, two-tailed, students t-test performed.

### 5.3.4 Loss of *Nfix* expression promotes B lymphopoiesis while impairing myelopoiesis

To investigate the physiological relevance of *Nfix* in hematopoiesis and lineage determination, the *Nfix*<sup>-/-</sup> mouse was studied. However, the loss of *Nfix* in mice leads to postnatal lethality at approximately 22 days after birth. The mice suffer from dramatic defects in the brain including brain hydrocephalus and complete or partial absence of the corpus callosum (Driller et al., 2007). As such *Nfix*<sup>-/-</sup> E14.5 FLCs were first analysed. Previous data suggested that *Nfix* expression is low in HSPCs isolated at the early embryonic stages (<E13.5) and is upregulated as HSPCs mature, with highest expression in the HSPCs of the adult BM (Holmfeldt et al., 2013). This data was corroborated using 2 publically available datasets downloaded from the Gene Expression Commons database (Seita et al., 2012), which both included 2 adult populations. The first data set comprised E14.5 FL HSCs, and HSCs from young (3 month old) and old (25 month old) mice. *Nfix* expression was very low at the fetal stage, but was highly expressed in the adult HSCs (Figure 5. 20A). The second model contains samples of HSPCs isolated from the yolk sac at D9, the AGM at D11.5, the FL at E12.5, E13.5 and E14.5, as well as from young mice at 6-8 weeks of age. A similar pattern to that reported by Holmfeldt et al was observed, with low *Nfix* expression in HSPCs during the embryonic stage of development and high expression in the adult mouse (Figure 5. 20B). Total FLCs were then isolated and analysed by flow cytometry for cells of the myeloid, B and T lineages. No significant differences between the expression of myeloid (CD11b, Gr1), B (B220, CD19) and T (CD4, CD8) cell surface markers were observed (Figure 5. 21). Cells isolated from WT and *Nfix*<sup>-/-</sup> FLCs were next plated in methylcellulose (M3434) to determine if loss of *Nfix* affected the ability of the FLCs to differentiate into myeloid cells *in vitro*. There was no difference in the number of colonies formed by the *Nfix*<sup>-/-</sup> cells compared to the WT (Figure 5. 22A). There was also no change in the type of colonies formed (Figure 5. 22B and C). Taken together these data suggest that loss of *Nfix* at this stage of embryonic development does not perturb lineage specification.

BM was then isolated from P10 WT and *Nfix*<sup>-/-</sup> mice. Analysis of markers of myeloid (CD11b, Gr1), B (B220, CD19) and T (CD4, CD8) cells was performed, however there was no significant difference in the distribution of these

differentiation markers in the *Nfix*<sup>-/-</sup> mice compared with WT controls (Figure 5. 23). To evaluate whether loss of *Nfix* in the neonatal mouse would affect myeloid differentiation from progenitor cells, BM cells isolated from WT and *Nfix*<sup>-/-</sup> P10 mice were plated in a methylcellulose assay (M3434). Colonies were counted and scored after 11 days, and cells were analysed for surface marker expression. Unlike colonies derived from the *Nfix*<sup>-/-</sup> FLCs, *Nfix* deficient BM cells yielded significantly fewer colonies than their WT counterparts (Figure 5. 24A). There was no significant difference to the type of colony produced (Figure 5. 24B). However cells derived from *Nfix*<sup>-/-</sup> BM expressed significantly lower percentages of mature myeloid markers Gr1 and F4/80 (Figure 5. 24C and D). The lymphoid potential of neonatal *Nfix*<sup>-/-</sup> BM was determined by co-culturing BM cells with OP9 cells in the presence of 5ng/ml FLT3 and 1ng/ml IL-7. An increase in B220<sup>+</sup> cells was observed after 4 and 6 days in culture compared with WT littermate control cells (Figure 5. 25). qPCR was performed on BM cells isolated from WT and *Nfix*<sup>-/-</sup> P10 mice and gene expression analysis showed that *Nfix* deficient BM cells have a marked disruption to the expression of key transcription factors associated with lineage specification (Figure 5. 26). The *Nfix*<sup>-/-</sup> BM cells revealed a decrease in expression of the *Id* genes, and *Mmp9*, the inverse of our overexpression data, as well as an upregulation of *Cd19* and *Pu.1* further supporting a role of *Nfix* in lymphoid cell fate.

These loss of function experiments, show that loss of *Nfix* in the neonatal BM leads to altered hematopoiesis by enhancing B cell development while disrupting myeloid differentiation, and that this effect is mediated by changes in key transcription factors associated with lineage specification.

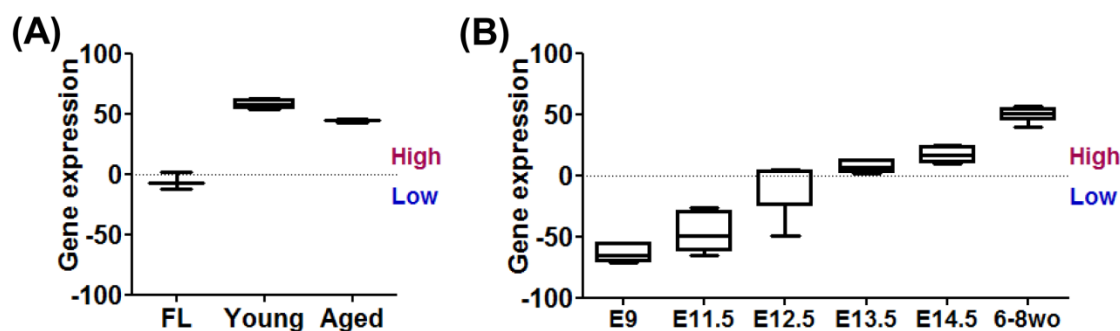


Figure 5. 20 - *Nfix* expression in fetal and adult HSC and HSPC.

(A) Analysis of *Nfix* expression in FL (n=3), young (3 months) (n=4) and old (25 months) (n=3) HSCs using a dataset (GSE ID:55525) (Seita et al., 2012) accessible from <https://gexc.stanford.edu/models/920/genes>. Error bars represent max and min *Nfix* expression values. (B) Analysis of *Nfix* expression in HSPCs derived from the yolk sac (E9)(n=6), AGM (E11.5)(n=6), FLCs (E12.5, E13.5, E14.5) (n=6) and 6-8 week old mice (n=5) using a dataset (GSE ID:34723) (Seita et al, 2012) accessible from <https://gexc.stanford.edu/models/920/genes>. Error bars represent max and min *Nfix* expression values. Values in (A) and (B) represent absolute profiling of gene expression. The dynamic-range (-100 to 100) and threshold for high/low expression (represented by grey line) for each probeset were obtained by mapping sample data against the Common Reference, generated from 11939 Affymetrix mouse 430 2.0 microarray data and 25229 Affymetrix human U133 Plus 2.0 microarray data, and Probeset Meta Profile.

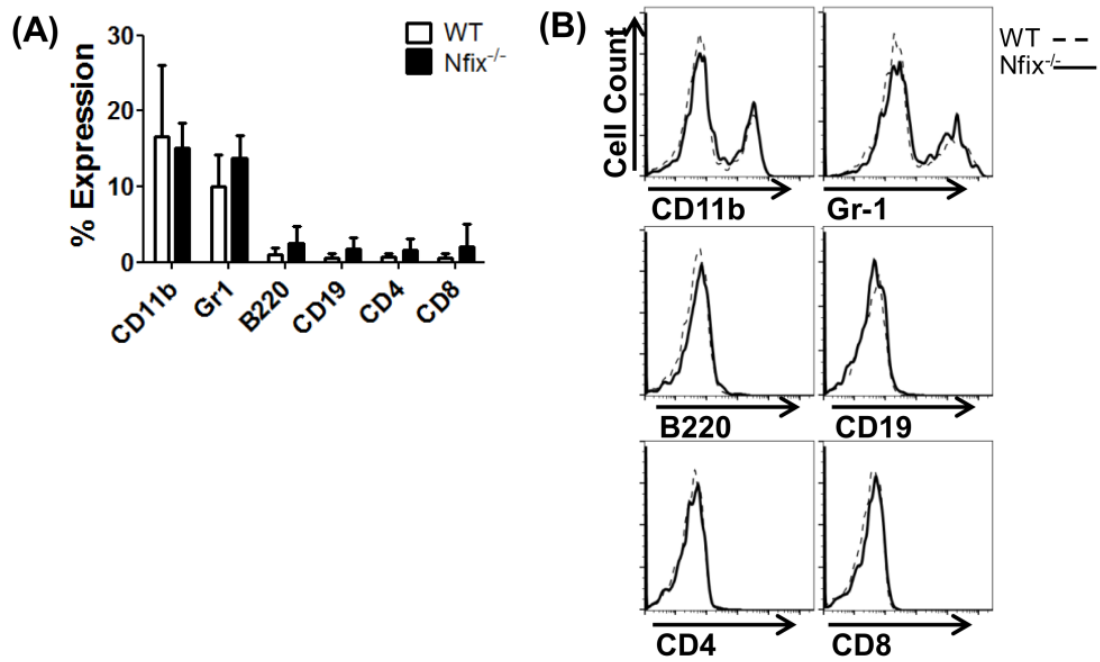


Figure 5. 21 - *Nfix*<sup>-/-</sup> FLCs do not display abnormal hematopoiesis.

FLCs were isolated from E14.5 WT and *Nfix*<sup>-/-</sup> embryos and analysed by flow cytometry. **(A)** Graph depicts mean percentage expression of cell surface markers +/- SD. Data is representative of n=6 WT samples, and n=6 KO samples from 3 independent litters. **(B)** Representative flow cytometry histograms of cell surface marker expression.

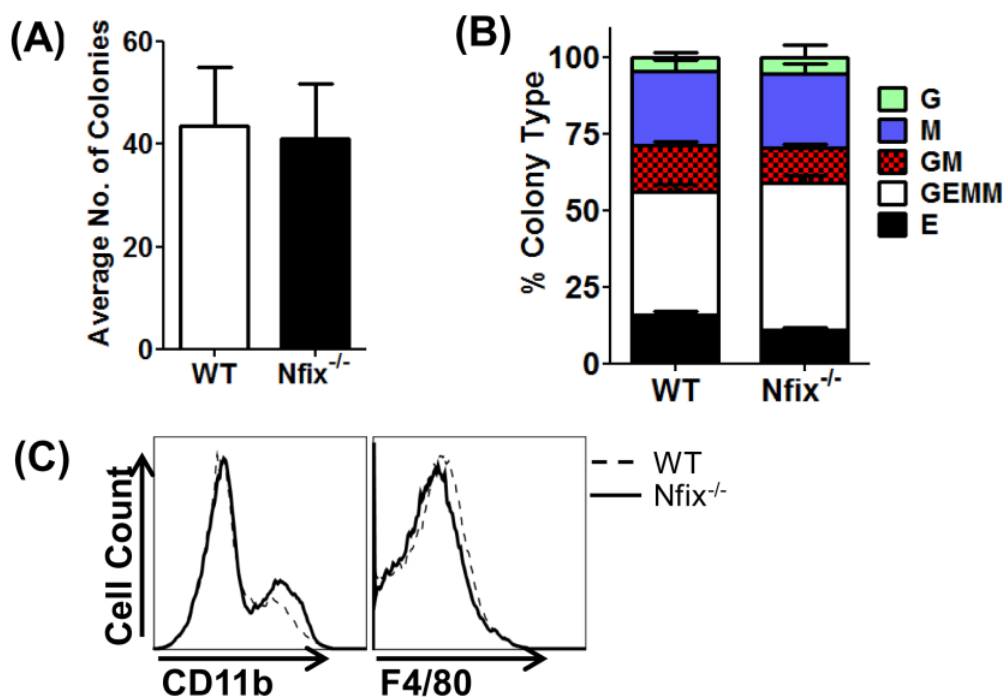


Figure 5. 22 - Loss of *Nfix* in the FLC does not affect myeloid differentiation *in vitro*.

WT and *Nfix*<sup>-/-</sup> FLCs were plated in methylcellulose media (M3434) and colonies counted and scored after 8 days according to morphological criteria. Bar charts represent (A) the average number of colonies normalised to GFP expression +/- SD and (B) The mean percentage of erythroid (E), granulocyte/erythrocyte/monocyte/megakaryocyte (GEMM), granulocyte/monocyte (GM) macrophage (M) and granulocyte (G) colonies are shown from 2 independent experiments +/- SEM. Data is representative of n=3 WT and n=4 KO samples. (C) Representative flow cytometric analysis of total cells from colony assay. This data is representative of n=2 WT and n=1 KO sample from 1 experiment.

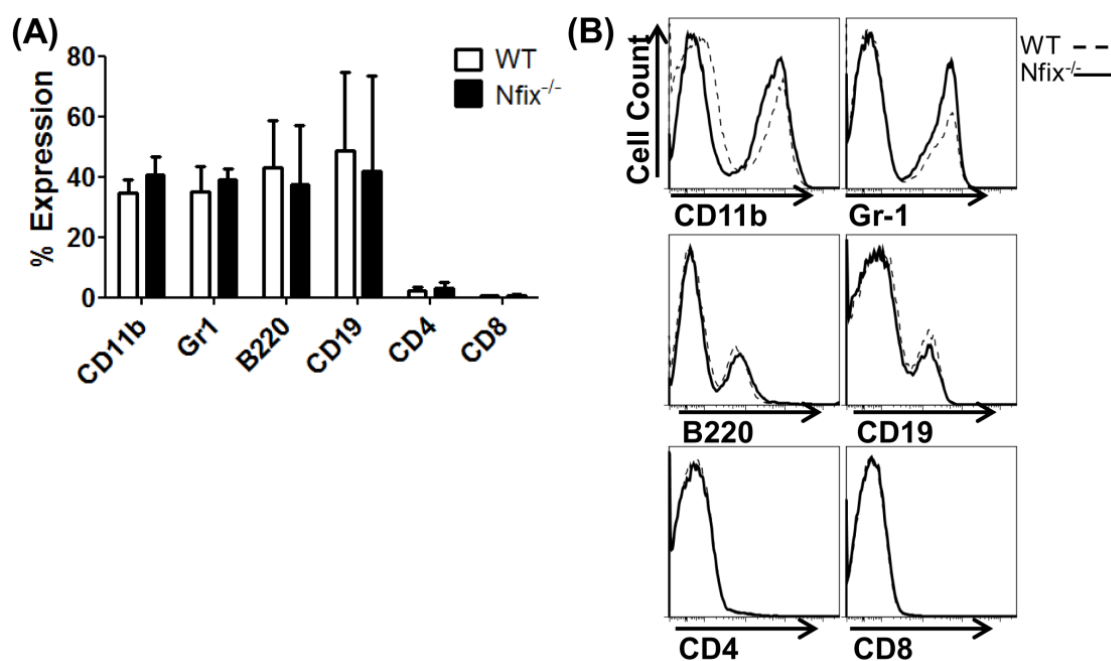


Figure 5.23 - *Nfix*<sup>-/-</sup> neonatal (P10) BM does not display abnormal hematopoiesis.

BM cells were isolated from P10 WT and *Nfix*<sup>-/-</sup> mice and analysed by flow cytometry. **(A)** Graph depicts mean percentage expression of cell surface markers +/- SD. Data is representative of n=5 WT samples, and n=5 KO samples from 2 independent litters. **(B)** Representative flow cytometry histograms of cell surface marker expression.

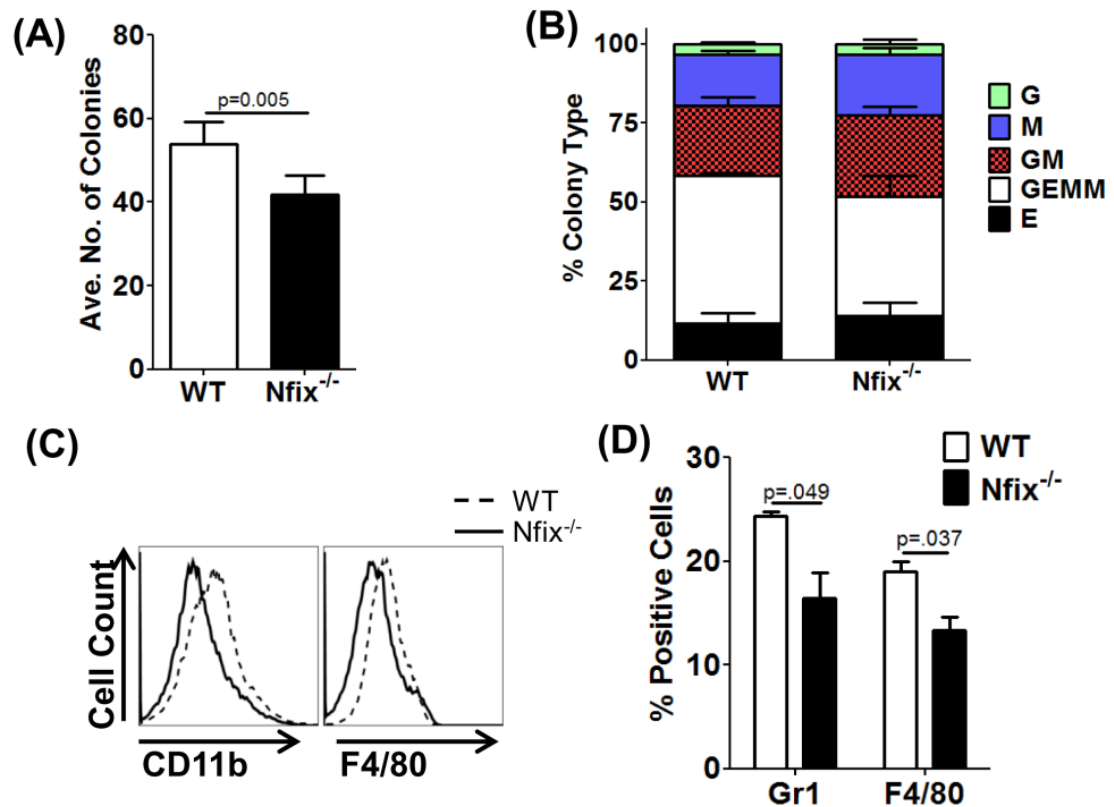


Figure 5. 24 Loss of *Nfix* disrupts myeloid differentiation *in vitro*

Total BM from WT or *Nfix* deficient mice was plated in methylcellulose (M3434). Colonies were counted and morphology assessed after 11 days. Bar chart represents (A) the mean number of colonies from 2 independent experiments +/- SD and (B) the mean percentage of erythroid (E), granulocyte/erythrocyte/monocyte/megakaryocyte (GEMM), granulocyte/monocyte (GM), macrophage (M) and granulocyte (G) colonies from 2 independent experiments +/- SEM. (C) Representative flow cytometric analysis of cells from colony assay. (D) Bar chart shows the mean percentages of Gr1<sup>+</sup> and F4/80<sup>+</sup> cells from 2 independent experiments +/- SD.

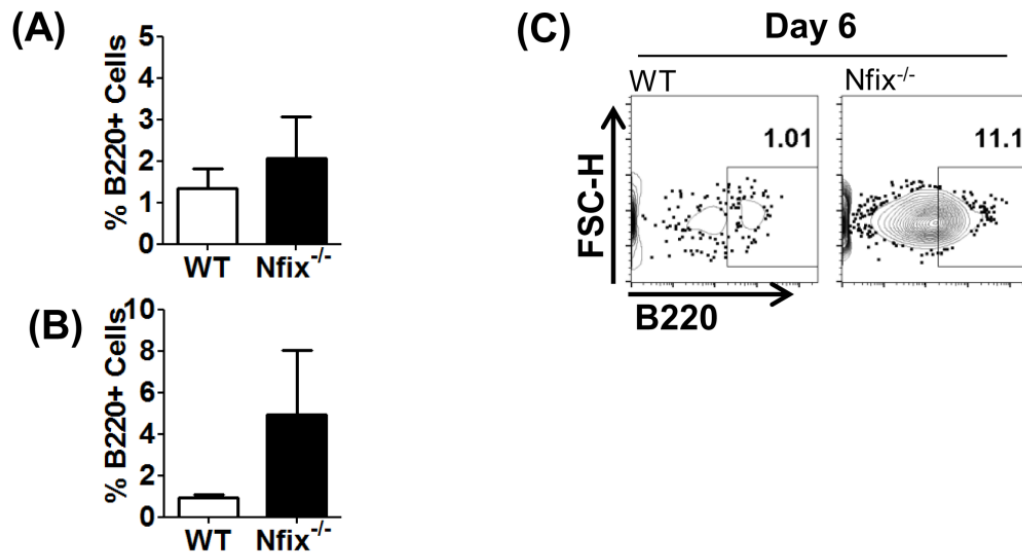


Figure 5. 25- Loss of *Nfix* enhances B cell differentiation in neonatal BM *in vitro*

Total BM from WT or *Nfix* deficient P10 mice was plated onto OP9 cells in the presence of 5ng/ml FLT3 and 1ng/ml IL-7, and analysed by flow cytometry on day 4 (A) and day 6 (B). Bar chart shows the mean percentages of B220<sup>+</sup> cells from 3 independent experiments +/- SD. (C) Representative flow cytometric analysis of cells expressing B220 at day 6.

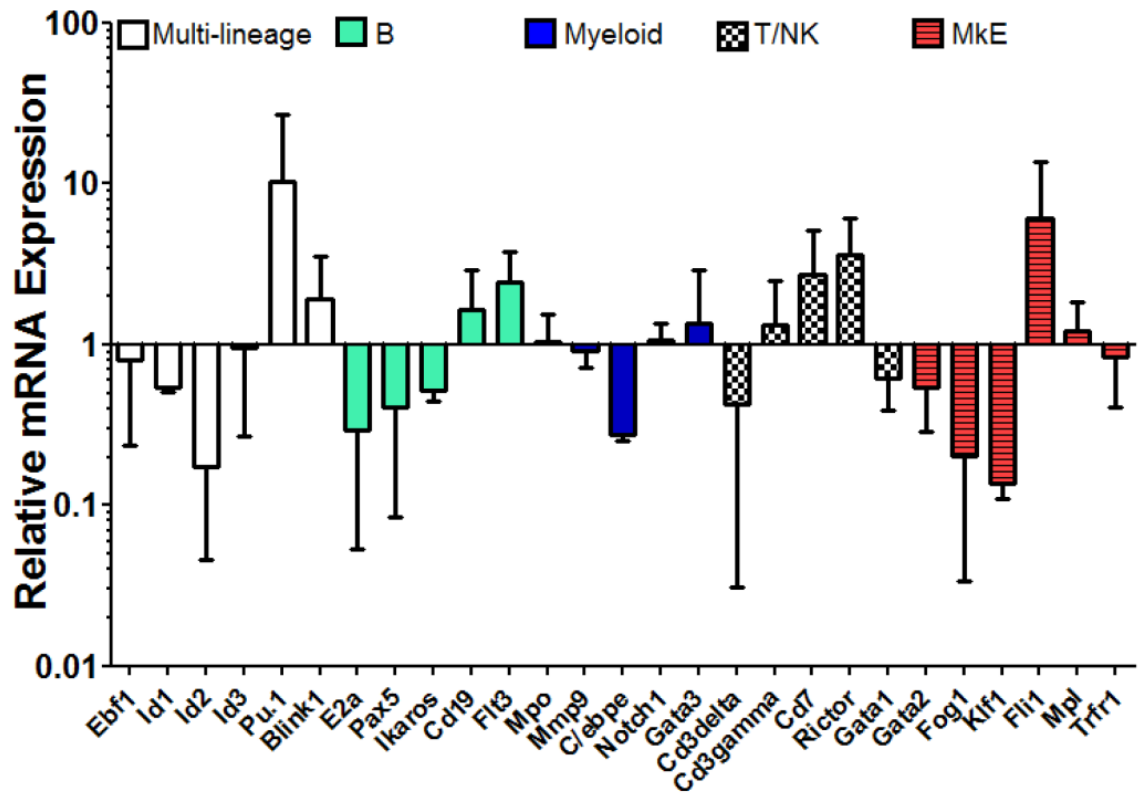


Figure 5. 26 - Gene expression analysis of WT and *Nfix*<sup>-/-</sup> BM.

Total BM was isolated from P10 WT or *Nfix* deficient mice and qPCR performed. Graphical presentation of relative mRNA expression of indicated genes assessed using high-throughput qPCR on the 48.48 Dynamic Array IFC system (Fluidigm™). Bars represent the average of 3 biological *Nfix*<sup>-/-</sup> replicates normalized to WT control, and error bars denote +/- SD.

## 5.4 Discussion

*Nfix* expression is downregulated as progenitor cells progress through B cell differentiation. NFIX overexpression prevents B cell differentiation in favour of myelopoiesis *in vivo* and *in vitro* causing a block at the pre-pro-B to pro-B cell stage of development, while loss of *Nfix* enhances B cell differentiation. These changes are coupled with alterations in the expression of key genes involved in lineage determination.

The data show that ectopic expression of NFIX drastically impairs B cell development in the murine hematopoietic system. While some B220<sup>+</sup>CD19<sup>+</sup> B cells persisted in the spleen, they were virtually absent from the BM compartment, and peripheral circulation. Gene expression analysis of both murine and human datasets revealed that *Nfix* mRNA expression was higher in the early B cell progenitor populations and its expression was downregulated as the cells commit and mature to the B cell lineage. In accordance with *Nfix* downregulation at this stage, an accumulation of B220<sup>lo</sup>CD43<sup>+</sup> early B cells was observed in the BM of NFIX chimeric mice. These data suggest that continued expression of NFIX impairs early-late B cell differentiation. Furthermore, *in vitro* experiments utilising the OP9 co-culture system, demonstrated that enforced NFIX expression in the HSPC compartment led to an almost complete absence of NFIX expressing cells at the end of the culture period. Those cells that did persist in culture expressed low levels of B220 and did not yet express CD19, consistent with the block at an early stage of development seen *in vivo*. When NFIX was overexpressed in total FLCs, containing a mixed pool of stem and progenitor populations, NFIX expressing cells were observed after 16 days in culture. However these cells were of myeloid origin. The culture system only contained cytokines for efficient B cell production and no cytokines to support myeloid differentiation. Together these data strongly suggest that NFIX has a functional role in lineage fate. To further ensure NFIX was blocking B cell development rather than having a toxic effect on B cells, it was overexpressed on a more mature lineage-committed B cell, the pro-B BA/F3 cell line. NFIX overexpression did not affect cell viability or cell growth after culture.

These findings are contrary to the observations made by Holmfeldt et al (2013). In their study they performed 2 competitive BM transplants - one with *Nfix*

knocked down in HSPCs using 2 shRNAs against *Nfix*, and the other utilising conditional *Nfix*<sup>fl/fl</sup> cells. In both transplants the authors reported no statistically significant difference in the distribution of myeloid, B and T cells in cells lacking *Nfix* compared with their respective control groups. However, there is a clear trend towards a higher proportion of B cells in their experiments using the *Nfix*<sup>fl/fl</sup> cells, and with one of the two *Nfix*-shRNAs (Figure 4D and H, Holmfeldt et al, 2013). Furthermore, despite using 2 markers to identify mature myeloid (CD11b/Gr1) and T (CD4/CD8) cells, the authors only use B220 as a marker for cells of the B lineage. B220 has been shown to be expressed in activated CD4+ T cells (Renno et al., 1998), a subset of NK cells (Rolink et al., 1996) and a subpopulation of dendritic cells (Nikolic et al., 2002), therefore without the use of another co-expressed B cell marker, such as CD19, these results are inconclusive.

The development of mature B cells from hematopoietic progenitors is regulated by the sequential expression of the transcription factors *E2A*, *EBF*, and *PAX5* (Cochrane et al., 2009). The earliest B cell progenitors express B220, together with CD43 (Mansson et al., 2007) and an accumulation of CD43+ B220<sup>lo</sup> cells was observed in our NFIX chimeric mice. It has been documented that the downregulation of both *Id2* and *Id3* is an essential event in B-lineage specification although the loss of either factor was not sufficient to promote B cell development (Benezra et al., 1990). Significant changes in *Id2* and *Id3* levels were observed in *Nfix*-deficient cells. This perturbation in the levels of *Id* gene expression would be consistent with promoting B cell differentiation. Our findings associate well with gene expression changes previously observed in LSKs lacking *Nfix* (Holmfeldt et al., 2013). LSKs isolated by FACS were transduced with control lentivirus or shRNA targeting *Nfix* and cultured for 7 days, then assessed for global transcriptional changes. Several B cell related genes were significantly upregulated in the LSKs with loss of *Nfix*. These included a 4 fold increase (p=.003) in Kruppel-like Factor 4 (*Klf4*), a transcription factor whose expression increases during B cell differentiation peaking in the mature B cell, and has also been shown to play an important role in B cell activation and proliferation (Klaewsongkram et al., 2007). A 3 fold increase (p=.003) was found in the expression of IL-7 receptor (*Il7r*). *Il7r* expression is required for the early stages of B cell development in mice (Namen et al., 1988). It is expressed

through B cell differentiation, and down-regulated in the mature B cell (Wei et al., 2000). *Stat1* showed a 2-fold ( $p=.02$ ) upregulation with loss of *Nfix* in the LSK, and is known play an essential role in B cell survival and proliferation (Lee et al., 2000). These transcriptional changes in B cell specific genes with loss of *Nfix* expression, supports the hypothesis that it plays a role in hematopoietic lineage determination.

In addition to a block in B cell development, NFIX overexpression caused an increase in the percentage of CD11b<sup>+</sup>Gr1<sup>+</sup> cells in the BM, spleen and PB of NFIX chimeric mice. Enforced NFIX expression on whole BM promoted myeloid differentiation in an *in vitro* colony forming assay, with an increase in expression of mature myeloid cell surface markers seen on cells from NFIX expressing colonies. From the HSC, NFIX expression did not drive myelopoiesis *in vitro*. However from CMP and GMP committed myeloid progenitors, NFIX overexpression enhanced myeloid differentiation. NFIX overexpression also induced myeloid differentiation in the 32D myeloblast cell line in the presence of IL-3, and significantly enhanced differentiation in the presence of G-CSF. As previously discussed in section 1.1.3.3.1, C/EBP $\alpha$  is a myeloid transcription factor essential for granulopoiesis (Zhang et al., 1997), highly expressed in GMPs where it is switched off and another family member, C/EBP $\epsilon$  is turned on to drive these committed progenitors to fully differentiate (Lekstrom-Himes, 2001). It has previously been shown that C/EBP $\alpha$  loss-of-function mutations decrease myeloid priming of HSCs while impairing myeloid-lineage commitment (Kueh et al., 2013). The down regulation of *Cebpa* that was observed in the BM of the *Nfix* deficient mice and the increase of *Cebpa* with NFIX overexpression in BAF/3 cells is consistent with dysregulation of myelopoiesis. It was also shown that ectopic expression of C/EBP $\alpha$  and ID1 can restore neutrophil development in myelodysplasia (Geest et al., 2009). The fact that *Nfix* deficient BM has both of these transcriptional regulators downregulated, underpins a functional role for NFIX in hematopoiesis.

In 32D cells overexpressing NFIX, a significant increase in *Gcsfr* expression was observed. The previously mentioned knockdown experiments performed by Holmfeldt et al on LSK cells, also revealed down-regulation of this myeloid specific gene with loss of *Nfix* (Holmfeldt et al., 2013). There was a 2-fold decrease ( $p=.02$ ) in *Csf3r* expression in LSKs lacking *Nfix*. The *Csf3r* gene

encodes the cell surface receptor for G-CSF, which initiates proliferation and maturation of BM granulocytes (Thomas et al., 2002). Furthermore, increased expression of *Pu1* was observed in the BM of *Nfix* deficient mice. PU.1 is a transcription factor with a well-documented role controlling myeloid and early B cell development, and PU.1 expression levels are important in the determination of lineage fate with high PU.1 levels in the MPP/LMPP favouring myelopoiesis and low levels favouring B cell lymphopoiesis (DeKoter and Singh, 2000). PU.1 expression increases with B cell maturation and its expression becomes dispensable once the progenitors are committed to the lymphoid lineage (Iwasaki et al., 2005). The modulation of *Pu1* seen in *Nfix*-deficient cells is consistent with the role of PU.1 in myeloid versus B lineage cell fate. Collectively these findings demonstrate that in stem and progenitor cells, NFIX expression can influence the cell fate decisions between myeloid and lymphoid lineages, possibly by direct modulation of downstream transcriptional targets.

While there is little in the literature describing the role of NFIX in hematopoietic differentiation, there are studies which support a role for NFIX in stem and progenitor cell differentiation in other tissues. *NFIX* is highly expressed in embryonic muscle progenitor cells (myoblasts), where it has been shown to activate a transcriptional program responsible for the embryonic to fetal myoblast transition. *NFIX* is then dramatically down-regulated in fetal myoblast cells. In this context *NFIX* behaves as a transcriptional activator by activating expression of the fetal-specific gene *Mck*, but also as a repressor by suppressing NFATc4 - a transcriptional activator of embryonic proteins (Calabria et al., 2009). Furthermore, in the human brain, the expression of the NFIX3 splice variant is dramatically upregulated during the differentiation of neural progenitors to astrocytes, and it has been shown to activate the *GFAP* promoter which induces glial differentiation from astrocytes (Singh et al., 2011). NFIX is also involved in neural progenitor cell differentiation by repressing the stem cell maintenance gene *Sox9* during the development of the hippocampus (Heng et al., 2014). Thus there is evidence from over tissues supporting the modulation of genes involved in stem and progenitor cell fate by NFIX.

Unlike the P10 BM, in the E14.5 fetal *Nfix*<sup>-/-</sup> liver, there was no apparent lineage effect from loss of *Nfix*. This may be due in part to the differential expression of *Nfix* in the HSPCs of the developing embryo and adult mouse, suggesting that the

role of *Nfix* in lineage determination may occur when it is more highly expressed in the adult mouse during steady state hematopoiesis. Other NFI family members may also be compensating for the loss of *Nfix*. The *NFIX* gene is not redundant in the CNS i.e. *Nfix* KO alone leads to lethality from brain malformations (Campbell et al., 2008). However its' necessity may be tissue specific. *Nfib* null mice die from severe respiratory dysfunction (Grunder et al., 2002) whereas the *Nfia*, *Nfic* or *Nfix* null mice display no obvious lung defects despite being expressed during lung development. Thus, in the embryonic hematopoietic system, *Nfix* may be dispensable and other NFI family members may compensate for *Nfix* loss. The most likely candidate for a compensatory role would be *Nfic*. Its expression in the E14.5 FLC HSPC is higher than *Nfia* or *Nfib* (Holmfeldt et al, 2013). *Nfic* and *Nfix* are frequently co-expressed at similar levels compared with other members in a tissue-specific manner. Endogenous *Nfic* and *Nfix* expression is high in the skeletal muscle, intermediate in the brain, heart, kidney, liver and lung, and low in the spleen and testis (Chaudhry et al., 1997), while *Nfia* and *Nfib* expression are different from *Nfic* and *Nfix*, and different from each other. It was also shown that in the developing embryo, detectable levels of both *Nfic* and *Nfix* appear at 11.5 days post coitus, whereas *Nfia* and *Nfib* occur at 10.5 days post coitus. There is already evidence to indicate that they may have overlapping functions. Expression of *NFIC* or *NFIX* in HeLa cells abrogates the induction of MMTV expression through glucocorticoid repression, whereas *NFIA* and *NFIB* do not (Chaudhry et al., 1997). Analysis of the expression of the other NFI family members in *Nfix*<sup>-/-</sup> FLCs may provide insight into our observations.

A recent study identified 36 factors that could reprogram a committed B cell into a myeloid cell and *Nfix* was one of these factors (Riddell et al., 2014). The data presented here demonstrate that *NFIX* can alter the fate of stem and progenitor cells. It can drive myelopoiesis from a committed progenitor cell and blocks B cell lymphopoiesis between the pre-pro and pro B cell stage. There is growing evidence to suggest that, despite being considered the earliest B cell precursor, pre-pro B cells retain some degree of multilineage potential with studies demonstrating this fraction can give rise to T, NK and dendritic cells (Nagasawa, 2006). As shown, *NFIX* overexpression in the committed pro-B cell line BAF/3, resulted in a 15 fold increase in *Cebpa* expression (Figure 5.19).

Enforced *Cebpa* expression has been shown to rapidly reprogram committed CD19<sup>+</sup> B cells into functional macrophages *in vitro* (Xie et al., 2004).

Collectively the data presented suggest that NFIX may act as a molecular switch at the myeloid/lymphoid branch point, potentially at the level of the MPP or LMPP, mediating changes in the expression of key lineage genes to restrict lineage potential in favour of myeloid differentiation.

This work has been published in O'Connor *et al*, 2015, provided in section 0.

## 6 General discussion

The data presented in this thesis represent findings which impact on 3 key areas -lineage determination in hematopoiesis, the pathophysiology of AML, and future therapeutic approaches in cancer treatment.

The process of hematopoiesis is an intricately regulated organisational system producing vast numbers of functionally and morphologically distinct blood cell types from a rare pool of long-lived HSCs. Understanding the regulation of this process will underpin our understanding of how its dysregulation results in leukaemia. The data in this thesis contribute to our understanding of lineage determination by identifying NFIX as a novel regulator of lineage fate decisions and by providing evidence that TRIB2 may influence the lymphoid lineage. The *Nfix* gene locus was identified as a retroviral insertion site in TRIB2-mediated myeloid leukaemia and in NOTCH1-mediated lymphoid leukaemia. TRIB2 overexpression results in the development of AML, its expression is highest in T cells and it is a NOTCH1 target gene, while NOTCH1 is a critical transcription factor in early T cell development and it is dysregulated in over 50% of T-ALL. It remains to be discerned what the exact relationship between NFIX, TRIB2 and NOTCH1 is, but it appears as though, together with CEBPA these genes may form a regulatory network involved in the bifurcation of the myeloid and lymphoid lineages. The data presented in chapter 5 show that NFIX overexpression drives myelopoiesis at the expense of B cell lymphopoiesis and that overexpression of NFIX in a committed B cell line results in a 15 fold increase in *Cebpa* expression. In addition, NFIX supports myeloid differentiation from the CMP and GMP but not the HSC. It is possible that at the level of the MPP/LMPP, NFIX may act as a molecular switch by activating *CEBPA* expression at the myeloid-lymphoid branch-point to promote myelopoiesis and thus inhibit lymphopoiesis. TRIB2 and NOTCH1 insertion into the NFIX locus may inhibit NFIX expression and its downstream effector C/EBP $\alpha$ , thus contributing to the resultant disease phenotypes. Overexpression of TRIB2 from the GMP induced a mature myeloid AML, but from the HSC induced a mixed lineage leukaemia even in a myeloid biased assay. As discussed in chapter 4, loss of TRIB2 from the hematopoietic compartment did not result in perturbation of lineage distribution. However, expression of TRIB2 is highest in the T cell compartment and it should be noted that our group have recently identified TRIB2 as a novel regulator of thymocyte

proliferation (Ling Liang et al, 2016 - details provided in section 0). As discussed in section 1.3.3.5 TRIB2 is also implicated in megakaryocyte and erythroid lineages where it is hypothesised to be activated by FOG1 in MkE precursor cells in order to degrade C/EBP $\alpha$  to permit MkE differentiation. The data presented suggest that TRIB2 mediated degradation of C/EBP $\alpha$  may also influence lymphopoiesis in a cell context dependent manner.

Collectively the data presented in chapter 3 show that TRIB2 degrades p42 through K48 mediated proteasomal ubiquitination but is unable to degrade p30, instead increasing oncogenic p30 expression in AML. Despite this, not only is C/EBP $\alpha$  expression essential for TRIB2 mediated AML, but it is the degradation of p42 which is the key driver of this oncogenic pathway. As previously discussed, the requirement of C/EBP $\alpha$  expression for TRIB2 leukaemia induction correlates with published studies (Collins et al., 2014, Ohlsson et al., 2014). A recent publication has provided a fresh perspective on the role of C/EBP $\alpha$  in leukaemogenesis. The authors demonstrated that loss of C/EBP $\alpha$  stunts AML induction by MLL-AF9 and MOZ-TIF2 (Ye et al, 2015). However upon treatment with GM-CSF and IL-3, *Cebpa* null cells differentiated and restoration of differentiation was sufficient to restore the ability of MLL-AF9 and MOZ-TIF2 to induce AML in these cells. Thus the authors hypothesise that it is not the presence of C/EBP $\alpha$  itself but rather the differentiation state of the cell which provides a transformation permissive environment. Our data fully supports this hypothesis as TRIB2 overexpression in the committed GMP produced a potent myeloid leukaemia whereas it was unable to initiate AML from the CMP or MPP. Indeed the hypothesis that the self-renewal capacity of putative LICs occurs once the immature stem cells reach a committed myeloid progenitor stage is also supported by the observation that only in the presence of p42 which promotes myeloid differentiation, did TRIB2 and p30 cooperate to decrease the latency of the AML. Together the data presented in chapter 3 and 4 support the emerging hypothesis that C/EBP $\alpha$  plays a dichotomous role in the pathophysiology of AML. On the one hand, its expression is required to promote myeloid differentiation until the cells reach a stage of maturation (GMP) permissive for oncogenic transformation. On the other hand, loss of C/EBP $\alpha$  at this stage contributes to leukaemogenesis by causing a block in differentiation as well as loss of cell cycle control through disrupted inhibition of E2F1.

The current standard approach to AML treatment, in place for over 40 years, is wholly inadequate. The complexity and heterogeneity of acute leukaemia is central to the difficulty in its successful treatment. Representing this heterogeneity in preclinical mouse models presents a fundamental obstacle in the development of targeted therapies for AML. The availability of human samples for preclinical research is also a limiting factor in drug development. Indeed clinical trials are also fraught with drawbacks, in particular in AML where in order to provide efficient treatment, multiple targets may need to be treated concurrently, and clinical trials generally deal with one drug.

Despite these factors there have been several exciting developments in the field recently. Next-generation sequencing has revolutionised our understanding of AML genetics and we are now seeing the emergence of several new types of treatment including small molecule drugs targeted against mutations in genes such as IDH1/2 and Flt3. One especially promising agent is the IDH2 inhibitor AG-221 which, in a phase 1 clinical trial, has been shown to achieve complete remission in 33% of AML patients bearing an IDH2 mutation (Rowe, 2015). The characterisation of unique cell surface markers present on leukaemic cells is opening the door for the development of antibody drug conjugates (ADC) in AML treatment. While there have been no successfully trialled ADCs to date - gemtuzumab ozagomicin which targets CD33 was withdrawn from the market - there are promising data now emerging. CD47, expressed at very low levels on healthy BM, is highly expressed on leukaemic cells (Majeti et al., 2009) and the humanised anti-CD47 antibody HuF9-G4 is currently in clinical trials with AML patients (Liu et al., 2015). Another promising avenue of AML therapy utilises chimeric antigen receptor (CAR)-expressing T cells to target cell surface markers on leukaemic cells. CD19 directed CAR-T cell therapy has yielded very promising results in the treatment of ALL and this technology is being adapted for the tailored treatment of AML (Ritchie et al., 2013). The data presented here support the further exploration of proteasome inhibition in the treatment of AML. Indeed TRIB2 mediated degradation of CEBPA has also been implicated in the progression of liver (Wang et al., 2013) and lung (Grandinetti et al., 2011) cancer, thus the development of clinically effective proteasome inhibitors could also impact on therapeutic strategies for treatment of these cancer types.

## 7 References

- ADOLFSSON, J., MANSSON, R., BUZA-VIDAS, N., HULTQUIST, A., LIUBA, K., JENSEN, C. T., BRYDER, D., YANG, L., BORGE, O. J., THOREN, L. A., ANDERSON, K., SITNICKA, E., SASAKI, Y., SIGVARDSSON, M. & JACOBSEN, S. E. 2005. Identification of Flt3+ lympho-myeloid stem cells lacking erythro-megakaryocytic potential a revised road map for adult blood lineage commitment. *Cell*, 121, 295-306.
- AILLES, L. E., GERHARD, B., KAWAGOE, H. & HOGGE, D. E. 1999. Growth characteristics of acute myelogenous leukemia progenitors that initiate malignant hematopoiesis in nonobese diabetic/severe combined immunodeficient mice. *Blood*, 94, 1761-72.
- AKASHI, K., TRAVER, D., MIYAMOTO, T. & WEISSMAN, I. L. 2000. A clonogenic common myeloid progenitor that gives rise to all myeloid lineages. *Nature*, 404, 193-7.
- AL-HAJJ, M., WICHA, M. S., BENITO-HERNANDEZ, A., MORRISON, S. J. & CLARKE, M. F. 2003. Prospective identification of tumorigenic breast cancer cells. *Proc Natl Acad Sci U S A*, 100, 3983-8.
- ALHARBI, R. A., PETTENGELL, R., PANDHA, H. S. & MORGAN, R. 2013. The role of HOX genes in normal hematopoiesis and acute leukemia. *Leukemia*, 27, 1000-8.
- ARGIROPOULOS, B., PALMQVIST, L., YUNG, E., KUCHENBAUER, F., HEUSER, M., SLY, L. M., WAN, A., KRYSTAL, G. & HUMPHRIES, R. K. 2008. Linkage of Meis1 leukemogenic activity to multiple downstream effectors including Trib2 and Ccl3. *Exp Hematol*, 36, 845-59.
- ARINOBU, Y., MIZUNO, S., CHONG, Y., SHIGEMATSU, H., IINO, T., IWASAKI, H., GRAF, T., MAYFIELD, R., CHAN, S., KASTNER, P. & AKASHI, K. 2007. Reciprocal activation of GATA-1 and PU.1 marks initial specification of hematopoietic stem cells into myeloerythroid and myelolymphoid lineages. *Cell Stem Cell*, 1, 416-27.
- ASOU, H., TASHIRO, S., HAMAMOTO, K., OTSUJI, A., KITA, K. & KAMADA, N. 1991. Establishment of a human acute myeloid leukemia cell line (Kasumi-1) with 8;21 chromosome translocation. *Blood*, 77, 2031-6.
- ATTAR, E. C., JOHNSON, J. L., AMREIN, P. C., LOZANSKI, G., WADLEIGH, M., DEANGELO, D. J., KOLITZ, J. E., POWELL, B. L., VOORHEES, P., WANG, E. S., BLUM, W., STONE, R. M., MARCUCCI, G., BLOOMFIELD, C. D., MOSER, B. & LARSON, R. A. 2013. Bortezomib added to daunorubicin and cytarabine during induction therapy and to intermediate-dose cytarabine for consolidation in patients with previously untreated acute myeloid leukemia age 60 to 75 years: CALGB (Alliance) study 10502. *J Clin Oncol*, 31, 923-9.
- BAILEY, F. P., BYRNE, D. P., ORUGANTY, K., EYERS, C. E., NOVOTNY, C. J., SHOKAT, K. M., KANNAN, N. & EYERS, P. A. 2015. The Tribbles 2 (TRB2) pseudokinase binds to ATP and autophosphorylates in a metal-independent manner. *Biochem J*, 467, 47-62.
- BAIN, G., MAANDAG, E. C., IZON, D. J., AMSEN, D., KRUISBEEK, A. M., WEINTRAUB, B. C., KROP, I., SCHLISSEL, M. S., FEENEY, A. J., VAN ROON, M. & ET AL. 1994. E2A proteins are required for proper B cell development and initiation of immunoglobulin gene rearrangements. *Cell*, 79, 885-92.
- BARREDA, D. R., HANINGTON, P. C. & BELOSEVIC, M. 2004. Regulation of myeloid development and function by colony stimulating factors. *Dev Comp Immunol*, 28, 509-54.
- BENEZRA, R., DAVIS, R. L., LOCKSHON, D., TURNER, D. L. & WEINTRAUB, H. 1990. The protein Id: a negative regulator of helix-loop-helix DNA binding proteins. *Cell*, 61, 49-59.
- BENNETT, J. M., CATOVSKY, D., DANIEL, M. T., FLANDRIN, G., GALTON, D. A., GRALNICK, H. R. & SULTAN, C. 1976. Proposals for the classification of the acute leukaemias. French-American-British (FAB) co-operative group. *Br J Haematol*, 33, 451-8.
- BERESHCHENKO, O., MANCINI, E., MOORE, S., BILBAO, D., MANSSON, R., LUC, S., GROVER, A., JACOBSEN, S. E., BRYDER, D. & NERLOV, C. 2009. Hematopoietic stem cell expansion precedes the generation of committed myeloid leukemia-initiating cells in C/EBPalpha mutant AML. *Cancer Cell*, 16, 390-400.
- BEZY, O., VEROCHET, C., GESTA, S., FARMER, S. R. & KAHN, C. R. 2007. TRB3 blocks adipocyte differentiation through the inhibition of C/EBPbeta transcriptional activity. *Mol Cell Biol*, 27, 6818-31.
- BHUSHAN, L. & KANDPAL, R. P. 2011. EphB6 receptor modulates micro RNA profile of breast carcinoma cells. *PLoS One*, 6, e22484.
- BIRKENKAMP, K. U., ESSAFI, A., VAN DER VOS, K. E., DA COSTA, M., HUI, R. C., HOLSTEGE, F., KOENDERMAN, L., LAM, E. W. & COFFER, P. J. 2007. FOXO3a induces differentiation of Bcr-Abl-transformed cells through transcriptional down-regulation of Id1. *J Biol Chem*, 282, 2211-20.

- BIRKENMEIER, E. H., GWYNN, B., HOWARD, S., JERRY, J., GORDON, J. I., LANDSCHULZ, W. H. & MCKNIGHT, S. L. 1989. Tissue-specific expression, developmental regulation, and genetic mapping of the gene encoding CCAAT/enhancer binding protein. *Genes Dev*, 3, 1146-56.
- BONNET, D. & DICK, J. E. 1997. Human acute myeloid leukemia is organized as a hierarchy that originates from a primitive hematopoietic cell. *Nat Med*, 3, 730-7.
- BRADLEY, L. M., DOUGLASS, M. F., CHATTERJEE, D., AKIRA, S. & BAATEN, B. J. 2012. Matrix metalloprotease 9 mediates neutrophil migration into the airways in response to influenza virus-induced toll-like receptor signaling. *PLoS Pathog*, 8, e1002641.
- BURGER, J. A. & BURKLE, A. 2007. The CXCR4 chemokine receptor in acute and chronic leukaemia: a marrow homing receptor and potential therapeutic target. *Br J Haematol*, 137, 288-96.
- BURGERING, B. M. & KOPS, G. J. 2002. Cell cycle and death control: long live Forkheads. *Trends Biochem Sci*, 27, 352-60.
- CALABRIA, E., CICILIOT, S., MORETTI, I., GARCIA, M., PICARD, A., DYAR, K. A., PALLAFACCHINA, G., TOTHOVA, J., SCHIAFFINO, S. & MURGIA, M. 2009. NFAT isoforms control activity-dependent muscle fiber type specification. *Proc Natl Acad Sci U S A*, 106, 13335-40.
- CAMPBELL, C. E., PIPER, M., PLACHEZ, C., YEH, Y. T., BAIZER, J. S., OSINSKI, J. M., LITWACK, E. D., RICHARDS, L. J. & GRONOSTAJSKI, R. M. 2008. The transcription factor Nfix is essential for normal brain development. *BMC Dev Biol*, 8, 52.
- CANCER RESEARCH UK. 2012. *AML incidence by sex and UK region*. [Online]. <http://www.cancerresearchuk.org/content/acute-myeloid-leukaemia-aml-incidence-statistics#heading-Zero>: Cancer Research UK.
- CARNICER, M. J., LASA, A., BUSCHBECK, M., SERRANO, E., CARRICONDO, M., BRUNET, S., AVENTIN, A., SIERRA, J., DI CROCE, L. & NOMDEDEU, J. F. 2008. K313dup is a recurrent CEBPA mutation in de novo acute myeloid leukemia (AML). *Ann Hematol*, 87, 819-27.
- CHAUDHRY, A. Z., LYONS, G. E. & GRONOSTAJSKI, R. M. 1997. Expression patterns of the four nuclear factor I genes during mouse embryogenesis indicate a potential role in development. *Dev Dyn*, 208, 313-25.
- CHAUDHURY, S. S., MORISON, J. K., GIBSON, B. E. & KEESHAN, K. 2015. Insights into cell ontogeny, age, and acute myeloid leukemia. *Exp Hematol*, 43, 745-55.
- CHEN, L., KOSTADIMA, M., MARTENS, J. H., CANU, G., GARCIA, S. P., TURRO, E., DOWNES, K., MACAULAY, I. C., BIELCZYK-MACZYNSKA, E., COE, S., FARROW, S., POUDEL, P., BURDEN, F., JANSEN, S. B., ASTLE, W. J., ATTWOOD, A., BARIANA, T., DE BONO, B., BRESCHI, A., CHAMBERS, J. C., CONSORTIUM, B., CHOUDRY, F. A., CLARKE, L., COUPLAND, P., VAN DER ENT, M., ERBER, W. N., JANSEN, J. H., FAVIER, R., FENECH, M. E., FOAD, N., FRESON, K., VAN GEET, C., GOMEZ, K., GUIGO, R., HAMPSHIRE, D., KELLY, A. M., KERSTENS, H. H., KOONER, J. S., LAFFAN, M., LENTAIGNE, C., LABALETTE, C., MARTIN, T., MEACHAM, S., MUMFORD, A., NURNBERG, S., PALUMBO, E., VAN DER REIJDEN, B. A., RICHARDSON, D., SAMMUT, S. J., SLODKOWICZ, G., TAMURI, A. U., VASQUEZ, L., VOSS, K., WATT, S., WESTBURY, S., FLICEK, P., LOOS, R., GOLDMAN, N., BERTONE, P., READ, R. J., RICHARDSON, S., CVEJIC, A., SORANZO, N., OUWEHAND, W. H., STUNNENBERG, H. G., FRONTINI, M. & RENDON, A. 2014. Transcriptional diversity during lineage commitment of human blood progenitors. *Science*, 345, 1251033.
- CHIM, C. S., WONG, A. S. & KWONG, Y. L. 2002. Infrequent hypermethylation of CEBPA promoter in acute myeloid leukaemia. *Br J Haematol*, 119, 988-90.
- CHRISTENSEN, J. L. & WEISSMAN, I. L. 2001. Flk-2 is a marker in hematopoietic stem cell differentiation: a simple method to isolate long-term stem cells. *Proc Natl Acad Sci U S A*, 98, 14541-6.
- CLEAVES, R., WANG, Q. F. & FRIEDMAN, A. D. 2004. C/EBPalpha30, a myeloid leukemia oncoprotein, limits G-CSF receptor expression but not terminal granulopoiesis via site-selective inhibition of C/EBP DNA binding. *Oncogene*, 23, 716-25.
- COCHRANE, S. W., ZHAO, Y., WELNER, R. S. & SUN, X. H. 2009. Balance between Id and E proteins regulates myeloid-versus-lymphoid lineage decisions. *Blood*, 113, 1016-26.
- COLLINS, C., WANG, J., MIAO, H., BRONSTEIN, J., NAWER, H., XU, T., FIGUEROA, M., MUNTEAN, A. G. & HESS, J. L. 2014. C/EBPalpha is an essential collaborator in Hoxa9/Meis1-mediated leukemogenesis. *Proc Natl Acad Sci U S A*, 111, 9899-904.
- COOMBS, C. C., TAVAKKOLI, M. & TALLMAN, M. S. 2015. Acute promyelocytic leukemia: where did we start, where are we now, and the future. *Blood Cancer J*, 5, e304.

- COZZIO, A., PASSEGUE, E., AYTON, P. M., KARSUNKY, H., CLEARY, M. L. & WEISSMAN, I. L. 2003. Similar MLL-associated leukemias arising from self-renewing stem cells and short-lived myeloid progenitors. *Genes Dev*, 17, 3029-35.
- DAHL, R., WALSH, J. C., LANCKI, D., LASLO, P., IYER, S. R., SINGH, H. & SIMON, M. C. 2003. Regulation of macrophage and neutrophil cell fates by the PU.1:C/EBPalpha ratio and granulocyte colony-stimulating factor. *Nat Immunol*, 4, 1029-36.
- DAKIC, A., METCALF, D., DI RAGO, L., MIFSUD, S., WU, L. & NUTT, S. L. 2005. PU.1 regulates the commitment of adult hematopoietic progenitors and restricts granulopoiesis. *J Exp Med*, 201, 1487-502.
- DEDHIA, P. H., KEESHAN, K., ULJON, S., XU, L., VEGA, M. E., SHESTOVA, O., ZAKS-ZILBERMAN, M., ROMANY, C., BLACKLOW, S. C. & PEAR, W. S. 2010. Differential ability of Tribbles family members to promote degradation of C/EBPalpha and induce acute myelogenous leukemia. *Blood*, 116, 1321-8.
- DEKOTER, R. P. & SINGH, H. 2000. Regulation of B lymphocyte and macrophage development by graded expression of PU.1. *Science*, 288, 1439-41.
- DELOGU, A., SCHEBESTA, A., SUN, Q., ASCHENBRENNER, K., PERLOT, T. & BUSSLINGER, M. 2006. Gene repression by Pax5 in B cells is essential for blood cell homeostasis and is reversed in plasma cells. *Immunity*, 24, 269-81.
- DESHPANDE, A. J., CUSAN, M., RAWAT, V. P., REUTER, H., KRAUSE, A., POTT, C., QUINTANILLA-MARTINEZ, L., KAKADIA, P., KUCHENBAUER, F., AHMED, F., DELABESSE, E., HAHN, M., LICHTER, P., KNEBA, M., HIDDEMANN, W., MACINTYRE, E., MECUCCI, C., LUDWIG, W. D., HUMPHRIES, R. K., BOHLANDER, S. K., FEURING-BUSKE, M. & BUSKE, C. 2006. Acute myeloid leukemia is propagated by a leukemic stem cell with lymphoid characteristics in a mouse model of CALM/AF10-positive leukemia. *Cancer Cell*, 10, 363-74.
- DRILLER, K., PAGENSTECHE, A., UHL, M., OMRAN, H., BERLIS, A., GRUNDER, A. & SIPPEL, A. E. 2007. Nuclear factor I X deficiency causes brain malformation and severe skeletal defects. *Mol Cell Biol*, 27, 3855-3867.
- DU, K., HERZIG, S., KULKARNI, R. N. & MONTMINY, M. 2003. TRB3: a tribbles homolog that inhibits Akt/PKB activation by insulin in liver. *Science*, 300, 1574-7.
- DUBRIDGE, R. B., TANG, P., HSIA, H. C., LEONG, P. M., MILLER, J. H. & CALOS, M. P. 1987. Analysis of mutation in human cells by using an Epstein-Barr virus shuttle system. *Mol Cell Biol*, 7, 379-87.
- DZIERZAK, E. & SPECK, N. A. 2008. Of lineage and legacy: the development of mammalian hematopoietic stem cells. *Nat Immunol*, 9, 129-36.
- EDER, K., GUAN, H., SUNG, H. Y., WARD, J., ANGYAL, A., JANAS, M., SARMA, G., DUDA, E., TURNER, M., DOWER, S. K., FRANCIS, S. E., CROSSMAN, D. C. & KISS-TOTH, E. 2008. Tribbles-2 is a novel regulator of inflammatory activation of monocytes. *Int Immunol*, 20, 1543-50.
- EPPERT, K., TAKENAKA, K., LECHMAN, E. R., WALDRON, L., NILSSON, B., VAN GALEN, P., METZELER, K. H., POEPPL, A., LING, V., BEYENE, J., CANTY, A. J., DANASKA, J. S., BOHLANDER, S. K., BUSKE, C., MINDEN, M. D., GOLUB, T. R., JURISICA, I., EBERT, B. L. & DICK, J. E. 2011. Stem cell gene expression programs influence clinical outcome in human leukemia. *Nat Med*, 17, 1086-93.
- ERAMO, A., LOTTI, F., SETTE, G., PILOZZI, E., BIFFONI, M., DI VIRGILIO, A., CONTICELLO, C., RUCO, L., PESCHLE, C. & DE MARIA, R. 2008. Identification and expansion of the tumorigenic lung cancer stem cell population. *Cell Death Differ*, 15, 504-14.
- FALINI, B., BOLLI, N., SHAN, J., MARTELLI, M. P., LISO, A., PUCCIARINI, A., BIGERNA, B., PASQUALUCCI, L., MANNUCCI, R., ROSATI, R., GORELLO, P., DIVERIO, D., ROTI, G., TIACCI, E., CAZZANIGA, G., BIONDI, A., SCHNITTGER, S., HAFERLACH, T., HIDDEMANN, W., MARTELLI, M. F., GU, W., MECUCCI, C. & NICOLETTI, I. 2006. Both carboxy-terminus NES motif and mutated tryptophan(s) are crucial for aberrant nuclear export of nucleophosmin leukemic mutants in NPMc+ AML. *Blood*, 107, 4514-23.
- FAZI, F., ROSA, A., FATICA, A., GELMETTI, V., DE MARCHIS, M. L., NERVI, C. & BOZZONI, I. 2005. A minicircuitry comprised of microRNA-223 and transcription factors NFI-A and C/EBPalpha regulates human granulopoiesis. *Cell*, 123, 819-31.
- FERRANDO, A. A., NEUBERG, D. S., STAUNTON, J., LOH, M. L., HUARD, C., RAIMONDI, S. C., BEHM, F. G., PUI, C. H., DOWNING, J. R., GILLILAND, D. G., LANDER, E. S., GOLUB, T. R. & LOOK, A. T. 2002. Gene expression signatures define novel oncogenic pathways in T cell acute lymphoblastic leukemia. *Cancer Cell*, 1, 75-87.
- FIELD-SMITH, A., MORGAN, G. J. & DAVIES, F. E. 2006. Bortezomib (Velcade trade mark) in the Treatment of Multiple Myeloma. *Ther Clin Risk Manag*, 2, 271-9.

- FLYGARE, J., RAYON ESTRADA, V., SHIN, C., GUPTA, S. & LODISH, H. F. 2011. HIF1alpha synergizes with glucocorticoids to promote BFU-E progenitor self-renewal. *Blood*, 117, 3435-44.
- FUJIWARA, Y., BROWNE, C. P., CUNNIFF, K., GOFF, S. C. & ORKIN, S. H. 1996. Arrested development of embryonic red cell precursors in mouse embryos lacking transcription factor GATA-1. *Proc Natl Acad Sci U S A*, 93, 12355-8.
- GAO, J., YAN, X. L., LI, R., LIU, Y., HE, W., SUN, S., ZHANG, Y., LIU, B., XIONG, J. & MAO, N. 2010. Characterization of OP9 as authentic mesenchymal stem cell line. *J Genet Genomics*, 37, 475-82.
- GEEST, C. R., BUITENHUIS, M., VELLENGA, E. & COFFER, P. J. 2009. Ectopic expression of C/EBPalpha and ID1 is sufficient to restore defective neutrophil development in low-risk myelodysplasia. *Haematologica*, 94, 1075-84.
- GELETU, M., BALKHI, M. Y., PEER ZADA, A. A., CHRISTOPEIT, M., PULIKKAN, J. A., TRIVEDI, A. K., TENEN, D. G. & BEHRE, G. 2007. Target proteins of C/EBPalpha30 in AML: C/EBPalpha30 enhances sumoylation of C/EBPalpha42 via up-regulation of Ubc9. *Blood*, 110, 3301-9.
- GEORGOPOULOS, K., BIGBY, M., WANG, J. H., MOLNAR, A., WU, P., WINANDY, S. & SHARPE, A. 1994. The Ikaros gene is required for the development of all lymphoid lineages. *Cell*, 79, 143-56.
- GIBBS, K. D., JR., JAGER, A., CRESPO, O., GOLTSEV, Y., TREJO, A., RICHARD, C. E. & NOLAN, G. P. 2012. Decoupling of tumor-initiating activity from stable immunophenotype in HoxA9-Meis1-driven AML. *Cell Stem Cell*, 10, 210-7.
- GOARDON, N., MARCHI, E., ATZBERGER, A., QUEK, L., SCHUH, A., SONEJI, S., WOLL, P., MEAD, A., ALFORD, K. A., ROUT, R., CHAUDHURY, S., GILKES, A., KNAPPER, S., BELDJORD, K., BEGUM, S., ROSE, S., GEDDES, N., GRIFFITHS, M., STANDEN, G., STERNBERG, A., CAVENAGH, J., HUNTER, H., BOWEN, D., KILLICK, S., ROBINSON, L., PRICE, A., MACINTYRE, E., VIRGO, P., BURNETT, A., CRADDOCK, C., ENVER, T., JACOBSEN, S. E., PORCHER, C. & VYAS, P. 2011. Coexistence of LMPP-like and GMP-like leukemia stem cells in acute myeloid leukemia. *Cancer Cell*, 19, 138-52.
- GODDARD, A. D., BORROW, J., FREEMONT, P. S. & SOLOMON, E. 1991. Characterization of a zinc finger gene disrupted by the t(15;17) in acute promyelocytic leukemia. *Science*, 254, 1371-4.
- GOUNARI, F., DE FRANCESCO, R., SCHMITT, J., VAN DER VLIET, P., CORTESE, R. & STUNNENBERG, H. 1990. Amino-terminal domain of NF1 binds to DNA as a dimer and activates adenovirus DNA replication. *EMBO J*, 9, 559-66.
- GRANDINETTI, K. B., STEVENS, T. A., HA, S., SALAMONE, R. J., WALKER, J. R., ZHANG, J., AGARWALLA, S., TENEN, D. G., PETERS, E. C. & REDDY, V. A. 2011. Overexpression of TRIB2 in human lung cancers contributes to tumorigenesis through downregulation of C/EBPalpha. *Oncogene*, 30, 3328-35.
- GREBIEN, F., VEDADI, M., GETLIK, M., GIAMBRUNO, R., GROVER, A., AVELLINO, R., SKUCHA, A., VITTORI, S., KUZNETSOVA, E., SMIL, D., BARSYTE-LOVEJOY, D., LI, F., PODA, G., SCHAPIRA, M., WU, H., DONG, A., SENISTERRA, G., STUKALOV, A., HUBER, K. V., SCHONEGGER, A., MARCELLUS, R., BILBAN, M., BOCK, C., BROWN, P. J., ZUBER, J., BENNETT, K. L., AL-AWAR, R., DELWEL, R., NERLOV, C., ARROWSMITH, C. H. & SUPERTI-FURGA, G. 2015. Pharmacological targeting of the Wdr5-MLL interaction in C/EBPalpha N-terminal leukemia. *Nat Chem Biol*, 11, 571-8.
- GREENBERGER, J. S., SAKAKEENY, M. A., HUMPHRIES, R. K., EAVES, C. J. & ECKNER, R. J. 1983. Demonstration of permanent factor-dependent multipotential (erythroid/neutrophil/basophil) hematopoietic progenitor cell lines. *Proc Natl Acad Sci U S A*, 80, 2931-5.
- GRIGOROPOULOS, N. F., PETTER, R., VAN 'T VEER, M. B., SCOTT, M. A. & FOLLOWS, G. A. 2013. Leukaemia update. Part 1: diagnosis and management. *BMJ*, 346, f1660.
- GRONOSTAJSKI, R. M. 2000. Roles of the NFI/CTF gene family in transcription and development. *Gene*, 249, 31-45.
- GRONOSTAJSKI, R. M., ADHYA, S., NAGATA, K., GUGGENHEIMER, R. A. & HURWITZ, J. 1985. Site-specific DNA binding of nuclear factor I: analyses of cellular binding sites. *Mol Cell Biol*, 5, 964-71.
- GROSSHANS, J. & WIESCHAUS, E. 2000. A genetic link between morphogenesis and cell division during formation of the ventral furrow in Drosophila. *Cell*, 101, 523-31.
- GRUNDER, A., EBEL, T. T., MALLO, M., SCHWARZKOPF, G., SHIMIZU, T., SIPPEL, A. E. & SCHREWE, H. 2002. Nuclear factor I-B (Nfib) deficient mice have severe lung hypoplasia. *Mech Dev*, 112, 69-77.

- GRUNDER, A., QIAN, F., EBEL, T. T., MINCHEVA, A., LICHTER, P., KRUSE, U. & SIPPEL, A. E. 2003. Genomic organization, splice products and mouse chromosomal localization of genes for transcription factor Nuclear Factor One. *Gene*, 304, 171-81.
- GRUNDLER, R., MIETHING, C., THIEDE, C., PESCHEL, C. & DUYSSTER, J. 2005. FLT3-ITD and tyrosine kinase domain mutants induce 2 distinct phenotypes in a murine bone marrow transplantation model. *Blood*, 105, 4792-9.
- GUIBAL, F. C., ALBERICH-JORDA, M., HIRAI, H., EBRALIDZE, A., LEVANTINI, E., DI RUSCIO, A., ZHANG, P., SANTANA-LEMONS, B. A., NEUBERG, D., WAGERS, A. J., REGO, E. M. & TENEN, D. G. 2009. Identification of a myeloid committed progenitor as the cancer-initiating cell in acute promyelocytic leukemia. *Blood*, 114, 5415-25.
- HANKEY, W., SILVER, M., SUN, B. S., ZIBELLO, T., BERLINER, N. & KHANNA-GUPTA, A. 2011. Differential effects of sumoylation on the activities of CCAAT enhancer binding protein alpha (C/EBPalpha) p42 versus p30 may contribute in part, to aberrant C/EBPalpha activity in acute leukemias. *Hematol Rep*, 3, e5.
- HANKS, S. K. & HUNTER, T. 1995. Protein kinases 6. The eukaryotic protein kinase superfamily: kinase (catalytic) domain structure and classification. *FASEB J*, 9, 576-96.
- HANNON, M. M., LOHAN, F., ERBILGIN, Y., SAYITOGU, M., O'HAGAN, K., MILLS, K., OZBEK, U. & KEESHAN, K. 2012. Elevated TRIB2 with NOTCH1 activation in paediatric/adult T-ALL. *Br J Haematol*, 158, 626-34.
- HARRIS, T. E., ALBRECHT, J. H., NAKANISHI, M. & DARLINGTON, G. J. 2001. CCAAT/enhancer-binding protein-alpha cooperates with p21 to inhibit cyclin-dependent kinase-2 activity and induces growth arrest independent of DNA binding. *J Biol Chem*, 276, 29200-9.
- HASEMANN, M. S., LAURIDSEN, F. K., WAAGE, J., JAKOBSEN, J. S., FRANK, A. K., SCHUSTER, M. B., RAPIN, N., BAGGER, F. O., HOPPE, P. S., SCHROEDER, T. & PORSE, B. T. 2014. C/EBPalpha is required for long-term self-renewal and lineage priming of hematopoietic stem cells and for the maintenance of epigenetic configurations in multipotent progenitors. *PLoS Genet*, 10, e1004079.
- HEIKE, T. & NAKAHATA, T. 2002. Ex vivo expansion of hematopoietic stem cells by cytokines. *Biochim Biophys Acta*, 1592, 313-21.
- HENG, Y. H., MCLEAY, R. C., HARVEY, T. J., SMITH, A. G., BARRY, G., CATO, K., PLACHEZ, C., LITTLE, E., MASON, S., DIXON, C., GRONOSTAJSKI, R. M., BAILEY, T. L., RICHARDS, L. J. & PIPER, M. 2014. NFIX regulates neural progenitor cell differentiation during hippocampal morphogenesis. *Cereb Cortex*, 24, 261-79.
- HEUSER, M., YUN, H., BERG, T., YUNG, E., ARGIROPOULOS, B., KUCHENBAUER, F., PARK, G., HAMWI, I., PALMQVIST, L., LAI, C. K., LEUNG, M., LIN, G., CHATURVEDI, A., THAKUR, B. K., IWASAKI, M., BILENKY, M., THIESSEN, N., ROBERTSON, G., HIRST, M., KENT, D., WILSON, N. K., GOTTGENS, B., EAVES, C., CLEARY, M. L., MARRA, M., GANSER, A. & HUMPHRIES, R. K. 2011. Cell of origin in AML: susceptibility to MN1-induced transformation is regulated by the MEIS1/AbdB-like HOX protein complex. *Cancer Cell*, 20, 39-52.
- HILL, R., KALATHUR, R. K., COLACO, L., BRANDAO, R., UGUREL, S., FUTSCHIK, M. & LINK, W. 2015. TRIB2 as a biomarker for diagnosis and progression of melanoma. *Carcinogenesis*, 36, 469-77.
- HOHAUS, S., PETROVICK, M. S., VOSO, M. T., SUN, Z., ZHANG, D. E. & TENEN, D. G. 1995. PU.1 (Spi-1) and C/EBP alpha regulate expression of the granulocyte-macrophage colony-stimulating factor receptor alpha gene. *Mol Cell Biol*, 15, 5830-45.
- HOLMFELDT, P., PARDIECK, J., SAULSBERRY, A. C., NANDAKUMAR, S. K., FINKELSTEIN, D., GRAY, J. T., PERSONS, D. A. & MCKINNEY-FREEMAN, S. 2013. Nfix is a novel regulator of murine hematopoietic stem and progenitor cell survival. *Blood*, 122, 2987-96.
- HU, M. C., LEE, D. F., XIA, W., GOLFMAN, L. S., OU-YANG, F., YANG, J. Y., ZOU, Y., BAO, S., HANADA, N., SASO, H., KOBAYASHI, R. & HUNG, M. C. 2004. I kappa B kinase promotes tumorigenesis through inhibition of forkhead FOXO3a. *Cell*, 117, 225-37.
- HUGHES, J. M., LEGNINI, I., SALVATORI, B., MASCIARELLI, S., MARCHIONI, M., FAZI, F., MORLANDO, M., BOZZONI, I. & FATICA, A. 2015. C/EBPalpha-p30 protein induces expression of the oncogenic long non-coding RNA UCA1 in acute myeloid leukemia. *Oncotarget*, 6, 18534-44.
- HUNTLY, B. J., SHIGEMATSU, H., DEGUCHI, K., LEE, B. H., MIZUNO, S., DUCLOS, N., ROWAN, R., AMARAL, S., CURLEY, D., WILLIAMS, I. R., AKASHI, K. & GILLILAND, D. G. 2004. MOZ-TIF2, but not BCR-ABL, confers properties of leukemic stem cells to committed murine hematopoietic progenitors. *Cancer Cell*, 6, 587-96.
- IKEDA, H., KANAKURA, Y., TAMAKI, T., KURIU, A., KITAYAMA, H., ISHIKAWA, J., KANAYAMA, Y., YONEZAWA, T., TARUI, S. & GRIFFIN, J. D. 1991. Expression and functional role of the proto-oncogene c-kit in acute myeloblastic leukemia cells. *Blood*, 78, 2962-8.

- IWASAKI, H., SOMOZA, C., SHIGEMATSU, H., DUPREZ, E. A., IWASAKI-ARAI, J., MIZUNO, S., ARINOBU, Y., GEARY, K., ZHANG, P., DAYARAM, T., FENYUS, M. L., ELF, S., CHAN, S., KASTNER, P., HUETTNER, C. S., MURRAY, R., TENEN, D. G. & AKASHI, K. 2005. Distinctive and indispensable roles of PU.1 in maintenance of hematopoietic stem cells and their differentiation. *Blood*, 106, 1590-600.
- JIN, G., YAMAZAKI, Y., TAKUWA, M., TAKAHARA, T., KANEKO, K., KUWATA, T., MIYATA, S. & NAKAMURA, T. 2007. Trib1 and Evi1 cooperate with Hoxa and Meis1 in myeloid leukemogenesis. *Blood*, 109, 3998-4005.
- JOHANSEN, L. M., IWAMA, A., LODIE, T. A., SASAKI, K., FELSHER, D. W., GOLUB, T. R. & TENEN, D. G. 2001. c-Myc is a critical target for c/EBPalpha in granulopoiesis. *Mol Cell Biol*, 21, 3789-806.
- JONES, K. A., KADONAGA, J. T., ROSENFELD, P. J., KELLY, T. J. & TJIAN, R. 1987. A cellular DNA-binding protein that activates eukaryotic transcription and DNA replication. *Cell*, 48, 79-89.
- KADIA, T. M., RAVANDI, F., O'BRIEN, S., CORTES, J. & KANTARJIAN, H. M. 2014. Progress in Acute Myeloid Leukemia. *Clin Lymphoma Myeloma Leuk*.
- KADOCH, C. & CRABTREE, G. R. 2015. Mammalian SWI/SNF chromatin remodeling complexes and cancer: Mechanistic insights gained from human genomics. *Sci Adv*, 1, e1500447.
- KATO, N., KITAURA, J., DOKI, N., KOMENO, Y., WATANABE-OKOCHI, N., TOGAMI, K., NAKAHARA, F., OKI, T., ENOMOTO, Y., FUKUCHI, Y., NAKAJIMA, H., HARADA, Y., HARADA, H. & KITAMURA, T. 2011. Two types of C/EBPalpha mutations play distinct but collaborative roles in leukemogenesis: lessons from clinical data and BMT models. *Blood*, 117, 221-33.
- KEESHAN, K., BAILIS, W., DEDHIA, P. H., VEGA, M. E., SHESTOVA, O., XU, L., TOSCANO, K., ULJON, S. N., BLACKLOW, S. C. & PEAR, W. S. 2010. Transformation by Tribbles homolog 2 (Trib2) requires both the Trib2 kinase domain and COP1 binding. *Blood*, 116, 4948-57.
- KEESHAN, K., HE, Y., WOUTERS, B. J., SHESTOVA, O., XU, L., SAI, H., RODRIGUEZ, C. G., MAILLARD, I., TOBIAS, J. W., VALK, P., CARROLL, M., ASTER, J. C., DELWEL, R. & PEAR, W. S. 2006. Tribbles homolog 2 inactivates C/EBPalpha and causes acute myelogenous leukemia. *Cancer Cell*, 10, 401-11.
- KEESHAN, K., SANTILLI, G., CORRADINI, F., PERROTTI, D. & CALABRETTA, B. 2003. Transcription activation function of C/EBPalpha is required for induction of granulocytic differentiation. *Blood*, 102, 1267-75.
- KEESHAN, K., SHESTOVA, O., USSIN, L. & PEAR, W. S. 2008. Tribbles homolog 2 (Trib2) and HoxA9 cooperate to accelerate acute myelogenous leukemia. *Blood Cells Mol Dis*, 40, 119-21.
- KIRSTETTER, P., SCHUSTER, M. B., BERESHCHENKO, O., MOORE, S., DVINGE, H., KURZ, E., THEILGAARD-MONCH, K., MANSSON, R., PEDERSEN, T. A., PABST, T., SCHROCK, E., PORSE, B. T., JACOBSEN, S. E., BERTONE, P., TENEN, D. G. & NERLOV, C. 2008. Modeling of C/EBPalpha mutant acute myeloid leukemia reveals a common expression signature of committed myeloid leukemia-initiating cells. *Cancer Cell*, 13, 299-310.
- KISS-TOTH, E., BAGSTAFF, S. M., SUNG, H. Y., JOZSA, V., DEMPSEY, C., CAUNT, J. C., OXLEY, K. M., WYLLIE, D. H., POLGAR, T., HARTE, M., O'NEILL, L. A., QWARNSTROM, E. E. & DOWER, S. K. 2004. Human tribbles, a protein family controlling mitogen-activated protein kinase cascades. *J Biol Chem*, 279, 42703-8.
- KLAEWSONGKRAM, J., YANG, Y., GOLECH, S., KATZ, J., KAESTNER, K. H. & WENG, N. P. 2007. Kruppel-like factor 4 regulates B cell number and activation-induced B cell proliferation. *J Immunol*, 179, 4679-84.
- KONDO, M., WEISSMAN, I. L. & AKASHI, K. 1997. Identification of clonogenic common lymphoid progenitors in mouse bone marrow. *Cell*, 91, 661-72.
- KRALOVICS, R., GUAN, Y. & PRCHAL, J. T. 2002. Acquired uniparental disomy of chromosome 9p is a frequent stem cell defect in polycythemia vera. *Exp Hematol*, 30, 229-36.
- KRIVTSOV, A. V., FIGUEROA, M. E., SINHA, A. U., STUBBS, M. C., FENG, Z., VALK, P. J., DELWEL, R., DOHNER, K., BULLINGER, L., KUNG, A. L., MELNICK, A. M. & ARMSTRONG, S. A. 2013. Cell of origin determines clinically relevant subtypes of MLL-rearranged AML. *Leukemia*, 27, 852-60.
- KROON, E., KROSL, J., THORSTEINSDOTTIR, U., BABAN, S., BUCHBERG, A. M. & SAUVAGEAU, G. 1998. Hoxa9 transforms primary bone marrow cells through specific collaboration with Meis1a but not Pbx1b. *EMBO J*, 17, 3714-25.
- KRUSE, U., QIAN, F. & SIPPEL, A. E. 1991. Identification of a fourth nuclear factor I gene in chicken by cDNA cloning: NFI-X. *Nucleic Acids Res*, 19, 6641.

- KRUSE, U. & SIPPEL, A. E. 1994. The genes for transcription factor nuclear factor I give rise to corresponding splice variants between vertebrate species. *J Mol Biol*, 238, 860-5.
- KUEH, H. Y., CHAMPHEKHAR, A., NUTT, S. L., ELOWITZ, M. B. & ROTHENBERG, E. V. 2013. Positive feedback between PU.1 and the cell cycle controls myeloid differentiation. *Science*, 341, 670-3.
- KUMAR, R., FOSSATI, V., ISRAEL, M. & SNOECK, H. W. 2008. Lin-Sca1+kit- bone marrow cells contain early lymphoid-committed precursors that are distinct from common lymphoid progenitors. *J Immunol*, 181, 7507-13.
- KUO, Y. Y., HOU, H. A., CHEN, Y. K., LI, L. Y., CHEN, P. H., TSENG, M. H., HUANG, C. F., LEE, F. Y., LIU, M. C., LIU, C. W., CHOU, W. C., LIU, C. Y., TANG, J. L., YAO, M. & TIEN, H. F. 2014. The N-terminal CEBPA mutant in acute myeloid leukemia impairs CXCR4 expression. *Haematologica*, 99, 1799-807.
- KVINLAUG, B. T., CHAN, W. I., BULLINGER, L., RAMASWAMI, M., SEARS, C., FOSTER, D., LAZIC, S. E., OKABE, R., BENNER, A., LEE, B. H., DE SILVA, I., VALK, P. J., DELWEL, R., ARMSTRONG, S. A., DOHNER, H., GILLILAND, D. G. & HUNTLY, B. J. 2011. Common and overlapping oncogenic pathways contribute to the evolution of acute myeloid leukemias. *Cancer Res*, 71, 4117-29.
- KWON, K., HUTTER, C., SUN, Q., BILIC, I., COBALEDA, C., MALIN, S. & BUSSLINGER, M. 2008. Instructive role of the transcription factor E2A in early B lymphopoiesis and germinal center B cell development. *Immunity*, 28, 751-62.
- LAM, K. & ZHANG, D. E. 2012. RUNX1 and RUNX1-ETO: roles in hematopoiesis and leukemogenesis. *Front Biosci (Landmark Ed)*, 17, 1120-39.
- LANOTTE, M., MARTIN-THOUVENIN, V., NAJMAN, S., BALERINI, P., VALENSI, F. & BERGER, R. 1991. NB4, a maturation inducible cell line with t(15;17) marker isolated from a human acute promyelocytic leukemia (M3). *Blood*, 77, 1080-6.
- LAPIDOT, T., SIRARD, C., VORMOOR, J., MURDOCH, B., HOANG, T., CACERES-CORTES, J., MINDEN, M., PATERSON, B., CALIGIURI, M. A. & DICK, J. E. 1994. A cell initiating human acute myeloid leukaemia after transplantation into SCID mice. *Nature*, 367, 645-8.
- LAVAU, C., LUO, R. T., DU, C. & THIRMAN, M. J. 2000. Retrovirus-mediated gene transfer of MLL-ELL transforms primary myeloid progenitors and causes acute myeloid leukemias in mice. *Proc Natl Acad Sci U S A*, 97, 10984-9.
- LAVAU, C., SZILVASSY, S. J., SLANY, R. & CLEARY, M. L. 1997. Immortalization and leukemic transformation of a myelomonocytic precursor by retrovirally transduced HRX-ENL. *EMBO J*, 16, 4226-37.
- LEE, C. K., SMITH, E., GIMENO, R., GERTNER, R. & LEVY, D. E. 2000. STAT1 affects lymphocyte survival and proliferation partially independent of its role downstream of IFN-gamma. *J Immunol*, 164, 1286-92.
- LEE, D. S., CHOUNG, H. W., KIM, H. J., GRONOSTAJSKI, R. M., YANG, Y. I., RYOO, H. M., LEE, Z. H., KIM, H. H., CHO, E. S. & PARK, J. C. 2014. NFI-C regulates osteoblast differentiation via control of osterix expression. *Stem Cells*, 32, 2467-79.
- LEKSTROM-HIMES, J. A. 2001. The role of C/EBP(epsilon) in the terminal stages of granulocyte differentiation. *Stem Cells*, 19, 125-33.
- LEROY, H., ROUMIER, C., HUYGHE, P., BIGGIO, V., FENAUX, P. & PREUDHOMME, C. 2005. CEBPA point mutations in hematological malignancies. *Leukemia*, 19, 329-34.
- LIANG, K. L., RISHI, L. & KEESHAN, K. 2013. Tribbles in acute leukemia. *Blood*, 121, 4265-70.
- LIN, F. T., MACDOUGALD, O. A., DIEHL, A. M. & LANE, M. D. 1993. A 30-kDa alternative translation product of the CCAAT/enhancer binding protein alpha message: transcriptional activator lacking antimitotic activity. *Proc Natl Acad Sci U S A*, 90, 9606-10.
- LIN, Z. Y., HUANG, Y. Q., ZHANG, Y. Q., HAN, Z. D., HE, H. C., LING, X. H., FU, X., DAI, Q. S., CAI, C., CHEN, J. H., LIANG, Y. X., JIANG, F. N., ZHONG, W. D., WANG, F. & WU, C. L. 2014. MicroRNA-224 inhibits progression of human prostate cancer by downregulating TRIB1. *Int J Cancer*, 135, 541-50.
- LINDSTROM, M. S. 2011. NPM1/B23: A Multifunctional Chaperone in Ribosome Biogenesis and Chromatin Remodeling. *Biochem Res Int*, 2011, 195209.
- LIONGUE, C., WRIGHT, C., RUSSELL, A. P. & WARD, A. C. 2009. Granulocyte colony-stimulating factor receptor: stimulating granulopoiesis and much more. *Int J Biochem Cell Biol*, 41, 2372-5.
- LIU, J., WANG, L., ZHAO, F., TSENG, S., NARAYANAN, C., SHURA, L., WILLINGHAM, S., HOWARD, M., PROHASKA, S., VOLKMER, J., CHAO, M., WEISSMAN, I. L. & MAJETI, R. 2015. Pre-Clinical Development of a Humanized Anti-CD47 Antibody with Anti-Cancer Therapeutic Potential. *PLoS One*, 10, e0137345.
- LIU, Y., HE, P., LIU, F., SHI, L., ZHU, H., ZHAO, J., WANG, Y., CHENG, X. & ZHANG, M. 2014. Prognostic significance of NPM1 mutations in acute myeloid leukemia: A meta-analysis. *Mol Clin Oncol*, 2, 275-281.

- LOHAN, F. & KEESHAN, K. 2013. The functionally diverse roles of tribbles. *Biochem Soc Trans*, 41, 1096-100.
- MAHMUD, D. L., M, G. A., DEB, D. K., PLATANIAS, L. C., UDDIN, S. & WICKREMA, A. 2002. Phosphorylation of forkhead transcription factors by erythropoietin and stem cell factor prevents acetylation and their interaction with coactivator p300 in erythroid progenitor cells. *Oncogene*, 21, 1556-62.
- MAJETI, R., BECKER, M. W., TIAN, Q., LEE, T. L., YAN, X., LIU, R., CHIANG, J. H., HOOD, L., CLARKE, M. F. & WEISSMAN, I. L. 2009. Dysregulated gene expression networks in human acute myelogenous leukemia stem cells. *Proc Natl Acad Sci U S A*, 106, 3396-401.
- MANCINI, E., SANJUAN-PLA, A., LUCIANI, L., MOORE, S., GROVER, A., ZAY, A., RASMUSSEN, K. D., LUC, S., BILBAO, D., O'CARROLL, D., JACOBSEN, S. E. & NERLOV, C. 2012. FOG-1 and GATA-1 act sequentially to specify definitive megakaryocytic and erythroid progenitors. *EMBO J*, 31, 351-65.
- MANSSON, R., HULTQUIST, A., LUC, S., YANG, L., ANDERSON, K., KHARAZI, S., AL-HASHMI, S., LIUBA, K., THOREN, L., ADOLFSSON, J., BUZA-VIDAS, N., QIAN, H., SONEJI, S., ENVER, T., SIGVARDSSON, M. & JACOBSEN, S. E. 2007. Molecular evidence for hierarchical transcriptional lineage priming in fetal and adult stem cells and multipotent progenitors. *Immunity*, 26, 407-19.
- MANSSON, R., ZANDI, S., ANDERSON, K., MARTENSSON, I.-L., JACOBSEN, S., BRYDER, D. & SIGVARDSSON, M. 2008. B-lineage commitment prior to surface expression of B220 and CD19 on hematopoietic progenitor cells. *Blood*, 112, 1048-1103.
- MATA, J., CURADO, S., EPHRUSSI, A. & RORTH, P. 2000. Tribbles coordinates mitosis and morphogenesis in *Drosophila* by regulating string/CDC25 proteolysis. *Cell*, 101, 511-22.
- MCCLURE, C., BRUDECKI, L., FERGUSON, D. A., YAO, Z. Q., MOORMAN, J. P., MCCALL, C. E. & EL GAZZAR, M. 2014. MicroRNA 21 (miR-21) and miR-181b couple with NFI-A to generate myeloid-derived suppressor cells and promote immunosuppression in late sepsis. *Infect Immun*, 82, 3816-25.
- MCKINNEY-FREEMAN, S., CAHAN, P., LI, H., LACADIE, S. A., HUANG, H. T., CURRAN, M., LOEWER, S., NAVEIRAS, O., KATHREIN, K. L., KONANTZ, M., LANGDON, E. M., LENGGERKE, C., ZON, L. I., COLLINS, J. J. & DALEY, G. Q. 2012. The transcriptional landscape of hematopoietic stem cell ontogeny. *Cell Stem Cell*, 11, 701-14.
- MEISTERERNST, M., ROGGE, L., DONATH, C., GANDER, I., LOTTSPEICH, F., MERTZ, R., DOBNER, T., FOCKLER, R., STELZER, G. & WINNACKER, E. L. 1988. Isolation and characterization of the porcine nuclear factor I (NFI) gene. *FEBS Lett*, 236, 27-32.
- MERMOD, N., O'NEILL, E. A., KELLY, T. J. & TJIAN, R. 1989. The proline-rich transcriptional activator of CTF/NF-I is distinct from the replication and DNA binding domain. *Cell*, 58, 741-53.
- METCALF, D. 2008. Hematopoietic cytokines. *Blood*, 111, 485-91.
- MEYER, C., HOFMANN, J., BURMEISTER, T., GROGER, D., PARK, T. S., EMERENCIANO, M., POMBO DE OLIVEIRA, M., RENNEVILLE, A., VILLARESE, P., MACINTYRE, E., CAVE, H., CLAPPIER, E., MASS-MALO, K., ZUNA, J., TRKA, J., DE BRAEKELEER, E., DE BRAEKELEER, M., OH, S. H., TSAUR, G., FECHINA, L., VAN DER VELDEN, V. H., VAN DONGEN, J. J., DELABESSE, E., BINATO, R., SILVA, M. L., KUSTANOVICH, A., ALEINIKOVA, O., HARRIS, M. H., LUND-AHO, T., JUUVONEN, V., HEIDENREICH, O., VORMOOR, J., CHOI, W. W., JAROSOVA, M., KOLENOVA, A., BUENO, C., MENENDEZ, P., WEHNER, S., ECKERT, C., TALMANT, P., TONDEUR, S., LIPPERT, E., LAUNAY, E., HENRY, C., BALLERINI, P., LAPILLONE, H., CALLANAN, M. B., CAYUELA, J. M., HERBAUX, C., CAZZANIGA, G., KAKADIYA, P. M., BOHLANDER, S., AHLMANN, M., CHOI, J. R., GAMEIRO, P., LEE, D. S., KRAUTER, J., CORNILLET-LEFEBVRE, P., TE KRONNIE, G., SCHAFFER, B. W., KUBETZKO, S., ALONSO, C. N., ZUR STADT, U., SUTTON, R., VENN, N. C., IZRAELI, S., TRAKHTENBROT, L., MADSEN, H. O., ARCHER, P., HANCOCK, J., CERVEIRA, N., TEIXEIRA, M. R., LO NIGRO, L., MORICKE, A., STANULLA, M., SCHRAPPE, M., SEDEK, L., SZCZEPANSKI, T., ZWAAN, C. M., COENEN, E. A., VAN DEN HEUVEL-EIBRINK, M. M., STREHL, S., DWORZAK, M., PANZER-GRUMAYER, R., DINGERMANN, T., KLINGEBIEL, T. & MARSCHALEK, R. 2013. The MLL recombinome of acute leukemias in 2013. *Leukemia*, 27, 2165-76.
- MINK, S., HARTIG, E., JENNEWEIN, P., DOPPLER, W. & CATO, A. C. 1992. A mammary cell-specific enhancer in mouse mammary tumor virus DNA is composed of multiple regulatory elements including binding sites for CTF/NFI and a novel transcription factor, mammary cell-activating factor. *Mol Cell Biol*, 12, 4906-18.
- MIYAMOTO, T., IWASAKI, H., REIZIS, B., YE, M., GRAF, T., WEISSMAN, I. L. & AKASHI, K. 2002. Myeloid or lymphoid promiscuity as a critical step in hematopoietic lineage commitment. *Dev Cell*, 3, 137-47.

- MIYOSHI, N., ISHII, H., MIMORI, K., TAKATSUNO, Y., KIM, H., HIROSE, H., SEKIMOTO, M., DOKI, Y. & MORI, M. 2009. Abnormal expression of TRIB3 in colorectal cancer: a novel marker for prognosis. *Br J Cancer*, 101, 1664-70.
- MULLER, C., CALKHOVEN, C. F., SHA, X. & LEUTZ, A. 2004. The CCAAT enhancer-binding protein alpha (C/EBPalpha) requires a SWI/SNF complex for proliferation arrest. *J Biol Chem*, 279, 7353-8.
- NAGASAWA, T. 2006. Microenvironmental niches in the bone marrow required for B-cell development. *Nat Rev Immunol*, 6, 107-16.
- NAGATA, K., GUGGENHEIMER, R. A., ENOMOTO, T., LICHY, J. H. & HURWITZ, J. 1982. Adenovirus DNA replication in vitro: identification of a host factor that stimulates synthesis of the preterminal protein-dCMP complex. *Proc Natl Acad Sci U S A*, 79, 6438-42.
- NAGATA, K., GUGGENHEIMER, R. A. & HURWITZ, J. 1983. Specific binding of a cellular DNA replication protein to the origin of replication of adenovirus DNA. *Proc Natl Acad Sci U S A*, 80, 6177-81.
- NAGEL, S., VENTURINI, L., PRZYBYLSKI, G. K., GRABARCZYK, P., SCHNEIDER, B., MEYER, C., KAUFMANN, M., SCHMIDT, C. A., SCHERR, M., DREXLER, H. G. & MACLEOD, R. A. 2011. Activation of Paired-homeobox gene PITX1 by del(5)(q31) in T-cell acute lymphoblastic leukemia. *Leuk Lymphoma*, 52, 1348-59.
- NAIK, S. H., PERIE, L., SWART, E., GERLACH, C., VAN ROOIJ, N., DE BOER, R. J. & SCHUMACHER, T. N. 2013. Diverse and heritable lineage imprinting of early haematopoietic progenitors. *Nature*, 496, 229-32.
- NAIKI, T., SAIJOU, E., MIYAOKA, Y., SEKINE, K. & MIYAJIMA, A. 2007. TRB2, a mouse Tribbles ortholog, suppresses adipocyte differentiation by inhibiting AKT and C/EBPbeta. *J Biol Chem*, 282, 24075-82.
- NAKAO, M., YOKOTA, S., IWAI, T., KANEKO, H., HORIIKE, S., KASHIMA, K., SONODA, Y., FUJIMOTO, T. & MISAWA, S. 1996. Internal tandem duplication of the flt3 gene found in acute myeloid leukemia. *Leukemia*, 10, 1911-8.
- NAMEN, A. E., LUPTON, S., HJERRILD, K., WIGNALL, J., MOCHIZUKI, D. Y., SCHMIERER, A., MOSLEY, B., MARCH, C. J., URDAL, D. & GILLIS, S. 1988. Stimulation of B-cell progenitors by cloned murine interleukin-7. *Nature*, 333, 571-3.
- NANDAKUMAR, S. K., JOHNSON, K., THROM, S. L., PESTINA, T. I., NEALE, G. & PERSONS, D. A. 2015. Low-level GATA2 overexpression promotes myeloid progenitor self-renewal and blocks lymphoid differentiation in mice. *Exp Hematol*, 43, 565-77 e1-10.
- NG, S. Y., YOSHIDA, T., ZHANG, J. & GEORGOPOULOS, K. 2009. Genome-wide lineage-specific transcriptional networks underscore Ikaros-dependent lymphoid priming in hematopoietic stem cells. *Immunity*, 30, 493-507.
- NIKOLIC, T., DINGJAN, G. M., LEENEN, P. J. & HENDRIKS, R. W. 2002. A subfraction of B220(+) cells in murine bone marrow and spleen does not belong to the B cell lineage but has dendritic cell characteristics. *Eur J Immunol*, 32, 686-92.
- NOTTA, F., DOULATOV, S., LAURENTI, E., POEPPL, A., JURISICA, I. & DICK, J. E. 2011. Isolation of single human hematopoietic stem cells capable of long-term multilineage engraftment. *Science*, 333, 218-21.
- NOTTA, F., ZANDI, S., TAKAYAMA, N., DOBSON, S., GAN, O. I., WILSON, G., KAUFMANN, K. B., MCLEOD, J., LAURENTI, E., DUNANT, C. F., MCPHERSON, J. D., STEIN, L. D., DROR, Y. & DICK, J. E. 2015. Distinct routes of lineage development reshape the human blood hierarchy across ontogeny. *Science*.
- NOVERSHTERN, N., SUBRAMANIAN, A., LAWTON, L. N., MAK, R. H., HAINING, W. N., MCCONKEY, M. E., HABIB, N., YOSEF, N., CHANG, C. Y., SHAY, T., FRAMPTON, G. M., DRAKE, A. C., LESKOV, I., NILSSON, B., PREFFER, F., DOMBKOWSKI, D., EVANS, J. W., LIEFELD, T., SMUTKO, J. S., CHEN, J., FRIEDMAN, N., YOUNG, R. A., GOLUB, T. R., REGEV, A. & EBERT, B. L. 2011. Densely interconnected transcriptional circuits control cell states in human hematopoiesis. *Cell*, 144, 296-309.
- NUTT, S. L., HEAVEY, B., ROLINK, A. G. & BUSSLINGER, M. 1999. Commitment to the B-lymphoid lineage depends on the transcription factor Pax5. *Nature*, 401, 556-62.
- O'BRIEN, C. A., POLLETT, A., GALLINGER, S. & DICK, J. E. 2007. A human colon cancer cell capable of initiating tumour growth in immunodeficient mice. *Nature*, 445, 106-10.
- OANCEA, C., RUSTER, B., HENSCHLER, R., PUCCHETTI, E. & RUTHARDT, M. 2010. The t(6;9) associated DEK/CAN fusion protein targets a population of long-term repopulating hematopoietic stem cells for leukemogenic transformation. *Leukemia*, 24, 1910-9.
- OGURO, H., DING, L. & MORRISON, S. J. 2013. SLAM family markers resolve functionally distinct subpopulations of hematopoietic stem cells and multipotent progenitors. *Cell Stem Cell*, 13, 102-16.

- OHLSSON, E., HASEMANN, M. S., WILLER, A., LAURIDSEN, F. K., RAPIN, N., JENDHOLM, J. & PORSE, B. T. 2014. Initiation of MLL-rearranged AML is dependent on C/EBPalpha. *J Exp Med*, 211, 5-13.
- OKAMOTO, H., LATRES, E., LIU, R., THABET, K., MURPHY, A., VALENZEULA, D., YANCOPOULOS, G. D., STITT, T. N., GLASS, D. J. & SLEEMAN, M. W. 2007. Genetic deletion of *Trb3*, the mammalian *Drosophila* tribbles homolog, displays normal hepatic insulin signaling and glucose homeostasis. *Diabetes*, 56, 1350-6.
- PABST, T. & MUELLER, B. U. 2007. Transcriptional dysregulation during myeloid transformation in AML. *Oncogene*, 26, 6829-37.
- PABST, T. & MUELLER, B. U. 2009. Complexity of CEBPA dysregulation in human acute myeloid leukemia. *Clin Cancer Res*, 15, 5303-7.
- PABST, T., MUELLER, B. U., ZHANG, P., RADOMSKA, H. S., NARRAVULA, S., SCHNITTGER, S., BEHRE, G., HIDDEMANN, W. & TENEN, D. G. 2001. Dominant-negative mutations of CEBPA, encoding CCAAT/enhancer binding protein-alpha (C/EBPalpha), in acute myeloid leukemia. *Nat Genet*, 27, 263-70.
- PALACIOS, R., KARASUYAMA, H. & ROLINK, A. 1987. Ly1+ PRO-B lymphocyte clones. Phenotype, growth requirements and differentiation in vitro and in vivo. *EMBO J*, 6, 3687-93.
- PARRY, P., WEI, Y. & EVANS, G. 1994. Cloning and characterization of the t(X;11) breakpoint from a leukemic cell line identify a new member of the forkhead gene family. *Genes Chromosomes Cancer*, 11, 79-84.
- PAZ-PRIEL, I. & FRIEDMAN, A. 2011. C/EBPalpha dysregulation in AML and ALL. *Crit Rev Oncog*, 16, 93-102.
- PEAR, W. S., MILLER, J. P., XU, L., PUI, J. C., SOFFER, B., QUACKENBUSH, R. C., PENDERGAST, A. M., BRONSON, R., ASTER, J. C., SCOTT, M. L. & BALTIMORE, D. 1998. Efficient and rapid induction of a chronic myelogenous leukemia-like myeloproliferative disease in mice receiving P210 bcr/abl-transduced bone marrow. *Blood*, 92, 3780-92.
- PEAR, W. S., NOLAN, G. P., SCOTT, M. L. & BALTIMORE, D. 1993. Production of high-titer helper-free retroviruses by transient transfection. *Proc Natl Acad Sci U S A*, 90, 8392-6.
- PEDERSEN, T. A., KOWENZ-LEUTZ, E., LEUTZ, A. & NERLOV, C. 2001. Cooperation between C/EBPalpha TBP/TFIIB and SWI/SNF recruiting domains is required for adipocyte differentiation. *Genes Dev*, 15, 3208-16.
- PEREZ-CASELLAS, L. A., WANG, X., HOWARD, K. D., REHAGE, M. W., STRONG, D. D. & LINKHART, T. A. 2009. Nuclear factor I transcription factors regulate IGF binding protein 5 gene transcription in human osteoblasts. *Biochim Biophys Acta*, 1789, 78-87.
- PEVNY, L., LIN, C. S., D'AGATI, V., SIMON, M. C., ORKIN, S. H. & COSTANTINI, F. 1995. Development of hematopoietic cells lacking transcription factor GATA-1. *Development*, 121, 163-72.
- PONGUBALA, J. M., NORTHRUP, D. L., LANCKI, D. W., MEDINA, K. L., TREIBER, T., BERTOLINO, E., THOMAS, M., GROSSCHEDL, R., ALLMAN, D. & SINGH, H. 2008. Transcription factor EBF restricts alternative lineage options and promotes B cell fate commitment independently of Pax5. *Nat Immunol*, 9, 203-15.
- PORSE, B. T., BRYDER, D., THEILGAARD-MONCH, K., HASEMANN, M. S., ANDERSON, K., DAMGAARD, I., JACOBSEN, S. E. & NERLOV, C. 2005. Loss of C/EBP alpha cell cycle control increases myeloid progenitor proliferation and transforms the neutrophil granulocyte lineage. *J Exp Med*, 202, 85-96.
- PORSE, B. T., PEDERSEN, T. A., XU, X., LINDBERG, B., WEWER, U. M., FRIIS-HANSEN, L. & NERLOV, C. 2001. E2F repression by C/EBPalpha is required for adipogenesis and granulopoiesis in vivo. *Cell*, 107, 247-58.
- PRONK, C. J., ROSSI, D. J., MANSSON, R., ATTEMA, J. L., NORDDAHL, G. L., CHAN, C. K., SIGVARDSSON, M., WEISSMAN, I. L. & BRYDER, D. 2007. Elucidation of the phenotypic, functional, and molecular topography of a myeloerythroid progenitor cell hierarchy. *Cell Stem Cell*, 1, 428-42.
- PUI, J. C., ALLMAN, D., XU, L., DEROCCO, S., KARNELL, F. G., BAKKOUR, S., LEE, J. Y., KADESCH, T., HARDY, R. R., ASTER, J. C. & PEAR, W. S. 1999. Notch1 expression in early lymphopoiesis influences B versus T lineage determination. *Immunity*, 11, 299-308.
- PUIFFE, M. L., LE PAGE, C., FILALI-MOUHIM, A., ZIETARSKA, M., OUELLET, V., TONIN, P. N., CHEVRETTE, M., PROVENCHER, D. M. & MES-MASSON, A. M. 2007. Characterization of ovarian cancer ascites on cell invasion, proliferation, spheroid formation, and gene expression in an in vitro model of epithelial ovarian cancer. *Neoplasia*, 9, 820-9.
- PULIKKAN, J. A., DENGLER, V., PEER ZADA, A. A., KAWASAKI, A., GELETU, M., PASALIC, Z., BOHLANDER, S. K., RYO, A., TENEN, D. G. & BEHRE, G. 2010. Elevated PIN1

- expression by C/EBPalpha-p30 blocks C/EBPalpha-induced granulocytic differentiation through c-Jun in AML. *Leukemia*, 24, 914-23.
- PUSKAS, L. G., JUHASZ, F., ZARVA, A., HACKLER, L., JR. & FARID, N. R. 2005. Gene profiling identifies genes specific for well-differentiated epithelial thyroid tumors. *Cell Mol Biol (Noisy-le-grand)*, 51, 177-86.
- QI, L., HEREDIA, J. E., ALTAREJOS, J. Y., SCREATON, R., GOEBEL, N., NIESSEN, S., MACLEOD, I. X., LIEW, C. W., KULKARNI, R. N., BAIN, J., NEWGARD, C., NELSON, M., EVANS, R. M., YATES, J. & MONTMINY, M. 2006. TRB3 links the E3 ubiquitin ligase COP1 to lipid metabolism. *Science*, 312, 1763-6.
- QIAN, F., KRUSE, U., LICHTER, P. & SIPPEL, A. E. 1995. Chromosomal localization of the four genes (NFIA, B, C, and X) for the human transcription factor nuclear factor I by FISH. *Genomics*, 28, 66-73.
- QUINTANA, E., SHACKLETON, M., FOSTER, H. R., FULLEN, D. R., SABEL, M. S., JOHNSON, T. M. & MORRISON, S. J. 2010. Phenotypic heterogeneity among tumorigenic melanoma cells from patients that is reversible and not hierarchically organized. *Cancer Cell*, 18, 510-23.
- RADOMSKA, H. S., HUETTNER, C. S., ZHANG, P., CHENG, T., SCADDEN, D. T. & TENEN, D. G. 1998. CCAAT/enhancer binding protein alpha is a regulatory switch sufficient for induction of granulocytic development from bipotential myeloid progenitors. *Mol Cell Biol*, 18, 4301-14.
- RECKZEH, K., BERESHCHENKO, O., MEAD, A., REHN, M., KHARAZI, S., JACOBSEN, S. E., NERLOV, C. & CAMMENGA, J. 2012. Molecular and cellular effects of oncogene cooperation in a genetically accurate AML mouse model. *Leukemia*, 26, 1527-36.
- RENNO, T., ATTINGER, A., RIMOLDI, D., HAHNE, M., TSCHOPP, J. & MACDONALD, H. R. 1998. Expression of B220 on activated T cell blasts precedes apoptosis. *Eur J Immunol*, 28, 540-7.
- RIDDELL, J., GAZIT, R., GARRISON, B. S., GUO, G., SAADATPOUR, A., MANDAL, P. K., EBINA, W., VOLCHKOV, P., YUAN, G. C., ORKIN, S. H. & ROSSI, D. J. 2014. Reprogramming committed murine blood cells to induced hematopoietic stem cells with defined factors. *Cell*, 157, 549-64.
- RISHI, L., HANNON, M., SALOME, M., HASEMANN, M., FRANK, A. K., CAMPOS, J., TIMONEY, J., O'CONNOR, C., CAHILL, M. R., PORSE, B. & KEESHAN, K. 2014. Regulation of Trib2 by an E2F1-C/EBPalpha feedback loop in AML cell proliferation. *Blood*, 123, 2389-400.
- RITCHIE, D. S., NEESON, P. J., KHOT, A., PEINERT, S., TAI, T., TANTON, K., CHEN, K., SHIN, M., WALL, D. M., HONEMANN, D., GAMBELL, P., WESTERMAN, D. A., HAURAT, J., WESTWOOD, J. A., SCOTT, A. M., KRAVETS, L., DICKINSON, M., TRAPANI, J. A., SMYTH, M. J., DARCY, P. K., KERSHAW, M. H. & PRINCE, H. M. 2013. Persistence and efficacy of second generation CAR T cell against the LeY antigen in acute myeloid leukemia. *Mol Ther*, 21, 2122-9.
- RODRIGUES, N. P., TIPPING, A. J., WANG, Z. & ENVER, T. 2012. GATA-2 mediated regulation of normal hematopoietic stem/progenitor cell function, myelodysplasia and myeloid leukemia. *Int J Biochem Cell Biol*, 44, 457-60.
- ROLINK, A., TEN BOEKEL, E., MELCHERS, F., FEARON, D. T., KROP, I. & ANDERSSON, J. 1996. A subpopulation of B220+ cells in murine bone marrow does not express CD19 and contains natural killer cell progenitors. *J Exp Med*, 183, 187-94.
- RORTH, P., SZABO, K. & TEXIDO, G. 2000. The level of C/EBP protein is critical for cell migration during Drosophila oogenesis and is tightly controlled by regulated degradation. *Mol Cell*, 6, 23-30.
- ROSA, A., BALLARINO, M., SORRENTINO, A., STHANDIER, O., DE ANGELIS, F. G., MARCHIONI, M., MASELLA, B., GUARINI, A., FATICA, A., PESCHLE, C. & BOZZONI, I. 2007. The interplay between the master transcription factor PU.1 and miR-424 regulates human monocyte/macrophage differentiation. *Proceedings of the National Academy of Sciences of the United States of America*, 104, 19849-54.
- ROSS, S. E., RADOMSKA, H. S., WU, B., ZHANG, P., WINNAY, J. N., BAJNOK, L., WRIGHT, W. S., SCHAUFLE, F., TENEN, D. G. & MACDOUGALD, O. A. 2004. Phosphorylation of C/EBPalpha inhibits granulopoiesis. *Mol Cell Biol*, 24, 675-86.
- ROSSI, P., KARSENTY, G., ROBERTS, A. B., ROCHE, N. S., SPORN, M. B. & DE CROMBRUGGHE, B. 1988. A nuclear factor 1 binding site mediates the transcriptional activation of a type I collagen promoter by transforming growth factor-beta. *Cell*, 52, 405-14.
- ROWE, J. M. 2015. Reasons for optimism in the therapy of acute leukemia. *Best Pract Res Clin Haematol*, 28, 69-72.
- RUPP, R. A., KRUSE, U., MULTHAUP, G., GOBEL, U., BEYREUTHER, K. & SIPPEL, A. E. 1990. Chicken NFI/TGGCA proteins are encoded by at least three independent genes: NFI-A,

- NFI-B and NFI-C with homologues in mammalian genomes. *Nucleic Acids Res*, 18, 2607-16.
- RYO, A., LIOU, Y. C., WULF, G., NAKAMURA, M., LEE, S. W. & LU, K. P. 2002. PIN1 is an E2F target gene essential for Neu/Ras-induced transformation of mammary epithelial cells. *Mol Cell Biol*, 22, 5281-95.
- SALMON-NGUYEN, F., BUSSON, M., DANIEL, M., LEBLANC, T., BERNARD, O. A. & BERGER, R. 2000. CALM-AF10 fusion gene in leukemias: simple and inversion-associated translocation (10;11). *Cancer Genet Cytogenet*, 122, 137-40.
- SALOME, M., CAMPOS, J. & KEESHAN, K. 2015. TRIB2 and the ubiquitin proteasome system in cancer. *Biochem Soc Trans*, 43, 1089-94.
- SANDA, T., LAWTON, L. N., BARRASA, M. I., FAN, Z. P., KOHLHAMMER, H., GUTIERREZ, A., MA, W., TATAREK, J., AHN, Y., KELLIHER, M. A., JAMIESON, C. H., STAUDT, L. M., YOUNG, R. A. & LOOK, A. T. 2012. Core transcriptional regulatory circuit controlled by the TAL1 complex in human T cell acute lymphoblastic leukemia. *Cancer Cell*, 22, 209-21.
- SARRY, J. E., MURPHY, K., PERRY, R., SANCHEZ, P. V., SECRETO, A., KEEFER, C., SWIDER, C. R., STRZELECKI, A. C., CAVELIER, C., RECHER, C., MANSAT-DE MAS, V., DELABESSE, E., DANET-DESNOYERS, G. & CARROLL, M. 2011. Human acute myelogenous leukemia stem cells are rare and heterogeneous when assayed in NOD/SCID/IL2Rgammac-deficient mice. *J Clin Invest*, 121, 384-95.
- SCHWIEGER, M., LOHLER, J., FISCHER, M., HERWIG, U., TENEN, D. G. & STOCKING, C. 2004. A dominant-negative mutant of C/EBPalpha, associated with acute myeloid leukemias, inhibits differentiation of myeloid and erythroid progenitors of man but not mouse. *Blood*, 103, 2744-52.
- SCOTT, E. W., SIMON, M. C., ANASTASI, J. & SINGH, H. 1994. Requirement of transcription factor PU.1 in the development of multiple hematopoietic lineages. *Science*, 265, 1573-7.
- SCOTT, L. M., CIVIN, C. I., RORTH, P. & FRIEDMAN, A. D. 1992. A novel temporal expression pattern of three C/EBP family members in differentiating myelomonocytic cells. *Blood*, 80, 1725-35.
- SEHER, T. C. & LEPTIN, M. 2000. Tribbles, a cell-cycle brake that coordinates proliferation and morphogenesis during Drosophila gastrulation. *Curr Biol*, 10, 623-9.
- SEITA, J., SAHOO, D., ROSSI, D. J., BHATTACHARYA, D., SERWOLD, T., INLAY, M. A., EHRlich, L. I., FATHMAN, J. W., DILL, D. L. & WEISSMAN, I. L. 2012. Gene Expression Commons: an open platform for absolute gene expression profiling. *PLoS One*, 7, e40321.
- SHIH, A. H., ABDEL-WAHAB, O., PATEL, J. P. & LEVINE, R. L. 2012. The role of mutations in epigenetic regulators in myeloid malignancies. *Nat Rev Cancer*, 12, 599-612.
- SHUKLA, S., SHUKLA, M., MACLENNAN, G. T., FU, P. & GUPTA, S. 2009. Deregulation of FOXO3A during prostate cancer progression. *Int J Oncol*, 34, 1613-20.
- SHULTZ, L. D., LYONS, B. L., BURZENSKI, L. M., GOTT, B., CHEN, X., CHALEFF, S., KOTB, M., GILLIES, S. D., KING, M., MANGADA, J., GREINER, D. L. & HANDGRETINGER, R. 2005. Human lymphoid and myeloid cell development in NOD/LtSz-scid IL2R gamma null mice engrafted with mobilized human hemopoietic stem cells. *J Immunol*, 174, 6477-89.
- SHULTZ, L. D., SCHWEITZER, P. A., CHRISTIANSON, S. W., GOTT, B., SCHWEITZER, I. B., TENNENT, B., MCKENNA, S., MOBRAATEN, L., RAJAN, T. V., GREINER, D. L. & ET AL. 1995. Multiple defects in innate and adaptive immunologic function in NOD/LtSz-scid mice. *J Immunol*, 154, 180-91.
- SINGH, S. K., HAWKINS, C., CLARKE, I. D., SQUIRE, J. A., BAYANI, J., HIDE, T., HENKELMAN, R. M., CUSIMANO, M. D. & DIRKS, P. B. 2004. Identification of human brain tumour initiating cells. *Nature*, 432, 396-401.
- SINGH, S. K., WILCZYNSKA, K. M., GRZYBOWSKI, A., YESTER, J., OSRAH, B., BRYAN, L., WRIGHT, S., GRISWOLD-PRENNER, I. & KORDULA, T. 2011. The unique transcriptional activation domain of nuclear factor-I-X3 is critical to specifically induce marker gene expression in astrocytes. *J Biol Chem*, 286, 7315-26.
- SITNICKA, E., BRAKEBUSCH, C., MARTENSSON, I. L., SVENSSON, M., AGACE, W. W., SIGVARDSSON, M., BUZA-VIDAS, N., BRYDER, D., CILIO, C. M., AHLENIUS, H., MARASKOVSKY, E., PESCHON, J. J. & JACOBSEN, S. E. 2003. Complementary signaling through flt3 and interleukin-7 receptor alpha is indispensable for fetal and adult B cell genesis. *J Exp Med*, 198, 1495-506.
- SLANY, R. K. 2009. The molecular biology of mixed lineage leukemia. *Haematologica*, 94, 984-93.
- SLOMIANY, B. A., D'ARIGO, K. L., KELLY, M. M. & KURTZ, D. T. 2000. C/EBPalpha inhibits cell growth via direct repression of E2F-DP-mediated transcription. *Mol Cell Biol*, 20, 5986-97.
- SMITH, L. T., HOHAUS, S., GONZALEZ, D. A., DZIENNIS, S. E. & TENEN, D. G. 1996. PU.1 (Spi-1) and C/EBP alpha regulate the granulocyte colony-stimulating factor receptor promoter in myeloid cells. *Blood*, 88, 1234-47.

- SO, C. W., KARSUNKY, H., PASSEGUE, E., COZZIO, A., WEISSMAN, I. L. & CLEARY, M. L. 2003. MLL-GAS7 transforms multipotent hematopoietic progenitors and induces mixed lineage leukemias in mice. *Cancer Cell*, 3, 161-71.
- STARNES, L. M., SORRENTINO, A., FERRACIN, M., NEGRINI, M., PELOSI, E., NERVI, C. & PESCHLE, C. 2010. A transcriptome-wide approach reveals the key contribution of NFI-A in promoting erythroid differentiation of human CD34(+) progenitors and CML cells. *Leukemia*, 24, 1220-3.
- STARNES, L. M., SORRENTINO, A., PELOSI, E., BALLARINO, M., MORSILLI, O., BIFFONI, M., SANTORO, S., FELLI, N., CASTELLI, G., DE MARCHIS, M. L., MASTROBERARDINO, G., GABBIANELLI, M., FATICA, A., BOZZONI, I., NERVI, C. & PESCHLE, C. 2009. NFI-A directs the fate of hematopoietic progenitors to the erythroid or granulocytic lineage and controls beta-globin and G-CSF receptor expression. *Blood*, 114, 1753-63.
- STEIN, E. M. & TALLMAN, M. S. 2016. Emerging therapeutic drugs for AML. *Blood*, 127, 71-8.
- SUNDSTROM, C. & NILSSON, K. 1976. Establishment and characterization of a human histiocytic lymphoma cell line (U-937). *Int J Cancer*, 17, 565-77.
- SWERDLOW, S. H., CANCER, I. A. F. R. O. & ORGANIZATION, W. H. 2008. *WHO Classification of Tumours of Haematopoietic and Lymphoid Tissues*, International Agency for Research on Cancer.
- TAKASATO, M., KOBAYASHI, C., OKABAYASHI, K., KIYONARI, H., OSHIMA, N., ASASHIMA, M. & NISHINAKAMURA, R. 2008. Trb2, a mouse homolog of tribbles, is dispensable for kidney and mouse development. *Biochem Biophys Res Commun*, 373, 648-52.
- TANG, B., WU, W., ZHANG, Q., SUN, Y., CUI, Y., WU, F., WEI, X., QI, G., LIANG, X., TANG, F., LI, Y. & FAN, W. 2015. Inhibition of tribbles protein-1 attenuates radioresistance in human glioma cells. *Sci Rep*, 5, 15961.
- THOMAS, J., LIU, F. & LINK, D. C. 2002. Mechanisms of mobilization of hematopoietic progenitors with granulocyte colony-stimulating factor. *Curr Opin Hematol*, 9, 183-9.
- TILL, J. E. & MCCULLOCH, E. 1961. A direct measurement of the radiation sensitivity of normal mouse bone marrow cells. *Radiat Res*, 14, 213-22.
- TIMCHENKO, N. A., HARRIS, T. E., WILDE, M., BILYEU, T. A., BURGESS-BEUSSE, B. L., FINEGOLD, M. J. & DARLINGTON, G. J. 1997. CCAAT/enhancer binding protein alpha regulates p21 protein and hepatocyte proliferation in newborn mice. *Mol Cell Biol*, 17, 7353-61.
- TODARO, G. J. & GREEN, H. 1963. Quantitative studies of the growth of mouse embryo cells in culture and their development into established lines. *J Cell Biol*, 17, 299-313.
- VALK, P. J., VERHAAK, R. G., BEIJEN, M. A., ERPELINCK, C. A., BARJESTE VAN WAALWIJK VAN DOORN-KHOSROVANI, S., BOER, J. M., BEVERLOO, H. B., MOORHOUSE, M. J., VAN DER SPEK, P. J., LOWENBERG, B. & DELWEL, R. 2004. Prognostically useful gene-expression profiles in acute myeloid leukemia. *N Engl J Med*, 350, 1617-28.
- VARDIMAN, J. W., THIELE, J., ARBER, D. A., BRUNNING, R. D., BOROWITZ, M. J., PORWIT, A., HARRIS, N. L., LE BEAU, M. M., HELLSTROM-LINDBERG, E., TEFFERI, A. & BLOOMFIELD, C. D. 2009. The 2008 revision of the World Health Organization (WHO) classification of myeloid neoplasms and acute leukemia: rationale and important changes. *Blood*, 114, 937-51.
- VINAY, D. S. & KWON, B. S. 2010. CD11c+CD8+ T cells: two-faced adaptive immune regulators. *Cell Immunol*, 264, 18-22.
- VYAS, P., AULT, K., JACKSON, C. W., ORKIN, S. H. & SHIVDASANI, R. A. 1999. Consequences of GATA-1 deficiency in megakaryocytes and platelets. *Blood*, 93, 2867-75.
- WAKITA, S., YAMAGUCHI, H., MIYAKE, K., MITAMURA, Y., KOSAKA, F., DAN, K. & INOKUCHI, K. 2011. Importance of c-kit mutation detection method sensitivity in prognostic analyses of t(8;21)(q22;q22) acute myeloid leukemia. *Leukemia*, 25, 1423-32.
- WANG, J., PARK, J. S., WEI, Y., RAJURKAR, M., COTTON, J. L., FAN, Q., LEWIS, B. C., JI, H. & MAO, J. 2013. TRIB2 acts downstream of Wnt/TCF in liver cancer cells to regulate YAP and C/EBPalpha function. *Mol Cell*, 51, 211-25.
- WANG, N. D., FINEGOLD, M. J., BRADLEY, A., OU, C. N., ABDELSAYED, S. V., WILDE, M. D., TAYLOR, L. R., WILSON, D. R. & DARLINGTON, G. J. 1995. Impaired energy homeostasis in C/EBP alpha knockout mice. *Science*, 269, 1108-12.
- WARNER, N. L., MOORE, M. A. & METCALF, D. 1969. A transplantable myelomonocytic leukemia in BALB-c mice: cytology, karyotype, and muramidase content. *J Natl Cancer Inst*, 43, 963-82.
- WEI, C., ZEFF, R. & GOLDSCHNEIDER, I. 2000. Murine pro-B cells require IL-7 and its receptor complex to up-regulate IL-7R alpha, terminal deoxynucleotidyltransferase, and c mu expression. *J Immunol*, 164, 1961-70.

- WEI, S. C., ROSENBERG, I. M., CAO, Z., HUETT, A. S., XAVIER, R. J. & PODOLSKY, D. K. 2012. Tribbles 2 (Trib2) is a novel regulator of toll-like receptor 5 signaling. *Inflamm Bowel Dis*, 18, 877-88.
- WEISSMAN, I. L., ANDERSON, D. J. & GAGE, F. 2001. Stem and progenitor cells: origins, phenotypes, lineage commitments, and transdifferentiations. *Annu Rev Cell Dev Biol*, 17, 387-403.
- WENNEMERS, M., BUSSINK, J., SCHEIJEN, B., NAGTEGAAL, I. D., VAN LAARHOVEN, H. W., RALEIGH, J. A., VARIA, M. A., HEUVEL, J. J., ROUSCHOP, K. M., SWEEP, F. C. & SPAN, P. N. 2011. Tribbles homolog 3 denotes a poor prognosis in breast cancer and is involved in hypoxia response. *Breast Cancer Res*, 13, R82.
- WILSON, A., MACDONALD, H. R. & RADTKE, F. 2001. Notch 1-deficient common lymphoid precursors adopt a B cell fate in the thymus. *J Exp Med*, 194, 1003-12.
- WOUTERS, B. J., JORDA, M. A., KEESHAN, K., LOUWERS, I., ERPELINCK-VERSCHUEREN, C. A., TIELEMANS, D., LANGERAK, A. W., HE, Y., YASHIRO-OHTANI, Y., ZHANG, P., HETHERINGTON, C. J., VERHAAK, R. G., VALK, P. J., LOWENBERG, B., TENEN, D. G., PEAR, W. S. & DELWEL, R. 2007. Distinct gene expression profiles of acute myeloid/T-lymphoid leukemia with silenced CEBPA and mutations in NOTCH1. *Blood*, 110, 3706-14.
- XIE, H., YE, M., FENG, R. & GRAF, T. 2004. Stepwise reprogramming of B cells into macrophages. *Cell*, 117, 663-76.
- XU, S., TONG, M., HUANG, J., ZHANG, Y., QIAO, Y., WENG, W., LIU, W., WANG, J. & SUN, F. 2014. TRIB2 inhibits Wnt/beta-Catenin/TCF4 signaling through its associated ubiquitin E3 ligases, beta-TrCP, COP1 and Smurf1, in liver cancer cells. *FEBS Lett*, 588, 4334-41.
- YAMAMOTO, M., UEMATSU, S., OKAMOTO, T., MATSUURA, Y., SATO, S., KUMAR, H., SATOH, T., SAITOH, T., TAKEDA, K., ISHII, K. J., TAKEUCHI, O., KAWAI, T. & AKIRA, S. 2007. Enhanced TLR-mediated NF-IL6 dependent gene expression by Trib1 deficiency. *J Exp Med*, 204, 2233-9.
- YAMAMOTO, R., MORITA, Y., OOEHARA, J., HAMANAKA, S., ONODERA, M., RUDOLPH, K. L., EMA, H. & NAKAUCHI, H. 2013. Clonal analysis unveils self-renewing lineage-restricted progenitors generated directly from hematopoietic stem cells. *Cell*, 154, 1112-26.
- YAMANAKA, R., BARLOW, C., LEKSTROM-HIMES, J., CASTILLA, L. H., LIU, P. P., ECKHAUS, M., DECKER, T., WYNshaw-BORIS, A. & XANTHOPOULOS, K. G. 1997. Impaired granulopoiesis, myelodysplasia, and early lethality in CCAAT/enhancer binding protein epsilon-deficient mice. *Proc Natl Acad Sci U S A*, 94, 13187-92.
- YANG, L., RAU, R. & GOODELL, M. A. 2015. DNMT3A in haematological malignancies. *Nat Rev Cancer*, 15, 152-65.
- YANG, M., BUSCHE, G., GANSER, A. & LI, Z. 2013. Morphology and quantitative composition of hematopoietic cells in murine bone marrow and spleen of healthy subjects. *Ann Hematol*, 92, 587-94.
- YE, M., ZHANG, H., AMABILE, G., YANG, H., STABER, P. B., ZHANG, P., LEVANTINI, E., ALBERICH-JORDA, M., ZHANG, J., KAWASAKI, A. & TENEN, D. G. 2013. C/EBP $\alpha$  controls acquisition and maintenance of adult haematopoietic stem cell quiescence. *Nat Cell Biol*, 15, 385-94.
- YE, M., ZHANG, H., YANG, H., KOEHE, R., STABER, P. B., CUSAN, M., LEVANTINI, E., WELNER, R. S., BACH, C. S., ZHANG, J., KRIVTSOV, A. V., ARMSTRONG, S. A. & TENEN, D. G. 2015. Hematopoietic Differentiation Is Required for Initiation of Acute Myeloid Leukemia. *Cell Stem Cell*.
- YOKOYAMA, T., KANNO, Y., YAMAZAKI, Y., TAKAHARA, T., MIYATA, S. & NAKAMURA, T. 2010. Trib1 links the MEK1/ERK pathway in myeloid leukemogenesis. *Blood*, 116, 2768-75.
- YOKOYAMA, T. & NAKAMURA, T. 2011. Tribbles in disease: Signaling pathways important for cellular function and neoplastic transformation. *Cancer Sci*, 102, 1115-22.
- YOKOYAMA, T., TOKI, T., AOKI, Y., KANEZAKI, R., PARK, M. J., KANNO, Y., TAKAHARA, T., YAMAZAKI, Y., ITO, E., HAYASHI, Y. & NAKAMURA, T. 2012. Identification of TRIB1 R107L gain-of-function mutation in human acute megakaryocytic leukemia. *Blood*, 119, 2608-11.
- ZANDI, S., MANSSON, R., TSAPOGAS, P., ZETTERBLAD, J., BRYDER, D. & SIGVARDSSON, M. 2008. EBF1 is essential for B-lineage priming and establishment of a transcription factor network in common lymphoid progenitors. *J Immunol*, 181, 3364-72.
- ZANELLA, F., RENNER, O., GARCIA, B., CALLEJAS, S., DOPAZO, A., PEREGRINA, S., CARNERO, A. & LINK, W. 2010. Human TRIB2 is a repressor of FOXO that contributes to the malignant phenotype of melanoma cells. *Oncogene*, 29, 2973-82.
- ZEISIG, B. B., GARCIA-CUELLAR, M. P., WINKLER, T. H. & SLANY, R. K. 2003. The oncoprotein MLL-ENL disturbs hematopoietic lineage determination and transforms a biphenotypic lymphoid/myeloid cell. *Oncogene*, 22, 1629-37.

- ZHANG, D. E., ZHANG, P., WANG, N. D., HETHERINGTON, C. J., DARLINGTON, G. J. & TENEN, D. G. 1997. Absence of granulocyte colony-stimulating factor signaling and neutrophil development in CCAAT enhancer binding protein alpha-deficient mice. *Proc Natl Acad Sci U S A*, 94, 569-74.
- ZHANG, P., BEHRE, G., PAN, J., IWAMA, A., WARA-ASWAPATI, N., RADOMSKA, H. S., AURON, P. E., TENEN, D. G. & SUN, Z. 1999. Negative cross-talk between hematopoietic regulators: GATA proteins repress PU.1. *Proc Natl Acad Sci U S A*, 96, 8705-10.
- ZHANG, P., IWASAKI-ARAI, J., IWASAKI, H., FENYUS, M. L., DAYARAM, T., OWENS, B. M., SHIGEMATSU, H., LEVANTINI, E., HUETTNER, C. S., LEKSTROM-HIMES, J. A., AKASHI, K. & TENEN, D. G. 2004. Enhancement of hematopoietic stem cell repopulating capacity and self-renewal in the absence of the transcription factor C/EBP alpha. *Immunity*, 21, 853-63.
- ZHANG, P., NELSON, E., RADOMSKA, H. S., IWASAKI-ARAI, J., AKASHI, K., FRIEDMAN, A. D. & TENEN, D. G. 2002. Induction of granulocytic differentiation by 2 pathways. *Blood*, 99, 4406-12.
- ZHOU, H., LUO, Y., CHEN, J. H., HU, J., LUO, Y. Z., WANG, W., ZENG, Y. & XIAO, L. 2013. Knockdown of TRB3 induces apoptosis in human lung adenocarcinoma cells through regulation of Notch 1 expression. *Mol Med Rep*, 8, 47-52.

## 8 Publications

List of publications:

“*Nfix* expression critically modulates early B lymphopoiesis and myelopoiesis”

Caitríona O’Connor, Joana Campos, Jason M. Osinski, Richard M. Gronostajski, Alison M. Michie, Karen Keeshan

PLOS ONE, 2015 Mar 17;10(3): e0120102. doi:10.1371/journal.pone.0120102

“TRIB2 regulates normal and stress-induced thymocytes proliferation”

Kai Ling Liang, Caitríona O’Connor, J. Pedro Veiga, Tommie V. McCarthy, Karen Keeshan

Cell Discovery, Accepted for publication Dec 10<sup>th</sup>, 2015

“The presence of C/EBP $\alpha$  and its degradation are both required for TRIB2 mediated leukaemia”

Caitríona O’Connor, Fiona Lohan, Joana Campos, Ewa Ohlsson, Mara Salomè, Ciarán Forde, Raik Artschwager, Robert M. Liskamp, Mary R. Cahill, Patrick A. Kiely, Bo Porse, Karen Keeshan

Oncogene, Accepted for publication Jan 11<sup>th</sup> 2016